



TECHNISCHE UNIVERSITÄT MÜNCHEN
TUM SCHOOL OF NATURAL SCIENCES

Azole Coupling Reactions via Combining Sulfonium Activation and Concepts of Catalytic Metalation

Nicolas W. Hilgert

Vollständiger Abdruck der von der TUM School of Natural Sciences der Technischen Universität München zur Erlangung des akademischen Grades eines

Doktors der Naturwissenschaften (Dr. rer. nat.)

genehmigten Dissertation.

Vorsitz: Prof. Dr. Bernd Reif

Prüfer der Dissertation: 1. Prof. Dr. Lukas Hintermann

2. Prof. Dr. Klaus Köhler

Die Dissertation wurde am 17.04.2023 bei der Technischen Universität München eingereicht und durch die TUM School of Natural Sciences am 09.05.2023 angenommen.

Für meine Eltern.

„Einer neuen Wahrheit ist nichts schädlicher als ein alter Irrtum.“
- Johann Wolfgang von Goethe.

The present thesis was carried out from May 2019 to December 2022 under the supervision of Prof. Dr. Lukas Hintermann at the Technical University of Munich.

Acknowledgments

First, I would like to thank Prof. Dr. Lukas Hintermann for giving me the opportunity to carry out my PhD in his group. I am grateful for his supporting guidance during my research and the vivid discussions in our meetings. His inspirational ideas were essential for the success of this project and I always appreciated working on new topics and enjoyed the freedom of developing my own ideas.

Furthermore, I want to thank Verena Widhopf and Christine Kretschmer for the support with all sorts of bureaucratic paper work, the analytical department, especially Jürgen Kudermann, and the chemical store and supply department with Daniel Lemma and Janina Räntsch.

Of course, the years spent in the lab during my PhD would not have been the same without my PhD colleagues Dr. Sebastian Helmbrecht, Dr. Philippe Klein, Dr. Katja Reinhardt and Christian Weindl, the postdoc colleagues in our lab PhD Junlin Zhang and PhD Lianjie Zhai, master student Theresa Appleson and the exchange students Mateja Markotic and Maria Kouridaki. Thank you for the comfortable working atmosphere. It has been a great pleasure to work with you in the last three years.

Moreover, I want to say thank you to my former students Oliver Jakob, Nicole Willeit, Benedict Horn, Kathrin Wendels, Mykhaylo Parkulab, Jonas Djossou and Raphael Etzensperger for having invested much time and energy into my research. They all did an amazing job in the lab and their contributions during their internships were essential in finishing the projects that are presented in this thesis.

Also, I am deeply grateful for having humans in my life I can always count on and for having absolutely great times with them aside from the working life. It definitely means a lot to me to share my life with you and you all have an individual contribution to the completion of this thesis: Aaron, Alex, Chris, Daniel, Eva, Fabi, Johanna, Jojo, Korbi, Lina, Lisa, Lukas, Maggie, Max, Michi, Moritz, Niklas, Tom, Vreni and all the others I did not mention particularly.

Lastly, I want to thank my whole family for always believing in me and supporting me in every possible way throughout my studies and PhD. The feeling of an anytime warm and welcoming home is irreplaceable. Additionally, for a few years now my life is enriched by the little nephews of my sister, it is wonderful seeing them grow up and putting chemistry aside. It goes without saying that I am sincerely thankful for having such loving parents, danke Mama, danke Papa.

Abstract

Within the scope of this work, the chemistry of pyrroles and indoles is investigated with regard to synthesis and general arylation and cross-coupling strategies with organometallic nucleophiles. A plethora of *N*-aryl-2,5-dimethylpyrroles was synthesized to serve as feedstock for further reactions. In one approach they were first brominated, then exposed to *n*-BuLi for halogen-lithium exchange followed by transmetalation with zinc chloride to provide organozinc species for NEGISHI cross-coupling reactions with various palladium catalysts, for instance the class of PEPPSI pre-catalysts. Whereas traditional cross-coupling strategies rely on halides or pseudo halides as electrophilic coupling partners, sulfonium salts represent an alternative, powerful and versatile class of electrophiles for cross-coupling reactions. In an alternative approach, the same *N*-aryl-2,5-dimethylpyrroles as well as selected indole precursors were activated with Tf₂O and a sulfoxide to give the corresponding sulfonium salt, which then underwent NEGISHI-type cross-coupling reactions with arylzinc tosylates obtained by nickel-catalyzed zincation of aryl sulfonates. The coupling conditions were extensively investigated in terms of catalyst complexes, steering ligands, ratio of reactants, time and temperature. The reaction scope was studied with regard to the structure of the sulfonium salt and the zincated sulfonate, respectively. Besides aryl tosylates, various other precursors for the organozinc reagent like mesylates, triflates, sulfamate esters and imidazolylsulfonates were tested. For evaluation of a complementary approach, the C–H arylation of caffeine with a brominated pyrrole as electrophile was tested with regards to typical conditions named above and CMD-additives.

The second part of this work focused on the catalytic generation of organozinc reagents from aryl sulfonates. The direct insertion of zinc into a C–X bond of aryl halides was typically limited to iodides and bromides. A NiCl₂–1,4-diazadiene catalyst-system, where diazadiene refers to diimines of glyoxal or diacetyl, bipyridines and related ligands, was previously developed and enables the insertion of zinc dust into the C–O bond of aryl sulfonates (tosylates, mesylates, triflates, sulfamates). Herein, this reaction methodology is further investigated. The scope of aryl tosylates is broadened, and an extensive ligand screening is conducted to tune the reactivity and gain knowledge about the substrate-ligand relationship. The potential for catalytic metalation by means of a combination of NiCl₂(dme) and several metal-mabiq (macrocylic biquinazoline) complexes is examined to gain insights into bimetallic catalysis.

The third part of the thesis evaluates the prospects of reductive cross-electrophile couplings of aryl tosylates with aryl and alkyl bromides. This concept avoids the use of preformed organometallic nucleophiles, otherwise mandatory for classical cross-coupling reactions. To achieve this goal two different electrophiles are allowed to react under the same conditions as in the catalytic metalation. Using the coupling of naphthyl tosylate and benzyl bromide as model reaction, a variety of reaction conditions are screened such as the ligand, reactant ratios and temperature. The reaction of an aryl tosylate with benzyl, aryl and alkyl bromides is then investigated under the optimized reaction conditions.

Zusammenfassung

Im Rahmen dieser Arbeit wurde die Chemie der Pyrrole und Indole hinsichtlich Synthese und allgemeiner Arylierungs- und Kreuzkupplungsstrategien mit organometallischen Nucleophilen untersucht. Eine Fülle an *N*-Aryl-2,5-dimethylpyrrolen wurde als Ausgangsmaterial synthetisiert. In einer Herangehensweise wurden diese zuerst bromiert und dann einem Halogen-Metall Austausch mit *n*-Butyllithium unterzogen, gefolgt von einer Transmetallierung mit Zinkchlorid um Organozinkverbindungen für NEGISHI Kreuzkupplungsreaktionen mit verschiedenen Palladiumkatalysatoren herzustellen, zum Beispiel die Klasse der PEPPSI Katalysatoren. Wohingegen klassische Kreuzkupplungsstrategien auf Halogeniden oder Pseudohalogeniden als elektrophile Kupplungspartner beruhen, stellen Sulfoniumsalze eine alternative, leistungsfähige und vielseitige Klasse an Elektrophilen für Kreuzkupplungsreaktionen dar. In einem alternativen Ansatz wurden die gleichen *N*-Aryl-2,5-dimethylpyrrole sowie ausgewählte Indole mit Tf_2O und einem Sulfoxid aktiviert, um die entsprechenden Sulfoniumsalze zu synthetisieren, die dann Kreuzkupplungen nach NEGISHI mit Arylzinktosylaten, hergestellt durch nickelkatalysierte Zinkierung von Arylsulfonaten, eingehen. Die Kupplungsbedingungen wurden umfangreich bezüglich Katalysatorkomplexen, Liganden, Verhältnis der Edukte, Zeit, Temperatur und Lösungsmittel untersucht. Der Umfang der Reaktion wurde hinsichtlich der Struktur der Sulfoniumsalze und der zinkierten Sulfonate erforscht. Außerdem wurden neben Aryltosylaten verschiedene, alternative Vorläufer der Organozinkverbindung getestet, darunter fallen Mesylate, Triflate, Sulfamatester und Imidazolylsulfonate. Ergänzend wurde die C-H Arylierung von Koffein mit einem bromierten Pyrrol als Elektrophil hinsichtlich ähnlicher Reaktionsbedingungen wie oben und mithilfe von CMD-Additiven untersucht.

Der zweite Teil dieser Arbeit fokussierte die katalytische Synthese von Organozinkreagenzien aus Arylsulfonaten. Die direkte Insertion von Zink in eine C-X Bindung von Arylhalogeniden war typischerweise auf Iodide und Bromide limitiert. Ein NiCl_2 -1,4-Diazadien Katalysatorsystem, wobei sich Diazadien auf Glyoxal- oder Diacetyldiimine, Bipyridine, oder verwandte Liganden bezieht, wurde im Vorfeld entwickelt und ermöglicht die Insertion von Zinkstaub in die C-O Bindung von Arylsulfonaten (Tosylate, Mesylate, Triflate, Sulfamate). Nun wurde diese Reaktion weiter untersucht. Die Reaktivität von verschiedenen Aryltosylaten wurde getestet und ein ausführliches Ligandenscreening wurde durchgeführt um die Reaktivität und Substrat-Ligand Beziehung besser einschätzen und nutzen zu können. Das Potenzial der katalytischen Metallierung mit dem etablierten $\text{NiCl}_2(\text{dme})$ und verschiedenen Metall-Mabiq (makrocyclisches Chinazolin) Komplexen wurde untersucht um Einblick in die bimetallische Katalyse zu bekommen.

Der dritte Teil dieser Arbeit untersuchte die Möglichkeiten einer reduktiven Kreuzelektrophilkupplung von Aryltosylaten mit Aryl- und Alkylbromiden. Dieses Konzept vermeidet die vorherige Synthese von organometallischen Nucleophilen, ansonsten zwingend erforderlich für klassische Kreuzkupplungsreaktionen. Um dieses Ziel zu erreichen wurden zwei verschiedene Elektrophile unter gleichen Bedingungen wie in der katalytischen Metallierung zur Reaktion gebracht. Mithilfe der Modellreaktion von einem Naphthyltosylat mit Benzylbromid wurden verschiedene Reaktionsbedingungen getestet, beispielsweise Liganden, Verhältnis der Edukte und Temperatur. Die Reaktion von einem Aryltosylat mit Benzyl-, Aryl- und Alkylbromiden wurde schließlich unter optimierten Reaktionsbedingungen getestet.

Table of Contents

1	Pyrroles – Syntheses and Coupling Reactions	1
1.1	Introduction – Quick History of Organic Chemistry	1
1.1.1	Natural and Commercial Products based on Pyrroles	2
1.1.2	Syntheses and Reactions of Pyrroles	4
1.1.2.1	Syntheses of Pyrroles	4
1.1.2.2	Halogenation of Pyrroles	7
1.1.2.3	Cross-Couplings and Arylations	8
1.1.3	Sulfonium Salts as Electrophiles	11
1.2	Aims and Objectives	13
1.3	Results and Discussion	15
1.3.1	Syntheses of Pyrrole Precursors	15
1.3.2	Halogenations of Pyrroles	18
1.3.3	NEGISHI Cross-Couplings of Metalated Pyrrolyl Halides	22
1.3.4	C–H Arylation of Pyrroles with Arylzinc Sulfonates <i>via</i> Sulfonium Activation	26
1.3.4.1	Synthesis of Pyrrole and Indole Sulfonium Salts	26
1.3.4.2	Screening of Reaction Conditions for Sulfonium Salt Cross- Coupling	29
1.3.4.3	Overview of Aryl Sulfonate Pro-Nucleophiles	38
1.3.4.4	Pyrrole C–H Arylation <i>via</i> Sulfonium Activation and NEGISHI cross-coupling	41
1.3.4.5	Indole C–H Arylation <i>via</i> Sulfonium Activation and NEGISHI cross-coupling	46
1.3.4.6	Screening of Alternative Aryl Sulfonates as Pre-Nucleophiles	48
1.3.4.7	Functionalization <i>via</i> β -Propionylation and Vinylation	49
1.3.5	Caffeine C–H Arylation with Pyrrolyl Halides	50
1.3.6	Attempted Pyrrole C–H Arylation with Aryl Tosylates	53
1.3.7	Attempted Pyrrole Amination with <i>N</i> -Methylpiperazine	54
1.4	Conclusion and Outlook	55
2	Catalytic Metalation – Zinc Insertion into Aryl Sulfonates	58
2.1	Introduction – Organometallic Chemistry	58
2.1.1	Preparation of Organometallic Reagents	59
2.1.1.1	Oxidative Addition	60
2.1.1.2	Halogen Metal Exchange	61

2.1.1.3	Transmetalation	62
2.1.1.4	Directed Metalation	63
2.1.2	The Role of Catalytic Metalation	65
2.1.2.1	Transition Metal-Catalyzed Metal Insertions: Aryl Halides	65
2.1.2.2	Transition Metal-Catalyzed Metal Insertions: Non-Halogen Leaving Groups	67
2.2	Aims and Objectives	69
2.3	Results and Discussion	71
2.3.1	Synthesis of Tosylates and Ligands	71
2.3.2	Ligand Screening	72
2.3.2.1	The Class of <i>N</i> -2,6-Diisopropylphenyl substituted Diazadienes	72
2.3.2.2	The Class of Pyridyl and Pyrazolyl Isoindoline Ligands	74
2.3.2.3	The Class of Mesitylamine derived Diazadiene Ligands	75
2.3.2.4	The Class of <i>N</i> -2,6-Dihaloaryl Diazadiene Ligands	76
2.3.3	Bimetallic Catalysis – Role of Mabiq Complexes	77
2.3.4	Optimization of Reaction Parameters	79
2.3.5	Catalytic Zincation of Pyrrolyl Halides and Sulfonium Salts	81
2.4	Conclusion and Outlook	82
3	Reductive Cross-Electrophile-Coupling involving Aryl Sulfonates	83
3.1	Introduction – No Need for Carbon Nucleophiles – An Alternative to Conventional Cross-Coupling	83
3.2	Aims and Objectives	86
3.3	Results and Discussion	87
3.3.1	Initial Condition Screening of Cross-Electrophile Coupling	87
3.3.2	Ligand Screening of Cross-Electrophile Coupling	89
3.3.3	Cross-Reductive Coupling Substrate Scope: Aryl Tosylate and Aryl or Alkyl Bromides	91
3.3.4	Cross-Reductive Coupling Substrate Scope: Aryl Tosylate and Alkyl Bromide	92
3.4	Conclusion and Outlook	93
4	Experimental Part	94
4.1	General Remarks	94
4.1.1	Chemicals and Solvents	94
4.1.2	Work Techniques	95
4.1.3	Analytics	95
4.1.4	Solutions, Bases and Catalysts	97
4.1.4.1	Preparation of a ZnCl ₂ solution	97
4.1.4.2	Synthesis of TMPZnCl · LiCl base	97
4.1.4.3	Synthesis of Pd-PEPPSI-IPr catalyst	97
4.2	Experimental Data to Chapter 1	98
4.2.1	General Procedures	98
4.2.1.1	General Procedure 1.1 for Synthesis of Pyrroles	98
4.2.1.2	General Procedure 1.2 for Synthesis of Sulfonium Salts	98
4.2.1.3	General Procedure 1.3 for Synthesis of Aryl Sulfonates	98

4.2.1.4	General Procedure 1.4 for Chlorination of Pyrroles	98
4.2.1.5	General Procedure 1.5 for Negishi Couplings via Trans- metalation of Pyrrolyl Halides	99
4.2.1.6	General Procedure 1.6 for Pyrrole and Indole C–H Arylation	99
4.2.1.7	General Procedure 1.7 for Caffeine Arylation with Pyrrolyl Halides	99
4.2.1.8	General Procedure 1.8 for Pyrrole Arylation with Aryl To- sylates	100
4.2.1.9	General Procedure 1.9 for Pyrrole Amination	100
4.2.2	Isolated Compounds and Analytical Data	101
4.2.2.1	Synthesis of Pyrrole Precursors	101
4.2.2.2	Synthesis of Indole Precursors	108
4.2.2.3	Synthesis of Sulfonium Salts	109
4.2.2.4	Synthesis of Aryl Sulfonates	113
4.2.2.5	Synthesis of Pyrrole Coupling Products	117
4.2.2.6	Synthesis of Indole Coupling Products	127
4.2.2.7	Synthesis of Propionic Acid Coupling Products	129
4.3	Experimental Data to Chapter 2	130
4.3.1	General Procedures	130
4.3.1.1	General Procedure 2.1 for Catalytic Zincation of Aryl To- sylates followed by Iodolysis	130
4.3.2	Isolated Compounds and Analytical Data	131
4.4	Experimental Data to Chapter 3	132
4.4.1	General Procedures	132
4.4.1.1	General Procedure 3.1 for Reductive Cross-Electrophile- Coupling	132
4.5	NMR Spectra	133

5 Appendix

List of Abbreviations

ANQ	acenaphthoquinone	DMG	directed metalation group
aq.	aqueous	DMPU	<i>N,N'</i> -dimethylpropyleneurea
Ar	aryl group	DMSO	dimethyl sulfoxide
Boc	tert-Butyloxycarbonyl	eq.	mole equivalent
<i>n</i> -BuLi	<i>n</i> -butyllithium	Et ₂ O	diethyl ether
<i>s</i> -BuLi	<i>sec</i> -butyllithium	FG	functional group
<i>t</i> -BuLi	<i>tert</i> -butyllithium	GC	gas chromatography
CC	column chromatography	GCMS	gas chromatography–mass spectrometry
DAD	diazadiene	HRMS	high resolution mass spectrometry
DBDMH	1,3-dibromo-5,5-dimethylhydantoin	IND	isoindoline
DCDMH	1,3-dichloro-5,5-dimethylhydantoin	LDA	lithium diisopropylamide
DCM	dichloromethane	LRMS	low resolution mass spectrometry
DIPA	2,6-diisopropylaniline	MABIQ	macrocyclic Biquinazoline
DMA	dimethylacetamide	Me	methyl
DMF	dimethylformamide	MESA	2,4,6-trimethylanilin

NBS	<i>N</i> -bromosuccinimide	sat.	saturated
NCS	<i>N</i> -chlorosuccinimide	SiO ₂	silica gel
NHC	<i>N</i> -heterocyclic carbene	sol.	solution
NMP	<i>N</i> -methyl-2-pyrrolidone	TBCA	tribromoisocyanuric acid
NMR	nuclear magnetic resonance	TCCA	trichloroisocyanuric acid
<i>N</i> -TIPS	triisopropylsilane	Tf ₂ O	trifluoromethanesulfonic anhydride
<i>o.n.</i>	over night	TFAA	trifluoroacetic anhydride
PEPPSI	pyridine-enhanced precatalyst preparation stabilization and initiation	TFE	trifluoroethanol
Ph	phenyl group	THF	tetrahydrofuran
PHE	1,10-phenanthroline	TLC	thin-layer chromatography
qNMR	quantitative NMR	TMEDA	<i>N,N,N',N'</i> -tetramethylethylenediamine
QUI	quinoline	TMOF	trimethyl orthoformate
<i>r.t.</i>	room temperature	TMP	2,2,6,6-tetramethylpiperidine
Rec.	recovery	TMS-Cl	trimethylsilyl chloride

1. Pyrroles – Syntheses and Coupling Reactions

1.1. Introduction – Quick History of Organic Chemistry

Since the proof of synthesis of urea in 1828¹ and breakthrough work on the structure of organic molecules in 1858², synthetic organic chemistry has greatly advanced in constructing complex organic molecules.³ The progress of chemical, synthetic methodology – the ability to form new bonds in an efficient and selective way – has contributed to and pushed on the total syntheses of naturally occurring or artificially designed, commercially used compounds.⁴ A sophisticated level of expertise has nowadays been reached in order to evaluate synthetic strategies and methods in terms of their efficiency.⁵ Essentially and generally accepted criteria like atom- and step-economy as well as the demands of green chemistry represent objective guidelines to evaluate any synthetic transformation or sequences of such.⁶ Although it is recognized as a challenging parameter, scalability of a reaction or sequence is mentioned less frequently.⁴ The importance of scalability is easily explained by recognizing that only scalable transformations can find industrial application in order to provide the desired product in large scale quantities. The scalability and economic criteria of a synthesis can be called practicality, representing a crucial factor for process chemists in industry. Hence, this concept affects society in its entirety, for instance economically in the synthesis of indispensable pharmaceuticals. Methods for minimizing the gap between academic and industrial synthesis are therefore desirable.⁷ In the past decades the utility of organometallic reagents and especially cross-coupling-reactions for achieving challenging transformations has been widely acknowledged. In terms of practicality, organometallic chemistry has made concise syntheses possible by providing efficient tools for bond formation. An ever-growing toolbox of organometallic reagents and catalysts is available to the synthetic organic chemist. Nearly every main group and transition

¹Wöhler, F. *Ann. Phys.*, **1828**, *88*, 253–256.

²Kekulé, F. A. *Liebigs Ann. Chem.*, **1858**, *104*, 129–159.

³Nicolaou, K. C.; Vourloumis, D.; Winssinger, N.; Baran, P. S. *Angew. Chem. Int. Ed.* **2000**, *39*, 44–122.

⁴Kuttruff, C. A.; Eastgate, M. D.; Baran, P. S. *Nat. Prod. Rep.* **2014**, *31*, 419–432.

⁵(a) Mulzer *J. Nat. Prod. Rep.* **2014**, *31*, 595–603. (b) Seebach, D. *Angew. Chem. Int. Ed.* **1990**, *29*, 1320–1367.

⁶(a) Trost, B. M. *Science* **1991**, *34*, 1471–1477. (b) Wender, P. A.; Verma, V. A.; Paxton T. J.; Pillow T. H. *Acc. Chem. Res.* **2008**, *41*, 40–49.

⁷Trost, B. M. *Angew. Chem. Int. Ed.* **1995**, *34*, 259–281.

metal has found its application or synthetic value, either as a catalyst or an organometallic nucleophile.⁸ The chemical and pharmaceutical industries apply these unique reactivity patterns made possible by transition metal catalysts like palladium, rhodium or nickel. The downside of these metals is their toxicity⁹ and purchase price.¹⁰ Thus, research is seeking after sustainable and environmentally benign methodologies enabling new and efficient reactions with broad substrate scopes. These intentions are summarized as green chemistry.

The research presented in this chapter pursues criteria of green chemistry by avoiding the use of halides as substrates (see chapter 1.1.3) and deals with a heterocycle which offers unique reactivity patterns: the electron-rich, five-membered and aromatic pyrrole ring. Its chemical behaviour becomes clear by looking at the limiting resonance structures: In total, there are five canonical structures possible and in four of them the positive charge is located at the nitrogen atom, the negative charge on carbon atoms, so as one would expect this results in a strong dipole moment. In comparison with other five-membered heterocycles it confirms the unique reactivity.¹¹ Quantitatively compared, the dipole moment of pyrrole is 1.81 D whereas the ones from furan (0.70 D) and thiophene (0.51 D) are much lower due to the weaker π donor effect (see figure 1.1). Hence, pyrrole is prone to electrophilic aromatic substitutions at the four carbon atoms.

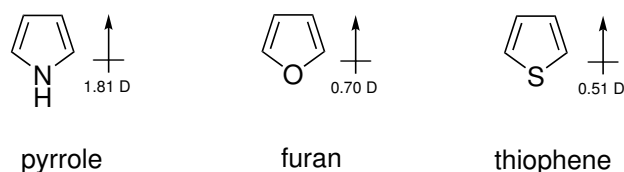


Figure 1.1: Dipole moment of selected five-membered, aromatic heterocycles.

1.1.1 Natural and Commercial Products based on Pyrroles

Heterocycles are abundantly found in natural products that possess a wide range of biological properties such as antibacterial, antiviral and antioxidant activities.¹² The five-membered and aromatic heterocycle pyrrole was first described by RUNGE as a component of coal tar in 1834¹³, but it was not until 1870 when the structure was correctly formulated by BAEYER.¹⁴ The name descends from the greek word *pyrrhos* which means fiery or reddish. Among heterocycles it is one of the most important ones because it is found in a broad range of natural products and commercial drugs. Polymers of pyrroles are of growing relevance in materials science. Its biological importance is ubiquitous due to being an essential structural fragment of the "pigments of life", the tetrapyrroles also

⁸Knochel, P. *Handbook of Functionalized Organometallics*; Wiley-VCH, Weinheim, **2005**.

⁹Weidmann, B.; Seebach, D. *Angew. Chem. Int. Ed.* **1983**, *22*, 31–45.

¹⁰Peña, K. A.; Kiselyov, K. *Biochem. J* **2015**, *470*, 65–76.

¹¹(a) Davies D. T. *Aromatische Heterocyclen*, VCH-Verl.-Ges, Weinheim, **1995**. (b) Vollhardt K. P. C.; Schore N. E. *Organische Chemie*, 4. Aufl., Wiley-VCH-Verl., Weinheim, **2007**.

¹²(a) Blunt, J. W.; Copp, B. R.; Keyzers, R. A.; Munro, M. H. G.; Prinsep, M. R. *Nat. Prod. Rep.* **2016**, *33*, 382–431. (b) Bhardwaj, V.; Gumber, D.; Abbot, V.; Dhiman, S.; Sharma, P. *RSC Adv.* **2015**, *5*, 15233–15266.

¹³Runge, F. F. *Ann. Phys.* **1834**, *31*, 67–78.

¹⁴Baeyer, A.; Emmerling A. *Ber. Dtsch. Chem. Ges.* **1870**, *3*, 514–517.

known as porphyrins¹⁵: heme (Fe-complex, cofactor of the protein hemoglobin), chlorophyll (Mg-complex, vital for photosynthesis) and cobalamin (Co-complex, vitamin B₁₂). Exemplary, important Fe(II)-protoporphyrin IX (Hematin) is shown in figure 1.2.

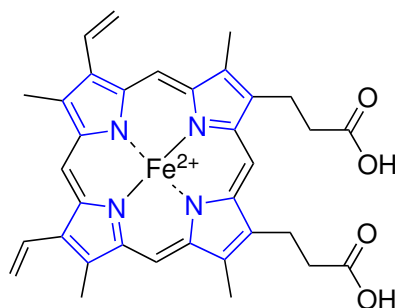


Figure 1.2: Structure of Fe(II)-Protoporphyrin IX (Hematin).

Pyrroles are found in many more compounds: Over the years many natural products have been isolated from plants or fungi, a selection is shown in figure 1.3. Pyrrolnitrin was isolated from the bacterial cells of a *Pseudomonas pyrocinia* and is known to possess antifungal and antibiotic properties.¹⁶ The class of lamellarins are from marine invertebrates and exhibit antitumor and anti-HIV activities.¹⁷ The pyrrole-imidazole family of alkaloids includes isolated natural products from marine sponges. The simplest, brominated member oroidin possesses antimalarial activity.¹⁸ Another class of marine alkaloids are the marinopyrroles which came to the fore in recent years due to their high activity against methicillin resistant bacteria. A beneficial feature because of antibiotic resistances.¹⁹

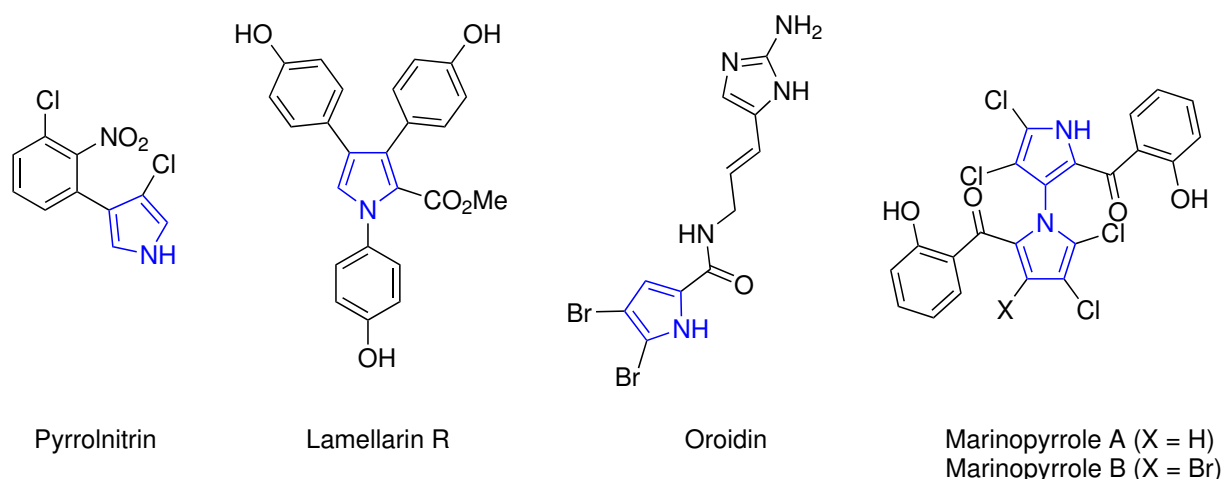


Figure 1.3: Natural products of pyrroles.

¹⁵Battersby A. *Science* **1994**, *264*, 1551–1557.

¹⁶(a) Gordee, R. S.; Matthews, T. R. *Appl. Microbiol.* **1969**, *17*, 690–694. (b) Kei, A.; Hiroshi, I.; Masanobu, K.; Akio, F.; Gakuzo, T. *Agric. Biol. Chem. Chem.* **1964**, *28*, 575–580.

¹⁷Fukuda T.; Ishibashi F.; Iwao M. *Heterocycles* **2011**, *83*, 491–529.

¹⁸Gademann K.; Kobylinska J. *Chem. Rec.* **2009**, *9*, 187–198.

¹⁹Clive D. L. J.; Cheng P. *Tetrahedron* **2013**, *69*, 5067–5078.

It comes as little surprise that the pyrrole ring has found great use in the design and development of pharmaceuticals (see figure 1.4). LB42908 belongs as an antitumor agent to a class of highly potent, selective, and non-peptidic inhibitors of the farnesyltransferase and is undergoing preclinical studies.²⁰ Sunitinib is a commercially available drug used for the oral treatment of renal cancer and acts as a multi-targeted receptor tyrosine kinase inhibitor.²¹ One of the best known pyrrole-containing pharmaceuticals is Atorvastatin. An inhibitor of HMG-CoA reductase, therefore used for the treatment of dyslipidemia and the prevention of cardiovascular diseases as a cholesterol-lowering agent. It is one of the most commonly prescribed drugs in history.²²

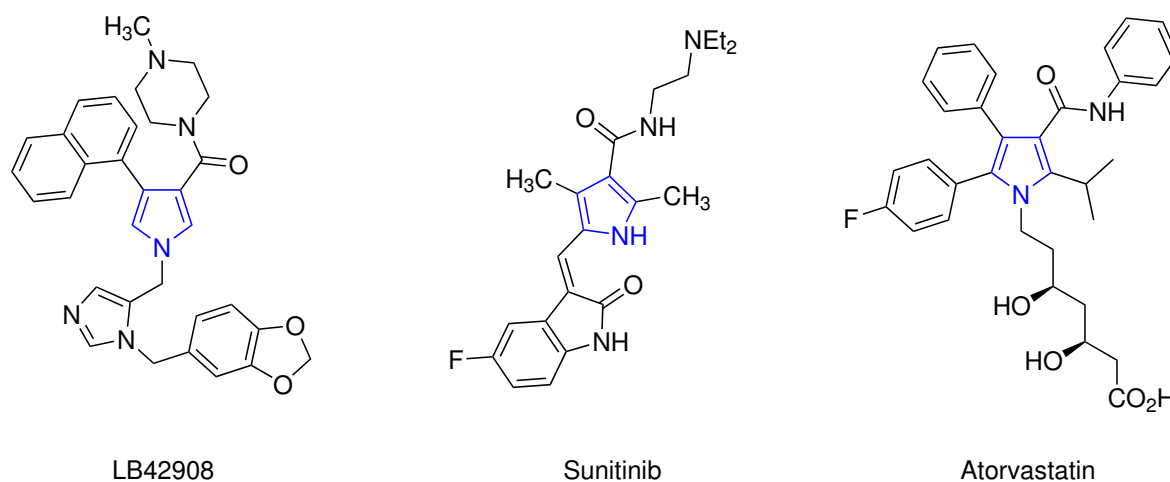


Figure 1.4: Commercial products of pyrroles.

1.1.2 Syntheses and Reactions of Pyrroles

1.1.2.1 Syntheses of Pyrroles

Several syntheses of pyrroles have been developed over time. Starting from the classic approaches toward more sophisticated ones selected procedures are described below:

Knorr Pyrrole Synthesis

In 1884, LUDWIG KNORR published the synthesis of pyrrole derivatives from α -amino- β -ketoesters and β -ketoesters (see scheme 1.1).²³ Since α -amino- β -ketoesters are prone to self-condensation they have to be prepared *in situ* by reduction of the oximo acetoacetate, another possible way would be the NEBER rearrangement of ketoximes. The reaction proceeds *via* condensation of the amine and the activated carbonyl group of the β -ketoester with an imine. The resulting imine then tautomerizes to an enamine. A cyclization, elimination of water and isomerization affords the corresponding tetrasubstituted pyrrole.

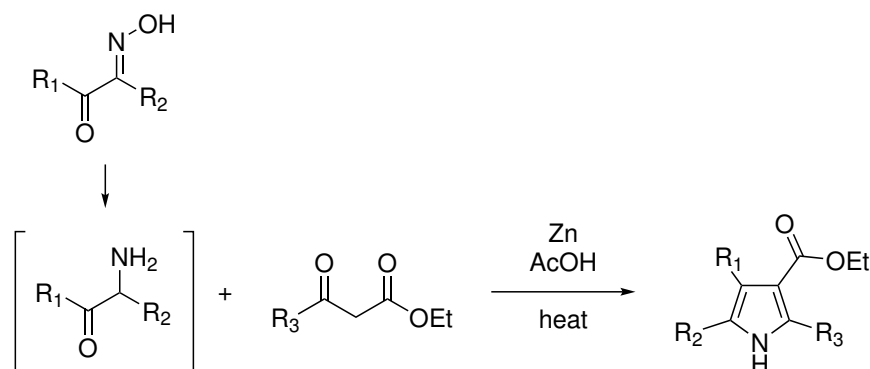
²⁰Lee, H.; Lee, J.; Lee, S.; Shin, Y.; Jung, W.; Kim, J.; Park, K.; Kim, K.; Cho, H. S.; Ro, S.; Lee, S.; Jeong, S. W.; Choi, T.; Chung, H.; Koh, J. S. *Bioorg. Med. Chem. Lett.* **2001**, *11*, 3069–3072.

²¹Estévez, V.; Villacampa, M.; Menéndez, J. C. *Chem. Soc. Rev.* **2014**, *43*, 4633–4657.

²²Hitchings A.; Lonsdale D.; Burrage D.; Baker E. *The Top 100 Drugs E-book: Clinical Pharmacology and Practical Prescribing*; Elsevier Health Sciences, London, **2014**.

²³Knorr, L. *Ber. Dtsch. Chem. Ges.* **1884**, *17*, 1635–1642.

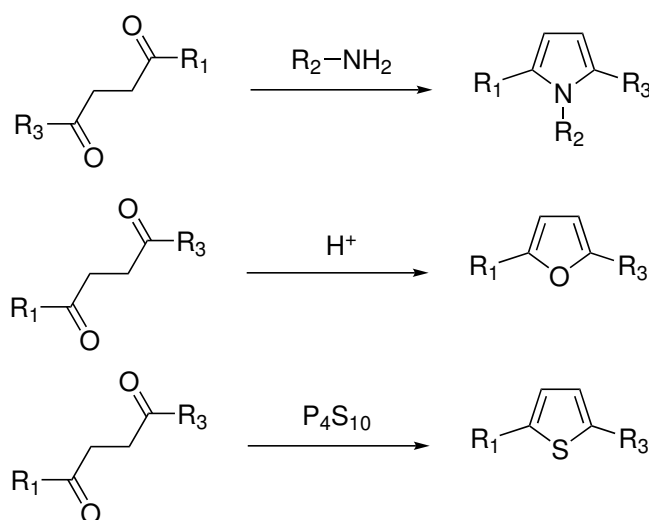
Zinc is needed as reducing agent and acetic acid as catalyst and H^+ donor. The original procedure from 1884 made use of two equivalents of ethyl acetoacetate of which one equivalent was converted to an α -aminoketone, whereas the second served as β -ketoester. Hence, the resulting product with $R_1 = R_3 = Me$ and $R_2 = CO_2Et$ is called Knorr's Pyrrole.



Scheme 1.1: The Knorr pyrrole synthesis.

Paal-Knorr Pyrrole Synthesis

In the same year a modified version of the KNORR pyrrole synthesis was concurrently published by german chemists CARL PAAL²⁴ and LUDWIG KNORR (see scheme 1.2).²⁵ This reaction allows the Brønsted acid- or Lewis acid-catalyzed formation of pyrrole derivatives from 1,4-dicarbonyl compounds and ammonia or primary amines. Due to its mild conditions it is a popular route to not only synthesize pyrroles but also other common five-membered heterocycles by either self-condensation of the dicarbonyl compound for furanes or substituting the amine with phosphorus pentasulfide (P_4S_{10}) for thiophenes. Mechanistically, the pyrrole synthesis proceeds *via* attack of the protonated carbonyl by the amine to form a hemiaminal.



Scheme 1.2: The Paal Knorr synthesis.

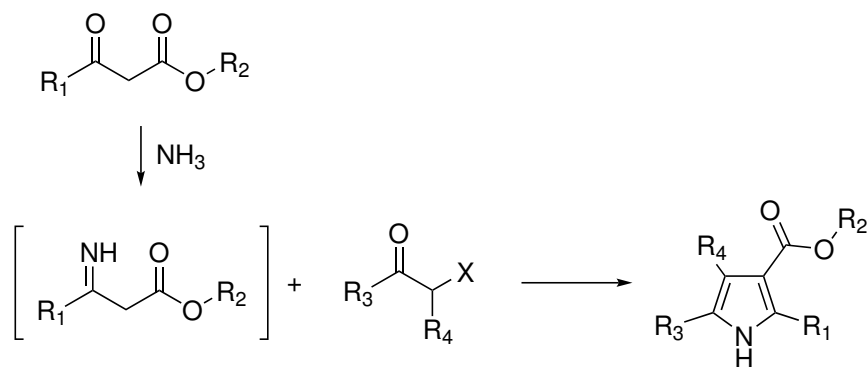
²⁴Paal, C. *Ber. Dtsch. Chem. Ges.* **1884**, *17*, 2756–2767.

²⁵Knorr, L. *Ber. Dtsch. Chem. Ges.* **1884**, *17*, 2863–2870.

The secondary amine then attacks the second ketone moiety to form a tetrahydropyrrole which then *via* dehydration forms the corresponding trisubstituted pyrrole. It is also possible to synthesize the *N*-unsubstituted pyrrole *via* use of ammonium hydroxide or ammonium acetate. Over the years miscellaneous syntheses have been developed catalyzed by iodine²⁶, RuCl₃²⁷, Fe³⁺-montmorillonite²⁸, lewis-acids such as titanium(IV)isopropoxide²⁹ or metal-free *via* microwave radiation.³⁰

Hantzsch Pyrrole Synthesis

In 1890 ARTHUR RUDOLF HANTZSCH published the reaction of a β -ketoester with ammonia or primary amines and α -haloketones to form substituted pyrroles (see 1.3).³¹ An enamine is formed *via* attack of the β -carbon of the β -ketoester by the amine. This enamine reacts with the α -haloketone and *via* an intramolecular nucleophilic attack a cyclization occurs. Final elimination of water and tautomerization yields the pyrrole.



Scheme 1.3: The Hantzsch pyrrole synthesis.

van Leusen Pyrrole Synthesis

Generally, the VAN LEUSEN reaction converts aldehydes and ketones to nitriles with the versatile reagent TosMIC (toluenesulfonylmethyl isocyanide).³² This unique CNC synthon can be used for the synthesis of various heterocycles such as oxazoles or imidazoles. The synthesis of pyrroles is made possible by the reaction of TosMIC with enones in presence of base (see scheme 1.4). A Michael addition followed by cyclization, elimination of the tosyl group and tautomerization furnishes the pyrrole.

²⁶Banik, B. K.; Samajdar, S.; Banik, I. *J. Org. Chem.* **2004**, *69*, 213–216.

²⁷De, S. K. *Catal. Lett.* **2008**, *124*, 174–177.

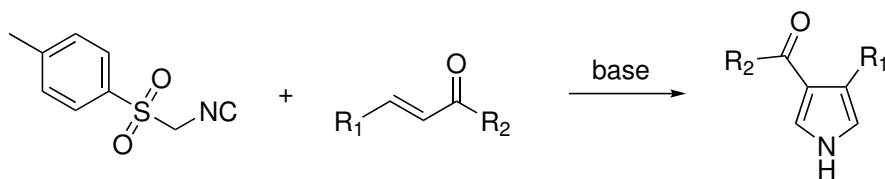
²⁸Song, G. Y.; Wang, B.; Wang, G.; Kang, Y. R.; Yang, T. and Yang, L. M. *Synth. Commun.* **2005**, *35*, 1051–1057.

²⁹Dong, Y.; Pai, N. N.; Ablaza, S. L.; Yu, S.-X.; Bolvig, S.; Forsyth, D. A. and Le Quesne, P. W. *J. Org. Chem.* **1999**, *64*, 2657–2666.

³⁰(a) Danks, T. N., *Tetrahedron Lett.* **1999**, *40*, 3957–3960. (b) Minetto, G.; Raveglia, L. F. and Taddei, M. *Org. Lett.* **2004**, *6*, 389–392.

³¹Hantzsch, A. *Ber. Dtsch. Chem. Ges.* **1890**, *23*, 1474–1478.

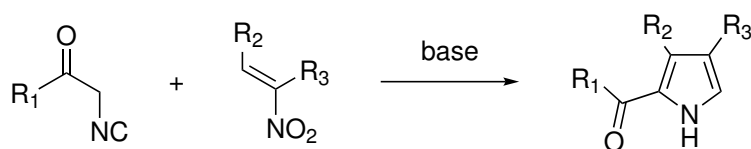
³²Oldenziel O. H.; Van Leusen D.; Van Leusen A. M. *J. Org. Chem.* **1977**, *42*, 3114–3118.



Scheme 1.4: The VAN LEUSEN pyrrole synthesis.

Barton–Zard Pyrrole Synthesis

This reaction was first reported by DEREK BARTON and SAMIR ZARD in 1985.³³ It allows the synthesis of pyrroles *via* the reaction of a α -isocyanoacetate with a nitroalkene under basic conditions. It proceeds comparably to the VAN LEUSEN reaction.



Scheme 1.5: The Barton-Zard pyrrole synthesis.

1.1.2.2 Halogenation of Pyrroles

In general, halogenations are essential transformations and an integral part in modern organic chemistry. Halogenated pyrroles commonly occur in natural products (e.g. oroidin in figure 1.3) as well as in commercial products (e.g. atorvastatin in figure 1.4). Due to the high toxicity and inconvenient handling of elemental chlorine and bromine a huge variety of reagents for synthesizing halogenated molecules has been developed. Preferably, the agents are stable, solid and easy to handle. Common, selected examples used in this chapter – especially suitable for aromatic systems – are shown in figure 1.5: The well-known *N*-chlorosuccinimide (NCS) and *N*-bromosuccinimide (NBS) function as convenient source of chlorine or bromine, respectively. They both deviate from the imide of succinic acid, succinimide. The next two agents are derived from 5,5-dimethylhydantoin and are able to transfer two equivalents of halogen: 1,3-dichloro-5,5-dimethylhydantoin (DCDMH) and 1,3-dibromo-5,5-dimethylhydantoin (DBDMH).³⁴

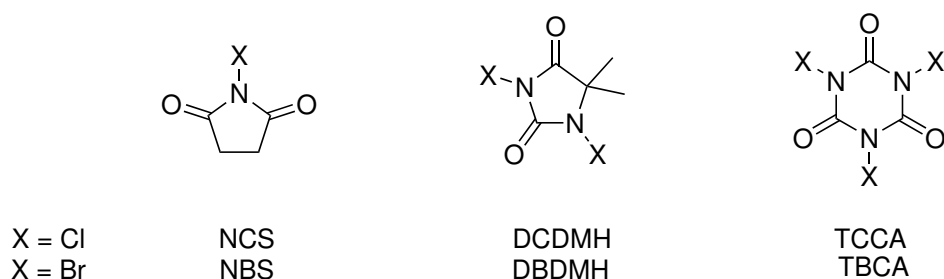


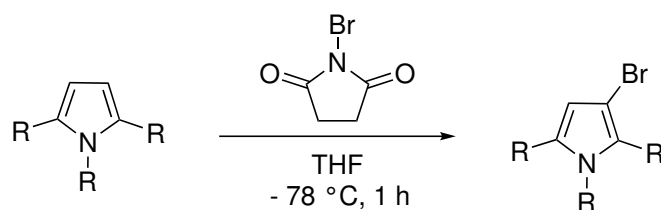
Figure 1.5: Various halogenating agents.

³³Barton D. H. R.; Zard S. Z. *J. Chem. Soc., Chem. Commun.* **1985**, 1098–1100.

³⁴(a) Chassaing C.; Haudrechy A.; Langlois Y. *Tetrahedron Lett.* **1997**, *38*, 4415–4416. (b) Alam A. *Synlett* **2005**, *15*, 2403–2404.

An even better atom economy is reached by trichloroisocyanuric acid (TCCA) or tribromoisocyanuric acid (TBCA), respectively.³⁵ These agents are able to transfer up to three equivalents of positive halogen.

Direct halogenations of pyrroles date back to reactions performed by LOUIS CARPINO from 1964³⁶. Later on, the scope was further investigated in line with the established route.³⁷ Scheme 1.6 shows an exemplary bromination of pyrrole. A huge drawback of these halogenated pyrroles as synthetic building blocks is their lability: they decompose rapidly if exposed to air or light and are therefore difficult to handle. As a consequence, substituting labile pyrrolyl halides by more suitable reagents is a research goal and topic of this chapter.

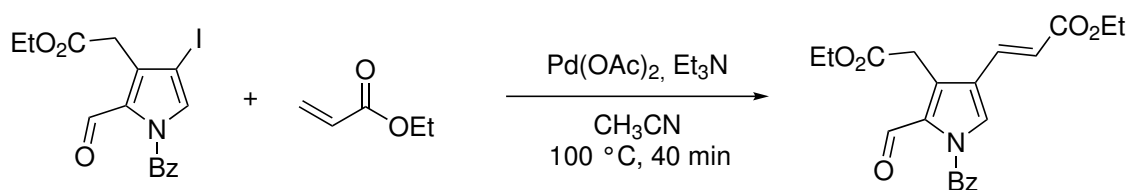


Scheme 1.6: Exemplary bromination of a pyrrole.

1.1.2.3 Cross-Couplings and Arylations

Due to the afore mentioned importance of the pyrrole heterocycle, the development of cross-coupling reactions involving pyrroles is a topic of interest in order to conveniently synthesize complex targets. Owing to the variety of coupling reactions reported in the literature only a few examples are presented with focus on halogenated pyrroles. In general, this chemistry is of lower importance for pyrroles when compared with other heterocycles.³⁸

The HECK chemistry was applied en route to porphobilinogen: C4-halogenated pyrrole reacts with ethyl acrylate to the β -substituted deprotected acrylate as major product (see scheme 1.7).³⁹



Scheme 1.7: HECK cross-coupling of a halogenated pyrrole.

³⁵(a) Motati D. R.; Uredi D.; Watkins E. B. *Chem. Sci.* **2018**, *9*, 1782–1785. (b) Gaspa S.; Carraro M.; Pisano L.; Porcheddu A.; De Luca L. *Eur. J. Org. Chem.* **2019**, *22*, 3544–3552. (c) Almeida L. S.; Esteves P. M.; de Mattos M. C. S. *Synthesis* **2006**, *2*, 221–223.

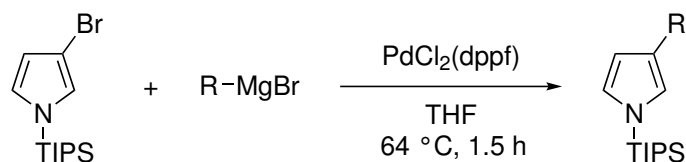
³⁶Carpino S. *J. Org. Chem.* **1965**, *30*, 736–739.

³⁷(a) Aiello E.; Dattolo G.; Cirrincione G.; Almerico A. M.; D'Asdia I. *J. Heterocyclic Chem.* **1982**, *19*, 977–979. (b) Gilow H. M.; Burton D. E. *J. Org. Chem.* **1981**, *46*, 2221–2225. (c) Dötz K.; Glänzer J. *Z. Naturforsch.* **1993**, *48b*, 1595–1602.

³⁸Banwell M. G.; Goodwin T. E.; Ng S.; Smith J. A.; Wong D. J. *Eur. J. Org. Chem.* **2006**, *14*, 3043–3060.

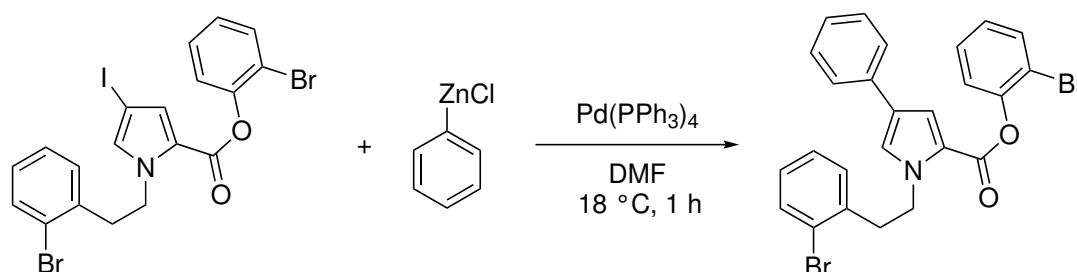
³⁹Demopoulos B. J.; Anderson H. J.; Loader C. E.; Faber K. *Can. J. Chem.* **1983**, *61*, 2415–2420.

Equally synthetically useful is the application of a KUMADA coupling where a *N*-TIPS-substituted pyrrole readily reacts with various GRIGNARD reagents under palladium catalysis furnishing 3-substituted pyrroles (see scheme 1.8).⁴⁰



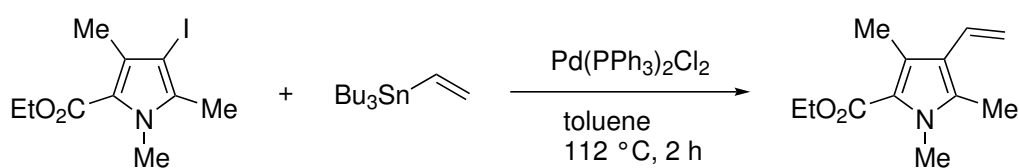
Scheme 1.8: KUMADA cross-coupling of a brominated pyrrole.

Unlike other coupling protocols, the NEGISHI cross-coupling is less common for pyrroles. A selected application in the synthesis of a Lamellarin (see figure 1.3) is shown in scheme 1.9.⁴¹



Scheme 1.9: NEGISHI cross-coupling of an iodinated pyrrole.

The first application of the STILLE-coupling in pyrrole chemistry was the Pd-catalyzed reaction of an iodinated pyrrole with tributylvinyltin to form important building blocks of bilirubins and biliverdins (see scheme 1.10).⁴²



Scheme 1.10: STILLE cross-coupling of an iodinated pyrrole.

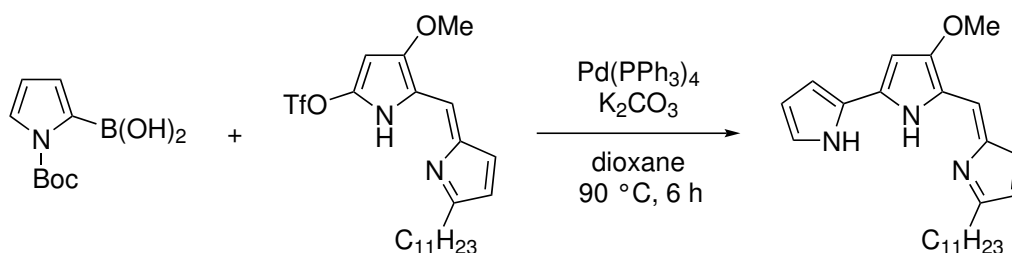
Among all established coupling protocols, the SUZUKI reaction is the best investigated one. An example where a *N*-Boc protected pyrrolyl boronic acid is coupled with a pyrrolyl triflate is shown in scheme 1.11.⁴³

⁴⁰Bray B. L.; Mathies P. H.; Naef R.; Solas D. R.; Tidwell T. T.; Artis D. R.; Muchowski J. M. *J. Org. Chem.* **1990**, *55*, 6317–6328.

⁴¹Banwell M. G.; Flynn B. L.; Hockless D. C. R.; Longmore R. W.; Rae A. D. *Aust. J. Chem.* **1999**, *52*, 755–766.

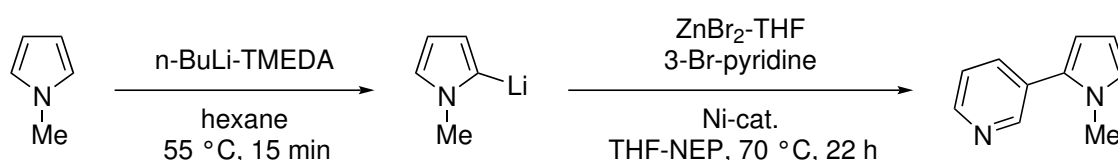
⁴²Wang J.; Scott A. I. *Tetrahedron Lett.* **1995**, *36*, 7043–7046.

⁴³D'Alessio R.; Rossi A. *Synlett* **1996**, *6*, 513–514.



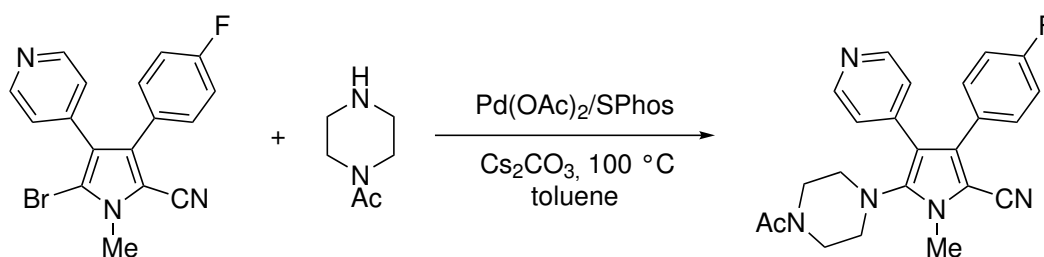
Scheme 1.11: Suzuki cross-coupling of a pyrrolyl triflate.

The synthetic value of pyrrole cross-couplings was demonstrated in the synthesis of β -nicotyrine: Direct *ortho*-lithiation of *N*-methylpyrrole followed by transmetalation with zinc bromide and nickel-catalyzed reaction with 3-bromopyridine led to the alkaloid metabolite of nicotine (see scheme 1.12).⁴⁴



Scheme 1.12: Synthesis of β -nicotyrine.

N-Arylation of halopyrroles, -pyrazoles, -imidazoles, and their benzo-fused analogues has long been a research interest. BULLINGTON and co-workers applied a BUCHWALD-HARTWIG type *N*-arylation in the synthesis of a kinase inhibitor *via* reacting a fully substituted pyrrole with acetylperazine (see scheme 1.13).⁴⁵



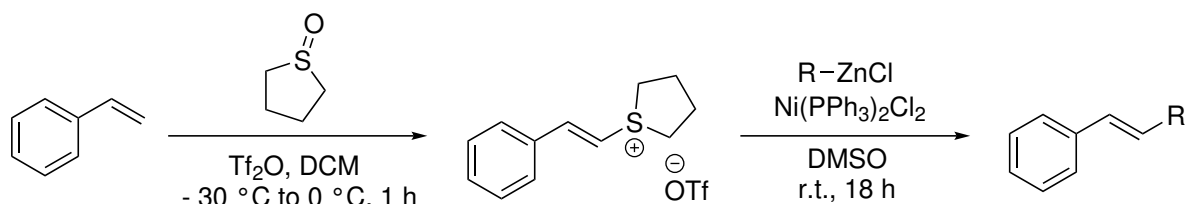
Scheme 1.13: *N*-Arylation of a pyrrole.

⁴⁴Gavryushin A.; Kofink C.; Manolikakes G.; Knochel P. *Org. Lett.* **2005**, *7*, 4871–4874.

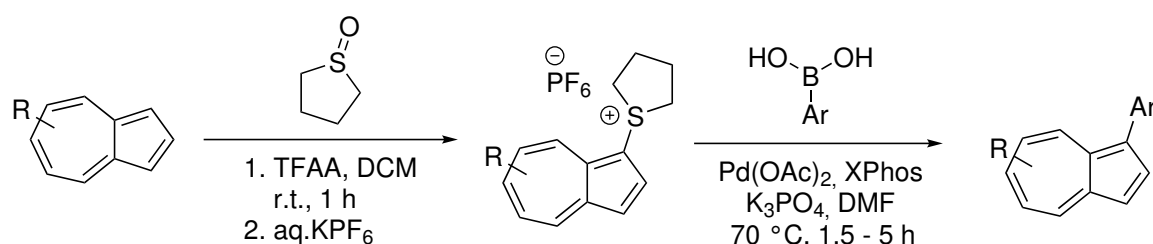
⁴⁵Bullington, J.; Argentieri, D.; Averill, K.; Carter, D.; Cavender, D.; Fahmy, B.; Fan, X.; Hall, D.; Heintzelman, G.; Jackson, P.; Leung, W.-P.; Li, X.; Ling, P.; Olini, G.; Razler, T.; Reuman, M.; Rupert, K.; Russell, R.; Siekierka, J.; Wadsworth, S.; Wolff, R.; Xiang, B.; Zhang, Y.-M. *Bioorg. Med. Chem. Lett.* **2006**, *16*, 6102–6106.

1.1.3 Sulfonium Salts as Electrophiles

Transition metal-catalyzed cross-coupling reactions undoubtedly represent an indispensable tool for the construction of carbon-carbon bonds. Traditionally, electrophilic coupling partners consist of halides or pseudo halides.⁴⁶ It was in 1997 when LIEBESKIND and co-workers published pioneering work using sulfonium salts as powerful and versatile electrophiles in cross-coupling reactions.⁴⁷ These salts show some inherent advantages compared to their oxygen analogues, sulfides and thioesters: facile oxidative addition, a neutral and less catalyst-poisoning sulfide as leaving group and being bench stable solids. After staying dormant for almost two decades the sulfur-mediated chemistry recently gained attraction (for a concise overview, see the cited reviews).⁴⁸ Precedent sulfonium salts consisted of either dialkyl or tetra methylene backbones. Examples are the interrupted PUMMERER/nickel-catalyzed cross-coupling of alkenyl sulfonium salts shown in scheme 1.14⁴⁹ or the Suzuki coupling of azulene sulfonium salts shown in scheme 1.15.⁵⁰



Scheme 1.14: Synthesis of alkenyl sulfonium salts and subsequent NEGISHI coupling.



Scheme 1.15: Synthesis of azulene sulfonium salts and subsequent SUZUKI coupling.

Later on, tetrafluorothianthrenium and dibenzothiophenium sulfonium salts were established, these synthetic linchpins enable site-selective C–H functionalizations and C–N

⁴⁶(a) de Meijere, A.; Diederich, F. In *Metal-Catalyzed Cross-Coupling Reactions*, 2nd Ed.; Wiley-VCH: Weinheim, **2004**. (b) Nishihara, Y. In *Applied Cross-Coupling Reactions*; 1st Ed.; Springer: Heidelberg, **2013**. (c) Hassan, J.; Sévignon, M.; Gozzi, C.; Schulz, E.; Lemaire, M. *Chem. Rev.* **2002**, *102*, 1359–1470. (d) Suzuki, A. *Angew. Chem. Int. Ed.* **2011**, *50*, 6722–6737.

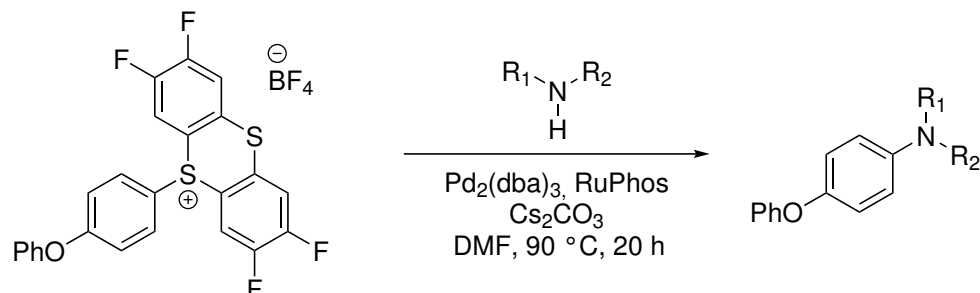
⁴⁷(a) Srogl, J.; Allred, G. D.; Liebeskind, L. S. *J. Am. Chem. Soc.* **1997**, *119*, 12376–12377. (b) Zhang, S.; Marshall, D.; Liebeskind, L. S. *J. Org. Chem.* **1999**, *64*, 2796–2804.

⁴⁸(a) Yorimitsu H. *Chem. Rec.* **2021**, *21*, 3356–3369. (b) Fan R.; Tan C.; Liu Y.; Wei Y.; Zhao X.; Liu X.; Tan J.; Yoshida H. *Chinese Chem. Lett.* **2021**, *32*, 299–312. (c) Kaiser D.; Klose I.; Oost R.; Neuhaus J.; Maulide N. *Chem. Rev.* **2019**, *119*, 8701–8780. (d) Kozhushkov S. I.; Alcarazo M. *Eur. J. Inorg. Chem.* **2020**, *26*, 24860–24871.

⁴⁹Aukland M. H.; Talbot F. J. T.; Fernández-Salas J. A.; Ball M.; Pulis A. P.; Procter D. J. *Angew. Chem. Int. Ed.* **2018**, *57*, 9785–9789.

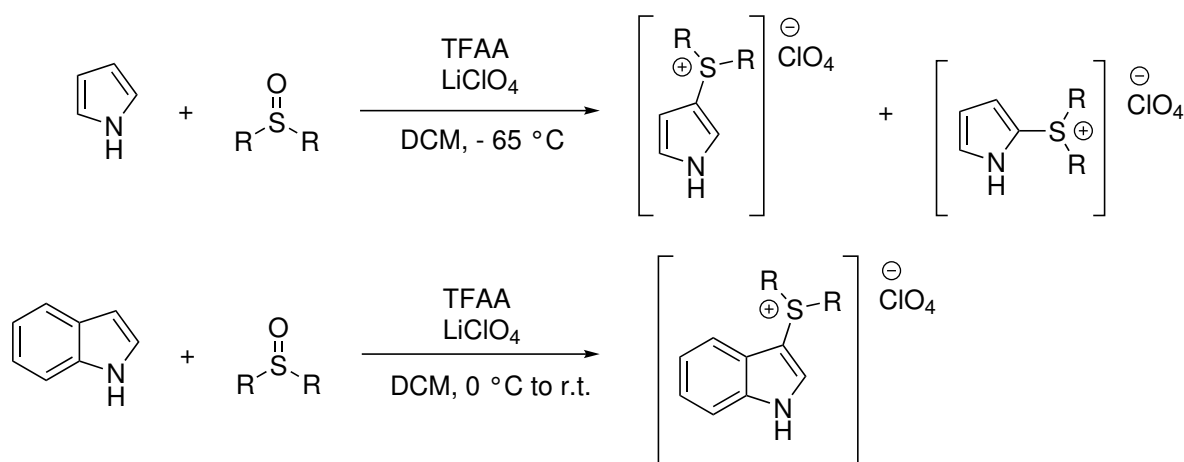
⁵⁰Cowper P.; Jin Y.; Turton M. D.; Kociok-Köhn G.; Lewis S. E. *Angew. Chem. Int. Ed.* **2016**, *55*, 2564–2568.

cross-couplings.⁵¹ An example for a C–N coupling is shown in scheme 1.16. This sort of reaction is made available for primary and secondary amines as well as aryl amines, amides, carbamates, ureas and even azoles, imides, pyridones and azides, for each substrate type with slightly modified procedures.



Scheme 1.16: C–N coupling of tetrafluorothiantrene sulfonium salts.

First syntheses of pyrrole and indole sulfonium salts were reported in the 1980s.⁵² At that time, the primary goal was the synthesis and elaboration of chemical and physical properties. The synthesis was achieved by allowing to react the unprotected *N*-heterocycles with activated sulfoxides like dimethyl sulfoxide or tetramethylene sulfoxide and trifluoroacetic anhydride (TFAA) in DCM at temperatures ranging from – 65 °C to room temperature.



Scheme 1.17: Synthesis of pyrrolyl and indolyl sulfonium salts. R = Me, (CH₂)₄

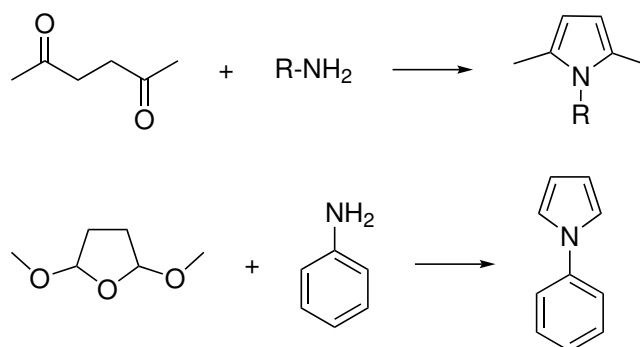
As expected, pyrrole gives a mixture of the 2- and 3-isomer due to its high reactivity. There is no literature-known application of these salts, despite a lack of easily accessible pyrrole electrophiles. Thus, interconnecting pyrroles with sulfonium activation is an appealing concept to investigate in order to get easier access to the corresponding coupling chemistry.

⁵¹(a) Berger F.; Plutschack M. B.; Riegger J.; Yu W.; Speicher S.; Ho M.; Frank N.; Ritter T. *Nature* **2019**, *567*, 223–228. (b) Engl P. S.; Häring A. P.; Berger F.; Berger G.; Pérez-Bitrián A.; Ritter T. *J. Am. Chem. Soc.* **2019**, *141*, 13346–13351. (c) Ye F.; Berger F.; Jia H.; Ford J.; Wortman A.; Börgel J.; Genicot C.; Ritter T. *Angew. Chem. Int. Ed.* **2019**, *58*, 14615–14761.

⁵²(a) Park K.; Daves G. D. *J. Org. Chem.* **1980**, *45*, 780–785. (b) Hartke K.; Tauber D.; Gerber H. *Tetrahedron* **1988**, *44*, 3261–3270. (c) Bellesia F.; Ghelfi F.; Grandi R.; Pagnoni U. M.; Pinetti A. *J. Heterocyclic Chem.* **1993**, *30*, 617–621.

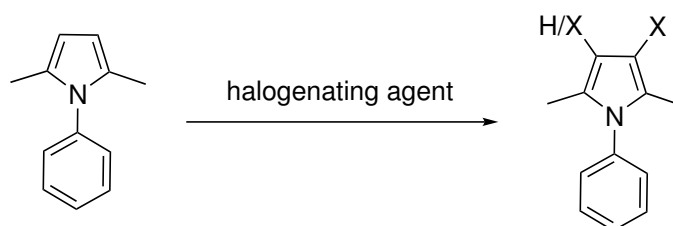
1.2. Aims and Objectives

As shown in chapter 1.1 the pyrrole ring is an important scaffold in organic chemistry. In the first part of this chapter in section 1.3.1 syntheses of various pyrroles by established methodologies are planned according to scheme 1.18.



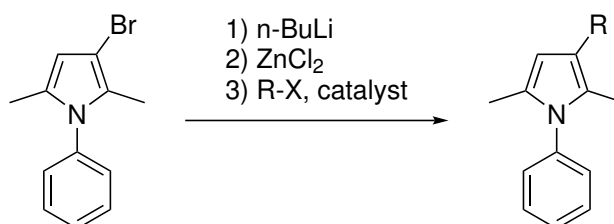
Scheme 1.18: Synthesis of pyrroles.

The prepared pyrroles are planned to undergo several halogenation reactions (see scheme 1.19, chlorination, bromination and iodination) in order to provide substrates for further coupling and arylation reactions.



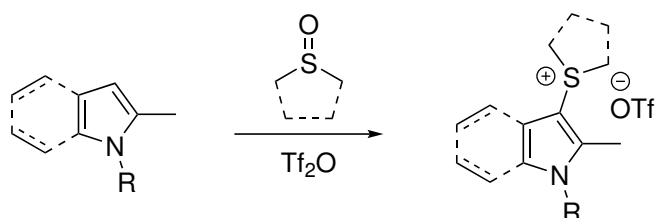
Scheme 1.19: Halogenation of pyrroles.

Generally, the coupling chemistry of pyrroles leaves room for improvements (see section 1.1.2.3). The current aims at developing complementary approaches to established methods rely on halides. The previously synthesized pyrrolyl substrates should easily undergo halogen-metal exchange, followed by *in situ* transmetalation with ZnCl₂ leading to the organozinc species. According to typical NEGISHI cross-coupling conditions the addition of an electrophile and a catalyst should furnish the coupling product.



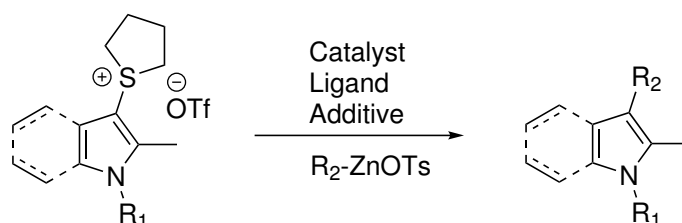
Scheme 1.20: Coupling reactions of pyrrolyl halides.

Halopyrroles, especially bromides, are labile compounds and inherently prone to decomposition or polymerization under air. We want to overcome this problem by synthesizing the corresponding sulfonium salts *via* a mild and selective methodology to make these difficult to activate substrates accessible for pyrrole cross-coupling (see scheme 1.21). Additionally, the same procedure will be applied to indoles.



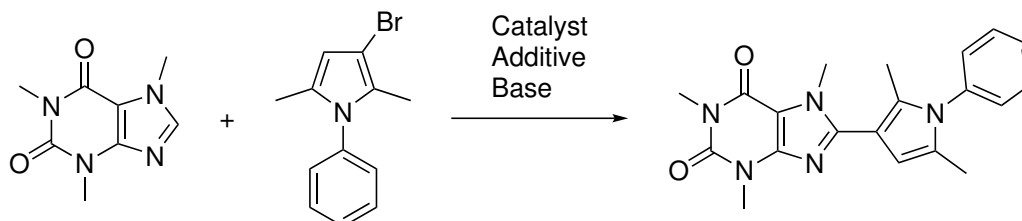
Scheme 1.21: Synthesis of azole sulfonium salts.

In the next step, the usefulness of the new sulfonium salts will be examined in NEGISHI cross-couplings. Since these reactions employ organozinc compounds, a combined application of two new "Umpolung" strategies will be demonstrated. An organozinc preparation out of aryl sulfonates (R_2 -ZnOTs) is chosen to further avoid the use of halides and provide a suitable nucleophile for the NEGISHI coupling reaction (see scheme 1.22).



Scheme 1.22: Coupling reactions of azole sulfonium salts.

Furthermore, an arylation reaction with caffeine as model C–H donor will be the subject of investigation to explore the use of pyrrolyl electrophiles in C–H arylation and cross-coupling reactions.

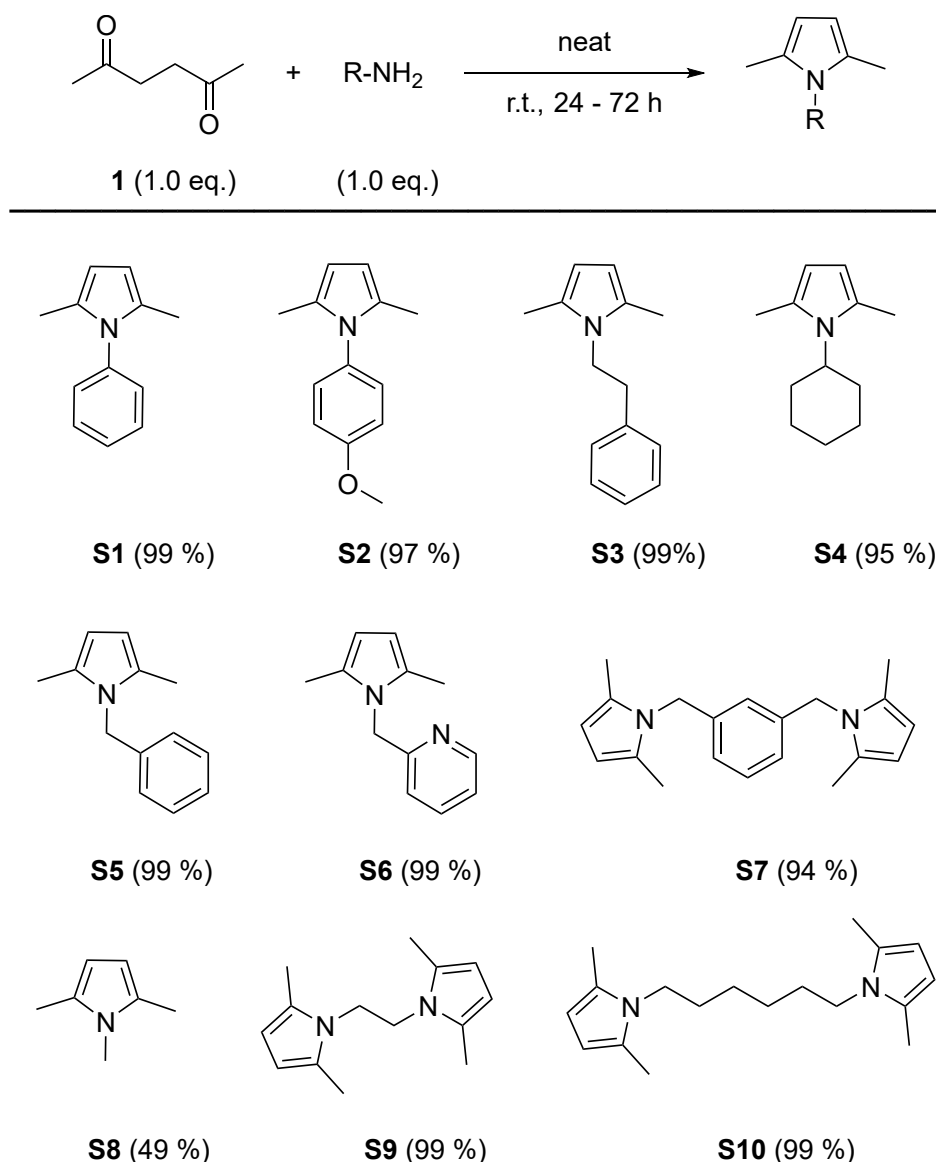


Scheme 1.23: C–H arylation reaction of caffeine with a pyrrolyl electrophile.

1.3. Results and Discussion

1.3.1 Syntheses of Pyrrole Precursors

At first, pyrroles were synthesized according to a procedure from TÖROK (see general procedure GP1.1 in subsection 4.2.1.1).⁵³ This version of the PAAL-KNORR reaction proceeds with respect to the conditions of green chemistry: no catalyst and solvent is required and simple stirring at room temperature yields the products in almost quantitative yields as shown in scheme 1.24.



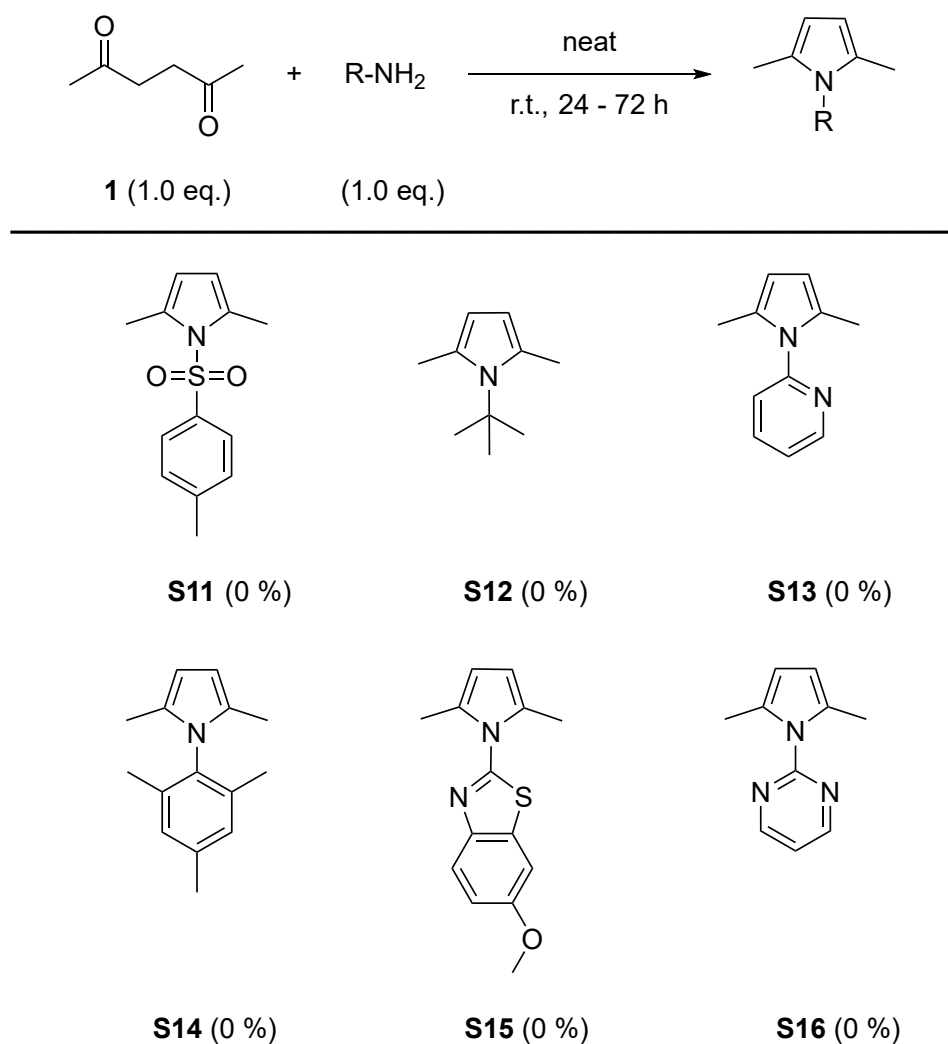
Scheme 1.24: Synthesis of various pyrrole derivatives from hexane-2,5-dione and the corresponding amine. Yields from isolated products.

The reaction of hexane-2,5-dione (**1**) with aniline yields 2,5-dimethyl-1-phenyl-1*H*-pyrrole (**S1**), the one with 4-methoxyaniline leads to 1-(4-methoxyphenyl)-2,5-dimethyl-1*H*-pyrrole

⁵³Cho H.; Madden R.; Nisanci B.; Török B. *Green Chem.* **2015**, *17*, 1088–1099.

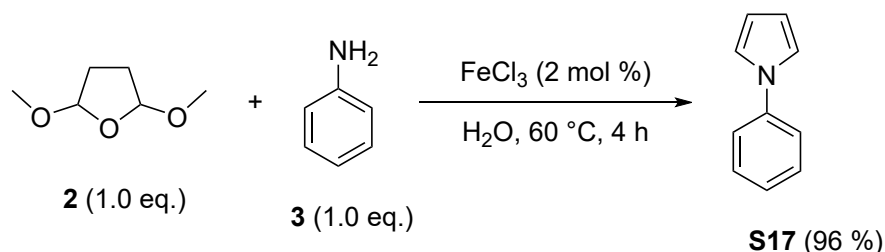
(**S2**), with 2-phenylethan-1-amine to 2,5-dimethyl-1-phenethyl-1*H*-pyrrole (**S3**), with cyclohexylamine to 1-cyclohexyl-2,5-dimethyl-1*H*-pyrrole (**S4**), with phenylmethanamine to 1-benzyl-2,5-dimethyl-1*H*-pyrrole (**S5**), with pyridin-2-ylmethanamine to 2-((2,5-dimethyl-1*H*-pyrrol-1-yl)methyl)pyridine (**S6**), with 1,3-phenylenedimethanamine to 1,3-bis((2,5-dimethyl-1*H*-pyrrol-1-yl)methyl)benzene (**S7**), with methylamine to 1,2,5-trimethyl-1*H*-pyrrole (**S8**) in diminished yield, with ethane-1,2-diamine to 1,2-bis(2,5-dimethyl-1*H*-pyrrol-1-yl)ethane (**S9**) and with hexane-1,6-diamine to 1,6-bis(2,5-dimethyl-1*H*-pyrrol-1-yl)hexane (**S10**).

Interestingly, this simple reaction protocol failed with some amines, as shown in scheme 1.25. Reactions with 4-methylbenzenesulfonamide (**S11**) and the bulkier tert-butylamine (**S12**) did not work. The latter and lower yield of trimethyl derivative **S8** indicate a reactivity problem with alkyl amines. Comparatively, electron-poor pyridin-2-amine (**S13**) and electron-rich 2,4,6-trimethylaniline (**S14**) furnished no pyrrole, and neither did the heterocyclic amines 6-methoxybenzo[*d*]thiazol-2-amine (**S15**) and pyrimidin-2-amine (**S16**).



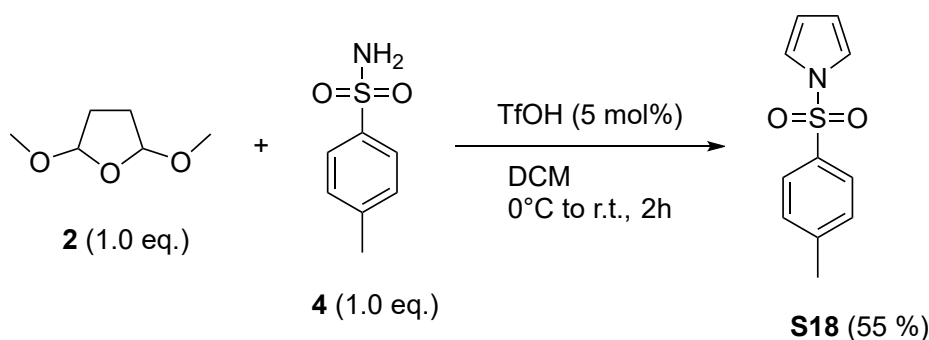
Scheme 1.25: Failed synthesis attempts of various pyrrole derivatives from hexane-2,5-dione and the corresponding amine.

The synthesis of pyrroles is also possible *via* a variation of the CLAUSON-KAAS reaction⁵⁴, a ring rearrangement reaction where an amine reacts with a 2,5-dialkoxytetrahydrofuran. In this case 2,5-dimethoxytetrahydrofuran (**2**) with aniline (**3**). Lewis acid-catalyzed (FeCl_3) ring opening led to attack of the primary amine to the carbocation. Elimination of methanol and subsequent ring closure delivered the unsubstituted pyrrole **S17** in almost quantitatively yield.



Scheme 1.26: Synthesis of 1-phenyl-1*H*-pyrrole **S17** *via* the CLAUSON-KAAS reaction.

Another variation of this reaction was applied in the synthesis of 1-tosyl-1*H*-pyrrole (**S18**).⁵⁵ Here, 2,5-dimethoxytetrahydrofuran (**2**) formed an *N*-tosylpyrrole with 4-methylbenzenesulfonamide (**4**) under acid catalysis with trifluoromethanesulfonic acid in 55 % yield. The lowered outcome may be explained by side reactions due to the acidic environment.



Scheme 1.27: Synthesis of 1-tosyl-1*H*-pyrrole **S18** *via* the CLAUSON-KAAS reaction.

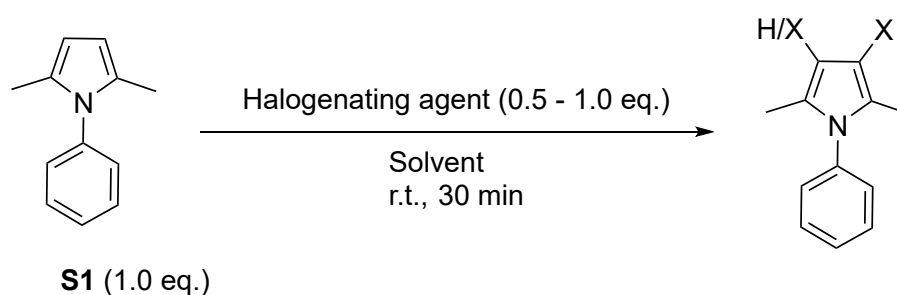
⁵⁴Azizi N.; Khajeh-Amiri A.; Ghafari H.; Bolourtchian M.; Saidib M. R. *Synlett* **2009**, 2245–2248.

⁵⁵Abid M.; Teixeira L.; Török B. *Tetrahedron Lett.* **2007**, *48*, 4047–4050.

1.3.2 Halogenations of Pyrroles

On route to establishing pyrroles in cross-coupling chemistry several halogenation strategies are available. As mentioned in chapter 1.1.2.2 various halogenating agents are commonly used and are part of a halogenation screening from pyrrol **S1**. Table 1.1 depicts the reaction setup where the pyrrole reacts at room temperature for 30 minutes with 1.0 equivalent of *N*-chlorosuccinimide (NCS) or *N*-bromosuccinimide (NBS)³⁷ and 0.5 equivalents of 1,3-dibromo-5,5-dimethylhydantoin (DBDMH)⁵⁶ in dichloromethane (DCM), dimethylformamide (DMF), acetonitrile (MeCN), tetrahydrofuran (THF) or trifluoroethanol⁵⁷ (TFE). The GC determined relative yields from integrated signals after 15 and 30 minutes are shown below.

Table 1.1: Screening of conditions for the halogenation of pyrroles. Relative yields are determined by GC-FID. S1 = substrate, X1 = monohalogenated, X2 = dihalogenated product.

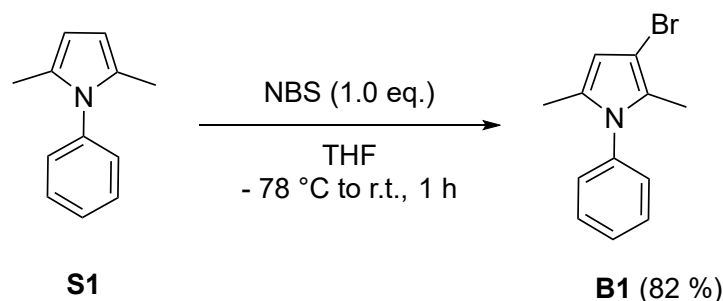


#	Reagent	Solvent	Yield [%] (15 min)			Yield [%] (30 min)		
			S1	X1	X2	S1	X1	X2
1	NCS	DCM	13	65	22	12	66	22
2	NCS	DMF	27	59	14	27	59	14
3	NCS	MeCN	0	99	1	0	99	1
4	NCS	THF	25	64	11	24	65	11
5	NCS	TFE	0	99	1	0	99	1
6	NBS	DCM	41	38	21	41	38	21
7	NBS	DMF	55	22	23	55	21	24
8	NBS	MeCN	48	14	38	48	13	39
9	NBS	THF	48	30	22	31	64	5
10	NBS	TFE	69	24	7	63	30	7
11	DBDMH	DCM	52	11	37	52	11	37
12	DBDMH	MeCN	23	69	8	22	69	9

⁵⁶Gao S.; Bethel T. K.; Kakeshpour T.; Hubbell G. E.; Jackson J. E.; Tepe J. J. *J. Org. Chem.* **2018**, *83*, 9250–9255.

⁵⁷Tang R.-J.; Milcent T.; Crousse B. *J. Org. Chem.* **2018**, *83*, 930–938.

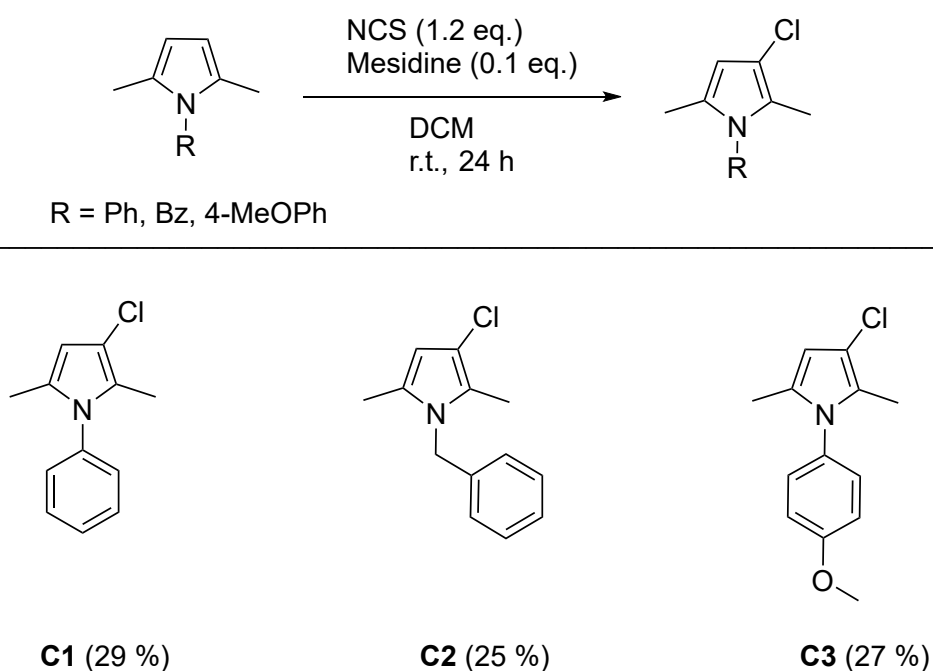
Due to the highly reactive substrate and conducting the halogenations at room temperature all reactions proceed rapidly and are not selective. In most cases there is no difference in conversion from 15 to 30 minutes. In entry 1 to 5 the yields from chlorination with *N*-chlorosuccinimide are shown. Reactions in DCM, DMF and THF show comparable, moderate yields from 59 % to 66 %, but in acetonitrile and trifluoroethanol the reaction shows an almost full conversion of 99 %. Bromination with *N*-bromosuccinimide (entry 6 to 10) delivers lower yields for the monobromination and sufficient yield is only reached with THF as a solvent (64 %). Interestingly, a mixture of substrate, mono- and dibromination is found for the other solvents and also with 1,3-dibromo-5,5-dimethylhydantoin in DCM (entry 11). Entry 12 is the best regarding monobromination. Due to economic reasons NBS in THF was chosen as ideal condition. To decrease the reactivity and avoid a mixture of bromination products the temperature for scale-up reactions was lowered to $-78\text{ }^{\circ}\text{C}$ as depicted in scheme 1.28.³⁷



Scheme 1.28: Bromination of pyrrole **S1**.

On a 20 mmol scale the monobrominated 3-bromo-2,5-dimethyl-1-phenyl-1*H*-pyrrole (**B1**) was isolated as a pale yellow resin in even higher yield (82 %). This may be because of the low temperature which allows a more controlled reaction and suppresses dibromination. The product **B1** has to be handled very carefully due to rapid decomposition under air and ambient temperatures. Due to its good accessibility and satisfactory reactivity it was used as substrate for further coupling reactions.

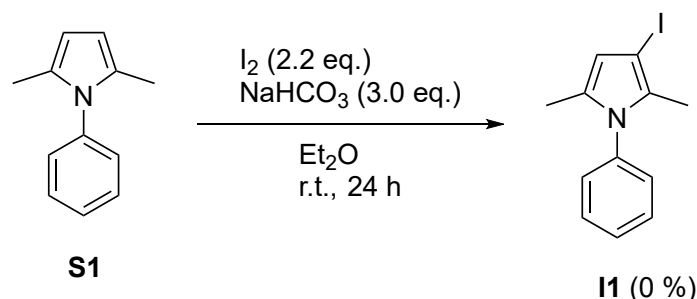
Another protocol relies on electrophilic halogenation with *N*-chlorosuccinimide, in particular with mesidine (2,4,6-trimethylaniline) as catalyst in DCM (see general procedure 1.4 in chapter 4.2.1.4). Three example substrates (3-chloro-2,5-dimethyl-1-phenyl-1*H*-pyrrole (**C1**), 1-benzyl-3-chloro-2,5-dimethyl-1*H*-pyrrole (**C2**) and 3-chloro-1-(4-methoxyphenyl)-2,5-dimethyl-1*H*-pyrrole (**C3**)) were synthesized and isolated in low yield as shown in scheme 1.29.⁵⁸ Surprisingly, the yields of this literature known protocol differ from the results in table 1.1.



Scheme 1.29: Chlorination reactions of various pyrroles. Yields are for isolated products.

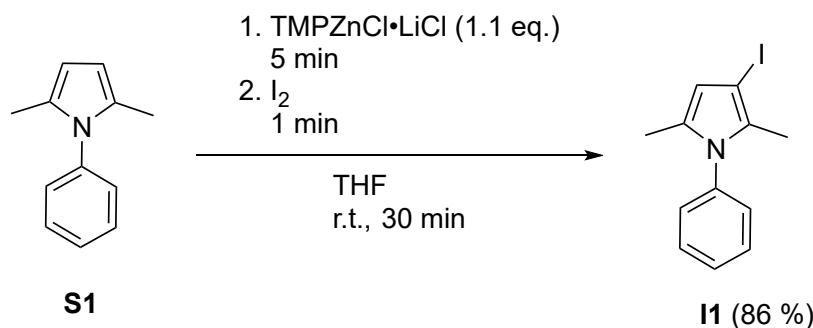
⁵⁸Samanta R. C.; Yamamoto H. *Chem. Eur. J.* **2015**, *21*, 11976–11979.

Following the chlorination and bromination, iodination reactions were investigated. A straightforward procedure for the iodination of pyrrole **S1** adapted from HE et al.⁵⁹, where also a 1,2,5-substituted pyrrole is iodinated, uses elemental iodine and the weak base sodium hydrogencarbonate in diethyl ether at room temperature as pictured in scheme 1.30. However, no product could be detected by GCMS and ¹H-NMR analysis.



Scheme 1.30: Iodination of pyrrole **S1**.

Consequently, a more sophisticated pathway was elaborated: A directed C–H metalation of pyrrole **S1** via the strong amide base TMPZnCl · LiCl was successful and delivered 3-iodo-2,5-dimethyl-1-phenyl-1*H*-pyrrole **I1** in 86 % yield (determined by GC analysis) after reaction with elemental iodine. The amide base was synthesized according to a literature procedure where 2,2,6,6-tetramethylpiperidine is lithiated with *n*-BuLi and transmetalated with ZnCl₂ (see chapter 4.1.4.2).⁶⁰ The concept of strong amide bases is further illustrated in chapter 2.1.1.4.



Scheme 1.31: Iodination of pyrrole **S1** *via* initial metalation. Yield determined by GC analysis.

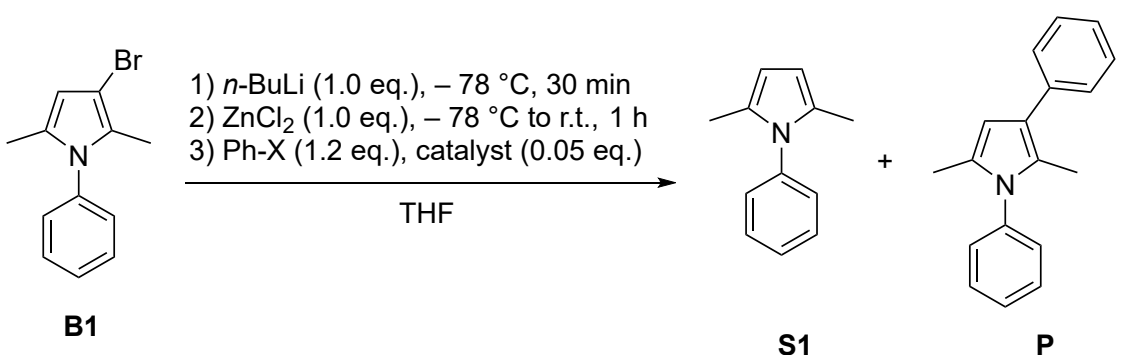
⁵⁹He, R.; Zeng, L.-F.; He, Y.; Wu, L.; Michelle Gunawan, A.; Zhang, Z.-Y. *Chem. Commun.* **2013**, *49*, 2064–2066.

⁶⁰Mosrin, M.; Bresser, T.; Knochel, P. *Org. Lett.* **2009**, *11*, 3406–3409.

1.3.3 Negishi Cross-Couplings of Metalated Pyrrolyl Halides

One of the most common procedures in coupling chemistry is the NEGISHI cross-coupling. The following procedure starts with a halogen-metal exchange reaction of the previously synthesized bromopyrrole **B1** with *n*-butyl lithium at $-78\text{ }^{\circ}\text{C}$ for 30 minutes. Subsequently, a ZnCl_2 -solution (see chapter 4.1.4.1) was added for transmetalation to zinc.) Finally, an electrophile (bromo- or iodobenzene) and a catalyst were added at the indicated temperature for the indicated time (see table 1.2).

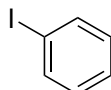
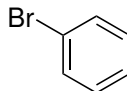
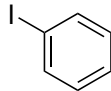
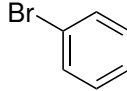
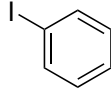
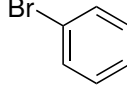
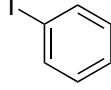
Table 1.2: Negishi cross-coupling reactions of pyrrole **B1** *via* lithiation and transmetalation with phenyl halides.



B1 1) *n*-BuLi (1.0 eq.), $-78\text{ }^{\circ}\text{C}$, 30 min
2) ZnCl_2 (1.0 eq.), $-78\text{ }^{\circ}\text{C}$ to r.t., 1 h
3) Ph-X (1.2 eq.), catalyst (0.05 eq.)

THF

S1 + **P**

#	Ph-X	Catalyst	T [$^{\circ}\text{C}$]	t [h]	B1 [%]	S1 [%]	P [%] ^{a)}
1		$\text{Pd}(\text{PPh}_3)_4$	r.t.	3	11	13	49
2		$\text{Pd}(\text{PPh}_3)_4$	50	2	9	60	15
3		$\text{Pd}(\text{PPh}_3)_4$	50	2	5	20	54
4		$\text{Pd}(\text{PPh}_3)_4$	70	20	1	28	46
5		$\text{Pd}(\text{PPh}_3)_4$	70	20	0	27	42
6		PEPPSI-IPr	r.t.	2	1	34	43
7		PEPPSI-IPr	r.t.	2	2	29	59

a) Yields in mol% were determined by qNMR-analysis. Reaction time and temperature refer to step 3.

Entry 1 in table 1.2 shows the first reaction with iodobenzene as electrophile and tetrakis-(triphenylphosphine)palladium as catalyst at room temperature. The outcome was sufficient for the first attempt with 49 % product **P**. The unusually high amount of **B1** indicates that insufficient amounts of *n*-BuLi had been used. The presence of **S1** indicates that either moisture found its way into the reaction mixture, for example *via* the ZnCl₂-solution, and hence *in situ* hydrolysis of the organometallic species or hydrolysis during the workup occurred due to a low conversion. Entries 2 and 3 were conducted at elevated temperatures: At 50 °C the less reactive bromide shows diminished yield and a high amount of hydrolysis product. The iodide shows a comparable yield. Increasing the temperature to 70 °C and prolonging the reaction time to 20 hours provides more product in case of the bromide (entry 4), but no improvement for the iodide (entry 5). By switching the catalyst to the PEPPSI-IPr Pd-NHC system (entries 6 and 7), satisfactory yields could be accomplished, even for the less reactive bromide.

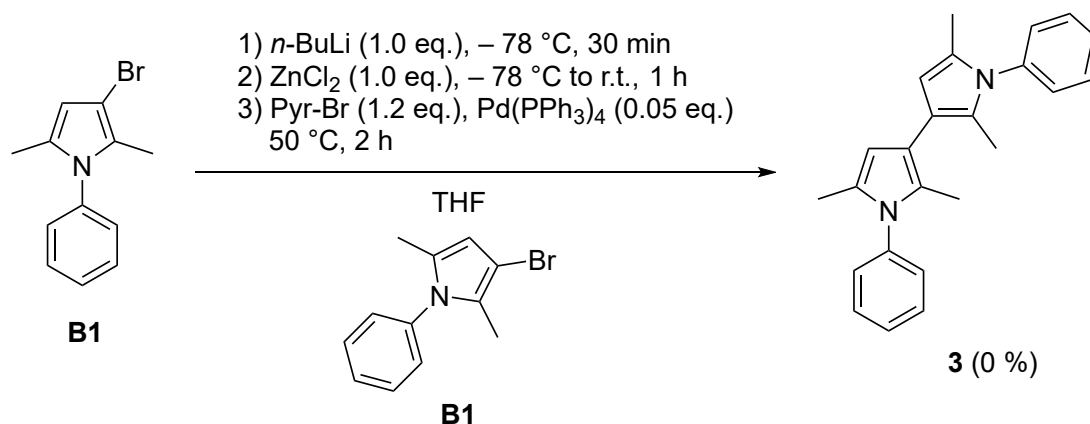
The reaction was further investigated with the PEPPSI-IPr catalyst using the same preparation protocol for the zinc species from pyrrole **B1** by halogen-metal exchange and subsequent transmetalation and the coupling reaction was performed at room temperature for 3 hours (see table 1.3). Entry 1 shows an improvement of yield for simple electrophile bromobenzene to 77 %. Further expanding the scope of this reaction with bromobenzonitrile (entry 2), bromopyridine (entry 3) and bromoanisole (entry 4) as electrophiles led to remarkable high yields ranging from 75 % to 79 %. As expected, entry 5 with a bromoaldehyde delivers the product in low yield. Presumably, side reactions occur because even hydrolysis product **S1** is not formed in noteworthy amounts. In entry 6 with bromoadamantane product **P** is only found in traces, but large amounts of **S1** were determined. In summary, this protocol delivers pyrrole coupling products starting from bromopyrrole **B1** *via* the Negishi coupling in mixed yields, strongly dependent on the substrates.

Table 1.3: Negishi cross-coupling reactions of pyrrole **B1** *via* lithiation and transmetalation, with selected aryl and alkyl halides.

#	R-Br	B1 [%]	S1 [%]	P [%] ^{a)}
1		2	11	77
2		1	9	79
3		3	14	78
4		4	11	75
5		2	5	22
6		4	78	2

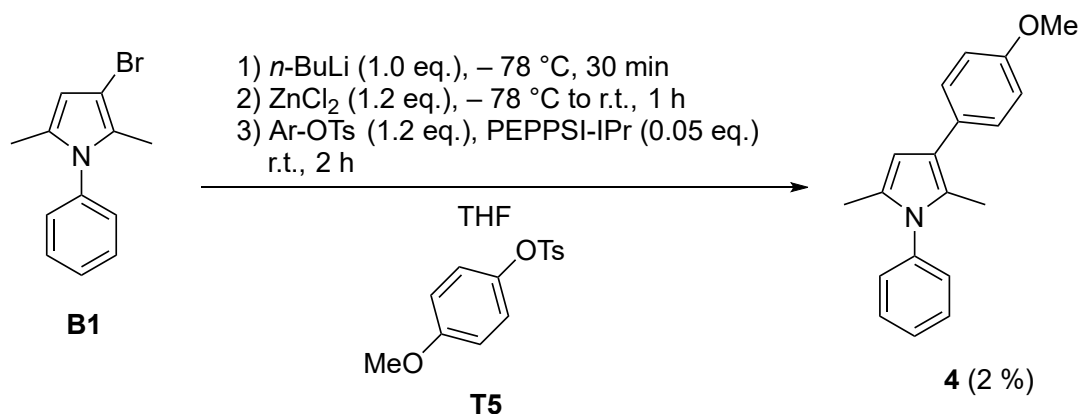
a) Yields in mol% were determined by qNMR-analysis.

The same reaction protocol but with another equivalent of brominated pyrrole **B1** instead of an aryl bromide led to no formation of coupling product 2,2',5,5'-tetramethyl-1,1'-diphenyl-1*H*,1'*H*-3,3'-bipyrrole (**3**).



Scheme 1.32: Attempted NEGISHI cross-coupling reaction of pyrrole **B1** *via* lithiation and transmetalation with pyrrole **B1**. Analytical yield was determined by qNMR-analysis.

Another coupling attempt with aryl tosylate **T5** as an alternative electrophile led to product 3-(4-methoxyphenyl)-2,5-dimethyl-1-phenyl-1*H*-pyrrole (**4**) only in traces.

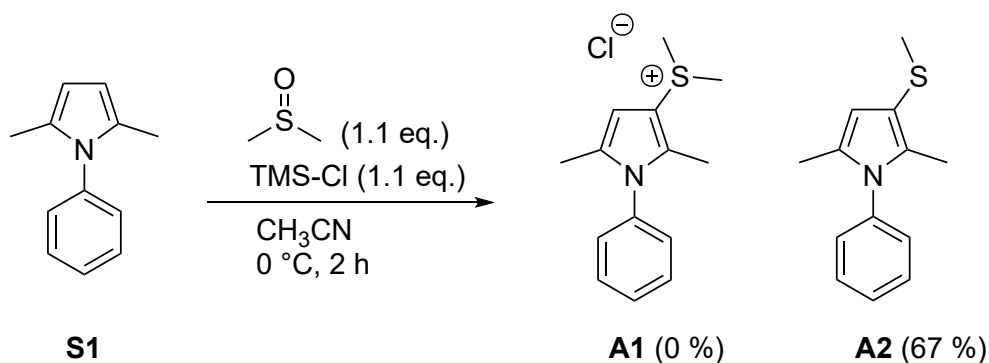


Scheme 1.33: Negishi cross-coupling reaction of pyrrole **B1** *via* lithiation and transmetalation with aryl tosylate **T5**. Analytical yield was determined by qNMR-analysis.

1.3.4 C–H Arylation of Pyrroles with Arylzinc Sulfonates *via* Sulfonium Activation

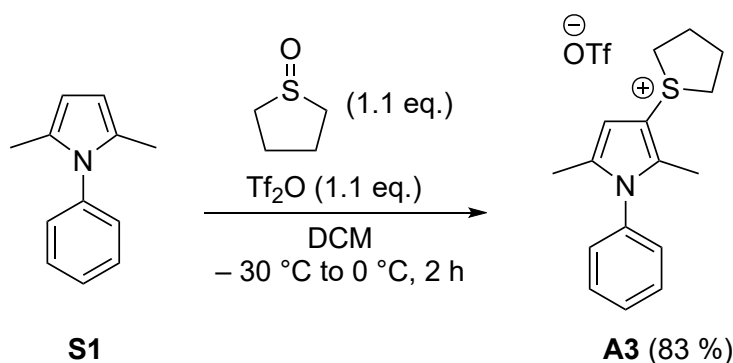
1.3.4.1 Synthesis of Pyrrole and Indole Sulfonium Salts

As discussed in chapter 1.1.3 the synthesis of sulfonium salts as powerful and versatile electrophiles in cross-coupling reactions may be applied to pyrroles and indoles.⁵² Whereas sulfonium salts are conventionally prepared *via* the corresponding thiol or thioether,⁴⁸ herein we attempted an interrupted PUMMERER-type direct C–H activation of pyrroles (scheme 1.34). The previously mentioned sulfide leaving groups, tetrafluorothiantrene and dibenzothiophene, are sterically demanding and laborious to synthesize. For the sake of atom economy, we chose smaller and commercially cheaper sulfoxides as starting materials. A synthesis of pyrrole sulfonium salt **A1** via reaction of pyrrole **S1** with DMSO and TMS-Cl in CH₃CN at 0 °C was evaluated. This reagent combination failed and analysis of the isolated product mixture indicated that demethylation to the corresponding thioether **A2** had taken place.



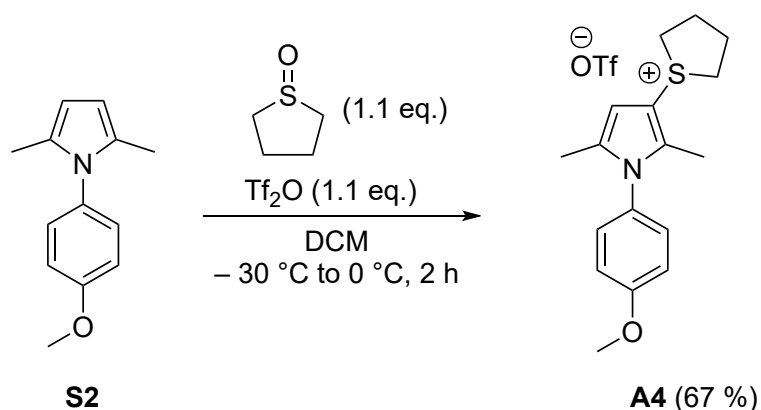
Scheme 1.34: Attempted synthesis of pyrrole sulfonium salt **A1**, returning thioether side product **A2**. Yields refer to isolated products.

Based on this result, another sulfoxide was identified as activated S-oxide precursor hoping to avoid this side reaction, namely tetrahydrothiophene 1-oxide.⁴⁹ Upon activation with the strong electrophile trifluoromethanesulfonic anhydride (Tf₂O) product pyrrole sulfonium salt **A3** was isolated in 83 % yield as an ochre, bench-stable solid (scheme 1.35).



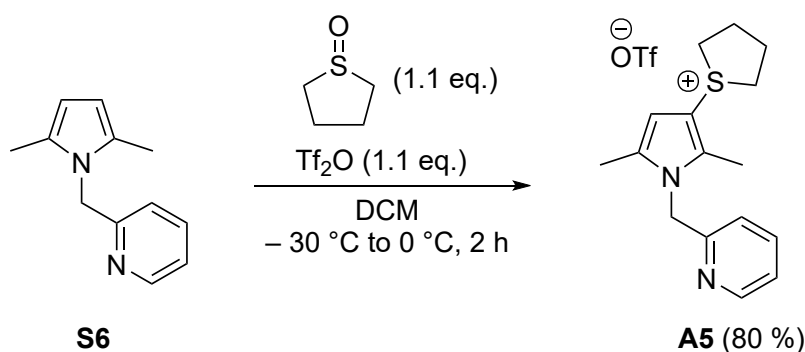
Scheme 1.35: Synthesis of pyrrole sulfonium salt **A3**. Yield refers to isolated product.

The same procedure was applied to pyrrole substrate **S2**. The anisole derivative **A4** was isolated in fair yield as an off-white solid (scheme 1.36).



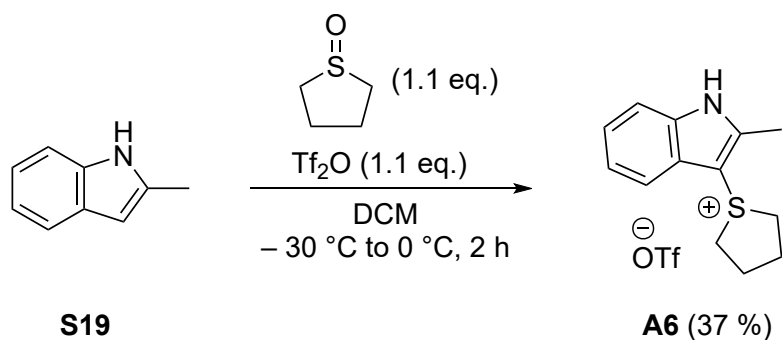
Scheme 1.36: Synthesis of pyrrole sulfonium salt **A4**. Yield refers to isolated product.

Another sulfonium salt **A5** was synthesized from *N*-heterobenzylic pyrrole **S6** using the same procedure in high yield as a red solid (scheme 1.37).



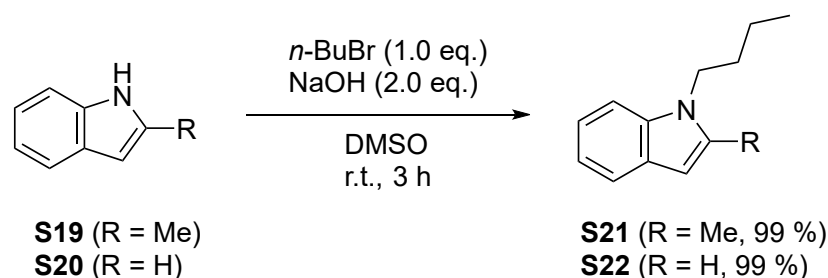
Scheme 1.37: Synthesis of pyrrole sulfonium salt **A5**. Yield refers to isolated product.

Applying this reaction to indole **S19** for formation of an indole sulfonium salt only led to a moderate yield of the corresponding product **A6**, most likely due to side reactions induced by the presence of the free N–H-group (scheme 1.38).



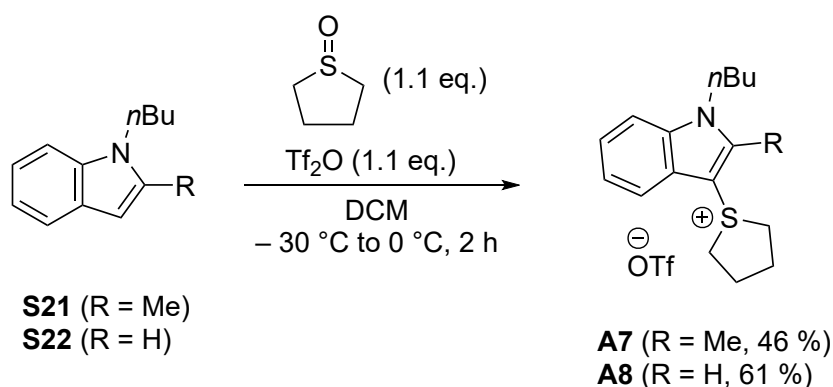
Scheme 1.38: Synthesis of indole sulfonium salt **A6**. Yield refers to isolated product.

This problem should be easily avoided by using *N*-substituted indoles. Simple *N*-alkylation of indoles **S19** and **S20** with *n*-butyl bromide in DMSO led to *N*-alkylated indoles **S21** and **S22** in near quantitative yields (see scheme 1.39).⁶¹



Scheme 1.39: Synthesis of *N*-butyl indoles **S21** and **S22**. Yields refer to isolated products.

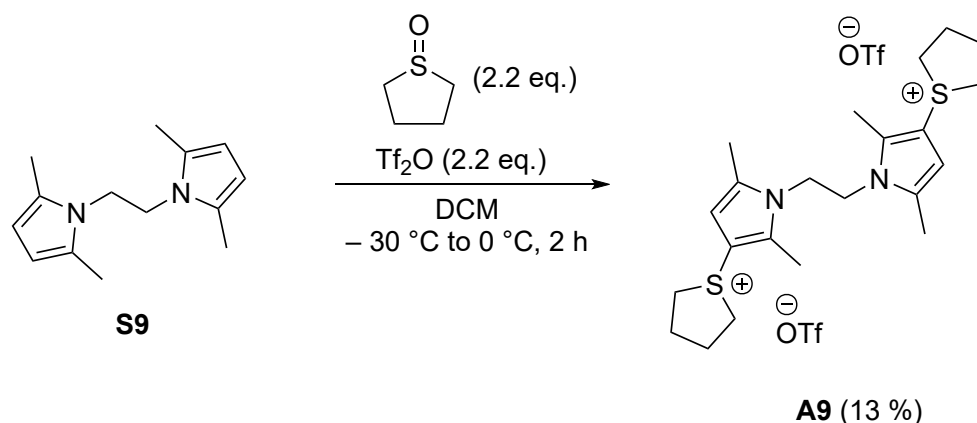
These substrates were now allowed to react with the previously used reactant combination tetrahydrothiophene 1-oxide and Tf_2O to give the new indole sulfonium salts **A7** and **A8** in 46 % and 61 % yield, respectively (scheme 1.40).



Scheme 1.40: Synthesis of *N*-butyl indole sulfonium salts **A7** and **A8**. Yields refer to isolated products.

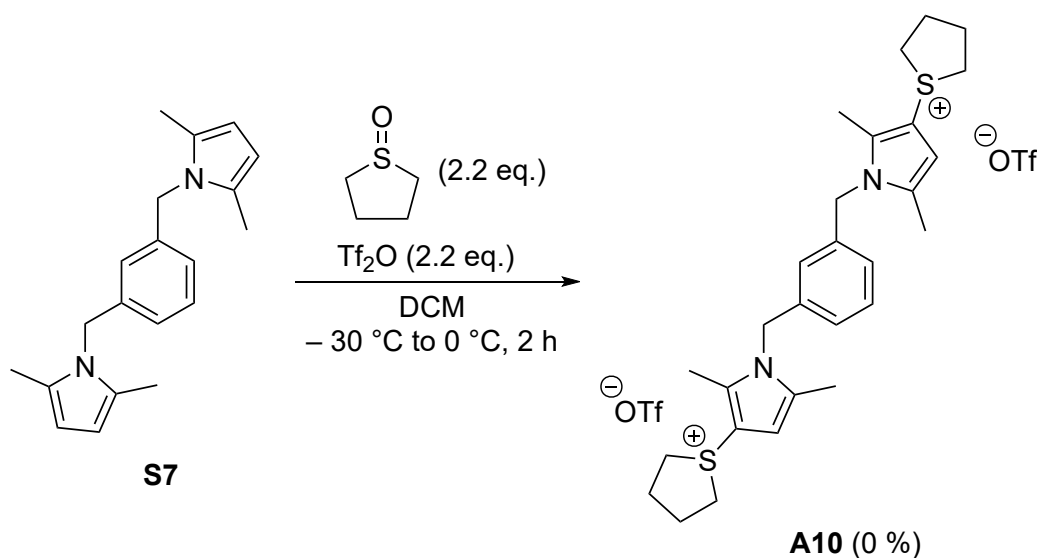
Further extending the available scope of sulfonium salts, the road led to the symmetric dipyrrole **S9** which yielded the corresponding bis-sulfonium salt in low yield as shown in scheme 1.41.

⁶¹Hong X.; Tan Q.; Liu B.; Xu B. *Angew. Chemie Int. Ed.* **2017**, *56*, 3961–3965.



Scheme 1.41: Synthesis of dipyrrole bis-sulfonium salt **A9**. Yield refers to isolated product.

Additionally, other *N*-heterocycles like pyrazole, imidazole and quinoline were submitted to the same conditions, but no sulfonium salt could be synthesized. The xylenyl-linked dipyrrole **S7** also did not afford the desired product (see scheme 1.42).



Scheme 1.42: Attempted synthesis of dipyrrole bis-sulfonium sulfonium salt **A10**.

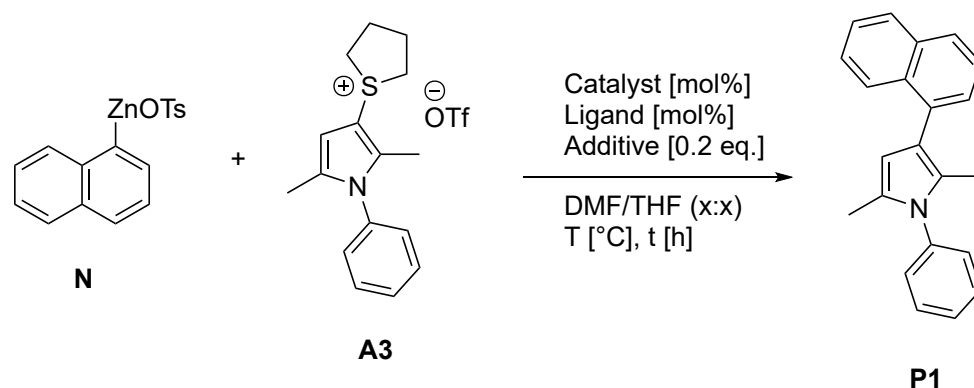
1.3.4.2 Screening of Reaction Conditions for Sulfonium Salt Cross-Coupling

With the successful synthesis of the above shown sulfonium salts, the road to a halogen-free NEGISHI-type cross-coupling reaction is now opened. The recently published catalytic zincation of aryl sulfonates from our group⁶² delivers the required nucleophilic coupling partner free from halides without the need of organometallic chemicals like *n*-BuLi and starting from aryl tosylates, which are among the most easily accessible derivatives of phenols and cheaper than their corresponding halides. The arylzinc sulfonates were synthesized from aryl tosylates, zinc dust and a nickel catalyst according to GP1.3 (see section 4.2.1.3). This catalytic metalation will be further discussed in chapter 2. Experimentally,

⁶²Klein, P.; Lechner, V. D.; Schimmel, T.; Hintermann, L. *Chem. - Eur. J.* **2019**, *26*, 176–180.

after completed zincation of the aryl tosylate, stirring was stopped, zinc dust settled, and the supernatant solution was transferred into a new Schlenk tube charged with the sulfonium salt, catalyst, ligand, additive, and co-solvent. The reaction was heated at the desired temperature. The detailed instructions are given in subsection 4.2.1.6 and 4.3.1.1. The conditions for the Negishi coupling with regard to the catalyst, solvent and temperature were tested. As model substrates the zincated 1-naphthyltosylate **N** was chosen in combination with pyrrole sulfonium salt **A3**.

Table 1.4: Screening of reaction conditions of the model NEGISHI coupling with Pd(OAc)₂ as precatalyst.



#	C ^{a)} (mol%)	L ^{a)} (mol%)	A ^{a)}	N eq.	Solv.	T[°C]	t[h]	P1[%] ^{b)}
1	Pd(OAc) ₂ (2)	SPhos (4)	-	1.3	1:0	r.t.	20	5
2	Pd(OAc) ₂ (2)	SPhos (4)	-	1.3	1:0	r.t.	20	37
3	Pd(OAc) ₂ (2)	SPhos (4)	-	1.3	1:0	r.t.	4	25
4	Pd(OAc) ₂ (4)	SPhos (8)	-	1.3	1:0	r.t.	4	15
5	Pd(OAc) ₂ (4)	XPhos (8)	-	1.3	1:0	r.t.	4	11
6	Pd(OAc) ₂ (4)	SPhos (8)	-	1.3	1:0	r.t.	20	13
7	Pd(OAc) ₂ (4)	SPhos (8)	-	1.3	1:0	60	20	14
8	Pd(OAc) ₂ (4)	SPhos (8)	-	1.3	1:1	r.t.	20	19
9	Pd(OAc) ₂ (4)	SPhos (8)	-	1.3	1:1	60	20	18
10	Pd(OAc) ₂ (4)	SPhos (8)	EtSH	1.3	1:0	r.t.	20	11
11	Pd(OAc) ₂ (4)	SPhos (8)	EtSH	1.3	1:1	r.t.	20	7
12	Pd(OAc) ₂ (2)	SPhos (4)	CySH	1.3	2:1	r.t.	40	13
13	Pd(OAc) ₂ (2)	SPhos (4)	-	2.0	1:0	r.t.	72	15
14	Pd(OAc) ₂ (10)	SPhos (20)	-	2.0	1:0	r.t.	20	63
15	Pd(OAc) ₂ (10)	SPhos (20)	-	2.0	1:1	r.t.	20	66

a) C = catalyst, L = ligand, A = additive. b) Yields in mol% were determined by qNMR-analysis.

The initial screening was conducted with a classic BUCHWALD catalyst system consisting of palladium(II) acetate and either ligand SPhos or XPhos. In entries 1 to 9 catalyst loadings range between 2 and 4 percent, and a slight excess of the nucleophile (1.3 eq.) was applied. Product **P1** was obtained in low yields and with mediocre reproducibility at room temperature. Reaction time varies between 4 and 20 hours, the temperature between room temperature (r.t.) and 60 °C. A finding from MINAMI *et al.* suggests that addition of various thiols to related desulfurative coupling reactions promotes C–S cleavage of the sulfonium salt.⁶³ Unfortunately, this additive effect was not observed in the present reaction by using either ethylthiol (ethyl mercaptan, entry 10 and 11) or cyclohexanethiol (entry 12). Further increasing the excess of the organozinc species to 2.0 equivalents was only successful with simultaneously higher catalyst loadings (10 mol%) as shown in entries 13 to 15. With those results in mind different catalysts were tested in order to lower the catalyst loading and find a more reactive combination.

⁶³Minami, H.; Nogi, K.; Yorimitsu, H. *Synlett* **2021**, 32, 1542–1546.

A new class of cross-coupling catalysts incorporating NHC ligands was discovered by the groups of HERRMANN⁶⁴, BELLER⁶⁵ and NOLAN.⁶⁶ These *N*-heterocyclic carbenes (NHC) offer unique properties and were enhanced by ORGAN⁶⁷ et al. by the introduction of PEPPSI (pyridine-enhanced precatalyst preparation, stabilization and initiation) precatalysts. These air-stable, easy to handle metal complexes proved their activity in cross-coupling reactions. Different palladium cross-coupling catalysts are shown in figure 1.6.

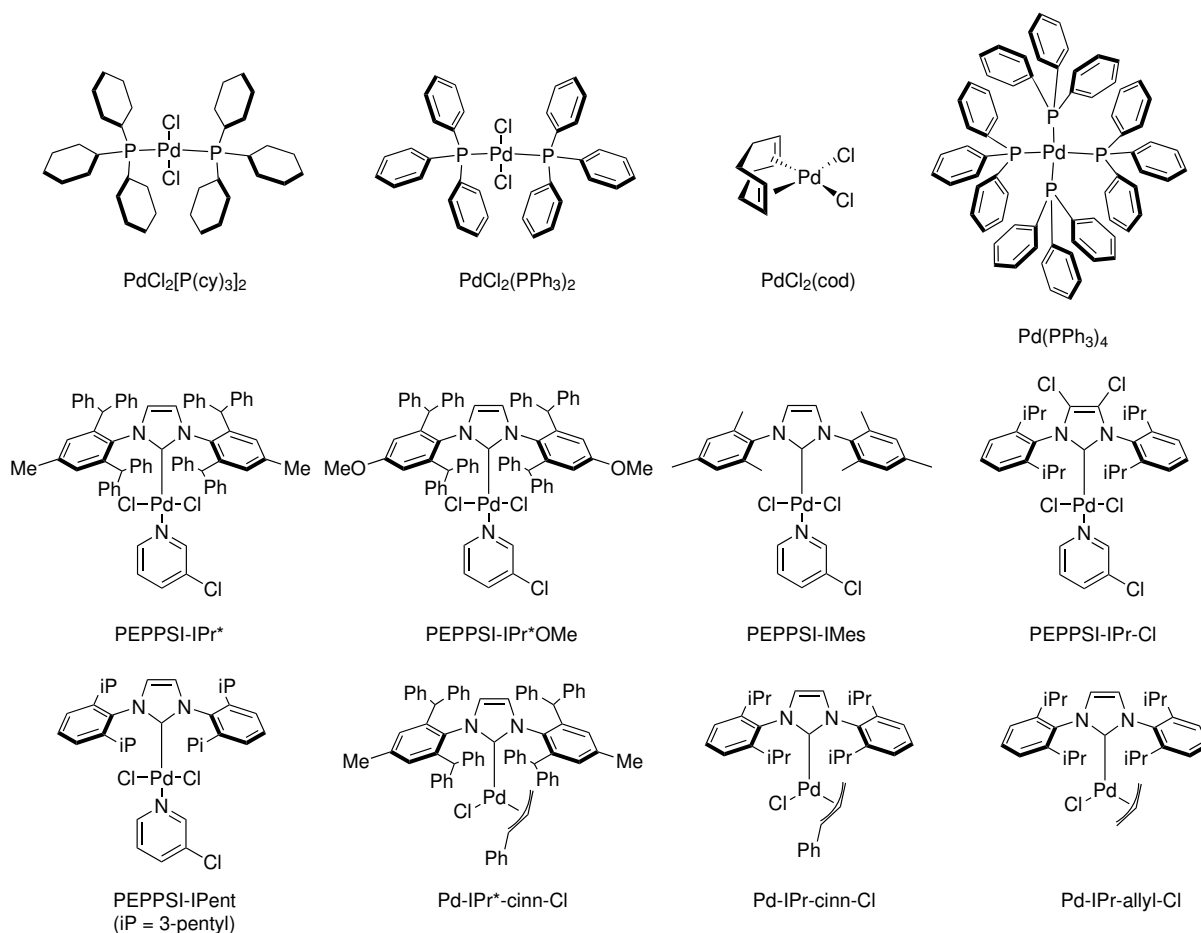


Figure 1.6: Palladium catalysts screened for reaction optimization.

The upper row shows established standard catalysts like $\text{PdCl}_2(\text{PPh}_3)_2$ or $\text{Pd}(\text{PPh}_3)_2$. The middle and lower row describe alternative PEPPSI catalyst systems such as PEPPSI-

⁶⁴(a) Herrmann, W. A.; Elison, M.; Fischer, J.; Köcher, C.; Artus, G. R. J. *Angew. Chem. Int. Ed.* **1995**, *34*, 2371–2374. (b) Herrmann, W. A.; Goossen, L. J.; Köcher, C.; Artus, G. R. J. *Angew. Chem. Int. Ed.* **1996**, *35*, 2805–2807. (c) Herrmann, W. A.; Köcher, C. *Angew. Chem. Int. Ed.* **1997**, *36*, 2162–2187.

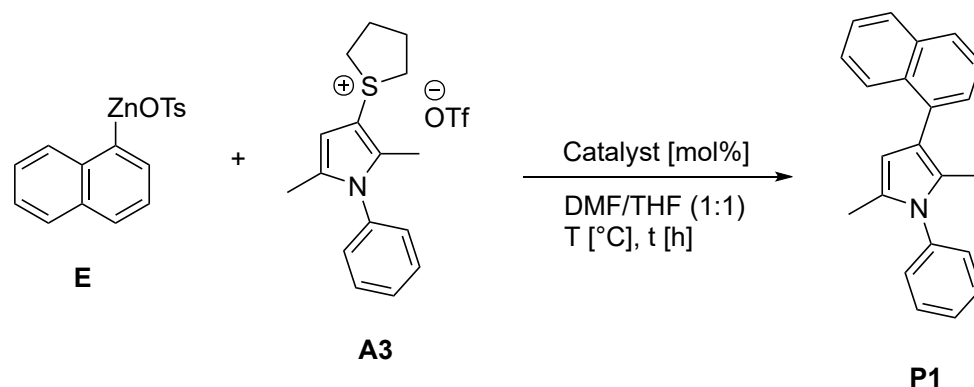
⁶⁵Selvakumar, K.; Zapf, A.; Beller, M. *Org. Lett.* **2002**, *4*, 3031–3033.

⁶⁶(a) Meiries, S.; Chartoire, A.; Slawin, A. M. Z.; Nolan, S. P. *Organometallics* **2012**, *8*, 3402–3409. (b) Meiries, S.; Speck, K.; Cordes, D. B.; Slawin, A. M. Z.; Nolan, S. P. *Organometallics* **2013**, *1*, 330–339.

⁶⁷(a) O'Brien, C. J.; Kantchev, E. A. B.; Valente, C.; Hadei, N.; Chass, G. A.; Lough, A.; Hopkinson, A. C.; Organ, M. G. *Chem. Eur. J.* **2006**, *12*, 4743–4748. (b) Organ, M. G.; Avola, S.; Dubovyk, I.; Hadei, N.; Kantchev, E. A. B.; O'Brien, C. J.; Valente, C. A. *Chem. Eur. J.* **2006**, *12*, 4749–4755. (c) Valente, C.; Belowich, M. E.; Hadei, N.; Organ, M. G. *Eur. J. Org. Chem.* **2010**, *23*, 4343–4354.

IPent⁶⁸, Pd(IPr*)(cinnamyl)Cl and Pd-IPr*-Cinn-Cl.⁶⁹ or Pd-IPr-Cinn-Cl⁷⁰ Table 1.5 shows results of the screening of different catalysts. In entries 1 to 3 the typical palladium sources deliver the product only in traces, even at elevated temperatures (60 °C, entry 4). Switching to the PEPPSI-IPr* catalyst in entry 5 the yield is still low. The different variations of the PEPPSI system and IPr ligands deliver low yields around 30 % as shown in entries 6 to 12, only the IPent and IPr-Allyl variant show higher yields.

Table 1.5: Screening of reaction conditions of sulfonium salt NEGISHI coupling with palladium catalysts.



#	Catalyst (mol%)	E eq. ^{a)}	Solv. rat.	T[°C]	t[h]	P1[%] ^{b)}
1	PdCl ₂ [P(cy) ₃] ₂ (5)	2.0	1:1	r.t.	20	1
2	PdCl ₂ (PPh ₃) ₂ (5)	2.0	1:1	r.t.	20	2
3	PdCl ₂ (cod) (5)	2.0	1:1	r.t.	20	1
4	Pd(PPh ₃) ₄ (2)	2.0	1:1	60	20	4
5	PEPPSI-IPr* (2)	2.0	1:1	60	20	5
6	PEPPSI-IPr*OMe (2)	2.0	1:1	60	20	26
7	PEPPSI-IMes (2)	2.0	1:1	60	20	28
8	PEPPSI-IPr-Cl (2)	2.0	1:1	60	20	32
9	PEPPSI-IPent (2)	2.0	1:1	60	20	83
10	Pd-IPr*-Cinn-Cl (2)	2.0	1:1	60	20	3
11	Pd-IPr-Cinn-Cl (2)	2.0	1:1	60	20	25
12	Pd-IPr-Allyl (2)	2.0	1:1	60	20	82

a) eq. = equivalents. b) Yields in mol% were determined by qNMR-analysis.

⁶⁸Organ, M. G.; Çalimsiz, S.; Sayah, M.; Hoi, K. H.; Lough, A. J. *Angew. Chem. Int. Ed.* **2009**, *48*, 2383–2387.

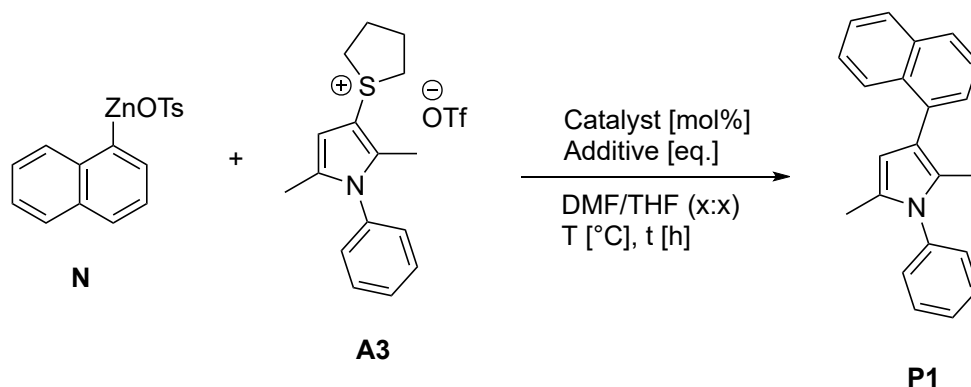
⁶⁹Chartoire, A.; Lesieur, M.; Falivene, L.; Slawin, A. M. Z.; Cavallo, L.; Cazin, C. S. J.; Nolan, S. P. *Chem. Eur. J.* **2012**, *18*, 4517–4521.

⁷⁰Chartoire, A.; Claver, C.; Corpet, M.; Krinsky, J.; Mayen, J.; Nelson, D.; Nolan, S. P.; Peñafiel, I.; Woodward, R.; Meadows, R. E. *Org. Process Res. Dev.* **2016**, *20*, 551–557.

One of the most commonly used and easy to synthesize PEPPSI catalysts is PEPPSI-IPr. Table 1.6 shows the optimization route for the coupling reaction with this catalyst.

The synthesis of this air and moisture stable Pd-NHC precatalyst was improved previously in our group. Originally, the suitable imidazolium salt IPr is heated with PdCl₂ and a huge excess of base such as K₂CO₃ (10.0 eq.) in the solvent 3-chloropyridine which simultaneously functions as co-ligand.⁶⁷ The improved version works at room temperature and 40 °C, respectively, and with lesser amount of base (1.5 eq.) and only 2.5 equivalents of 3-chloropyridine in acetone as solvent (see section 4.1.4.3). Comparably, a less toxic and wasteful procedure was established.⁷¹

Table 1.6: Screening of reaction conditions of sulfonium salt NEGISHI coupling with PEPPSI-IPr catalyst.



#	Catalyst (mol%)	Add. (eq.) ^{a)}	N eq. ^{a)}	Solv. rat.	T[°C]	t[h]	P1[%] ^{b)}
1	PEPPSI-IPr (2)	CySH (0.4)	2.0	1:1	r.t.	72	13
2	PEPPSI-IPr (2)	-	1.3	1:0	r.t.	4	23
3	PEPPSI-IPr (2)	CySH (0.2)	1.3	2:1	r.t.	40	39
4	PEPPSI-IPr (2)	-	2.0	1:1	r.t.	4	47
5	PEPPSI-IPr (2)	CySH (0.2)	2.0	1:1	r.t.	72	51
6	PEPPSI-IPr (5)	-	2.0	1:0	r.t.	20	77
7	PEPPSI-IPr (10)	CySH (0.2)	2.0	1:1	r.t.	20	78
8	PEPPSI-IPr (5)	-	2.0	1:1	r.t.	20	81
9	PEPPSI-IPr (10)	-	2.0	1:0	r.t.	20	82
10	PEPPSI-IPr (2)	-	2.0	1:1	r.t.	20	88

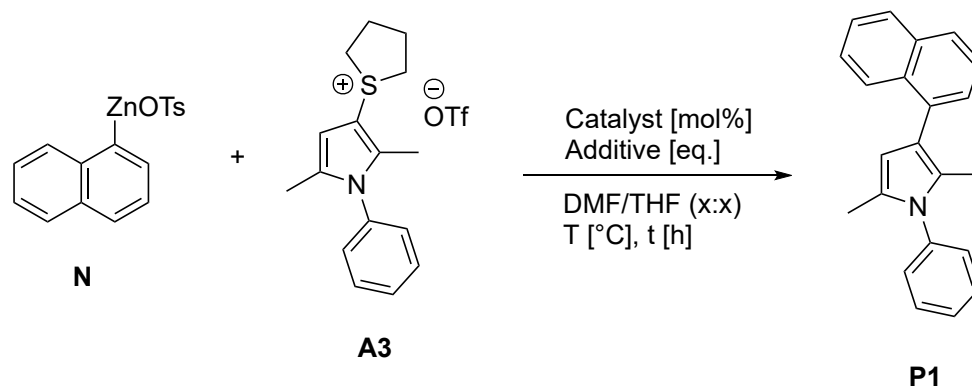
a) eq. = equivalents, N = nucleophile. b) Yields in mol% were determined by qNMR-analysis.

⁷¹Klein, Philippe (2020). The Multifunctional Component Catalyst Principle (MFCCP): Design of Functional Catalyst Precursors for Systematic Reaction Development [Doctoral dissertation]. Technische Universität München.

In entries 1, 3, 5 and 7 the use of cyclohexanethiol as promoting additive is evaluated again, but no significant yield increase compared to its absence was achieved.⁶³ Notably, at higher catalyst loading (entry 7, 10 mol%) an analytical yield of 78 % was reached. Entry 2 shows that even with 2 % of PEPPSI-IPr, a slight excess of nucleophile **N** (1.3 eq.), ambient temperature and a short reaction time of 4 h the product **P1** was delivered at 23 %. Increasing the amount of organozinc species to 2.0 equivalents doubled the yield to 47 % in entry 4 and adding more catalyst (5 mol%) as well as prolonging the reaction time to 20 h yields 77 % (entry 6). Addition of the co-solvent tetrahydrofuran (THF) proved to be slightly beneficial comparing entries 6 and 8. Further confirmation of this condition is delivered by comparing entries 9 and 10: They show almost the same amount of product, but the first requires 10 mol% of PEPPSI-IPr, whereas the second uses the 1:1 mixture of dimethylformamide (DMF) and THF.

Table 1.7 further shows the optimization route for the coupling reaction with this catalyst. Entries 1 to 4 evaluate a very low catalyst loading of 1 mol%. Even then, a notable product synthesis takes place helped by increased temperatures up to 60 °C. In entries 5 to 8 higher reaction temperatures (60 and 80 °C) at different reaction times (2 and 20 h) were tested, but no sufficing distinction was detected. Small differences in this high yield range may be due to measuring inaccuracy. Entries 9 and 10 display the highest yield of this screening table but for the sake of atom economy no catalyst loading in this range was chosen. For extending the scope of reaction and hence utilizing different aryl tosylates the reaction time was prolonged to 20 h to assure complete conversion. Therefore, conditions in entry 7 with a low palladium loading and a prolonged reaction time were chosen for subsequent experiments.

Table 1.7: Screening of reaction conditions of sulfonium salt NEGISHI coupling with PEPPSI-IPr catalyst.

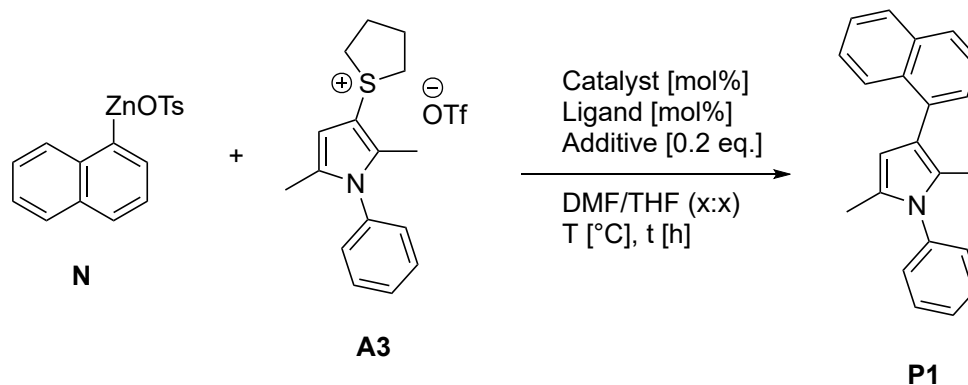


#	Cat. (mol%) ^{a)}	Add. (eq.) ^{a)}	N eq. ^{a)}	Solv. rat.	T[°C]	t[h]	P1[%] ^{b)}
1	PEPPSI-IPr (1)	-	2.0	1:2	r.t.	20	20
2	PEPPSI-IPr (1)	-	2.0	1:2	r.t.	20	21
3	PEPPSI-IPr (1)	-	2.0	1:1	40	20	75
4	PEPPSI-IPr (1)	-	2.0	1:1	60	20	78
5	PEPPSI-IPr (2)	-	2.0	1:1	60	20	88
6	PEPPSI-IPr (2)	-	2.0	1:1	80	20	89
7	PEPPSI-IPr (2)	-	2.0	1:1	60	2	92
8	PEPPSI-IPr (2)	-	2.0	1:1	80	2	93
9	PEPPSI-IPr (10)	-	2.0	1:1	r.t.	20	94
10	PEPPSI-IPr (10)	-	2.0	1:1	r.t.	20	95

a) Cat. = catalyst, eq. = equivalents, N = nucleophile. b) Yields in mol% were determined by qNMR-analysis.

Several common nickel catalysts were also investigated. Unfortunately, the NEGISHI reaction with sulfonium electrophiles seems to be incompatible with any chosen condition and catalyst as shown in table 1.8.

Table 1.8: Screening of reaction conditions of NEGISHI coupling with nickel catalysts.



#	Cat. (mol%) ^{a)}	Add. (eq.) ^{a)}	N eq. ^{a)}	Solv. rat.	T[°C]	t[h]	P1[%] ^{b)}
1	Ni(PPh ₃) ₂ Cl ₂ (10)	-	2.0	1:1	r.t.	20	0
2	Ni(PPh ₃) ₂ Cl ₂ (10)	CySH (0.2)	1.3	2:1	r.t.	20	0
3	Ni(PPh ₃) ₂ Cl ₂ (5)	-	1.3	1:0	r.t.	20	0
4	NiCl ₂ (bpy) (10)	-	1.3	1:0	r.t.	20	0
5	NiCl ₂ (bpy) (10)	-	1.3	1:0	r.t.	20	0
6	NiCl ₂ (bpy) (10)	CySH (0.2)	1.3	2:1	r.t.	20	0
7	Ni(PCy ₃) ₂ Cl ₂ (10)	-	1.3	1:1	r.t.	20	0
8	Ni(PCy ₃) ₂ Cl ₂ (2)	-	2.0	1:0	r.t.	20	0
9	NiCl ₂ (dme) (10)	CySH (0.2)	1.3	2:1	r.t.	20	0

a) Cat. = catalyst, eq. = equivalents, N = nucleophile. b) Yields in mol% were determined by qNMR-analysis.

1.3.4.3 Overview of Aryl Sulfonate Pro-Nucleophiles

Figure 1.7 provides an overview of the aryl tosylates used as pro-nucleophiles *via* catalytic zincation in the following sections for the NEGISHI cross-coupling with pyrrole and indole sulfonium salts. If not mentioned otherwise, the corresponding aryl tosylates were previously synthesized in the working group and were available for the present project.

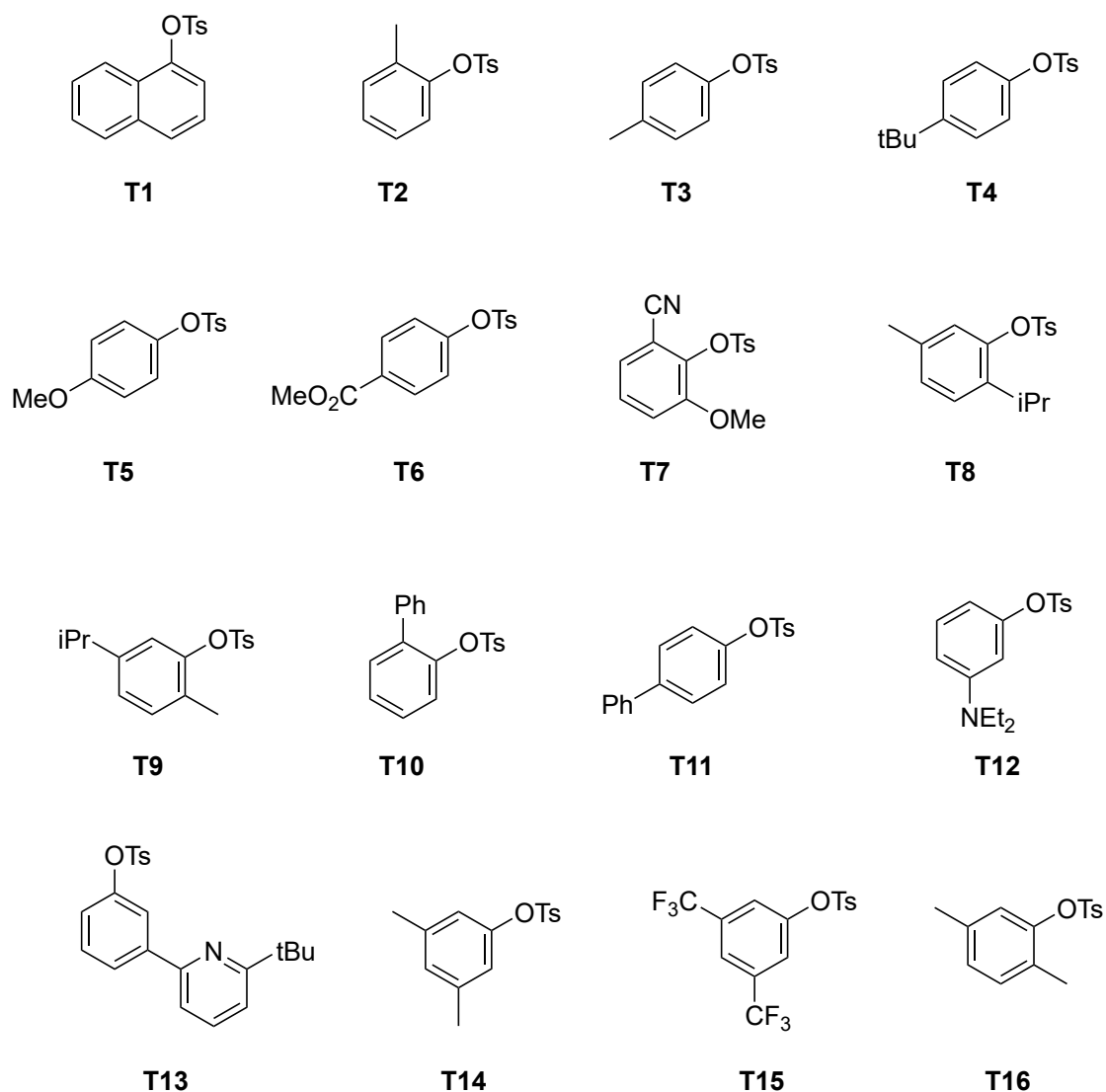
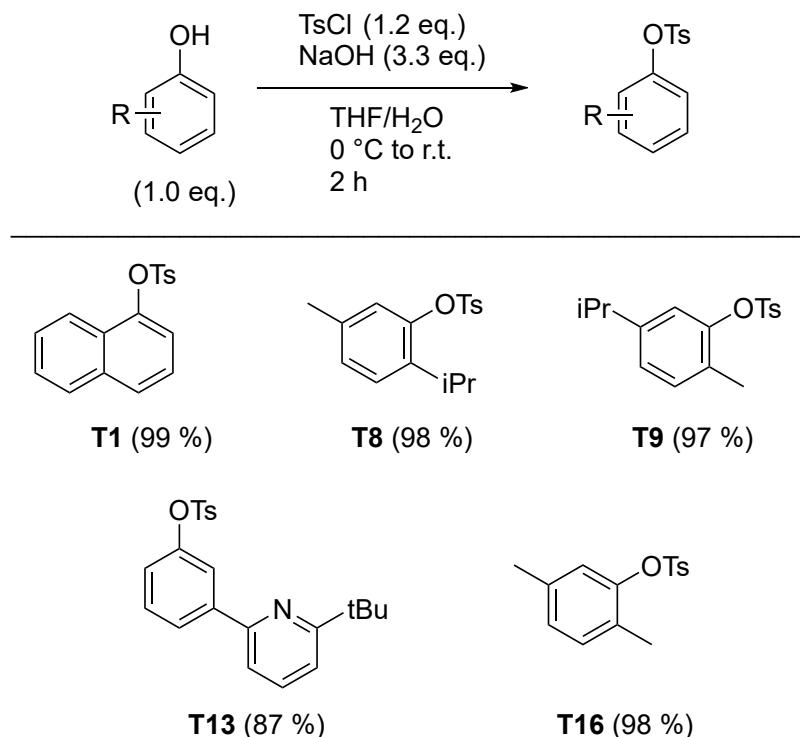


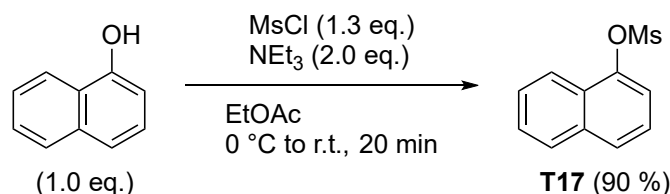
Figure 1.7: Overview of utilized aryl tosylates for NEGISHI cross-coupling.

Several aryl tosylates were synthesized according to a procedure of LEI,⁷² in which the sulfonation of hydroxyarenes takes place in an economically benign manner in a non-halogenated solvent mixture (THF/H₂O) with cheap bases like NaOH or K₂CO₃ and requires no chromatography for the isolation of the products. Conversely, prevailing methods include DCM as solvent and triethylamine or pyridine as base.⁷³ The screening substrate **T1** as well as thymol- (**T8**) and carvacrol-derived tosylates (**T9**), a pyridin-containing tosylate (**T13**) and the simple 2,5-dimethylsubstituted tosylate **T16** were all synthesized by the new procedure.



Scheme 1.43: Synthesis of aryl tosylates by the LEI procedure. Yields refer to isolated product.

To broaden the scope of applicable sulfonates as pro-nucleophiles additional substrates were synthesized and later tested in section 1.3.4.6. A simple substitution reaction of 1-naphthol with methanesulfonyl chloride under basic conditions delivers the mesylate **T17** in very high yield (90 %, see 1.44).⁷²

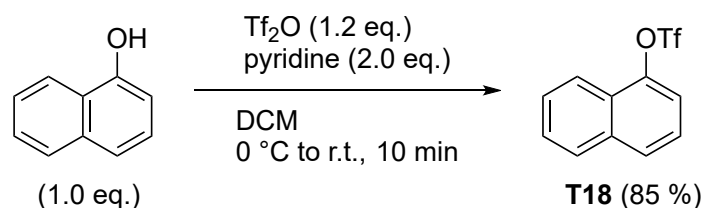


Scheme 1.44: Synthesis of naphthalene-1-yl methanesulfonate **T17**. Yield refers to isolated product.

⁷²Lei X.; Jalla A.; Shama M. A. A.; Stafford J. M.; Cao B. *Synthesis* **2015**, *47*, 2578–2585.

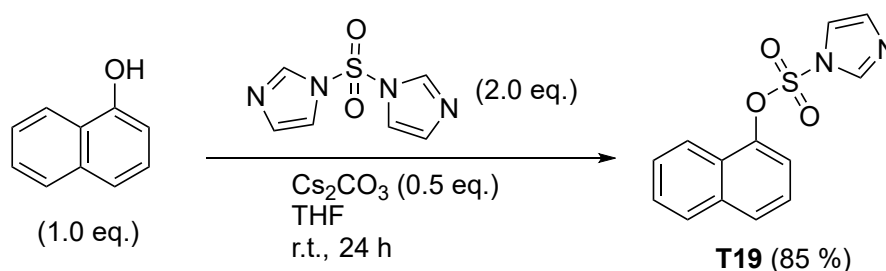
⁷³(a) Schade, M. A.; Metzger, A.; Hug, S.; Knochel, P. *Chem. Commun.* **2008**, *26*, 3046–3048. (b) Zim, D.; Lando, V. R.; Dupont, J.; Monteiro, A. L. *Org. Lett.* **2001**, *3*, 3049–3051. (c) Gooßen, L. J.; Rodríguez, N.; Lange, P. P.; Linder, C. *Angew. Chem.* **2010**, *122*, 1129–1132.

Triflate **T18** is obtained by reaction of 1-naphthol with trifluoromethanesulfonic anhydride and pyridine in DCM (85 %, see scheme 1.45).⁷⁴



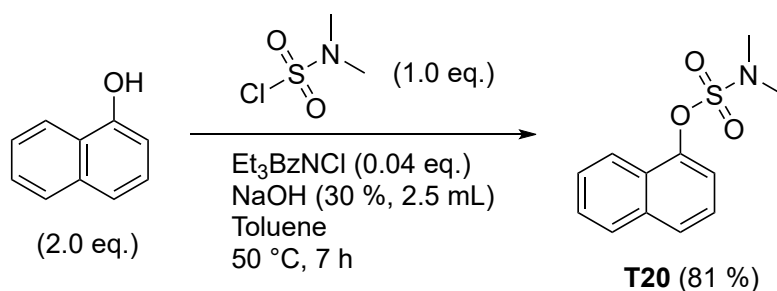
Scheme 1.45: Synthesis of naphthalene-1-yl trifluoromethanesulfonate **T18**. Yield refers to isolated product.

Aryl imidazolysulfonates have been introduced as electrophilic coupling partners in cross-coupling reactions.⁷⁵ They offer improved reactivity over aryl tosylates and improved stability and lower cost over aryl triflates. The synthesis of **T19** is conducted with a slight excess of reagent 1,1'-sulfonyldiimidazole with a substoichiometric amount of cesium carbonate in THF at room temperature as shown in scheme 1.46.



Scheme 1.46: Synthesis of naphthalene-1-yl 1*H*-imidazole-1-sulfonate **T19**. Yield refers to isolated product.

Another class of sulfur electrophiles are sulfamate esters. Substrate **T20** was synthesized *via* reaction with *N,N*-dimethylsulfamoyl chloride and benzyltriethylammonium chloride as catalyst in toluene at 50 °C for 7 h.⁷⁶



Scheme 1.47: Synthesis of naphthalene-1-yl dimethylsulfamate **T20**. Yield refers to isolated product.

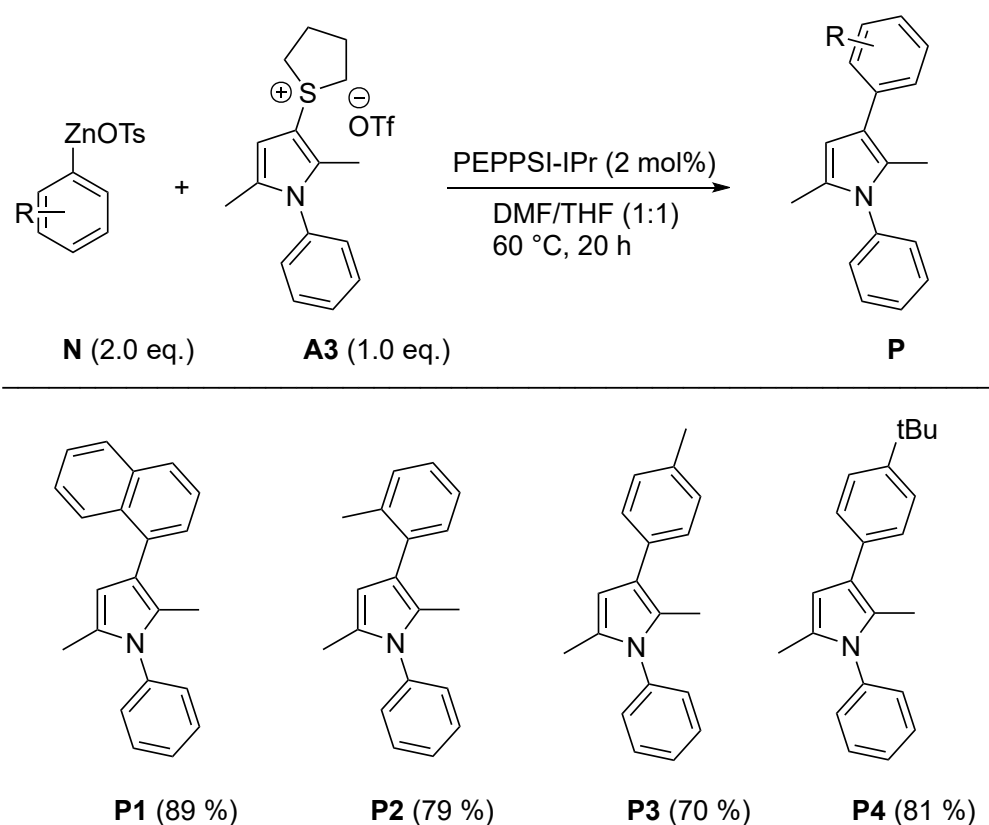
⁷⁴Thompson, A.; Kabalka, G.; Akula, M.; Huffman, J. *Synthesis* **2005**, 54–55.

⁷⁵Albaneze-Walker, J.; Raju, R.; Vance, J. A.; Goodman, A. J.; Reeder, M. R.; Liao, J.; Maust, M. T.; Irish, P. A.; Espino, P.; Andrews, D. R. *Org. Lett.* **2009**, *11*, 1463–1466.

⁷⁶Spillane, W. J.; Taheny, A. P.; Kearns, M. M. *J. Chem. Soc., Perkin Trans. 1* **1982**, 677–679.

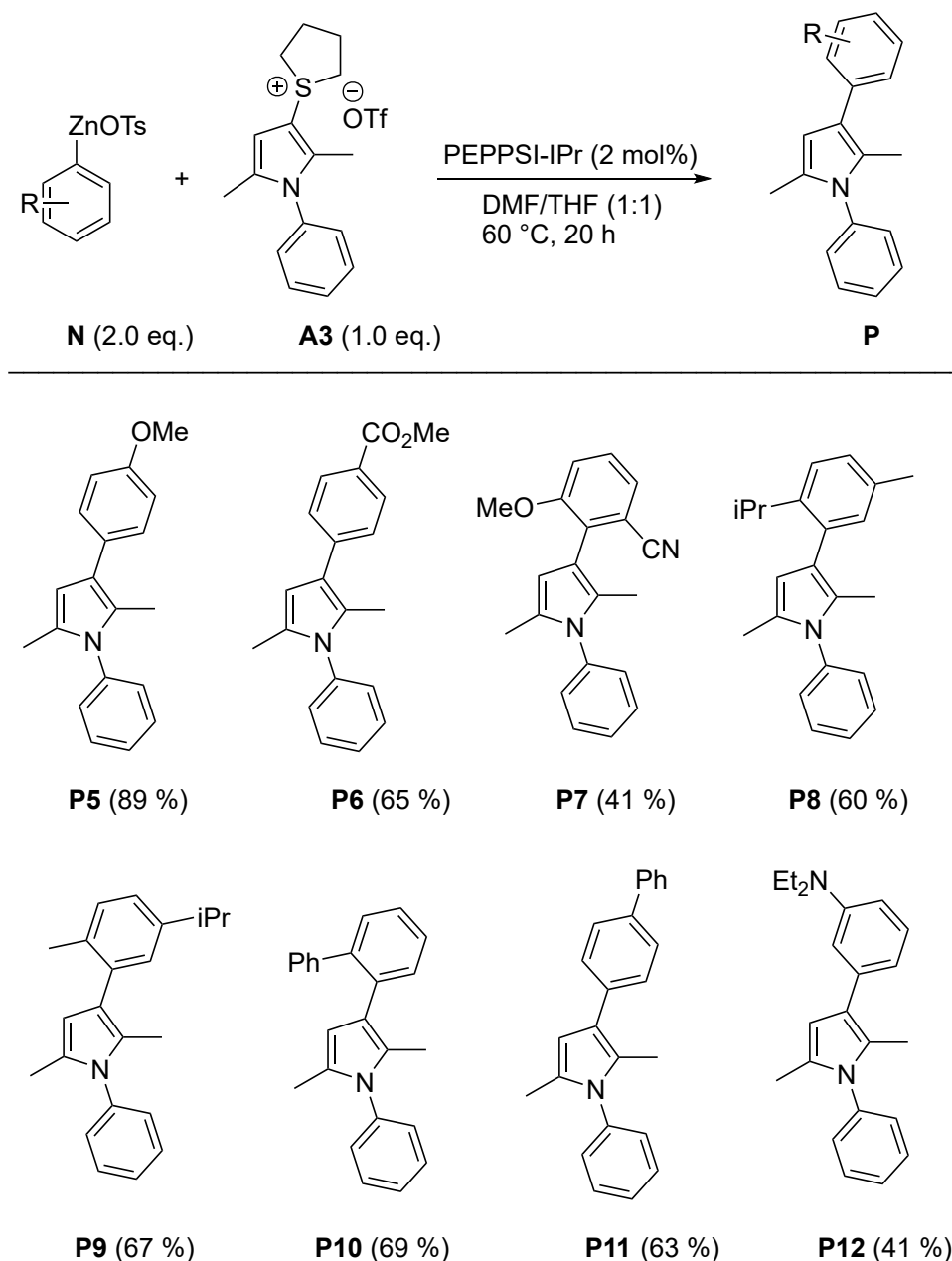
1.3.4.4 Pyrrole C–H Arylation *via* Sulfonium Activation and Negishi cross-coupling

After optimization of the reaction parameters for the sulfonium salt NEGISHI coupling (1.3.4.2), the scope of the reaction was explored with various nucleophiles **N** synthesized *via* catalytic zincation of aryl tosylates using pyrrole sulfonium salt **A3** as model electrophile, and with the optimized conditions chosen from table 1.6 (see scheme 1.48). The zincated 1-naphthyltosylate **T1** delivered the isolated coupling product **P1** in 89 % yield. Alkylated cresol-derived tosylates **T2** and **T3** (*o*-Me, *p*-Me) and the more sterically demanding version with a *tert*-butyl group **T4** delivered the corresponding coupling products **P2**, **P3** and **P4** in high yields.



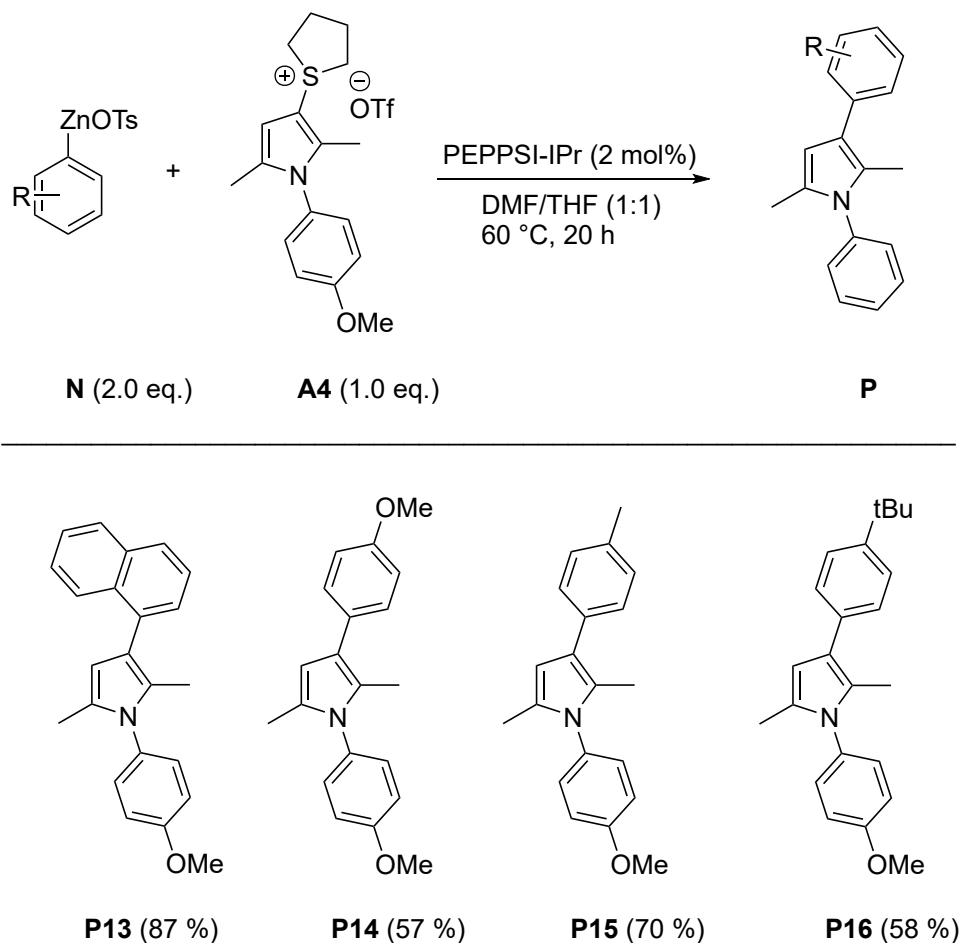
Scheme 1.48: NEGISHI cross-coupling reactions of pyrrole sulfonium salt **A3**. Yields refers to isolated products.

Electron-rich product **P5** was delivered in even higher yield from tosylate **T5** as shown in scheme 1.49. More demanding acceptor substrate **T6** still furnishes the product but in diminished yield (**P6**). Aryl tosylates derived from *o*-vanilline (**T7**), thymol (**T8**) and carvacrol (**T9**), electron-neutral tosylates (**T10**, **T11**) as well as an amine-containing tosylate (**T12**) also delivered the coupling products in satisfactory yield (**P7**, **P8**, **P9**, **P10**, **P11** and **P12**). Most of these arylated pyrroles were not yet known in the literature.



Scheme 1.49: NEGISHI cross-coupling reactions of pyrrole sulfonium salt **A3**. Yields refers to isolated products.

Extension of the scope with respect to the sulfonium salt was explored with anisole derivative **A4** which was synthesized analogously to salt **A3** as shown in section 1.3.4.1. The zincated naphthyl tosylate **T1** was successfully allowed to react with the pyrrole sulfonium salt to give **P13**, and then analogously with zincated electron-rich methoxy tosylate **T5** to give **P14**. Methyl and *t*Bu substituted tosylates **T3** and **T4** furnished products **P15** and **P16** (see scheme 1.50).

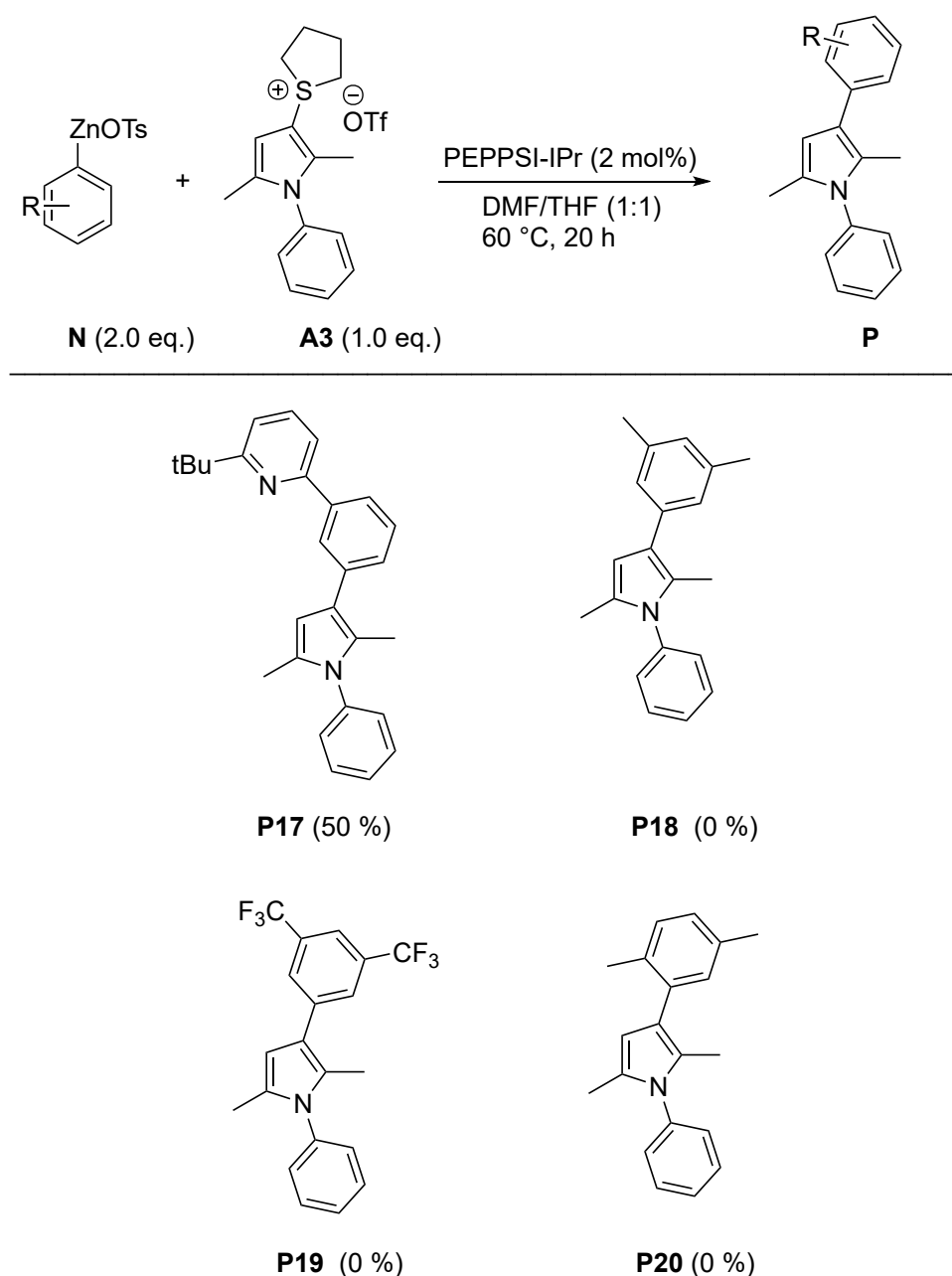


Scheme 1.50: NEGISHI cross-coupling reactions of pyrrole sulfonium salt **A4**. Yields refers to isolated products.

All the reactions so far were performed in a two-step process where at first the catalytic zincation of the aryl sulfonate is conducted and secondly the coupling reaction with the sulfonium salt in another Schlenk tube. Consequently, a one-pot reaction was evaluated with addition of sulfonium salt **A3** to the zincated naphthyl tosylate, leading to the product in only 22 % yield. This may indicate an undesirable influence of remaining zinc or nickel catalyst from the initial metalation step in the ensuing palladium cross-coupling.

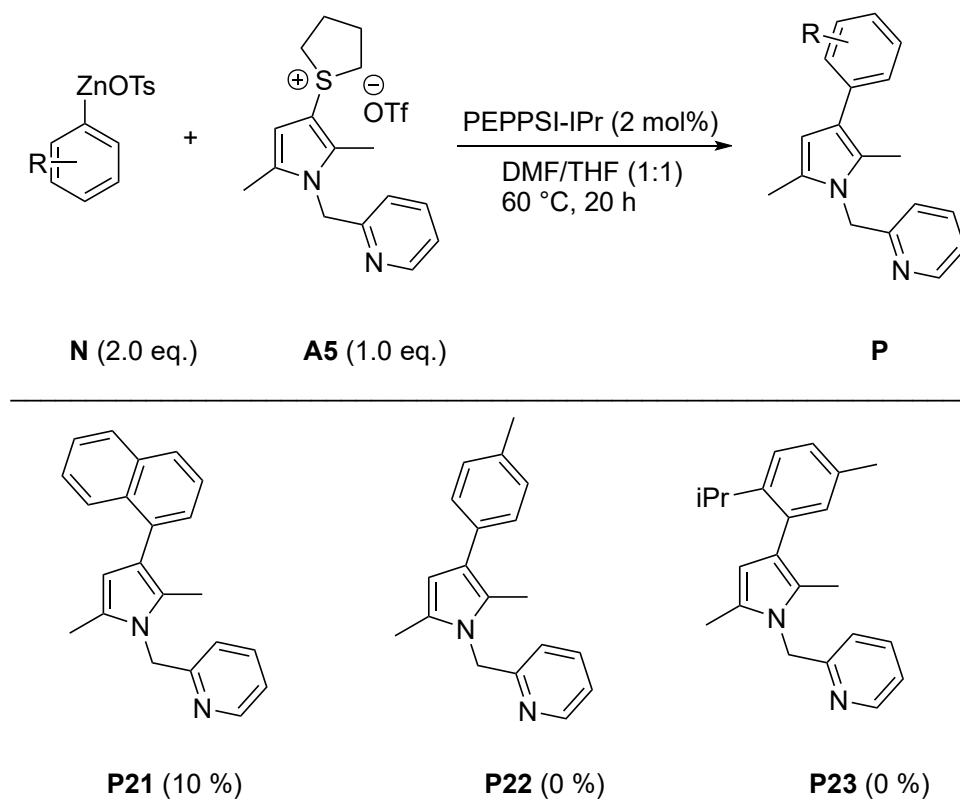
For completeness, a number of reactions will be presented here which did not work as expected or returned the desired product in diminished yield.

Various zincated aryl tosylates failed to react with pyrrole sulfonium salt **A3**. Pyridin-derived tosylate **T13** delivered **P17** in satisfying yield according to qNMR, but no isolation was conducted. Surprisingly, alkylated product **P18** was not formed contrarily to alkylated products **P2**, **P3**, **P8** and **P9**. This may be due to the electronically different *meta*-position of the methyl substituent because *ortho*- and *para*-substituents work well. Aryl tosylate substituted with the strong electronegative CF₃-group also showed no reaction (**P19**) as well as 2,5-dimethylsubstituted tosylate (**P20**).



Scheme 1.51: Unsuccessful NEGISHI cross-coupling reactions of pyrrole sulfonium salt **A3**. Yields were determined by qNMR-analysis.

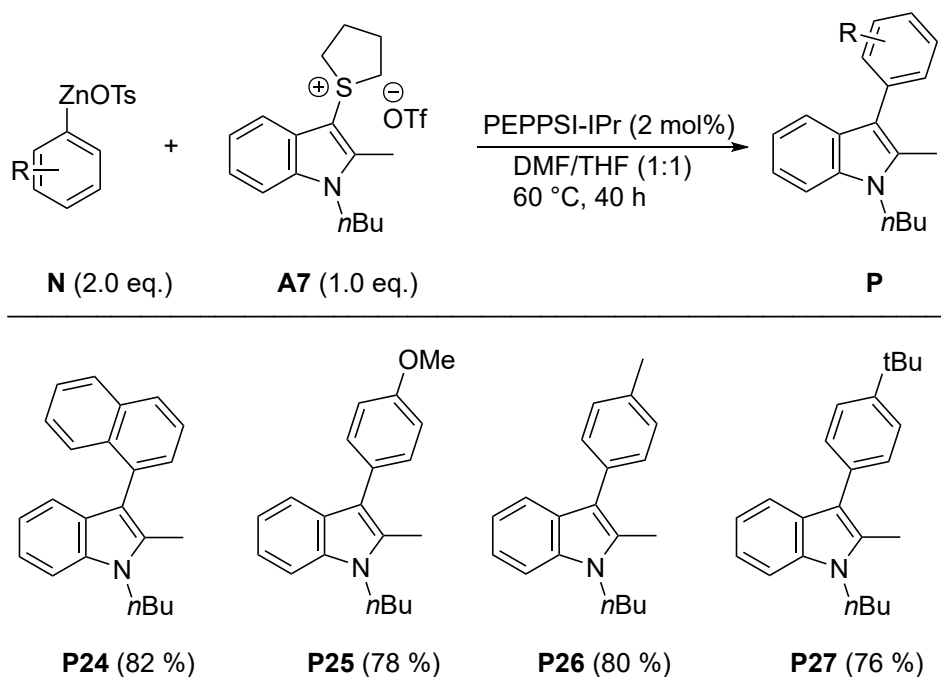
Reactions conducted under the same, optimized conditions as above and with well-established catalytically zincated aryl sulfonates (see **P1**, **P3**, or **P8**) but another sulfonium salt, pyridin-derived **A5**, led to a very low (**P21**) or no conversion (**P22**, **P23**).



Scheme 1.52: NEGISHI cross-coupling reactions of pyrrole sulfonium salt **A5**. Yields were determined by qNMR-analysis.

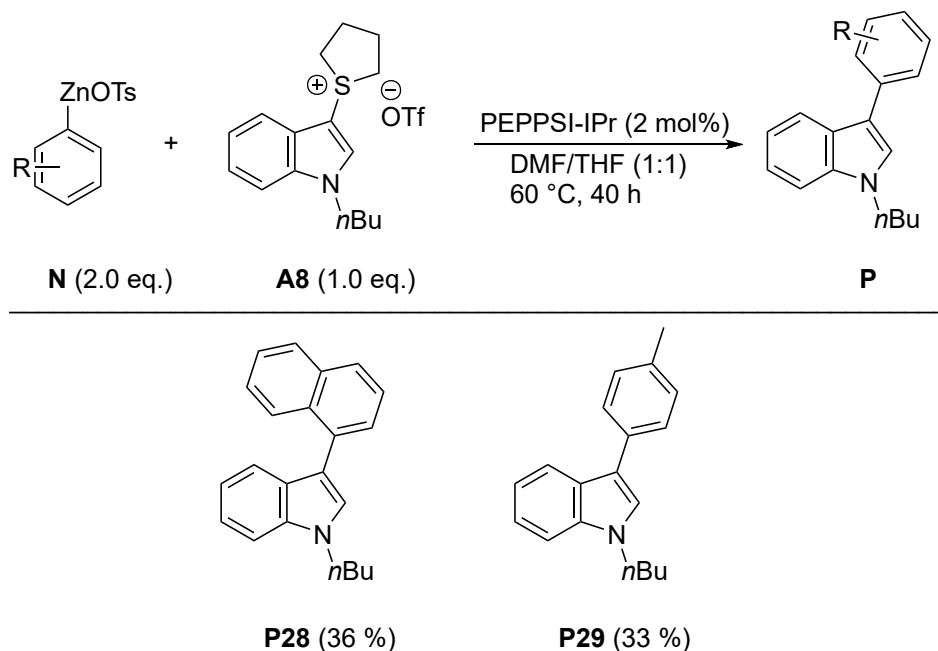
1.3.4.5 Indole C–H Arylation *via* Sulfonium Activation and Negishi cross-coupling

The next step was the evaluation with respect to other azole sulfonium salts. A range of trisubstituted indoles was successfully synthesized from indole sulfonium salt (**A7**) by cross-coupling with organozinc species. Since sulfonium salt **A7** is itself obtained directly from *N*-alkyl indole **S21**, the overall process corresponds to a C–H arylation of that heterocycle. The isolated yield of those reaction products could be greatly improved by extending the reaction time to 40 h.



Scheme 1.53: NEGISHI cross-coupling reactions of indoles. Yields from isolated products.

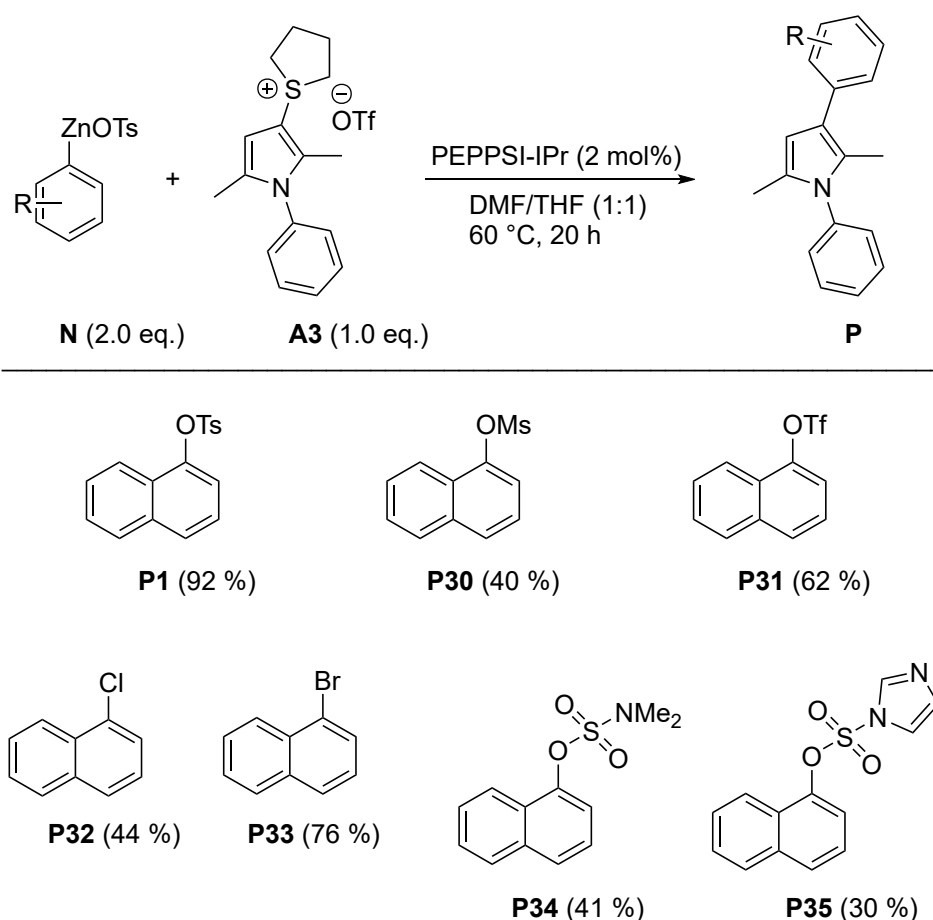
Changing the sulfonium salt to indole derivative **A8** the yield reduced to 36 % (**P28**) and 33 % (**P29**) with tosylates **T1** and **T3**, respectively. This change might be due to a missing structural common to better working sulfonium salts like **A3**, **A4** and **A7**: the methyl group in 2-position, which may explain the lower yield due to missing inductive effects.



Scheme 1.54: NEGISHI cross-coupling reactions of indole sulfonium salt **A8**. Yields were determined by qNMR-analysis.

1.3.4.6 Screening of Alternative Aryl Sulfonates as Pre-Nucleophiles

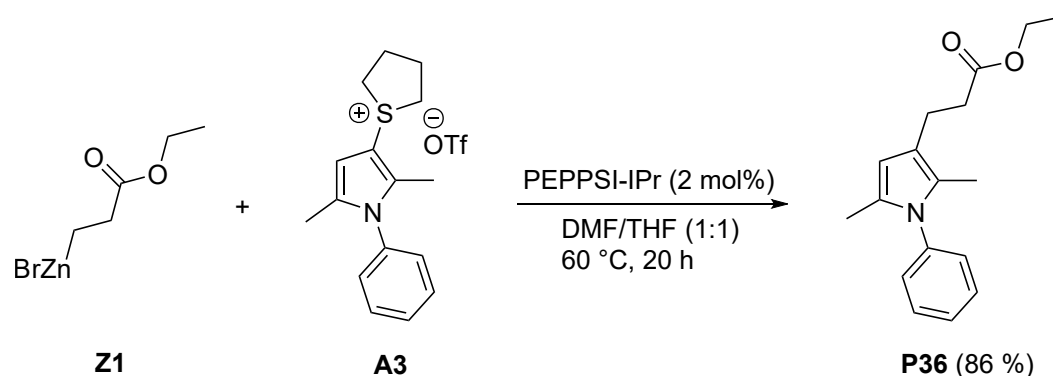
Having established the coupling protocol with tosylates and various sulfonium salts, a determination of the generality of the conversion regarding the aryl sulfonate is investigated. The catalytic zincation can also be performed with other leaving groups. Compared to the reference reaction providing model product **P1** (92 % yield determined via quantitative NMR) naphthyl mesylate (**P30**) and naphthyl triflate (**P31**) as pre-nucleophiles returned the same product in declined yield. The chloride and bromide pre-nucleophiles reacted as expected in accordance with their established proneness for zincation (**P32** and **P33**) whereas the fluoride shows no activity. The interesting, alternative electrophilic partners sulfamate ester **P34** and the imidazolylsulfonate **P35** still show some conversion.



Scheme 1.55: NEGISHI cross-coupling reactions of pyrrole sulfonium salt **A3** with catalytically zincated aryl sulfonates obtained from various aryl sulfonates. Yields were determined by qNMR-analysis.

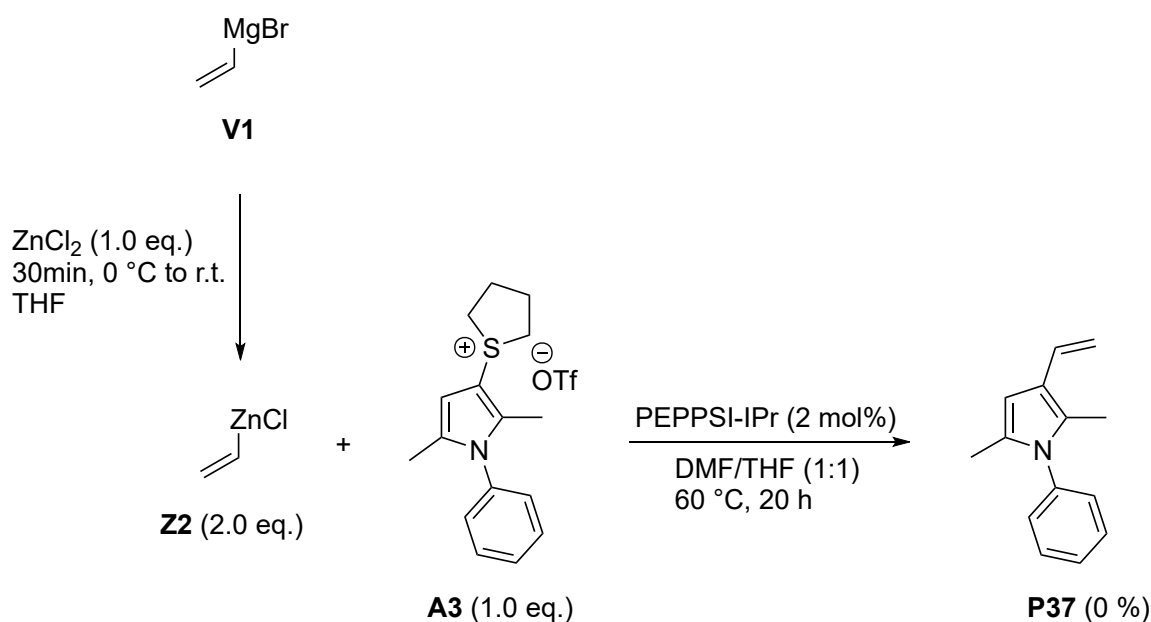
1.3.4.7 Functionalization *via* β -Propionylation and Vinylation

As mentioned in subsection 1.1.1 the Fe(II)-protoporphyrin IX (hematin) as porphyrin is of biological importance. It bears vinyl and propionic acid groups at the 3- and 4-position of the pyrrole core. Herein, the pyrrole sulfonium salt **A3** is allowed to react with zincated 3-bromopropanoate **Z1** to investigate a route to synthetic substructures of hematins. The established coupling conditions from the previous sections were applied. After 20 h at 60 °C with PEPPSI-IPr as catalyst the product **P36** is isolated in a promising yield as shown in scheme 1.56. The ^1H - and ^{13}C -NMR spectra are consistent with the structure except the missing carbon atom from the keto group. This initial result opens up room toward future reactions with other pyrrole salts or alkyl bromides.



Scheme 1.56: NEGISHI cross-coupling reaction of pyrrole sulfonium salt **A3** with zincated ethyl 3-bromopropanoate **Z1**. Yield refers to isolated product.

Next, the second reaction regarding the functional groups in hematins is tested: A vinylation of pyrrole sulfonium salt **A3**. Transmetalation of vinyl magnesium bromide **V1** with ZnCl_2 leads to **Z2** which subsequently is then allowed to react with sulfonium salt **A3**. Unfortunately, no product formation could be detected in this coupling attempt.



Scheme 1.57: Attempted NEGISHI cross-coupling reaction of pyrrole sulfonium salt **A3** with vinylzinc reagent **Z2**. Yield determined by qNMR-analysis.

1.3.5 Caffeine C–H Arylation with Pyrrolyl Halides

C–H arylation reactions of heteroaromatics represent an important class of catalytic coupling reactions. Since pyrroles, especially halogenated pyrroles, are not in the focus of research in this field a general reaction screening is conducted in order to evaluate the overall feasibility of a direct C–H arylation of caffeine **E** as model C–H donor with bromopyrrole **B1**. Remarkable results had been achieved by the group of YOU who reported the palladium-catalyzed arylation of heterocycles through C–H bond activation with pivalic acid as additive.⁷⁷ They carried out the arylation of caffeine with bromobenzene in DMF in the presence of pivalic acid resulting in 85 % of phenylcaffeine after seven hours at 120 °C. In accordance with that work and following up on previous results from our group, Pd(OAc)₂ and PdCl₂(MeCN)₂ were chosen as the most promising catalysts in combination with two equivalents of either K₂CO₃ or K₃PO₄ as base. The use of several, previously synthesized carboxylic acid additives proved to be beneficial for the conversion, as expected.

These carboxylic acid or ammonium carboxylate additives function as concerted-metalation-deprotonation (CMD) reagents and are based on sterically hindered alkyl carboxylic acids. For this screening, pivalic acid (Add. 1), its tetrabutylammonium salt (Add. 3), sterically more demanding additive 2-isopropyl-2,3-dimethylbutanoic acid (Add. 2) and its tetrabutylammonium salt (Add. 4) were used (see figure 1.8). Several groups reported applications of tetraalkylammonium carboxylates as nucleophilic oxygen sources in catalysis.⁷⁸ Among alkyl ammonium derivatives, these salts might not offer the highest reactivity but are readily available and inexpensive.⁷⁹ The detailed experimental procedure for the screening can be found in subsection 4.2.1.7

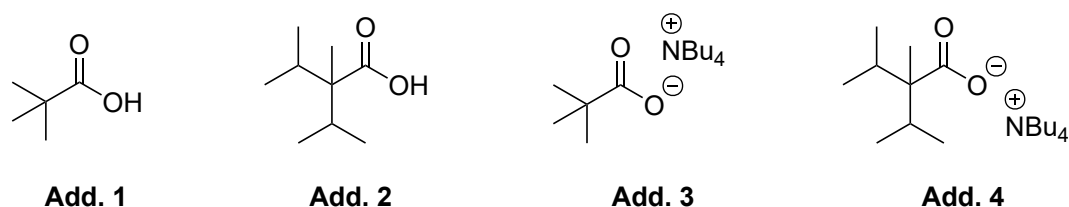


Figure 1.8: CMD-additives applied in the caffeine C–H arylation.

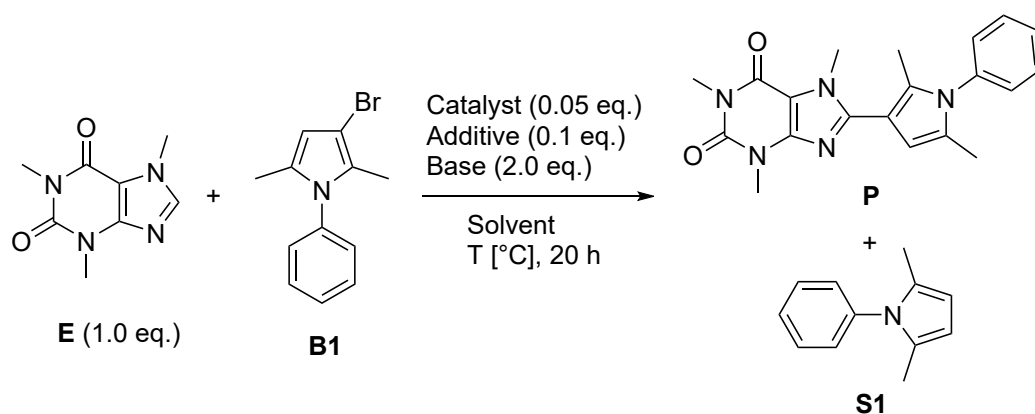
⁷⁷Zhao, D.; Wang, W.; Lian, S.; Yang, F.; Lan, J.; You, J. *Chem. Eur. J.* **2009**, *15*, 1337–1340.

⁷⁸Kurcok, P.; Smiga, M.; Jedlinski, Z. *J. Polym. Sci. A Polym. Chem.* **2002**, *40*, 2184–2189

⁷⁹Starks, C. M.; Liotta, C. L.; Halpern, M. E. *Phase-Transfer Catalysts in Phase-Transfer Catalysis*, Springer Netherlands, Dordrecht, 1994; pp 123–206.

The reaction conditions are defined by an excess of bromopyrrole **B1** (1.5 – 2.0 eq.) and temperatures ranging from 100 to 120 °C. In order to achieve these temperatures high-boiling solvents like DMF, dimethylacetamide (DMA) or *N*-methyl-2-pyrrolidone (NMP) were used. All three additives utilized in table 1.9 in entries 1 to 12 delivered the product **P** only in distinct, but low amounts below 10 mol%. The problem may be an insufficient activated caffeine C8–H bond in presence of bases K₂CO₃ or K₃PO₄, poor reactivity of bromopyrrole **B1** to oxidative addition to the palladium catalyst or slow reductive elimination. Even doubling the amount of the bromopyrrole did not improve the outcome (entries 4, 8 and 12).

Table 1.9: C–H arylation of caffeine **E** with pyrrolyl bromide **B1**.

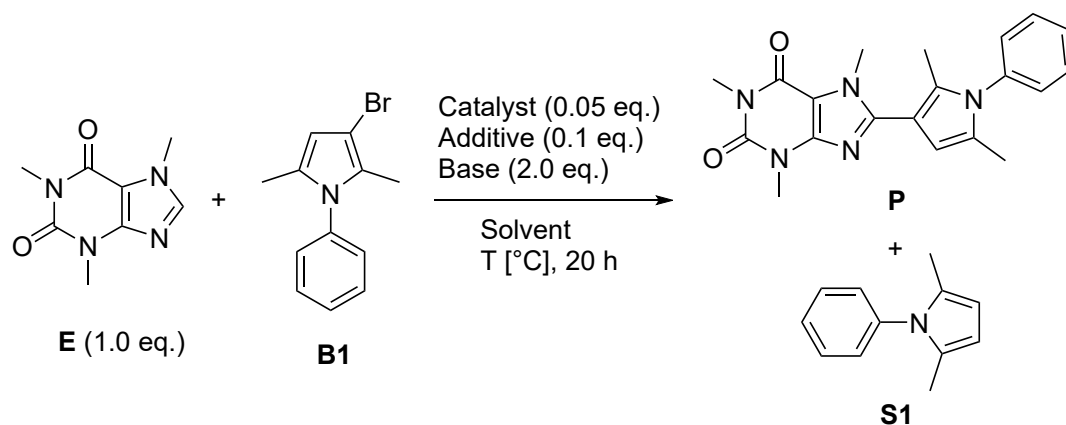


#	Catalyst	Additive	Base	Solv.	B1(eq.)	T[°C]	E	B1	S1	P ^{a)}
1	PdCl ₂ (MeCN) ₂	1	K ₂ CO ₃	DMF	1.5	100	71	80	6	5
2	PdCl ₂ (MeCN) ₂	1	K ₂ CO ₃	DMF	1.5	120	65	85	9	5
3	PdCl ₂ (MeCN) ₂	1	K ₃ PO ₄	DMF	1.5	120	45	66	6	7
4	Pd(OAc) ₂	1	K ₃ PO ₄	DMF	2.0	120	31	39	3	5
5	PdCl ₂ (MeCN) ₂	3	K ₂ CO ₃	DMF	1.5	100	61	51	2	4
6	PdCl ₂ (MeCN) ₂	3	K ₂ CO ₃	DMF	1.5	120	49	88	6	5
7	PdCl ₂ (MeCN) ₂	3	K ₃ PO ₄	DMF	1.5	120	46	62	6	7
8	Pd(OAc) ₂	3	K ₃ PO ₄	DMF	2.0	120	32	49	3	6
9	PdCl ₂ (MeCN) ₂	2	K ₂ CO ₃	DMF	1.5	100	4	83	8	7
10	PdCl ₂ (MeCN) ₂	2	K ₂ CO ₃	DMF	1.5	120	60	91	4	4
11	PdCl ₂ (MeCN) ₂	2	K ₃ PO ₄	DMF	1.5	120	55	60	9	8
12	Pd(OAc) ₂	2	K ₃ PO ₄	DMF	2.0	120	37	59	4	4

a) Yields in mol% were determined by qNMR-analysis.

Table 1.10 uses the same model substrate and reaction conditions with one change: Now additive Add. 4 is used and shows improved results in entry 18 with 14 % yield and in entry 19 with 24 % yield. The other attempts showed the same results as previously, namely the product could only be found in traces. Generally speaking, the productivity of this reaction is low and a more reactive reaction system has to be found. Due to strong overlay of signals as well as partial loss of reactants by the work-up procedure a discussion of recovered or decomposed starting material is left out. The detailed experimental procedure can be found in subsection 4.2.1.7.

Table 1.10: C–H arylation of caffeine **E** with pyrrolyl bromide **B1**.



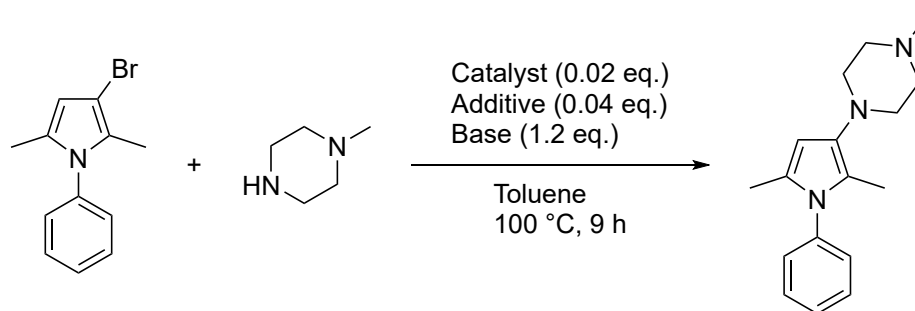
#	Catalyst	Additive	Base	Solv.	B1(eq.)	T[°C]	E	B1	S1	P ^{a)}
13	PdCl ₂ (MeCN) ₂	4	K ₂ CO ₃	DMF	1.5	100	25	78	9	12
14	PdCl ₂ (MeCN) ₂	4	K ₂ CO ₃	DMF	1.5	120	73	90	5	4
15	PdCl ₂ (MeCN) ₂	4	K ₃ PO ₄	DMF	1.5	120	40	72	5	4
16	Pd(OAc) ₂	4	K ₃ PO ₄	DMF	2.0	120	39	65	3	6
17	PdCl ₂ (MeCN) ₂	4	K ₂ CO ₃	DMF	1.5	100	32	83	9	7
18	PdCl ₂ (MeCN) ₂	4	K ₃ PO ₄	DMF	1.5	100	34	81	4	14
19	PdCl ₂ (MeCN) ₂	4	K ₂ CO ₃	DMA	1.5	100	3	65	10	24
20	PdCl ₂ (MeCN) ₂	4	K ₃ PO ₄	DMA	1.5	100	62	90	5	3
21	PdCl ₂ (MeCN) ₂	4	K ₂ CO ₃	DMA	1.5	120	28	69	15	12
22	PdCl ₂ (MeCN) ₂	4	K ₂ CO ₃	NMP	1.5	100	52	91	2	2
23	Pd(OAc) ₂	4	K ₂ CO ₃	DMF	1.5	100	27	82	9	6
24	Pd(OAc) ₂	4	K ₃ PO ₄	DMF	1.5	100	32	83	4	9
25	Pd(OAc) ₂	4	K ₂ CO ₃	NMP	1.5	100	56	95	2	1
26	Pd(OAc) ₂	4	K ₃ PO ₄	NMP	1.5	100	46	90	9	3
27	Pd(OAc) ₂	4	K ₂ CO ₃	DMA	1.5	100	6	78	6	10

a) Yields in mol% were determined by qNMR-analysis.

1.3.7 Attempted Pyrrole Amination with *N*-Methylpiperazine

Palladium-catalyzed amination reactions of aryl halides with primary or secondary amines are a convenient synthetic route to arylamines. This chemistry was mainly developed by BUCHWALD and HARTWIG. Amination reactions of halopyrroles are scarcely found in the literature therefore a few conditions were tested herein according to general procedure 9 in subsection 4.2.1.9. The results are shown in table 1.11. Here, bromopyrrole **B1** is allowed to react with *N*-methylpiperazine (**S**) under various conditions. Entry 1 displays standard conditions for aryl bromides and secondary amines found by GURAM and BUCHWALD in 1995.⁸² Entries 2 and 3 vary the catalyst⁸³ and entries 4 and 5 use the BINAP ligand: a fully substituted and 2-brominated pyrrole was aminated with Boc-piperazine under very similar conditions as in entries 2 and 3 by BULLINGTON.⁸⁴ However, none of the conditions below could furnish even traces of the pyrrole product.

Table 1.11: Screening of conditions for amination reaction of pyrrolyl halide B1 with *N*-methylpiperazine.



	B1 (1.0 eq.)	S (1.2 eq.)		P
#	Catalyst	Base	Additive	Yield[%] ^{a)}
1	PdCl ₂	NaOtBu	-	0
2	PdCl ₂ (PCy ₃) ₂	NaOtBu	-	0
3	PdCl ₂ (MeCN) ₂	NaOtBu	PCy ₃	0
4	Pd(OAc) ₂	Cs ₂ CO ₃	BINAP	0
5	Pd(dba) ₂	Cs ₂ CO ₃	BINAP	0

a) Yields in mol% were determined by qNMR-analysis.

⁸²Guram A.; Rennels R.; Buchwald S. *Angew. Chem. Int. Ed.* **1995**, *34*, 1348–1350.

⁸³Reddy N. P.; Tanaka M. *Tetrahedron Lett.* **1997**, *38*, 4807–4810.

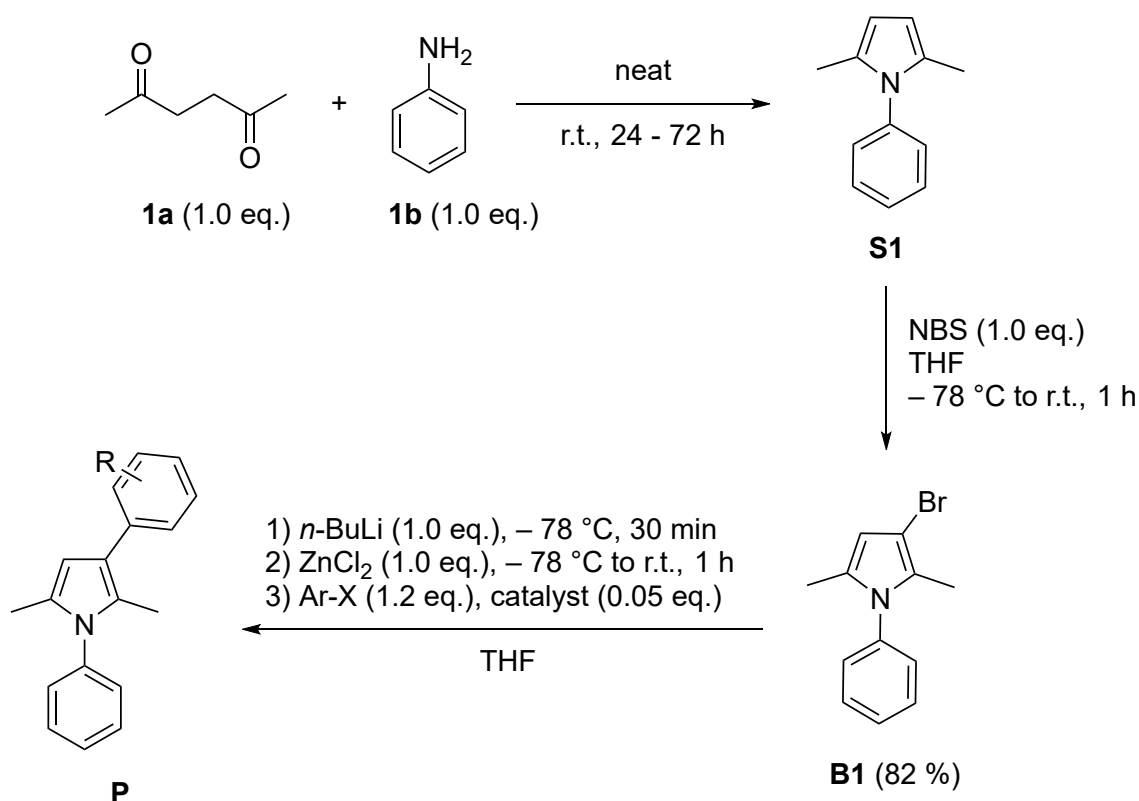
⁸⁴Bullington et al. *Bioorg. Med. Chem. Lett.* **2006**, *16*, 6102–6106.

1.4. Conclusion and Outlook

In summary, a plethora of 2,5-dimethyl substituted *N*-aryl pyrroles were synthesized (chapter 1.3.1) *via* a solvent-free procedure. The scope covers mostly *N*-aryl, *N*-cyclohexyl, *N*-benzyl and bridged *N*-*N*-alkyl pyrroles (**S1**–**S10**). Some reactions did not work, for example with *N*-pyridin or *N*-benzothiazole substitution (**S11**–**S16**). The *N*-phenyl substituted pyrrole (**S17**) or the *N*-tosyl pyrrole (**S18**) were also synthesized.

In chapter 1.3.2 several halogenation strategies were tested to convert pyrroles into halopyrrole electrophiles. A screening with different halogenating agents led to a concise synthesis of bromopyrrole **B1** as convenient model substrate for cross-coupling reactions. Additionally, a chlorination procedure adapted from the literature was successfully applied to several pyrroles (**C1**–**C3**). Iodination via directed C–H metalation was also possible (**I1**).

Subsequently, the bromopyrrole **B1** underwent halogen-metal exchange with *n*-butyl lithium and transmetalation with ZnCl₂ to give a pyrrolylzinc reagent suitable for NEGISHI cross-coupling with several aryl and heteroaryl halides as described in chapter 1.3.3. The general route to functionalized pyrroles (**P**) is shown in scheme 1.59.



Scheme 1.59: General access route to substituted pyrroles **P** *via* synthesis of **S1** from hexane-2,5-dione (**1a**) and aniline (**1b**), bromination of pyrrole **S1** and halogen-metal exchange, transmetalation and NEGISHI coupling of **B1** with aryl halides.

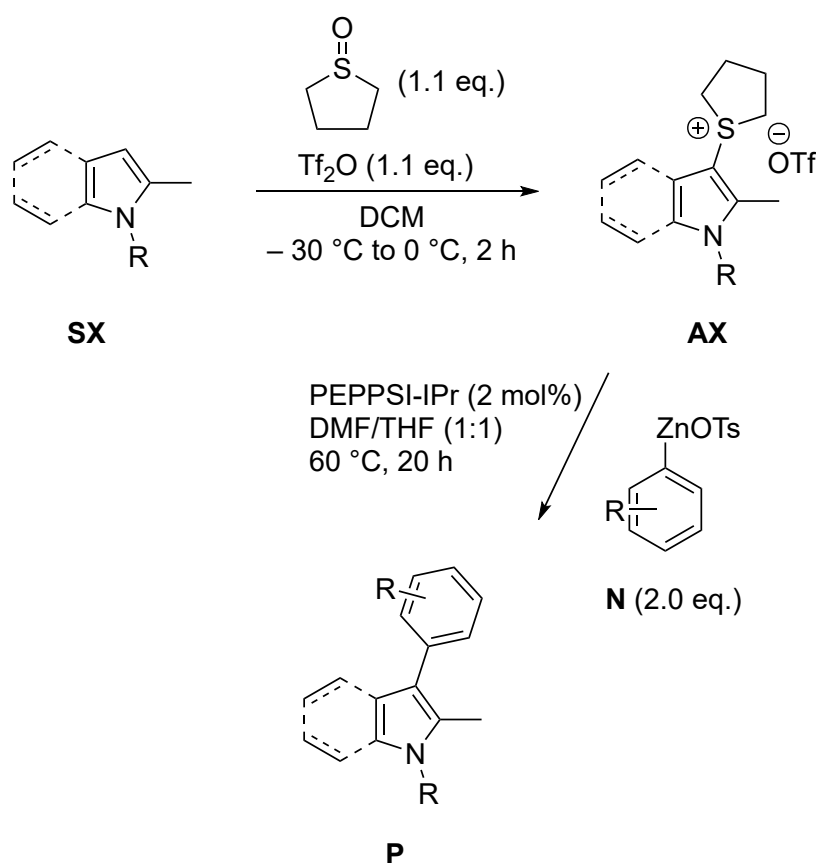
To broaden the scope of the presented procedure, further investigation of the coupling of other synthesized halopyrroles with various aryl or alkyl halide coupling partners are desirable.

Yet, the focus of our research moved to the exploration of new pyrrole and indole sulfonium salts as powerful, alternative and stable electrophiles for azole cross-coupling reactions. Various sulfonium salts **AX** were accessible *via* mild and selective sulfonio-ylation of the *N*-heterocycles **SX** with an *in situ* reagent from tetrahydrothiophene 1-oxide and trifluoromethanesulfonic anhydride at low temperatures (**A1–A9**).

Based upon an extensive screening with different catalysts, ligands, temperatures, reaction times and solvent mixtures, optimal conditions were found (PEPPSI-IPr 2 mol%, DMF/THF 1:1, 60 °C, 20 h) for the subsequent cross-coupling with organozinc nucleophiles **N**. The source of the nucleophile is a catalytic zincation of aryl tosylates that will be precisely described in the following chapter 2. Coupling with an excess of organozinc species (2.0 eq.) delivers several new, functionalized pyrroles (**P1–P16**) in satisfying to high yield. Unfortunately, some zincated aryl tosylates did not show any conversion (**P17–P22**).

The scope of sulfonium NEGISHI coupling was extended to another type of *N*-heterocycle. Previously synthesized indole sulfonium salts were allowed to react with the same organozinc species to deliver six functionalized indoles (**P23–P28**).

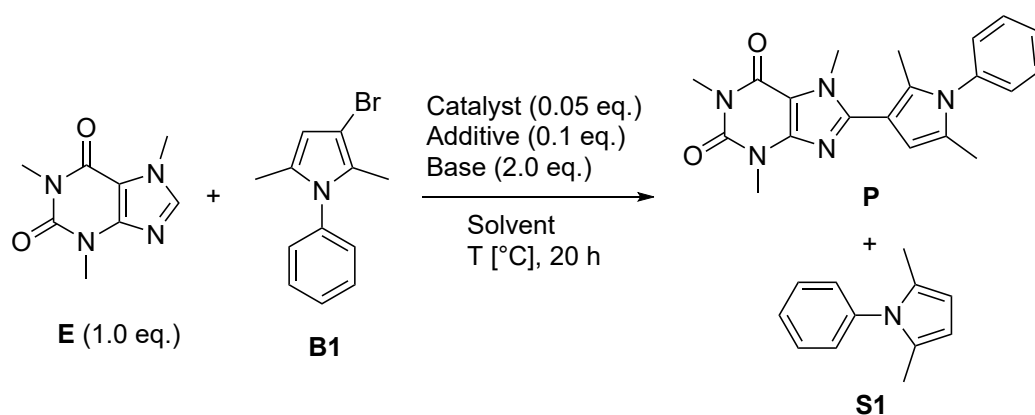
This general route to C–H arylated pyrroles and indoles (**P**) *via* sulfonium activation and NEGISHI coupling is shown in scheme 1.60.



Scheme 1.60: Synthesis of pyrrole and indole sulfonium salts and subsequent NEGISHI cross-coupling with catalytically zincated aryl tosylates.

In summary, this reaction protocol provides access to a plethora of building blocks for pyrrole and indole synthesis. Several readily synthesized but not yet utilized sulfonium salts should be amenable to cross-coupling with organozinc species. The direct zincation of these sulfonium salts might be an interesting topic of research because the group of YORIMITSU has shown the general amenability of the generation of organozinc reagents from aryl- and styryl sulfonium salts, respectively, using a nickel catalyst and zinc Dust.⁸⁵ Furthermore, application of other coupling protocols such as the SUZUKI or HECK reactions should be promising.

In parallel, access to substituted pyrroles by direct C–H arylation was investigated. An extensive screening with different catalysts, additives and bases at two temperatures revealed that the reaction is in principle possible, but the coupling yields achieved were not yet satisfactory and should be further investigated.



Scheme 1.61: C–H arylation of caffeine **E** with bromopyrrole **B1**.

⁸⁵(a) Yamada K.; Yanagi T.; Yorimitsu H. *Org. Lett.* **2020**, *22*, 9712–9718. (b) Yamada K.; Kintzel M.; Perry G. J. P.; Saito H.; Yorimitsu H. *Org. Lett.* **2022**, *24*, 7446–7449.

2. Catalytic Metalation – Zinc Insertion into Aryl Sulfonates

2.1. Introduction – Organometallic Chemistry

The synthesis of cacodyl (Tetramethyldiarsane) in 1760⁸⁶ as the first organometallic compound was the beginning of organometallic chemistry. Later on, the syntheses of the first transition metal containing species diethylzinc by Frankland in 1848⁸⁷ and Zeise's salt (Potassium trichloro(ethene)platinate(II)) in 1850⁸⁸ were remarkable achievements. Since then, organometallic compounds have developed into indispensable tools for organic synthesis – as catalysts, bases or carbon nucleophiles.⁸⁹

Organometallic compounds are defined by containing at least one chemical bond between a carbon atom and a metal. The reactivity of these species is explained by the polarized nature of the carbon-metal bond due to the difference in electronegativity. As most metals are significantly less electronegative than carbon, the negatively polarized carbon is able to react as a nucleophile, similar to a carbanion. Because of their intrinsic chemical properties organometallic species exhibit an instability under non-inert gas atmosphere or moisture. Therefore, working with this compound class requires using inert-gas atmosphere and the exclusion of moisture, especially with pyrophoric molecules like *tert*-butyllithium.

The predominant application of organometallic compounds lies in the field of efficient carbon-carbon bond formation. Forming these bonds is a crucial step in the synthesis of complex organic frameworks. Appropriately chosen organometallic derivatives have to be compatible with the presence of various functional groups. Therefore, undesired protection group strategies are often avoided crucially enhancing atom- and step-economy.⁹⁰ The *in situ* synthesized organometallics exhibit an extensively tunable reactivity enabling broad applications to many different conditions and substrates. This adaptability arises on the one hand from the level of polarization of the carbon-metal bond and on the other hand from the properties of the metal-ligand bond. A ligand bound to the metal moiety offers diverse regulating effects on the reactivity.⁹¹

⁸⁶Gassicourt, L. C. C. d. *Mem. Math. Phys. Acad. Sci. Paris* **1760**, *3*, 623–625.

⁸⁷(a) Frankland, E. *Liebigs Ann. Chem.* **1848**, *71*, 171–213. (b) Frankland, E. *J. Chem. Soc.* **1848**, *2*, 263–296.

⁸⁸Frankland, E. *J. Chem. Soc.* **1850**, *2*, 263–296.

⁸⁹Seyferth, D. *Organometallics* **2001**, *20*, 2940–2955.

⁹⁰Boudier, A.; Bromm, L. O.; Lotz, M.; Knochel, P. *Angew. Chem.* **2000**, *112*, 4584–4606.

⁹¹Trost, B. M. *Angew. Chem. Int. Ed.* **1995**, *34*, 259–281.

Lithium, magnesium, zinc, copper and boron compounds belong to the most commonly used organometallic reagents.⁹² The different reactivity of these compounds derives from their carbon-metal bond character. Table 2.1 shows the electronegativity difference $\Delta\chi$ for different carbon-metal bonds. The values are based on the Allred-Rochow electronegativity scale.⁹³

Table 2.1: Electronegativity difference ($\Delta\chi$) for different carbon-metal bonds.

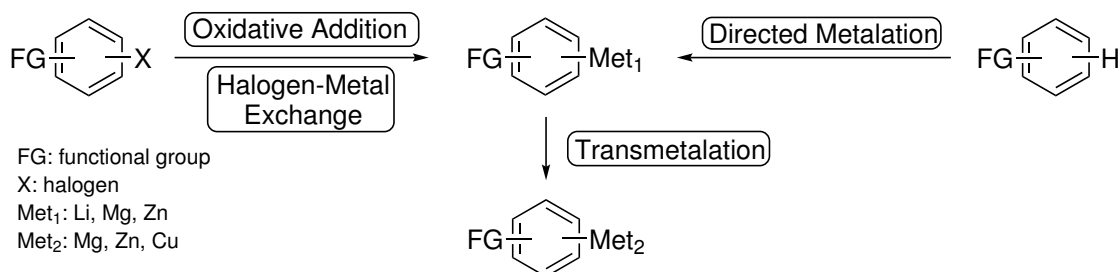
M	Li	Mg	Zn	Cu	B
$\Delta\chi$ (C-M)	1.53	1.27	0.84	0.75	0.49

Carbon-lithium bonds have strongly ionic character with a $\Delta\chi$ comparable to the salt sodium bromide ($\Delta\chi = 1.73$). The C-Mg bond has also noticeable ionic character, whereas C-Zn, C-Cu and C-B bonds are increasingly less polarized and consequently more covalent, their $\Delta\chi$ is lower than that of a C-O bond (1.00).

Generally speaking, a more ionic C-M bond is expected to induce higher reactivity and the corresponding organometallic compound to be more nucleophilic. Predominantly covalent C-M bonds provide less reactive organometallic reagents, enabling more selective transformations and higher tolerance for sensitive functionalities as a result. Common experimental strategies used in reaction sequences including these species are the application of low temperatures, use of apolar solvents and introduction of protecting groups to control the reactivity. Doubtless, the endeavor of finding the compromise between reactivity and functional group tolerance is one of the most important objectives.

2.1.1 Preparation of Organometallic Reagents

Organometallic reagents are commonly prepared by oxidative addition, transmetalation, halogen metal exchange or directed metalation as depicted in scheme 2.1. This chapter briefly describes each synthesis. In the literature many variations of these general methods can be found. Additionally, other related methods (e.g. carbo- or hydrometalation) can be used are not further mentioned here, since the overview focuses on substitution reactions.⁹⁴



Scheme 2.1: Preparation of organometallic reagents *via* different methods.

⁹²Klatt, T.; Markiewicz, J. T.; Sämann, C.; Knochel, P. *J. Org. Chem.* **2014**, *79*, 4253–4269.

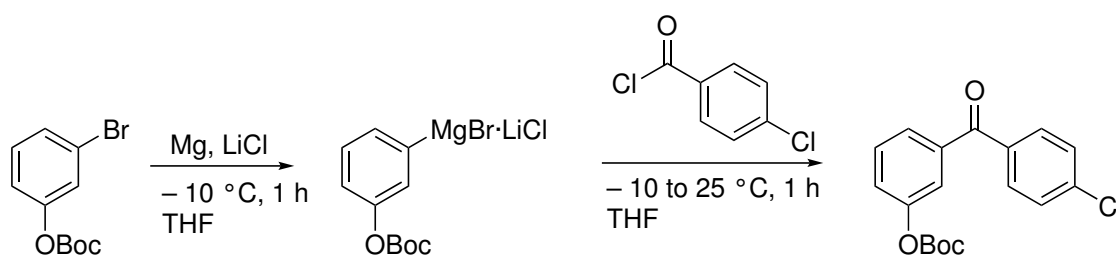
⁹³Allred, A. L.; Rochow, E. G. *J. Inorg. Nucl. Chem.* **1958**, *5*, 264–268.

⁹⁴(a) Spessard, G. O.; Miessler, G. L. *Organometallic chemistry*, Oxford University Press, New York, 2010. (b) Elschenbroich, C. *Organometallics*, Wiley-VCH, Weinheim, 2006. (c) Flynn, A. B.; Ogilvie, W. W. *Chem. Rev.* **2007**, *107*, 4698–4745.

2.1.1.1 Oxidative Addition

One of the first organometallic compounds synthesized by FRANKLAND in 1850⁹⁵ using zinc and GRIGNARD in 1900⁹⁶ using magnesium were prepared by oxidative addition. The metal inserts directly into a carbon-halogen bond under oxidation of the metal and reduction of the carbon atom. Magnesium insertion is performed with magnesium turnings which are usually deactivated due to an oxide layer. It can be removed by the use of iodine or 1,2-dibromoethane. If performed in this way, the reaction requires elevated temperatures. Besides magnesium and zinc insertion, lithium insertions were developed by ZIEGLER⁹⁷, WITTIG⁹⁸ and GILMAN.⁹⁹ Their ease of preparation and their broad applications in organic synthesis made these new reagents an instant success. As a result of this fundamental contribution GRIGNARD was awarded a Nobel Prize in chemistry in 1912.

The performance of the oxidative insertion of elemental magnesium into organic halides can be significantly increased by using LiCl as additive, which also avoids aggregation as shown by the group of KNOCHEL.¹⁰⁰ These reactions offer high regioselectivity and tolerance of sensitive functional groups like esters, ketones, aldehydes or nitriles. An example for the oxidative addition of magnesium into an arylbromide and the following trapping reaction with 4-chlorobenzoyl chloride is displayed in scheme 2.2.¹⁰¹



Scheme 2.2: Oxidative insertion of magnesium into 3-bromophenyl *t*-butyl carbonate and subsequent trapping with 4-chlorobenzoyl chloride.

Zinc insertion is also commonly used in synthesis. Organozinc reagents feature a high functional group tolerance, favorable reactivity and non-toxic byproducts. Major drawback is their liability when exposed to air which leads to hydrolysis *via* air moisture. Often expensive organic iodides have to be used as starting materials, but this can be avoided by applying a method developed by RIEKE,¹⁰² in which highly active zinc is prepared by reduction of ZnCl₂ with lithium naphthalide to access organozinc reagents from less reactive arylbromides.

⁹⁵Frankland, E. *Liebigs Ann. Chem.* **1848**, *71*, 171–213.

⁹⁶Grignard, V. *Compt. Rend. Acad. Sci. Paris* **1900**, *130*, 1322–1324.

⁹⁷Ziegler, K.; Colonius, H. *Liebigs Ann. Chem.* **1930**, *479*, 135–149.

⁹⁸Wittig, G. *Naturwissenschaften* **1942**, *30*, 696–703.

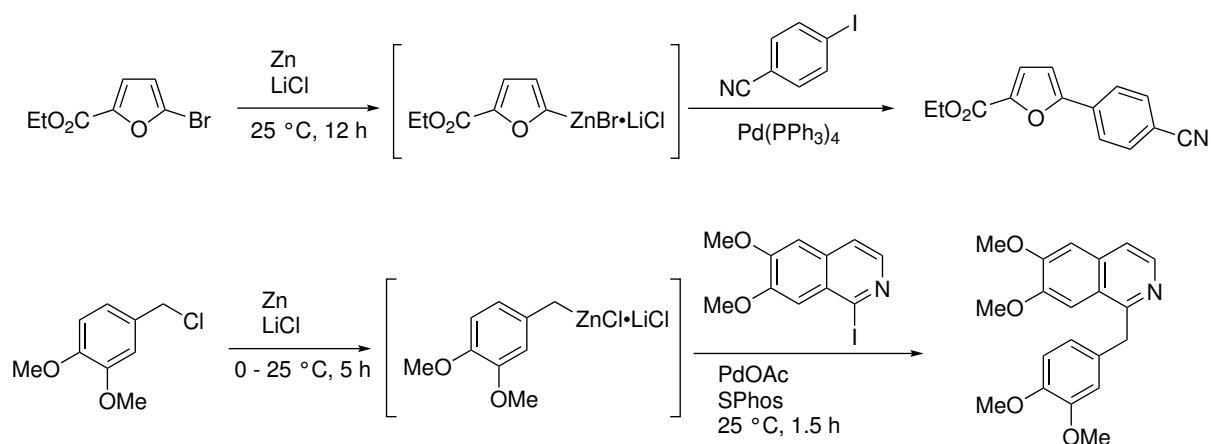
⁹⁹Gilman, H.; Jones, R. G.; Woods, L. H. *J. Org. Chem.* **1952**, *17*, 1630–1634.

¹⁰⁰(a) Piller, F. M.; Appukktuttan, P.; Gavryushin, A.; Helm, P.; Knochel, P. *Angew. Chem. Int. Ed.* **2008**, *47*, 6802–6806. (b) Krasovskiy, A.; Knochel, P. *Angew. Chem. Int. Ed.* **2004**, *43*, 3333–3336.

¹⁰¹Piller, F.; Knochel, P. *Chem. Eur. J.* **2009**, *15*, 7192–7202.

¹⁰²(a) Rieke R. D.; Li P. T.-J.; Burns T. P.; Uhm S. T. *J. Org. Chem.* **1981**, *46*, 4322–4326. (b) Zhu L.; Wehmeyer R. M.; Rieke R. D. *J. Org. Chem.* **1991**, *56*, 1445–1453.

In 2006, KNOCHEL and co-workers demonstrated that the use of commercially available zinc powder also allows the synthesis of highly functionalized zinc reagents from aryl and benzyl halides even in presence of sensitive functional groups like esters, nitriles and aldehydes.¹⁰³ Thus, a 2-furyl bromide could be converted into the corresponding organozinc compound and subsequently coupled with an iodide in a NEGISHI coupling. The reaction protocol is not limited to bromides: A benzylic chloride was applied in a two-step synthesis of the opium alkaloid antispasmodic drug papaverine (see scheme 2.3).



Scheme 2.3: Oxidative insertion of organohalides in the presence of LiCl and subsequent coupling reactions.

The role of LiCl has been investigated by experimental, computational, and analytical studies.¹⁰⁴ For example, a positive effect of LiCl is the increased solubility of the resulting organometallic reagent.

Facile transmetalation of organozinc species to palladium in NEGISHI cross-coupling reactions has made organozinc compounds a powerful tool in organic synthesis, as evidenced by the award of EI-ICHI NEGISHI along with RICHARD F. HECK and AKIRA SUZUKI with the Nobel Prize in Chemistry in 2010 for their work on new types of C–C-bond formation by catalytic cross-coupling.¹⁰⁵

2.1.1.2 Halogen Metal Exchange

Generally, a halogen-metal exchange occurs by the reaction of an organohalide with an organometal reagent like butyl lithium¹⁰⁶ or isopropylmagnesium chloride¹⁰⁷. Driving force of this reaction is the formation of the thermodynamically most stable carbanion.

¹⁰³(a) Krasovskiy A.; Malakhov V.; Gavryushin A.; Knochel P. *Angew. Chem. Int. Ed.* **2006**, *45*, 6040–6044. (b) Boudet N.; Sase S.; Sinha P.; Liu C. Y.; Krasovskiy A.; Knochel P. *J. Am. Chem. Soc.* **2007**, *129*, 12358–12359.

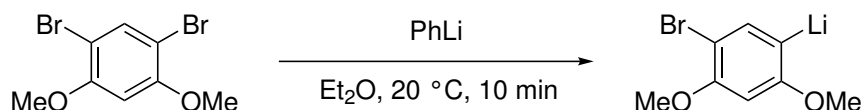
¹⁰⁴(a) Koszinowski K.; Böhler P. *Organometallics* **2009**, *28*, 771–779. (b) Liu C.-Y.; Wang X.; Furuyama T.; Yasuike S.; Muranaka A.; Morokuma K.; Uchiyama M. *Chem. Eur. J.* **2010**, *16*, 1780–1784. (c) Feng C.; Cunningham D. W.; Easter Q. T.; Blum S. A. *J. Am. Chem. Soc.* **2016**, *138*, 11156–11159. (d) Jess. K.; Kitagawa K.; Tagawa T.; Blum S. A. *J. Am. Chem. Soc.* **2019**, *141*, 9879–9884.

¹⁰⁵Wu X. F.; Anbarasan P.; Neumann H.; Beller M. *Angew. Chem. Int. Ed.* **2010**, *49*, 9047–9050.

¹⁰⁶Rottländer, M.; Knochel, P. *Angew. Chem. Int. Ed.* **1998**, *40*, 1801–1804.

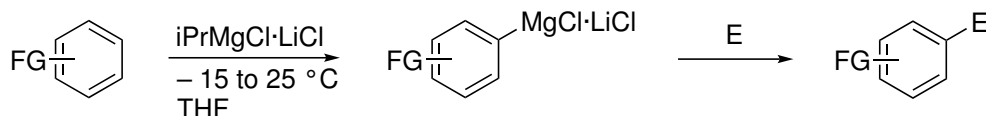
¹⁰⁷Ren, H.; Knochel, P. *Chem. Commun.* **2006**, 726–728.

In 1931 PRÉVOST¹⁰⁸ discovered halogen-metal exchange as a major new route for converting organic halides into organometallic compounds. For instance, cinnamyl bromide was treated with ethylmagnesium bromide to furnish cinnamylmagnesium bromide. During the early development of this method, the inherent efficiency of the I–Li exchange process was recognized and successfully utilized. The group of WITTIG was the first to report a halogen-metal exchange by bromine-lithium exchange of 1,3-dimethoxy-4,6-dibromobenzene with phenyllithium in 1938 pictured in scheme 2.4.¹⁰⁹ Shortly thereafter, GILMAN reported his independent discovery of the halogen-lithium exchange.¹¹⁰



Scheme 2.4: Wittig's first identified halogen-lithium exchange.

The low functional group tolerance of organolithium species made exchange reactions with other metals desirable. A remarkable discovery was achieved by KNOCHEL and co-workers in 2004¹¹¹: *i*PrMgCl · LiCl was synthesized by complexing the known exchange reagent *i*PrMgCl with one equivalent of LiCl. This new reagent called "Turbo Grignard" increases reaction rates dramatically and makes high-yielding preparations of a broad range of functionalized aryl- and heteroarylmagnesium species possible (see scheme 2.5).



Scheme 2.5: Preparation of functionalized arylmagnesium reagents and subsequent trapping with an electrophile; FG = F, Cl, Br, CN, CO₂R, OMe.

2.1.1.3 Transmetalation

Transmetalation reactions offer another pathway towards organometallic reagents. When a magnesium or lithium organometallic species is treated with another metal, the more stable carbon–metal bond forms. The driving force of this metathesis is the formation of the most covalent bond, for example it is possible to transmetalate an organolithium reagent using ZnCl₂, whereas the other way round it is not possible with LiCl and a zinc organyl. A major advantage lies in the preparation of relatively stable organometallic species, therefore enabling the use of sensitive scaffolds and tolerating various functional groups. Commonly used metal salts for transmetalation are MgCl₂, ZnCl₂ and CuCN. The resulting newly formed magnesium, zinc and copper species are often required for specific synthetic protocols such as NEGISHI cross-couplings.

Furthermore, in the presence of a zinc salt and lithium chloride, magnesium inserts into the carbon bromine bond of ethyl 4-bromobenzoate and is then rapidly transmetalated to

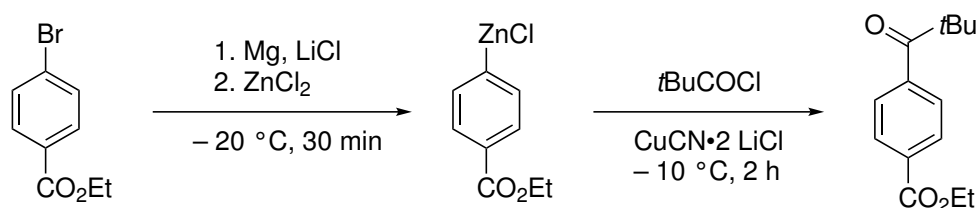
¹⁰⁸Prévost, C. *Bull. Soc. Chim. Fr.* **1931**, *49*, 1372–1381.

¹⁰⁹Wittig, G.; Pockels, U.; Dröge, H. *Chem. Ber.* **1938**, *71*, 1903–1912.

¹¹⁰Gilman, H.; Langham, W.; Jacoby, A. L. *J. Am. Chem. Soc.* **1939**, *61*, 106–112.

¹¹¹Krasovskiy, A.; Knochel, P. *Angew. Chem. Int. Ed.* **2004**, *43*, 3333–3336.

the more stable zinc species, which after copper-mediated acylation with pivaloyl chloride leads to the ketone (see scheme 2.6).¹¹²



Scheme 2.6: Magnesium insertion followed by *in situ* transmetalation to zinc and subsequent trapping with *t*BuCOCl.

2.1.1.4 Directed Metalation

The previous methods discussed in subsection 2.1.1.1 and 2.1.1.2 represent carbon-halogen functionalizations, thus starting materials containing halides. This moiety is not necessary for base-mediated directed metalations because a direct deprotonation of substrates occurs leading to a better atom-economy. Pioneering work by GILMAN¹¹³ and WITTIG¹¹⁴ paved the way for further investigations by SНИЕCKUS¹¹⁵, HAUSER¹¹⁶, EATON¹¹⁷ and MULZER¹¹⁸. The fourth important pathway toward organometallic compounds traditionally uses amide bases with one of its most prominent examples lithium diisopropylamide (LDA)¹¹⁹ or alkyl organometallics (*n*-BuLi/*sec*-BuLi etc.). These amide bases however tend to form aggregates and often react sluggishly, thus requiring a large excess of metalating reagent. Due to their high reactivity, their strong nucleophilicity, and their low functional group tolerance they often suffer under undesired side reactions. Another massive drawback is the low stability of organolithium reagents at ambient temperature. Thus, low temperatures (–78 to –100 °C) are often necessary to avoid decomposition. Furthermore, a major drawback is their selectivity because usually there is more than one C–H bond in a substrate. Consequently, the development of sophisticated reagents controlling the regioselectivity is essential.

A breakthrough for metalation chemistry came with the mixed lithium magnesium base TMPMgCl · LiCl¹²⁰ and mixed lithium zinc base TMPZnCl · LiCl¹²¹ (TMP = Tetramethylpiperidin) shown in scheme 2.7.

¹¹²Klatt T.; Markiewicz J. T.; Sämann C.; Knochel P. *J. Org. Chem.* **2014**, *79*, 4253–4269.

¹¹³Gilman H.; Bebb R. L. *J. Am. Chem. Soc.* **1939**, *61*, 109–112.

¹¹⁴Wittig G.; Fuhrmann G. *Ber. Dtsch. Chem. Ges.* **1940**, *73*, 1197–1218.

¹¹⁵Snieckus V. *Chem. Rev.* **1990**, *90*, 879–933.

¹¹⁶Hauser C. R.; Walker H. G. *J. Am. Chem. Soc.* **1947**, *69*, 295–297.

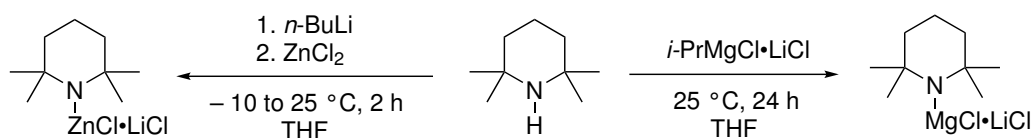
¹¹⁷Eaton P. E.; Lee C. H.; Xiong Y. *J. Am. Chem. Soc.* **1989**, *111*, 8016–8018.

¹¹⁸Schlecker W.; Huth A.; Ottow E.; Mulzer J. *J. Org. Chem.* **1995**, *60*, 8414–8416.

¹¹⁹Hamell H.; Levine R. *J. Org. Chem.* **1950**, *15*, 162–168.

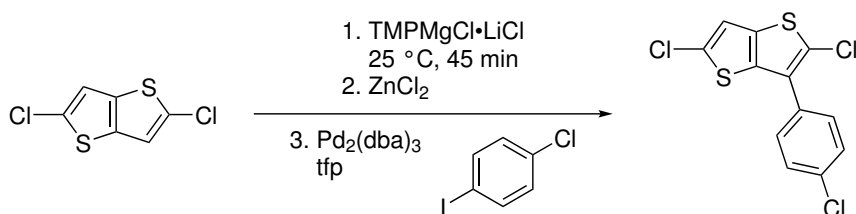
¹²⁰Krasovskiy, A.; Krasovskaya, V.; Knochel, P. *Angew. Chem. Int. Ed.* **2006**, *45*, 2958–2961.

¹²¹(a) Mosrin M.; Knochel P. *Org. Lett.* **2009**, *11*, 1837–1840. (b) Bresser T.; Monzon G.; Mosrin M.; Knochel P. *Org. Process Res. Dev.* **2010**, *14*, 1299–1303.



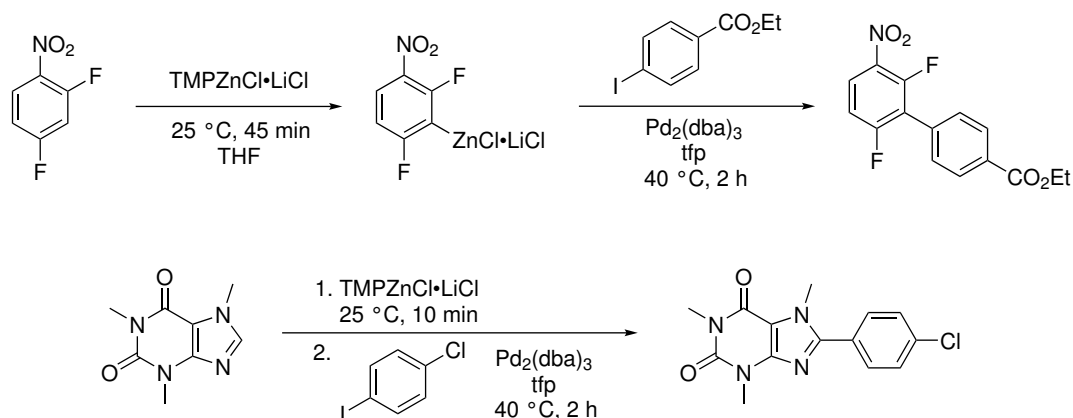
Scheme 2.7: Synthesis of TMP-derived bases.

They combine superior kinetic basicity, high solubility in THF, excellent stability of the solutions and high functional group tolerance at convenient conditions. Similarly as in the case of $i\text{-PrMgCl} \cdot \text{LiCl}$ earlier mentioned, the lithium chloride breaks up the aggregates and therefore provides a kinetically highly reactive base. Another advantage is their easy access out of 2,2,6,6-tetramethylpiperidine. Several variations of these bases such as $(\text{TMP})_2\text{Zn}_2 \cdot \text{MgCl}_2 \cdot 2 \text{LiCl}$ have been investigated.¹²² Typically applied synthesis procedures are shown below: Scheme 2.8 shows a regioselective metalation of 2,5-dichlorothiopheno[3,2b]thiophene with $\text{TMPMgCl} \cdot \text{LiCl}$ followed by subsequent chemoselective NEGISHI cross-coupling with 1-chloro-4-iodobenzene.¹²³



Scheme 2.8: Metalation with $\text{TMPMgCl} \cdot \text{LiCl}$ and subsequent NEGISHI cross-coupling.

As shown in scheme 2.9 directed zincation of 2,4-difluoro-1-nitrobenzene with $\text{TMPZnCl} \cdot \text{LiCl}$ and again subsequent NEGISHI cross-coupling delivers the ester. Interestingly, the more sophisticated heterocycle caffeine was also metalated and followed the same reaction protocol.¹²⁴



Scheme 2.9: Metalation with $\text{TMPZnCl} \cdot \text{LiCl}$ and subsequent NEGISHI cross-coupling.

¹²²(a) Wunderlich S. H.; Knochel P. *Angew. Chem. Int. Ed.* **2007**, *46*, 7685–7688. (b) Wunderlich S. H.; Knochel P. *Org. Lett.* **2008**, *10*, 4705–4707.

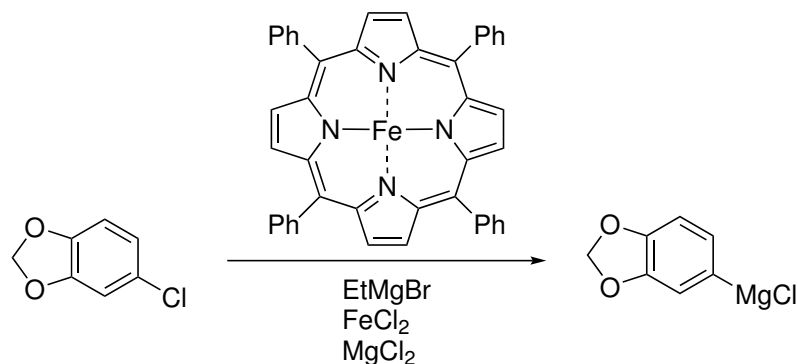
¹²³Kunz T.; Knochel P. *Chem. – Eur. J.* **2011**, *17*, 866–872.

¹²⁴Mosrin M.; Knochel P. *Org. Lett.* **2009**, *11*, 1837–1840.

2.1.2 The Role of Catalytic Metalation

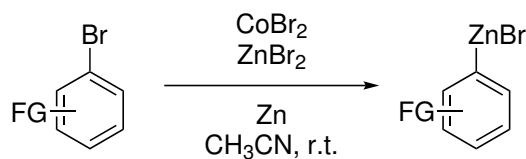
2.1.2.1 Transition Metal-Catalyzed Metal Insertions: Aryl Halides

The generation of organometallic species is also possible catalyzed by transition metals or complexes thereof. In 2000, BOGDANOVIĆ discovered a preparation method of Grignard compounds catalyzed by iron, manganese, cobalt and copper porphyrin complexes.¹²⁵



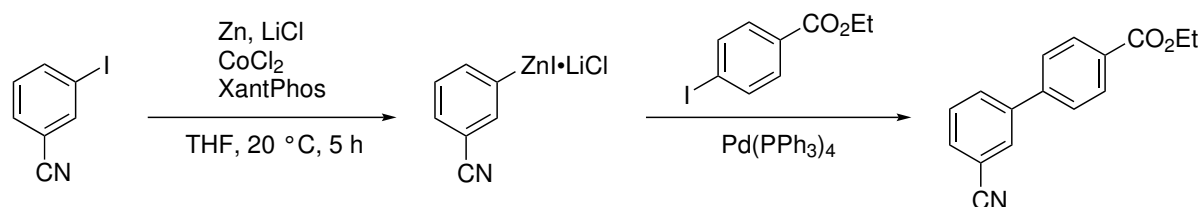
Scheme 2.10: Iron-catalyzed GRIGNARD formation.

GOSMINI further showed that various polyfunctional arylzinc reagents can efficiently be prepared under Co-catalysis using cobalt halides (see scheme 2.11).¹²⁶



Scheme 2.11: Cobalt-catalyzed zinc insertion into aryl bromide.

Furthermore, YOSHIKAI has reported that CoCl_2 catalyzes the zinc insertion into various aryl halides which can subsequently undergo Pd-catalyzed cross-couplings.¹²⁷ Thus, 3-iodobenzonitrile is converted into the corresponding zinc reagent and provides in a NEGISHI coupling the expected biphenyl (see scheme 2.12).



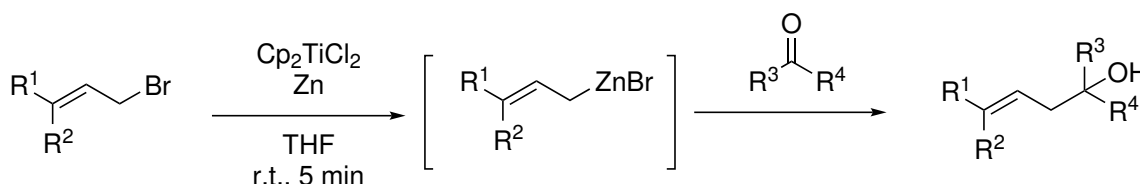
Scheme 2.12: Cobalt-catalyzed zinc insertion into an aryl iodide and subsequent NEGISHI coupling.

¹²⁵Bogdanović, B.; Schwickardi, M. *Angew. Chem. Int. Ed.* **2000**, *39*, 4610–4612.

¹²⁶(a) Kazmierski I.; Gosmini C.; Paris J. M.; Périchon J. *Tetrahedron Lett.* **2003**, *44*, 6417–6420. (b) Gosmini C.; Amatore M.; Claudel S.; Périchon J., *Synlett* **2005**, *14*, 2171–2174. (c) Fillon H.; Gosmini C.; Périchon J. *J. Am. Chem. Soc.* **2003**, *125*, 3867–3870.

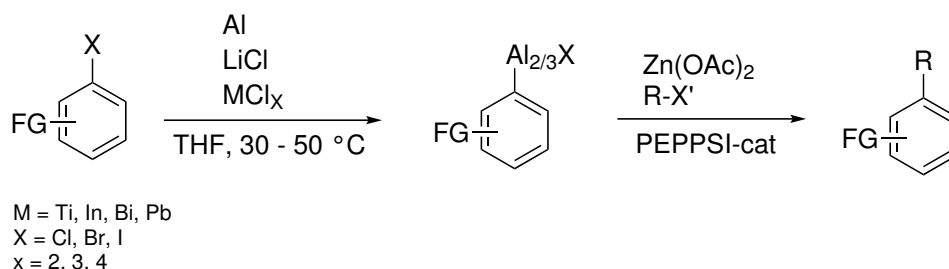
¹²⁷Jin M. Y.; Yoshikai N. *J. Org. Chem.* **2011**, *76*, 1972–1978.

The preparation of polyfunctional organozinc halides is also possible by catalytic systems consisting of InCl_3 or $\text{In}(\text{acac})_3$, respectively, and LiCl . The insertion to a range of aryl, heteroaryl and alkyl bromides proceeds smoothly in THF/DMPU (1:1) at 50 °C.¹²⁸ Furthermore, in 2009 ASHFELD presented a titanium-catalyzed activation of alkyl halides.¹²⁹ A mild protocol was developed where an alkyl halide is catalytically activated by the titanocene complex and subsequent transmetalation furnishes the active organometallic species which then undergoes an addition to carbonyl derivatives (see scheme 2.13).



Scheme 2.13: Titanium-catalyzed zinc insertion into alkyl bromides and subsequent addition to carbonyl derivatives.

Furthermore, group 13 elements are also able to form organometallic species. The synthesis of functionalized organoaluminums by direct insertion of aluminium into aryl halides is made possible with metal chlorides (TiCl_4 , BiCl_3 , InCl_3 or PbCl_2). Of course, these species are readily available for further coupling reactions after transmetalation with zinc acetate.¹³⁰



Scheme 2.14: Metal-catalyzed aluminum insertion into aryl halides and subsequent transmetalation and cross-coupling.

A similar protocol was investigated for the generation of organoindium species. Direct insertion of indium is made possible in the presence of LiCl and/or cobalt-bathophenanthroline or LiI , respectively.¹³¹

Interestingly, direct metal insertion is also possible via addition of a catalytic amount of C_{60} -fullerene (3 mol%) and a mixture of commonly used metal salts (see scheme 2.15).

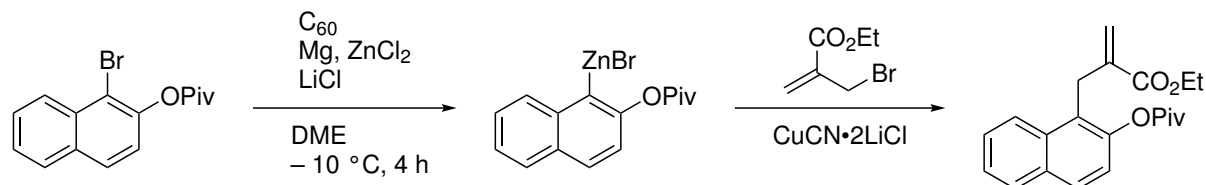
¹²⁸(a) Klatt, T.; Blümke, T.; Ganiek, M.; Knochel, P. *Synthesis* **2013**, *46*, 290–294. (b) Benischke, A. D.; Le Corre, G.; Knochel, P. *Chem. Eur. J.* **2017**, *23*, 778–782.

¹²⁹Fleury, L. M.; Ashfeld, B. L. *Org. Lett.* **2009**, *11*, 5670–5673.

¹³⁰Blümke, T.; Chen, Y.-H.; Peng, Z.; Knochel, P. *Nat. Chem.* **2010**, *2*, 313–318.

¹³¹(a) Chen, Y.-H.; Knochel, P. *Angew. Chem. Int. Ed.* **2008**, *47*, 7648–7651. (b) Adak, L.; Yoshikai, N. *J. Org. Chem.* **2011**, *76*, 7563–7568. (c) Chen B.; Zhi B.; Wang C.; Chu X.; Shen Z.; Loh T. *Org. Lett.* **2018**, *20*, 1902–1905.

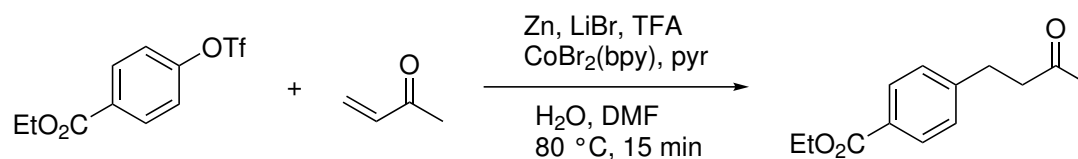
1-bromonaphthalen-2-yl pivalate was converted to the corresponding organozinc reagent at $-10\text{ }^{\circ}\text{C}$ within 4 h reaction time. Under the same conditions, in the absence of C_{60} -fullerene, only a poor conversion was obtained ($<5\%$). Subsequently, the organozinc reagent efficiently reacts in a copper-catalyzed allylation with allylic bromide.¹³²



Scheme 2.15: C_{60} -fullerene-catalyzed zinc insertion into an aryl bromide and subsequent allylation.

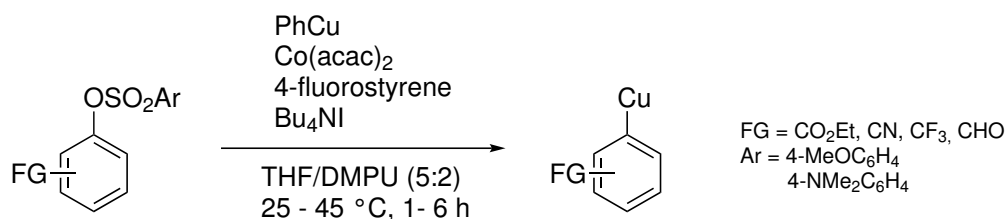
2.1.2.2 Transition Metal-Catalyzed Metal Insertions: Non-Halogen Leaving Groups

In terms of green chemistry the use of non-halogen leaving groups is inevitable. The following procedure avoid the use of halides such as bromides and iodides. In scheme 2.16 no prior formation of sensitive organometallic species is necessary and a cobalt-catalyzed direct conjugate addition of aryl triflates to methyl vinyl ketone took place.¹³³



Scheme 2.16: Cobalt-catalyzed conjugate addition of an activated aryl triflate to methyl vinyl ketone.

Copper-catalyzed reactions and functionalized copper reagents are by now common synthetic elements in modern organometallic chemistry. Their preparation relies on their corresponding aryl bromides or iodides. KNOCHEL and co-workers found a cobalt-catalyzed sulfonate/copper exchange reaction.¹³⁴



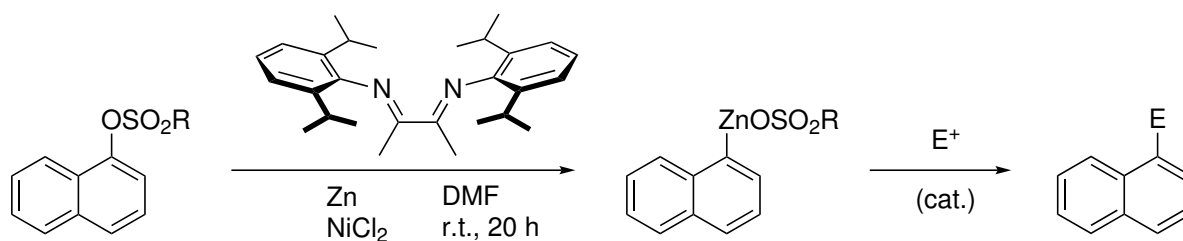
Scheme 2.17: Cobalt-catalyzed aryl sulfonate/copper exchange reaction.

¹³²Shen Z.; Knochel P. *ACS Catal.* **2015**, *5*, 2324–2328.

¹³³Amatore, M.; Gosmini, C. *Synlett* **2009**, *7*, 1073–1076.

¹³⁴Rohbogner C. J.; Diéne C. R.; Korn T. J.; Knochel P. *Angew. Chem. Int. Ed.* **2010**, *49*, 1874–1877.

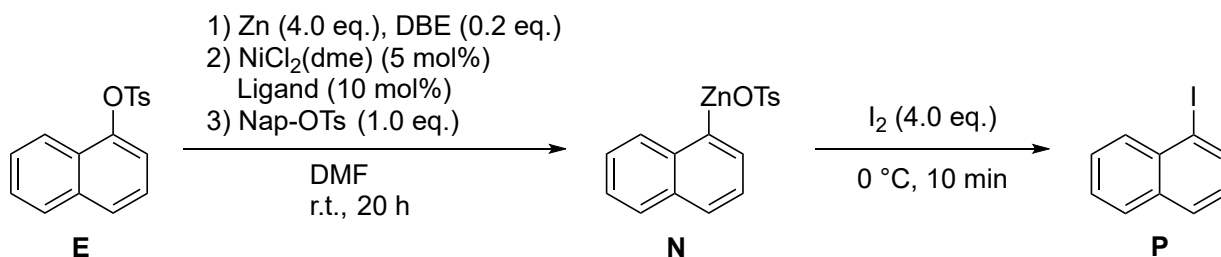
The generation of organozinc reagents typically relies on the direct insertion of zinc into the C–X bond of aryl or alkyl bromides or iodides. HINTERMANN and co-workers recently published a catalytic zincation protocol of aryl sulfonates.⁶² The synthesis proceeds via a NiCl₂-1,4-diazadiene catalyst system (1,4-diazadiene stands for diacetyl diimines, phenanthroline, bipyridine and related ligands).



Scheme 2.18: Nickel-catalyzed zincation of aryl tosylates.

2.2. Aims and Objectives

As shown in section 2.1.1 there exist several methods to synthesize organometallic compounds, for example oxidative addition or halogen metal exchange. Another pathway gaining more and more attraction is the catalytic metalation of substrates illustrated in section 2.1.2. The current chapter focuses on the generation of organozinc reagents (**N**) by nickel diazadiene complex catalyzed zinc insertion into aryl sulfonates (**E**), a methodology introduced by our working group and described in scheme 2.19.⁶²



Scheme 2.19: Nickel-catalyzed zincation of aryl tosylates.

In the first part the synthesis of aryl tosylates and ligands according to literature known procedures is conducted for testing in the catalytic metalation. The second part consists of an extensive ligand screening of several diazadienes. The core structure of these ligands is shown in figure 2.1. The aniline-derived *N*-aryl group is substituted with alkyl or halide substituents and the diimine backbone is built up from either 1,2-dicarbonyl compounds glyoxal, diacetyl or acenaphthenequinone. Additionally, alternative ligand structures incorporating pyridines, quinazolines, pyrazoles or isoindolines are tested.

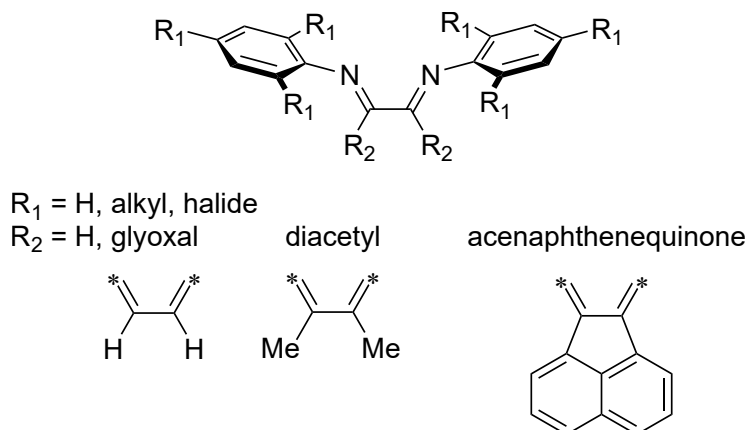


Figure 2.1: Ligand core structure for 1,4-diazadienes used in Ni-catalyzed zincation.

In the third part the catalytic metalation is tested with a bimetallic catalyst system: Instead of combining the established $\text{NiCl}_2(\text{dme})$ precatalyst with a free 1,4-diazadiene ligand, a second metal complex is added: Namely, the macrocyclic biquinazoline Mabiq with either nickel, copper, cobalt or iron as central metal atom, where an *in situ* catalyst may be formed by coordination of NiCl_2 at the ligand periphery (Fig. 2.2).

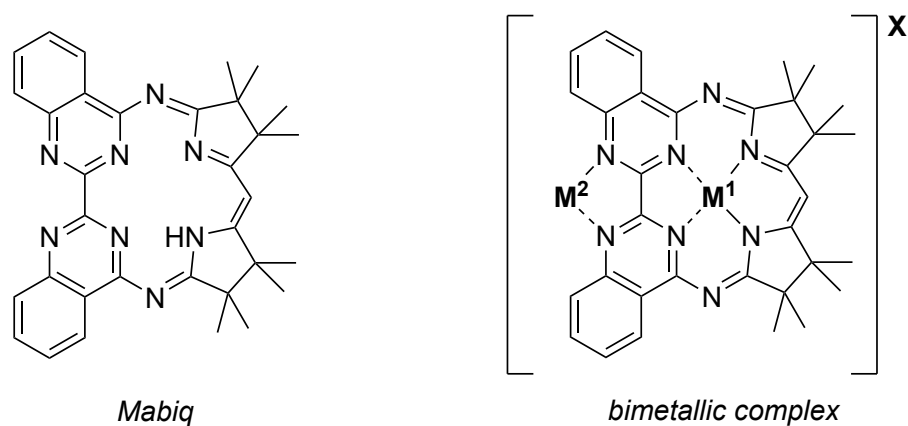
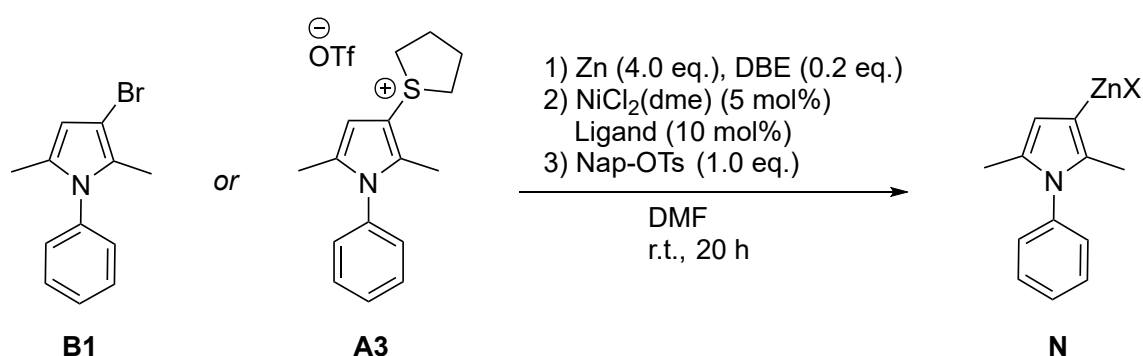


Figure 2.2: General structure of Mabiq and bimetallic complexes thereof. $M_1 = \text{Ni, Cu, Co, Fe}$. $M_2 = \text{Ni}$. $X = \text{OTf, Cl, PF}_6$.

In the fourth part the influence of general reaction parameters on reaction outcome are investigated, as for example the effect of excess equivalents of zinc. Furthermore, effects of additives such as lithium chloride^{103,135}, SOCl_2 , or trimethyl orthoformate (TMOF) are tested. A reaction progress study of tosylate consumption and organozinc formation is conducted.

In the fifth part the catalytic zincation conditions are applied to bromopyrrole **B1** and pyrrole sulfonium salt **A3** with the aim of generating zinc nucleophile **N** as depicted in scheme 2.20.



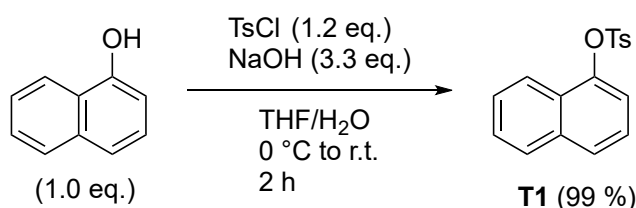
Scheme 2.20: Nickel-catalyzed zincation of bromopyrrole **B1** and sulfonium salt **A3**.

¹³⁵(a) Feng, C.; Cunningham, D. W.; Easter, Q. T.; Blum, S. A. *J. Am. Chem. Soc.* **2016**, *138*, 11156–11159. (b) Jess, K.; Kitagawa, K.; Tagawa, T. K. S.; Blum, S. A. *J. Am. Chem. Soc.* **2019**, *141*, 9879–9884.

2.3. Results and Discussion

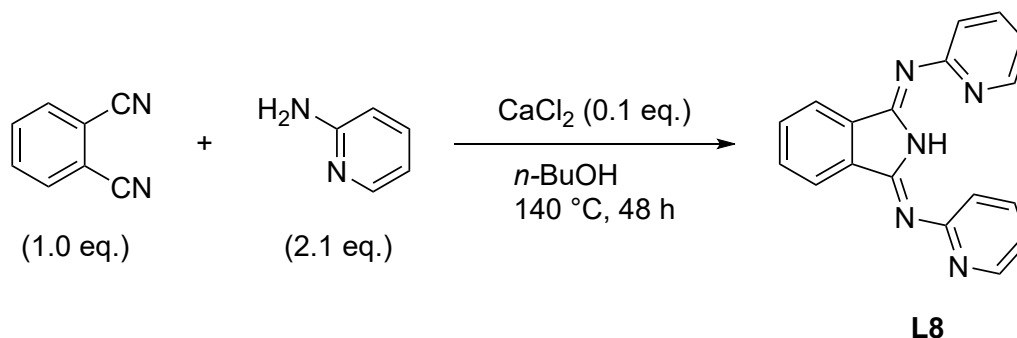
2.3.1 Synthesis of Tosylates and Ligands

The synthesis of model tosylate **T1** as substrate in the catalytic zincation is conducted according to a literature procedure.⁷² The sulfonylation of 1-naphthol takes place in an economically benign manner in a non-halogenated solvent mixture (THF/H₂O) with the cheap base NaOH. Typically, prevailing methods include DCM and triethylamine or pyridine as base.⁷³ Additionally, the isolation of the products occurs chromatography-free and in stoichiometric yield. Unless mentioned otherwise in the following sections, the corresponding aryl tosylates were previously synthesized and were available for subsequent reactions.



Scheme 2.21: Synthesis of aryl tosylate **T1**. Yield from isolated product.

The synthesis of ligand **L8** is conducted according to the procedure from GOGOI et. al.¹³⁶ Alkaline earth salt CaCl₂ apparently acts as weak LEWIS acid and activates the nitrile which facilitates the nucleophilic addition of the primary aromatic amine pyridin-2-amine yielding isoindoline-1,3-diimine **L8** (see scheme 2.22).



Scheme 2.22: Synthesis of ligand **L8**. Yield refers to isolated product.

If not mentioned otherwise in the following sections, the corresponding ligands were previously synthesized within the research group and were available for subsequent reactions.

¹³⁶(a) Siegl, W. O. *J. Org. Chem.* **1977**, *42*, 1872–1878. (b) Gogoi, K.; Saha, S.; Mondal, B.; Deka, H.; Ghosh, S.; Mondal, B. *Inorg. Chem.* **2017**, *56*, 14438–14445.

2.3.2 Ligand Screening

In this section the study of ligand effects upon the performance of Ni-catalyzed zincation of aryl sulfonates is described. The diimine backbone is built up of glyoxal, diacetyl or acenaphthenequinone and is substituted with aniline derivatives which contain isopropyl, methyl or halide substituents (see figure 2.3). Additionally, alternative structural motifs such as isoindolines fused with pyridins or isopropylimines and pyridin with pyrazole are of interest. These ligand structures differ in their steric demand and electronic structure.

2.3.2.1 The Class of *N*-2,6-Diisopropylphenyl substituted Diazadienes

In this subsection the following ligands are tested: **L1** DIPA-^{Me}DAD which stands for diisopropylaniline diazadiene with methyl groups in the backbone, **L2** DIPA-^{HMe}DAD for diisopropylaniline diazadiene with H and methyl groups, **L3** DIPA-^{Et}DAD for diisopropylaniline diazadiene with ethyl groups, **L4** DIPA-^{ANQ}DAD for diisopropylaniline diazadiene with acenaphthoquinone backbone, **L5** DIPA-^HQUI for diisopropylaniline imine with quinoline, **L6** DIPA-^HPYR for diisopropylaniline imine with pyridine and **L7** DIPA-^{Ph}IPK as a mixed ketoimine ligand. The chemical structures are depicted in figure 2.3.

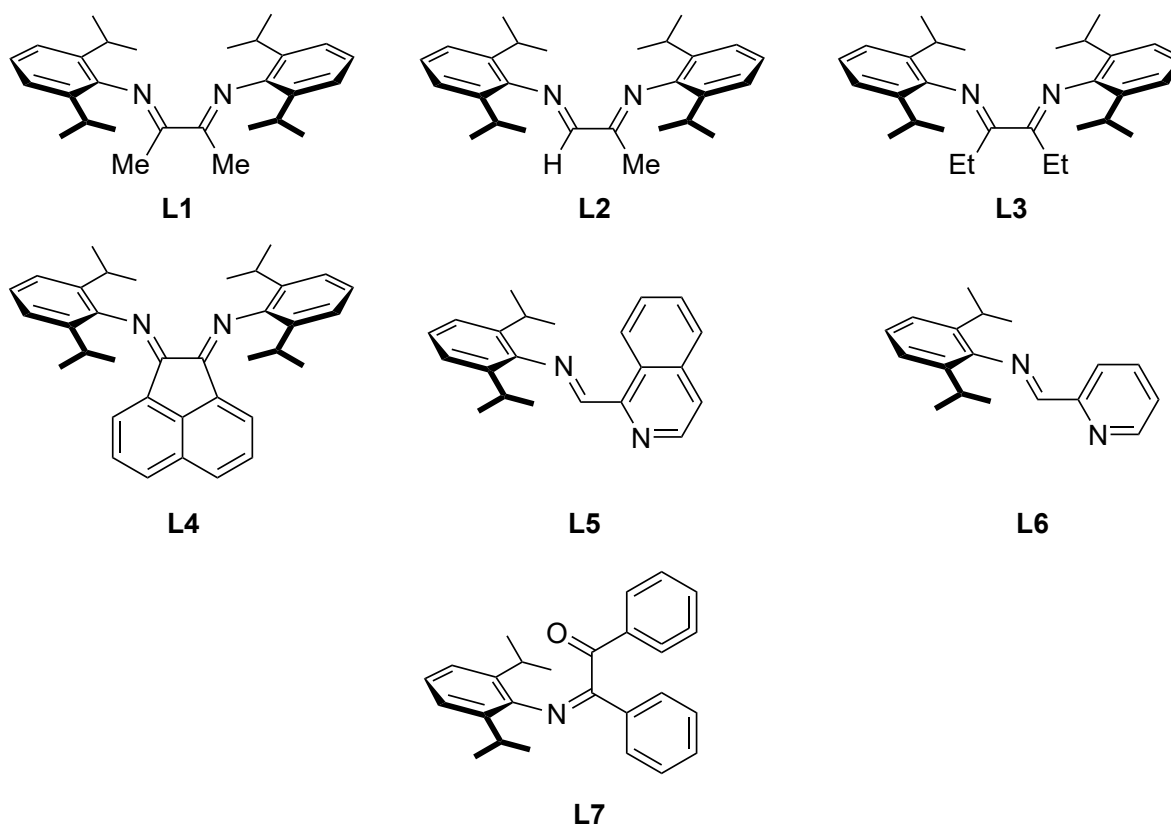


Figure 2.3: Ligands of the class of *N*-2,6-diisopropylphenyl substituted diazadienes.

Table 2.2 shows the results of the screening by listing the composition of the reaction mixture. Entry 1 shows results for the already tested ligand **L1**. The similar ligand **L2** where only one methyl group is changed to a hydrogen in the backbone works almost as good. Surprisingly, ligand **L3** with ethyl groups at the imine backbone shows no conversion (92 % aryl tosylate recovered). Apparently, the alkyl side chain cannot be longer than methyl. **L4** with an acenaphthoquinone backbone displays very low activity. Substituting one diisopropylaniline unit of the diazadiene with heteroaryls quinoline (**L5**) and pyridin (**L6**) provides highly active catalysts. Only traces of starting material could be detected. These ligands might be useful for future applications, for example for aryl tosylates where standard ligand **L1** induces insufficient catalytic activity. Alternative ligand structure **L7** was completely inactive in this catalysis, this might be due to the oxygen which interferes with the coordination to the nickel center.

Table 2.2: Screening of ligands for catalytic zincation.

#	Ligand	Ar-OTs	Ar-H	Ar-OH	Ar-Ar	Ar-I	Recovery
1	L1: DIPA- ^{Me} DAD	0	2	0	0	97	99
2	L2: DIPA- ^{HMe} DAD	0	4	0	0	93	99
3	L3: DIPA- ^{Et} DAD	92	0	0	0	0	92
4	L4: DIPA- ^{ANQ} DAD	79	0	0	0	20	99
5	L5: DIPA- ^H QUI	1	3	0	0	95	99
6	L6: DIPA- ^H PYR	4	6	0	3	86	99
7	L7: DIPA- ^{Ph} IPK	98	0	0	0	0	98

Yields are given in percentage and were determined by qNMR-analysis. Reaction component analysis in mol% relative to initial **T1**.

Recovery is the sum of analytically detected compounds with Ar groups.

2.3.2.2 The Class of Pyridyl and Pyrazolyl Isoindoline Ligands

Here, **L8** DPYR-^HIND which stands for dipyrindyl isoindoline diimine, **L9** DPYR-^HPYR for dipyrazol pyridine and **L10** DIPI-^HIND for diisopropyl isoindoline diimine are tested. The ligand structures are shown in figure 2.4.

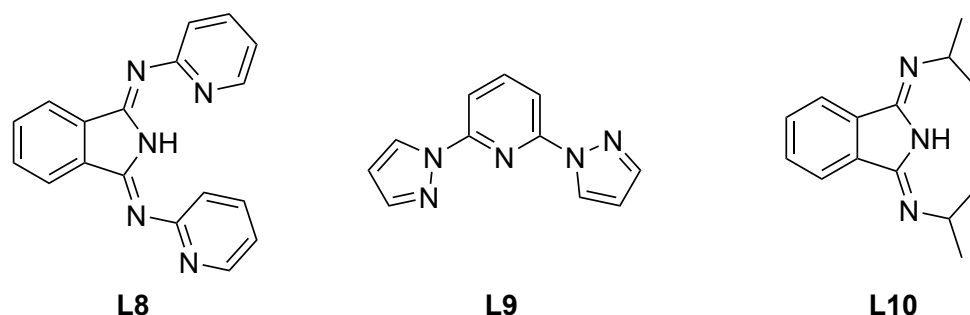


Figure 2.4: Ligands of the class of pyridyl and pyrazolyl isoindolines.

This class of ligands generally does not work very well (see table 2.3). The isoindoline ligands **L8** in entry 1 and **L10** in entry 3 show no conversion of the starting tosylate. This tridentate coordination pattern and electronic environment seemingly is incompatible with this reaction. Only ligand **L9** with the pyridin-bridged pyrazoles offers a low conversion. The multidentate structure and absence of a N–H donor might enable a coordination to the catalytic nickel center.

Table 2.3: Screening of ligands for catalytic zincation.

#	Ligand	Ar-OTs	Ar-H	Ar-OH	Ar-Ar	Ar-I	Recovery
1	L8: DPYR- ^H IND	89	0	0	0	0	89
2	L9: DPYR- ^H PYR	68	14	0	0	17	99
3	L10: DIPI- ^H IND	93	0	0	0	0	93

Yields are given in percentage and were determined by qNMR-analysis. Reaction component analysis in mol% relative to initial **T1**.

Recovery is the sum of analytically detected compounds with Ar groups.

2.3.2.3 The Class of Mesitylamine derived Diazadiene Ligands

In this section the two mesitylamine derived diazadienes **L11** MESA-^{Me}DAD which stands for mesitylamine diazadine with methyl substituents and **L12** MESA-^{ANQ}DAD for mesitylamine diazadine with acenaphthoquinone backbone are tested (figure 2.5).

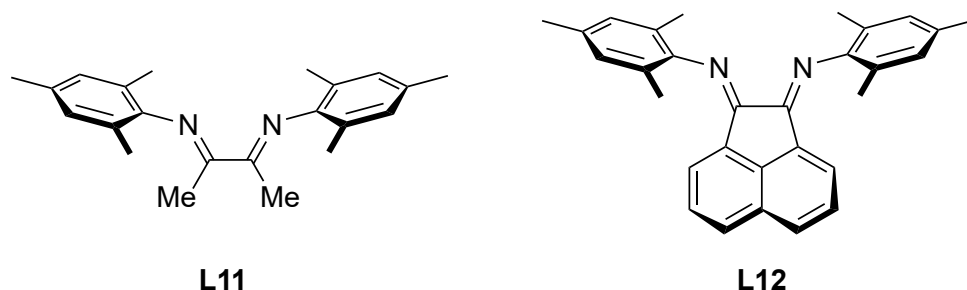


Figure 2.5: Ligands of the class of mesitylamine derived diazadines.

Both ligands provide almost the same conversion and amount of product formed (87 % and 88 %) and therefore they also qualify for further utilization. Whereas ligand **L4** also bearing an acenaphthoquinone backbone delivers only 20 % of product, the result with **L12** shows that the ANQ backbone need not to be excluded from ligand development.

Table 2.4: Screening of ligands for catalytic zincation.

#	Ligand	Ar-OTs	Ar-H	Ar-OH	Ar-Ar	Ar-I	Recovery
1	L11: MESA- ^{Me} DAD	2	7	0	0	87	96
2	L12: MESA- ^{ANQ} DAD	6	3	0	0	88	97

Yields are given in percentage and were determined by qNMR-analysis. Reaction component analysis in mol% relative to initial **T1**.

Recovery is the sum of analytically detected compounds with Ar groups.

2.3.2.4 The Class of *N*-2,6-Dihaloaryl Diazadiene Ligands

The last tested class comprises ligand **L13** BrMe-^{Me}DAD which stands for 2,6-dibromo-4-methylaniline derived diazadiene with methyl groups and **L14** ClH-^{Me}DAD for 2,6-dichloroaniline derived diazadiene with methyl groups in the backbone.

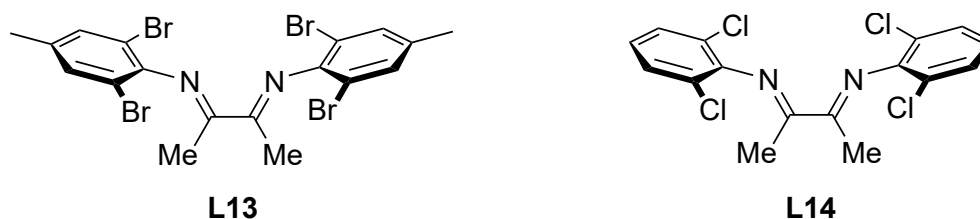


Figure 2.6: Ligands of the class of 2,6-dihaloaryl diazadienes.

Here, the quite similar structure to the mesityl aniline diazadiene with methyl substituents differs only in the 2- and 6-position of the aniline where bromide or chloride is substituted. Clearly, this distinction brings down the conversion to 53 % and 54 %, respectively. A too high amount of aryl tosylate is recovered (see table 2.5).

Table 2.5: Screening of ligands for catalytic zincation.

#	Ligand	Ar-OTs	Ar-H	Ar-OH	Ar-Ar	Ar-I	Recovery
1	L13: BrMe- ^{Me} DAD	42	0	0	0	53	95
2	L14: ClH- ^{Me} DAD	39	0	0	0	54	95

Yields are given in percentage, are average from two reactions and were determined by qNMR-analysis.

Reaction component analysis in mol% relative to initial **T1**.

Recovery is the sum of analytically detected compounds with Ar groups.

2.3.3 Bimetallic Catalysis – Role of Mabiq Complexes

The macrocyclic biquinazoline ligand Mabiq was first mentioned in 1988.¹³⁷ Since then a plethora of complexes containing this ligand have been isolated, for example with Ni,¹³⁸ Cu,¹³⁹ Co,¹⁴⁰ or Fe¹⁴¹, where the counteranion mostly consists of a triflate, chloride or hexafluorophosphate (PF₆⁻). Some of these complexes have successfully been applied in catalysis¹⁴² and other applications, as for example a light-driven MARKOVNIKOV-selective C- and N-Alkylation of indoles and indazoles.¹⁴³

The catalytic metalation with the nickel-diazadiene system poses an ideal opportunity to further incorporate this macrocyclic complex in another catalysis. The Mabiq ligand features a structural similarity to porphyrins where a metal center atom is surrounded by four nitrogen heterocycles in a conjugated system as shown in figure 2.7. Additionally, the mabiq ligands have a peripheral coordination site for another metal atom (M²). As a result a bimetallic complex is formed which could bear interesting metal-metal interactions and activity modulation in catalytic reactions.

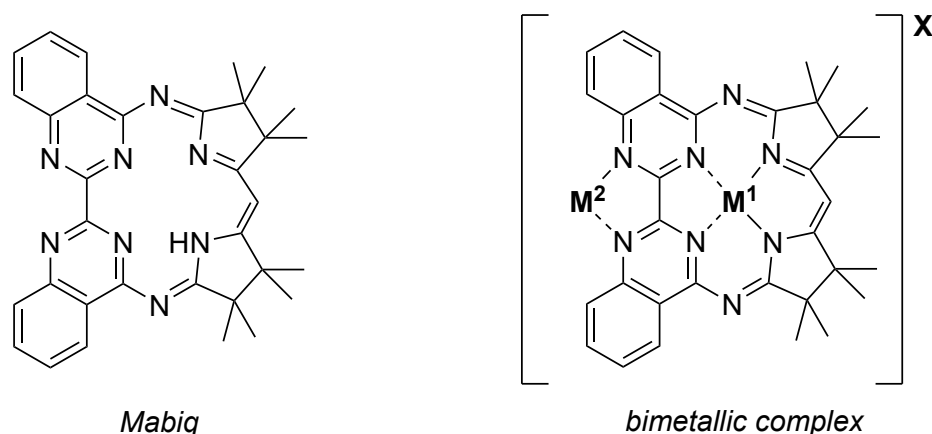


Figure 2.7: General structure of Mabiq and Mabiq complexes. M¹ = Ni, Cu, Co, Fe, M² = Ni. X = OTf, Cl, PF₆.

In table 2.6 the screening results with various mabiq complexes are shown. In entry 1 a catalytic run with a Ni(II)-mabiq complex is shown in which no additional NiCl₂(dme) was added, therefore no bimetallic catalysis could take place. There is no activity for the catalytic metalation and full recovery of the starting material. If one adds a co-catalytic amount of NiCl₂(dme) to either nickel (entry 2) or copper (entry 3) mabiq-complex, workup by iodolysis furnishes the reaction product in 63 % and 68 % yield, respectively.

¹³⁷Mueller, E.; Bernardinelli, G.; Von Zelewsky, A. *Inorg. Chem.* **1988**, *27*, 4645–4651.

¹³⁸Grübel, M.; Bosque, I.; Altmann, P. J.; Bach, T.; Hess, C. R. *Chem. Sci.* **2018**, *9*, 3313–3317.

¹³⁹Stark, H. S.; Altmann, P. J.; Sproules, S.; Hess, C. R. *Inorg. Chem.* **2018**, *57*, 6401–6409.

¹⁴⁰(a) Puttock, E. V.; Banerjee, P.; Kaspar, M.; Drennen, L.; Yufit, D. S.; Bill, E.; Sproules, S.; Hess, C. R. *Inorg. Chem.* **2015**, *54*, 5864–5873. (b) Kaspar, M.; Altmann, P. J.; Pöthig, A.; Sproules, S.; Hess, C. R. *Chem. Commun.* **2017**, *53*, 7282–7285.

¹⁴¹Banerjee, P.; Company, A.; Weyhermüller, T.; Bill, E.; Hess, C. R. *Inorg. Chem.* **2009**, *48*, 2944–2955.

¹⁴²Lauenstein, R.; Mader, S. L.; Derondeau, H.; Esezobor, O. Z.; Block, M.; Römer, A. J.; Jandl, C.; Riedle, E.; Kaila, V. R. I.; Hauer, J.; Thyraug, E.; Hess, C. R. *Chem. Sci.* **2021**, *12*, 7521–7532.

¹⁴³Esezobor, O. Z.; Zeng, W.; Niederegger, L.; Grübel, M.; Hess, C. R. *J. Am. Chem. Soc.* **2022**, *144*, 2994–3004.

The cobalt complexes in entry 4 and 5, regardless of the oxidation state, deliver less product and a higher amount of unreacted starting material when analogously combined with NiCl₂(dme) (39 % and 27 %). The best catalytic activity is obtained with an iron(II) mabiq-complex which delivers 84 % of iodinated product **P**. Generally, the amount of protonolysis product **Ar-H** is rather high, which is likely due to water contamination in the reaction system.

Table 2.6: Screening of mabiq complexes for catalytic zincation.

#	M-MABIQ	Ar-OTs	Ar-H	Ar-OH	Ar-Ar	Ar-I	Rec.
1 ^{a)}	Ni ^{II} (Mabiq)OTf	97	0	0	0	0	97
2	Ni ^{II} (Mabiq)OTf	2	31	0	0	63	96
3	Cu ^{II} (Mabiq)OTf	1	27	0	0	68	96
4	Co ^{II} (Mabiq)Cl ₂	39	22	0	0	35	96
5	Co ^I (Mabiq)Cl	27	24	0	0	47	98
6	[Fe ^{II} (Mabiq)(MeCN) ₂]PF ₆	0	7	0	0	84	91

Yields are average from two reactions, given in percentage and were determined by qNMR-analysis. ^{a)}No addition of NiCl₂(dme).

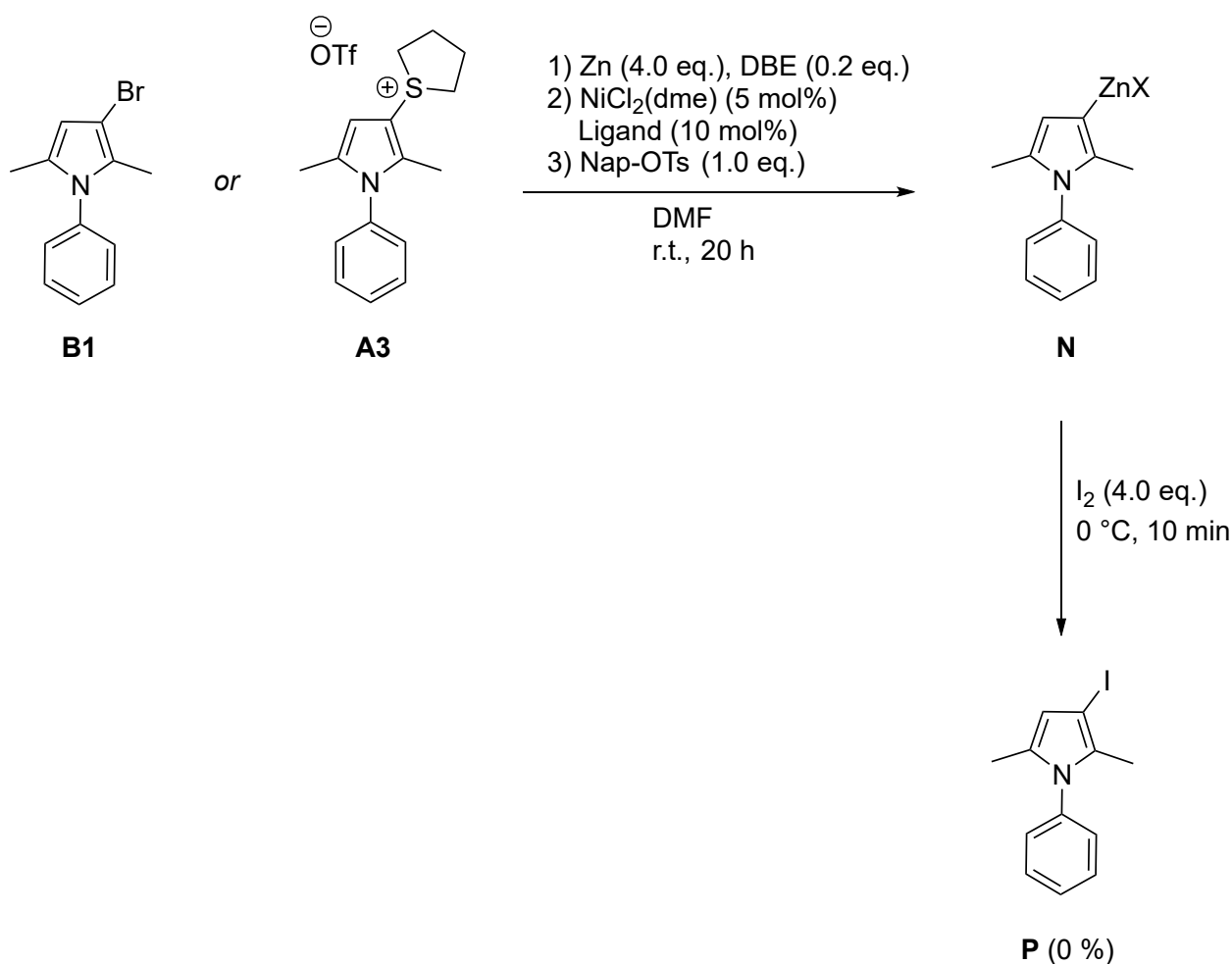
2.3.4 Optimization of Reaction Parameters

A recurring problem in the nickel-catalyzed zincation of aryl sulfonates is the contamination of the reaction system with traces of water which leads to the generation of variable amounts of ArH besides the desired aryl zinc species. This leads to reproducibility problems whenever newly synthesized precatalyst, ligand, substrates or a new solvent batch is used in the catalytic reaction. To address the problem of water contamination, the potentially beneficial effect of water binding additives was tested. In entry 1 0.1 equivalents of thionyl chloride are added to the reaction mixture. In theory, it should react with traces of water to hydrochloric acid and SO₂, but the outcome was not beneficial and the catalytic system gave inferior results with only 46 % of product and 53 % of hydrolysis side product naphthalene. The second tested additive is trimethyl orthoformate which normally is used for methoxymethylenylation or formylation, but is also an efficient dehydrating agent. Here, it should react with water to give methanol and methyl formate. The outcome in entry 2 did not yield a major improvement relative to the standard reaction conditions, and the generation of 7 % naphthalene indicates that the drying effect of this reagent is limited (91 % **P**). As mentioned earlier the addition of lithium chloride proved beneficial for many (direct) metal insertions. Entries 3 and 4 probe this concept with addition of 2.0 equivalents of LiCl at 50 °C. However, the amount of homo coupling rises to almost 20 %, and the zincation yield reduced, while the level of hydrolysis product is high. The results of those runs may have been affected by the elevated temperature. One of the best-known techniques to eliminate traces of water is the use of molecular sieves, especially for storing solvents. Addition of 0.1 g pre-dried sieves (3 Å) to the catalytic reaction delivers results comparable to those under best conditions (94 % **P**) and is therefore recommended for future use in reaction systems suffering from water contamination. The standard zincation protocol uses 4.0 equivalents of zinc which is a rather large excess and thus reduces the atom economy of the reaction. In entries 6 and 7 less equivalents are tested: 2.0 eq. deliver the same result which means that this amount can safely be used, but 1.5 eq. show an incomplete conversion of starting material. Entry 8 displays a combination of lithium chloride addition, less zinc and a shorter reaction time of 2 h and still 81 % of product **P** are furnished.

2.3.5 Catalytic Zincation of Pyrrolyl Halides and Sulfonium Salts

Since access to pyrrolyl zinc species is traditionally only possible via halogen-lithium exchange, followed by transmetalation with zinc chloride, it would be desirable to have a more direct access to pyrrolyl zinc species *via* direct insertion of zinc metal into pyrrolyl electrophiles such as halopyrroles or the readily available pyrrolyl sulfonium salts (section 1.3.4.1). Recent work in the group of YORIMITSU has in fact shown that sulfonium salts can be catalytically zincated by means of a nickel catalyst.¹⁴⁴

Therefore, we have performed cursory experiments in which the catalytic zincation protocol is applied to previously synthesized bromopyrrole **B1** and pyrrole sulfonium salt **A3**. Unfortunately, both electrophiles are incompatible with this reaction.



Scheme 2.23: Yields were determined by qNMR- and GCMS-analysis.

¹⁴⁴Minami H.; Nogi K.; Yorimitsu H. *Synlett* **2020**, 31, A–E.

2.4. Conclusion and Outlook

The screening substrate **T1** and the ligand **L8** were successfully synthesized and tested in a standardized protocol for nickel-catalyzed zincation of aryl sulfonates. A broad ligand screening resulted in two very well-working ligands (**L2** DIPA-^{HMe}DAD and **L6** DIPA-^{HQUI}) shown in figure 2.8 which give results on par with the previous reference ligand **L1**. Promising results were also obtained with ligand **L6** DIPA-^{HPYR} (86 %), **L11** MESA-^{Me}DAD (87 %) and **L12** MESA-^{ANQ}DAD (88 %). *Via* variation of the diimine backbone and the *N*-aryl group, many more combinations of ligands are available and may be investigated.

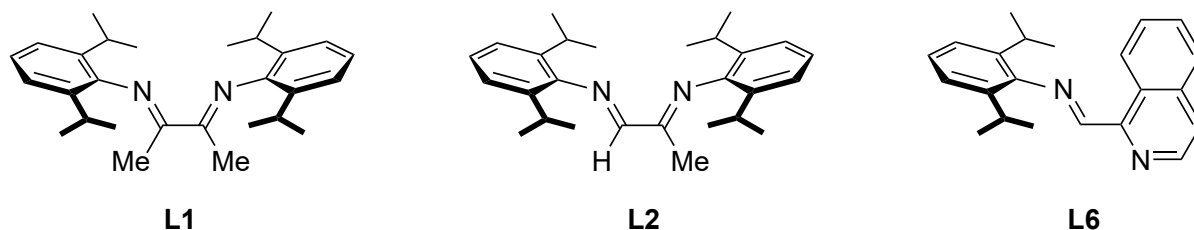


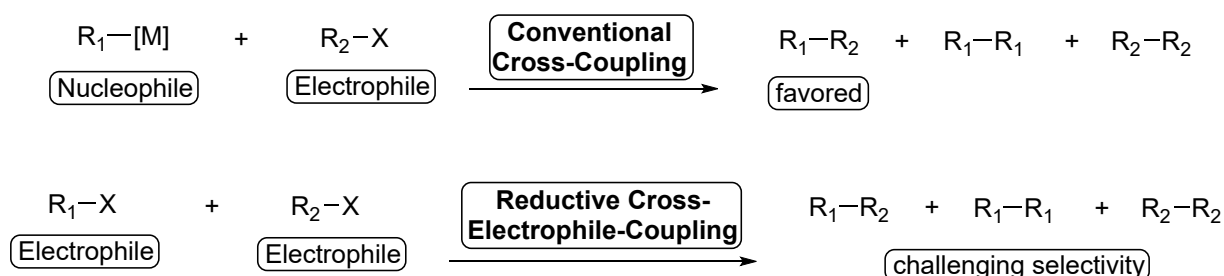
Figure 2.8: Best ligands from the screening for catalytic zincation.

The use of various metal mabiq complexes in combination with NiCl₂ in a bimetallic catalysis provided mixed results. Catalytic runs with metal mabiq complexes were in principle successful and the results clearly indicate that they act as ligands for an exometallic nickel complex, which acts as a catalyst for the zincation reaction of aryl sulfonates. However, the individual reaction runs with end-point yields do not permit a more detailed discussion of the effect of the core metal (M¹) on catalyst performance. The amount of hydrolysis product in those runs was also rather high, which is presumably due to water contamination introduced into the reaction system from unknown sources. On the other hand, the amount of metal mabiq complexes available for the current study was limited, such that more extensive catalysis studies could not be readily performed. Kinetic experiments could deliver more insights into the role of the core metal M¹ and its potential to modulate the catalytic activity of the nickel center (M²). Water contamination is a recurring problem that negatively affects the reproducibility of the catalytic zincation reaction by producing varying levels of hydrolysis product (ArH). Application of molecular sieves as additive for eliminating traces of water is possible without reduction of yield and may prove useful in future work. The catalytic zincation did not work in case of halopyrroles and pyrrolyl sulfonium salts. Generally speaking, the nickel-catalyzed zincation of aryl sulfonates makes chemoselective zincations possible and may be applied in synthesis due to the broad availability of phenols and their easy conversion into sulfonates.

3. Reductive Cross-Electrophile-Coupling involving Aryl Sulfonates

3.1. Introduction – No Need for Carbon Nucleophiles – An Alternative to Conventional Cross-Coupling

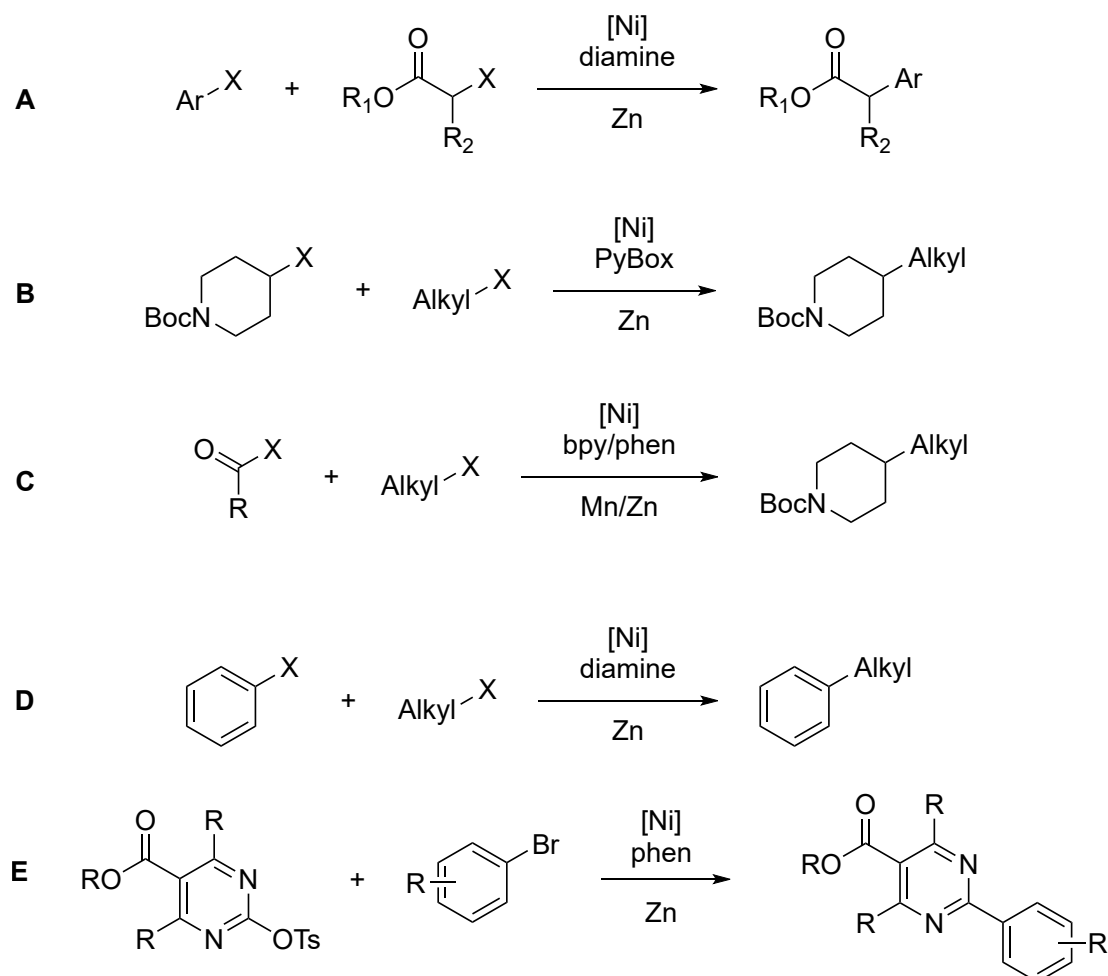
Undoubtedly, transition metal-catalyzed cross-coupling reactions have undergone an impressive development in the last decades and represent an indispensable tool for the creation of C–C bonds. Catalytic methods avoiding the challenges of preformed carbon nucleophiles are of great interest due to skipping instable organometallic species and time-consuming prior preparations. Reactions between two bench stable electrophiles – like ready available organic halides – under reductive conditions have seen a rapid development as powerful tool for cross-coupling sequences.¹⁴⁵ In particular, nickel catalysts, characterized by low reduction potential, can undergo rapid oxidative addition. However, due to their chemical similarity both electrophiles are prone to undergo oxidative addition with low chemoselectivity. In case of aryl sulfonates their inherent low reactivity may constitute another serious drawback. Scheme 3.1 illustrates the differences between conventional cross-coupling reactions with a nucleophile and an electrophile where there is a distinct favored product, and reductive cross-electrophile couplings. Therefore, optimizing selectivity and minimizing side reactions, for instance homocoupling, are major goals of such research.



Scheme 3.1: Comparison of conventional redox-neutral cross-couplings and reductive cross-electrophile couplings.

¹⁴⁵(a) Everson, D. A.; Weix, D. J. *J. Org. Chem.* **2014**, *79*, 4793–4798. (b) Moragas, T.; Correa, A.; Martin, R. *Chem. Eur. J.* **2014**, *20*, 8242–8258. (c) Everson, D. A.; Jones, B. A.; Weix, D. J. *J. Am. Chem. Soc.* **2012**, *134*, 6146–6159. (d) Weix, D. J. *J. Acc. Chem. Res.* **2015**, *48*, 1767–1775.

The straightforward homocoupling of electrophiles has been known for over 150 years. The first example was published by WURTZ¹⁴⁶ and TOLLENS and FITTIG¹⁴⁷ using stoichiometric amounts of sodium metal as the reducing agent and elevated temperatures. Besides homocoupling, the cross-coupling of aryl halides with alkyl halides was also realized. The first disclosure of Ni-mediated reductive homocoupling of halide electrophiles was by SEMMELHACK in 1971.¹⁴⁸ Recently, this coupling method has seen many new developments as depicted in scheme 3.2. A seminal report by DURANDETTI and coworkers¹⁴⁹ employed an α -haloester with an aryl halide. This cross-coupling is effected by a catalytic Ni(II) source and stoichiometric Zn metal (Scheme A). This finding has been extended by the groups of WEIX, GONG, and MOLANDER with new couplings employing many C(sp²) (aryl, vinyl, acyl) and C(sp³) coupling partners (Scheme B, C, D, E).¹⁵⁰



Scheme 3.2: Selected examples of Ni-catalyzed reductive cross-electrophile couplings.

¹⁴⁶Wurtz, A. *Ann. Chem. Pharm.* **1855**, *96*, 364–375.

¹⁴⁷Tollens, B.; Fittig, R. *Ann. Chem. Pharm.* **1864**, *131*, 303–323.

¹⁴⁸Semmelhack, M. F.; Helquist, P. M.; Jones, L. D. *J. Am. Chem. Soc.* **1971**, *93*, 5908–5910.

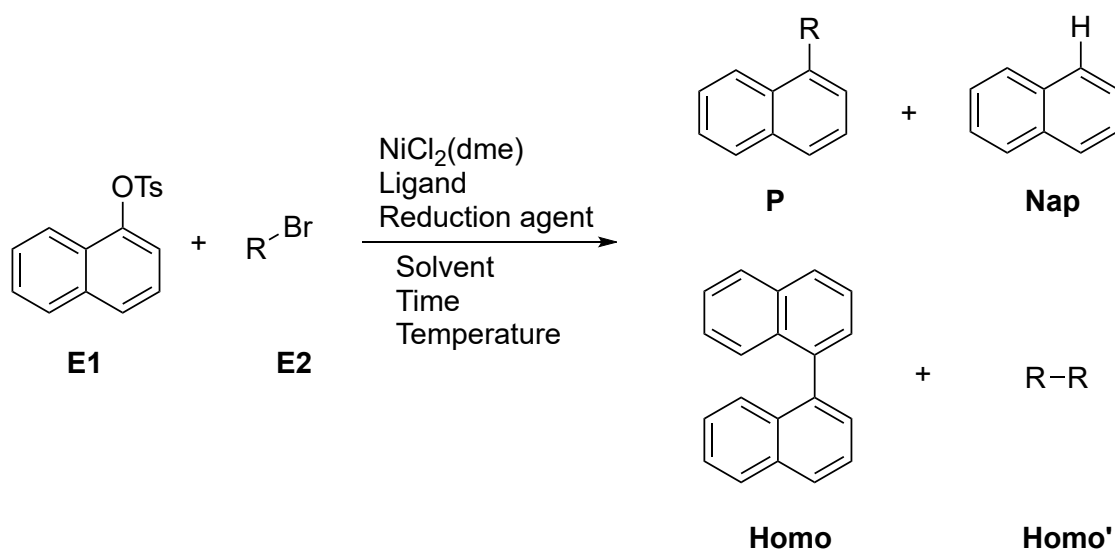
¹⁴⁹Durandetti, M.; Gosmini, C.; Périchon, J. *Tetrahedron* **2007**, *63*, 1146–1153.

¹⁵⁰(a) Everson, D. A.; Shrestha, R.; Weix, D. J. *J. Am. Chem. Soc.* **2010**, *132*, 920–921. (b) Gu, J.; Wang, X.; Xue, W.; Gong, H. *Org. Chem. Front.* **2015**, *2*, 1411–1421.

When employing two electrophiles, some means of differentiation between the coupling partners must be achieved to avoid generation of a mixture of homo- and cross-coupled products. While an unsophisticated method would be to apply a huge excess of one reagent, this does not prevent the formation of dimers. Notably, selectivity can successfully be accomplished in the above shown examples by combining electrophiles with different carbon hybridizations.

3.2. Aims and Objectives

The aim of this chapter is to study the appealing principle of coupling two different electrophiles without the need of a preformed nucleophile. In the previous chapter aryl tosylates were extensively studied in terms of catalytic metalations with a nickel-diazadiene catalyst system. Now, the screening substrate naphthalen-1-yl 4-methylbenzenesulfonate (**E1**) will be the subject of a reductive cross-electrophile-coupling with aryl, benzyl and alkyl bromides **E2** in a screening setup as shown in scheme 3.3, taking advantage of a similar catalytic system.



Scheme 3.3: .

The reaction outcome will be analyzed by qNMR for the amount of product **P**, hydrolysis product naphthalene (**Nap**) and homocoupling products of electrophile **E1** (**Homo**) and **E2** (**Homo'**), which will shed light on the overall reaction selectivity. Several catalyst–ligand combinations will be tested with $\text{NiCl}_2(\text{dme})$ as metal precursor. The goal is to investigate the general reactivity regarding a reductive cross-coupling of this nickel catalyst in combination with typical ligands for the established catalytic zincation.

3.3. Results and Discussion

3.3.1 Initial Condition Screening of Cross-Electrophile Coupling

The initial condition screening setup relied on the previously utilized naphthyl tosylate **E1**, which is allowed to react with benzyl bromide **E2** as cross-electrophile at different temperatures, mostly in DMF solution with zinc dust as reducing agent (table 3.1). The catalyst and ligand are adopted from the catalytic metalation chemistry from chapter 2 in the same mole percentage: NiCl₂(dme) (5 mol%) and diimine **L1** DIPA-^{Me}DAD (10 mol%, see figure 3.1). The reaction is conducted in a one-pot procedure where all components are added at the same time after activation of the zinc powder (see 4.4.1.1).

Table 3.1: Reductive cross-electrophile coupling of 1-naphthyltosylate with benzylbromide.

O=C1C=CC=C2C(=C1)C=C(C=C2)OS(=O)(=O)c3ccccc3 + BrCc1ccccc1

$\xrightarrow[\text{Solvent, Time, Temperature}]{\text{NiCl}_2(\text{dme}) (5 \text{ mol } \%), \text{DIPA-}^{\text{Me}}\text{DAD} (10 \text{ mol } \%), \text{Reducing agent}}$

c1ccc(cc1)Cc2ccccc2 + c1ccc2c(c1)ccc(C)cc2 + c1ccc2c(c1)ccc(Cc3ccccc3)cc2

P **Nap** **Homo**

#	Cat. 2	E2 eq.	Red. Ag. _[eq.]	Solv.	t _[h]	T _[°C]	Homo	Homo'	Nap	P
1	-	1.0	Zn (4.0)	DMF	20	r.t.	2	2	86	8
2 ^{a)}	-	1.0	Zn (4.0)	DMF	20	r.t.	2	3	89	1
3	-	1.0	Zn (4.0)	THF	20	r.t.	1	15	85	14
4	-	1.0	Zn (4.0)	DMF	20	50	3	4	80	14
5	-	1.0	Zn (4.0)	DMF	20	80	1	2	66	30
6	-	1.5	Zn (4.0)	DMF	20	80	1	7	42	55
7	-	2.0	Zn (4.0)	DMF	20	80	2	10	34	63
8	-	2.0	Zn (4.0)	DMF	40	80	2	24	38	58
9	-	2.0	Zn (4.0)	DMF	20	100	2	12	37	60
10	-	2.0	Zn (4.0)	DMF	40	100	2	8	47	46
11 ^{b)}	Pd(OAc) ₂	1.0	Zn (4.0)	DMF	20	r.t.	14	9	27	2
12	Pd(OAc) ₂	1.0	Zn (4.0)	DMF	20	80	1	6	83	15
13	PdCl ₂ (MeCN) ₂	1.0	Zn (4.0)	DMF	20	80	2	8	81	11
14 ^{c)}	-	1.0	Mn (2.0)	DMF	20	r.t.	0	0	0	0
15 ^{c)}	Pd(OAc) ₂	1.0	Mn (2.0)	DMF	20	r.t.	0	36	0	0

Yields were determined by qNMR-analysis. ^{a)}Bromide addition after 20 h. ^{b)}Recovery **E1**: 56 %. ^{c)}Recovery **E1**: >95 %.

Figure 3.1 illustrates the chemical structure of the used ligand. It is the same diisopropylaniline derived diazadiene with methyl groups in the backbone that serves as reference ligand in the nickel-catalyzed zincation of aryl sulfonates 2.

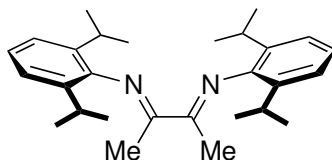


Figure 3.1: Ligand **L1** DIPA-^{Me}DAD.

Entry 1 shows unmodified zincation conditions, where the reaction system delivers mostly the reduction product naphthalene (**Nap**) in 86 % yield after aqueous workup, but also a small amount of the desired cross-coupling product with 8 %. Generally speaking, the large amount of product **Nap** indicates a successful metalation of the aryl tosylate but no or less successful coupling with the second electrophile benzyl bromide (**E2**). Hence, due to a missing conversion the zinc intermediate is accumulated and protonated during the workup procedure. Additionally, if not explicitly stated in the table, the amount of residual substrates **E1** and **E2** is only detected in traces or not at all by qNMR analysis. In entry 2 the benzyl bromide is added 20 h after complete zincation, but no improvement of yield is detected. A switch to THF as solvent (entry 3) and slightly elevating the temperature to 50 °C (entry 4) leads to the right path, since both changes increase the yield of coupling product.

Increasing simultaneously the temperature further to 80 °C and the number of equivalents of **E2** to 1.5 eq. and 2.0 eq. gradually increase the yield of product **P** as shown in entries 5, 6 and 7. Prolonging the reaction time and further increasing the temperature do not improve the yield (entries 8 and 9) or are disadvantageous (entry 10). The groups of ACKERMANN and WEIZ proposed a bimetallic catalysis when coupling two electrophiles.¹⁵¹ This strategy was tested in entries 11 to 13 and 15, but there is no sign of increased reactivity for the coupling step and tosylate reduction is the major reaction.

Another commonly used reducing agent in cross-reductive coupling is elemental manganese.¹⁵² This agent was tested in entries 14 and 15 but was incompatible with the current reaction setup as evident from the recovered amount of >95 % of the starting tosylate.

¹⁵¹Ackerman, L. K. G.; Lovell, M. M.; Weix, D. J. *Nature* **2015**, *524*, 454–457.

¹⁵²(a) Komeyama, K.; Michiyuki, T.; Osaka, I. *ACS Catal.* **2019**, *9*, 9285–9291. (b) Komeyama, K.; Tsunemitsu, R.; Michiyuki, T.; Yoshida, H.; Osaka, I. *Molecules* **2019**, *24*, 1458–1466.

3.3.2 Ligand Screening of Cross-Electrophile Coupling

To further improve the reaction conditions for cross-electrophile coupling, a selection of well-working ligands from the catalytic zincation, namely: DIPA-^HPYR (**L6**), DIPA-^HPHE (**L15**), DIPA-^HQUI (**L5**), MESA-^{Me}DAD (**L11**), MESA-^{ANQ}DAD (**L12**) and 1,10-phenanthroline (PHE, **L16**) is tested in the model reaction between **E1** and **E2** under the reductive coupling conditions showed in figure 3.2. The ligands consist of a diisopropylaniline or mesityl amine derived diimines substituted with pyridin, quinoline, acenaphthoquinone or phenanthroline backbones.

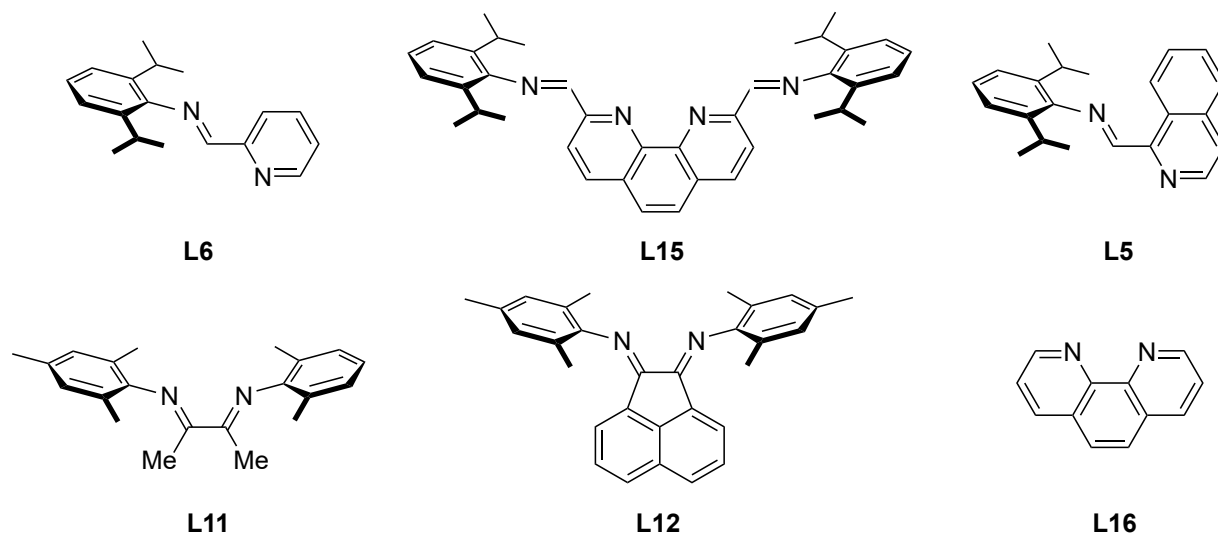


Figure 3.2: Ligands used in the screening in table 3.2.

3.3.3 Cross-Reductive Coupling Substrate Scope: Aryl Tosylate and Aryl or Alkyl Bromides

Continuing the studies with the best working ligand (DIPA-^HQUI) and reaction conditions from above several bromide electrophiles were allowed to react with naphthyl tosylate. In entry 1, the alkylic 1-bromooctane mostly returned unreacted tosylate (83 %) besides 14 % of coupling product. The aryl bromides 4-bromoanisole in entry 2 and 4-bromotoluene in entry 3 provide little coupling product and large amounts of the reduction product *via* the zincation of **E1** is detected. This suggests a selectivity problem when coupling two aryl C(sp²) centers. Entry 4 with 2-bromopyridine as second electrophile besides **E1** gave the best coupling yield with 28 %.

Table 3.3: Reductive cross-electrophile coupling of 1-naphthyltosylate with aryl and alkyl bromides.

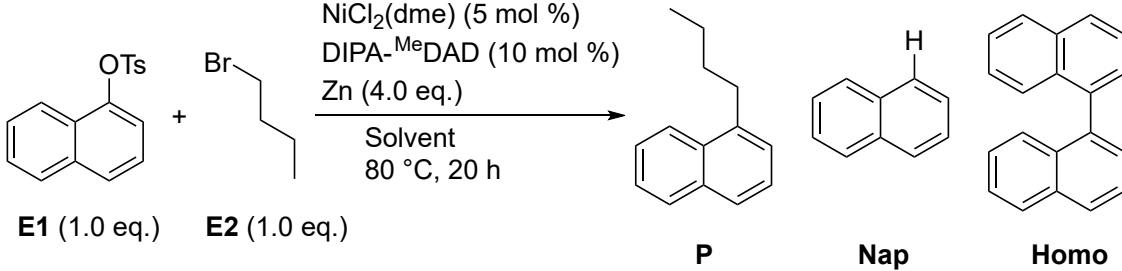
	#	R-Br	E1	Homo	Nap	P
	1		83	0	0	14
	2		0	10	79	9
	3		21	0	72	6
	4		1	28	42	28

Yields were determined by qNMR-analysis.

3.3.4 Cross-Reductive Coupling Substrate Scope: Aryl Tosylate and Alkyl Bromide

Another set of reaction conditions was investigated with regards to an aryl-alkyl coupling of naphthyl tosylate with 1-bromobutane. Entry 1 shows the result under the previous conditions (table 3.2) which provide no product with alkyl bromide. In entry 2 the additive $\text{Et}_4\text{NI}^{153}$ is added but no product formation occurred. Neither did addition of a palladium source improve the situation. The large amount of recovered starting material **E1** in all entries suggests that these conditions already fail at the metalation step.

Table 3.4: Reductive cross-electrophile coupling of 1-naphthyltosylate with 1-bromobutane.



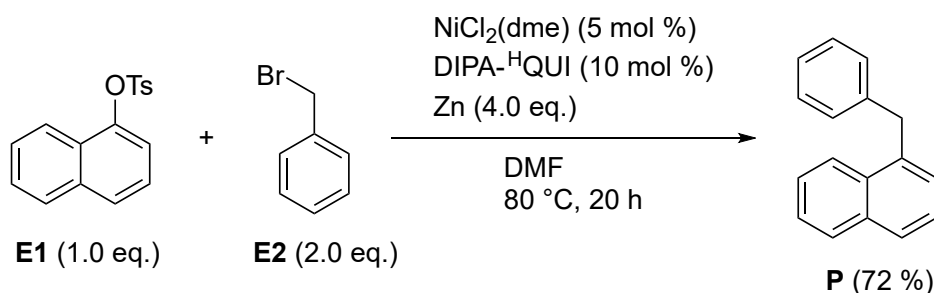
	#	Catalyst 2	Solv.	E1	Homo	Nap	P
	1	-	THF	35	10	50	0
	2 ^{a)}	-	THF	27	6	66	0
	3	$\text{Pd}(\text{OAc})_2$	DMF	50	11	35	3

Yields were determined by qNMR-analysis. ^{a)} Addition of Et_4NI (0.2 eq.).

¹⁵³Iyoda, M.; Otsuka, H.; Sato, K.; Nisato, N.; Oda, M. *Bull. Chem. Soc. Jpn.* **1990**, *63*, 80–87.

3.4. Conclusion and Outlook

In summary, the principle of reductive cross-electrophile-coupling was successfully applied to the reaction of an aryl tosylate and various aryl or alkyl bromides. For the first time, the conditions of our nickel-catalyzed zincation of aryl sulfonates⁶² could be extended to an *in situ* reductive coupling without the need of preforming a carbon nucleophile. Exemplary, the best result was achieved in a coupling of an aryl sulfonate with a benzylic bromide with the formation of 1-benzyl-naphthalene in 72 % yield (scheme 3.4).



Scheme 3.4: Nickel-catalyzed reductive cross-electrophile coupling of 1-naphthyltosylate with benzyl-bromide.

Despite this initial success, there is ample room for improvement for this setup. Typical reaction parameters like the solvent, base or additives can be investigated to improve the substrate range and selectivity of this catalytic reaction. Also, different types of electrophiles such as the sulfonium salts described in chapter 1 should be included in future studies.

4. Experimental Part

4.1. General Remarks

4.1.1 Chemicals and Solvents

Unless otherwise specified, all **reagents and solvents** were obtained from commercial suppliers and were used without further purification. Technical quality solvents for use in silica gel flash column chromatography, crystallizations or work-up procedures were distilled prior use. Water used in reactions or work-up procedures was deionized water from the tap.

Solvents for water-free reactions were filtered over aluminum oxide (Sigma Aldrich, neutral, Brockmann I), degassed by argon bubbling *via* a cannula for 15 minutes and stored over molecular sieves (3 Å or 4 Å). The residual water content was determined by Karl-Fischer-titration, using a coulometric Karl-Fischer titration apparatus from Schott Instruments Titroline KF trace.¹⁵⁴ Acetonitrile was dried over molecular sieves (4 Å). The solvents listed below (see table 4.1) were purchased as 'extra-dry' from commercial suppliers with a water content below 50 ppm.

Table 4.1: Purchased dry solvents.

Solvent	Purity [%]	Information	Supplier
DMA	99.5	extra dry over molecular sieve 4 Å, AcroSeal™, ACROS Organics™	Fisher Scientific
DMF	99.8	extra dry over molecular sieve 4 Å, AcroSeal™, ACROS Organics™	Fisher Scientific
DMSO	≥ 99.9	anhydrous	Sigma Aldrich
MeOH	99.9	extra dry, AcroSeal™, ACROS Organics™	Fisher Scientific

Zinc dust for catalytic zincation was pre-treated to obtain a reproducible quality also with the usual 'aged' samples present in many laboratories: zinc powder (150 g; BASF) was stirred in aqueous HCl (0.5 M, 150 mL) for two hours, filtered through a glass filter. The zinc on the filter was washed with H₂O (100 mL), EtOH (2 x 100 mL) and Et₂O (3

¹⁵⁴D. B. G. Williams, M. Lawton, *J. Org. Chem.* **2010**, *75*, 8351–8354.

x 100 mL) and pre-dried on the filter by sucking air with a water-jet vacuum (fast flow) for 15 minutes. The zinc powder was transferred into a 100 mL Schlenk flask and dried in vacuum (0.01 mbar) at 40 °C for three hours, when it presented itself as free-flowing powder. Vacuum drying was continued overnight at room temperature. The powder was stored under argon until further use.

$\text{PdCl}_2(\text{MeCN})_2$ was prepared by a literature procedure and stored in a Schlenk tube under argon.¹⁵⁵ Larger amounts were stored in a glovebox.

$\text{NiCl}_2(\text{dme})$ was prepared by the *Inorganic Syntheses* procedure and stored in a Schlenk tube under argon.¹⁵⁶ Larger amounts were stored in a glovebox.

Inorganic bases (potassium carbonate, caesium carbonate, potassium phosphate) were finely ground and pre-dried for two days at 150 °C in an oven (20 % ventilation). The solids were further dried in vacuum (0.8 – 1.2 mbar) at 300 °C for at least two hours using a tube furnace (type LOSA) from HTM Reetz GmbH. Potassium bicarbonate was dried for three days at 60 °C in an oven (20 % ventilation). The hygroscopic bases were stored either in a Schlenk flask or inside a glovebox under argon.

Molecular sieves (3 Å and 4 Å) were dried for five hours in vacuum (0.8 – 1.2 mbar) at 400 °C and stored under argon.

Celite® (545, treated with sodium carbonate, flux calcined) was purchased from Fisher Scientific (H33152) and used as filter aid either on a suction filter or in a Pasteur pipette.

4.1.2 Work Techniques

Air and moisture sensitive reactions were carried out under Argon (Westfalen, 4.6) using Standard Schlenk techniques.¹⁵⁷

Heating and cooling: Oil baths were filled with silicon oil (Gruessing, silicon oil M100). Schlenk tubes were heated in an aluminum block. Freezing mixtures of 0 °C were obtained by mixing ice and water. Temperatures below 0 °C were reached with appropriate mixtures (–15 °C: NaCl-ice 1:3 or –78 °C: dry ice saturated isopropanol or acetone). Temperatures were controlled with a digital contact thermometer.

Flash column chromatography was performed on silica gel 60 (Acros, 35–70 μm) as stationary phase with the eluent mixtures given for the corresponding procedures. Positive air pressure (0.1 – 0.3 bar) was used for flash elution.

4.1.3 Analytics

Qualitative thin-layer chromatography (TLC) was performed on silica-coated glass plates (Merck, silica gel 60 F254). Compounds were detected under UV light ($\lambda = 254$ or 366 nm) and by staining with Mostain solution prepared from 10.0 g $(\text{NH}_4)_6[\text{Mo}_7\text{O}_{24}]_4 \cdot \text{H}_2\text{O}$,

¹⁵⁵M. Rimoldi, F. Ragaini, E. Gallo, F. Ferretti, P. Macchi, N. Casati, *Dalton Trans.* **2012**, 41, 3648–3658.

¹⁵⁶L. G. Ward, J. Pipal, *Inorg. Synth.* **1972**, 13, 154–164.

¹⁵⁷J. Houben, T. Weyl, *Die Methoden Der Organischen Chemie (Weyls Methoden)*, Vol. 4, G. Thieme, **1924**.

200 mg $\text{Ce}(\text{SO}_4) \cdot 4 \text{H}_2\text{O}$, 12 mL H_2SO_4 (conc.) in 190 mL water) by dipping and gently heating the plate with a heat-gun.

NMR spectroscopy: NMR spectra were recorded at 300 K either on a Bruker AVHD-300, AVHD-400, AVHD-500 or AVHD-500cr spectrometer. Proton NMR spectra were recorded with a relaxation delay d_1 of 20 s between the pulses. Chemical shifts are reported in parts per million (ppm) relative to the signal of tetramethylsilane. Multiplicities are abbreviated as follows: s - singlet, d - doublet, t - triplet, q - quartet, quint - quintet, sext - sextet, sept - septet, m - multiplet, br - broad signal. Coupling constants (J) are indicated in Hertz (Hz).

Quantitative NMR (qNMR) analysis was carried out as follows: The crude reaction mixture was homogeneously dissolved in an appropriate solvent (CDCl_3 or dichloromethane, if suitable). An internal standard (see table 4.2) was added *via* Hamilton μL syringe (or as weighed amount of solid) and the solution was homogenized by swirling. In case of a non-deuterated solvent, a sample of the reaction mixture (ca. 50 μL) was added to an NMR tube containing CDCl_3 (450 μL) and the sample was homogenized. If CDCl_3 was used for dissolution, a sample of the reaction mixture (500 μL) was transferred to an empty NMR tube without further dilution. A proton NMR ($d_1 = 20$ s, 16 scans) was measured.¹⁵⁸ The yield of the reaction is determined by comparison of the integral of the internal standard with the integral of characteristic signals of the reaction product(s) and starting material(s) in the ^1H -NMR spectra.

Table 4.2: qNMR Standards.

Molecule	Signal
1,1,2,2-tetrachloroethane	^1H -NMR (500 MHz, CDCl_3): δ 5.91 (s, 2H)
1,1,2-trichloroethylene	^1H -NMR (500 MHz, CDCl_3): δ 6.45 (s, 1H)

High resolution mass spectrometry (HRMS) were carried out by the analytical core labs at Technical University of Munich. ESI-HRMS were recorded on a Thermo Fisher Scientific LTQ FT Ultra ion trap with a Fourier Transform Ion Cyclotron Resonance (FT-ICR) MS detector.

Gas chromatography–mass spectrometry (GC-MS) measurements were recorded on an Agilent Technologies 7890B gas chromatograph with a HP-5ms UI Columns by Agilent coupled to an Agilent Technologies 5977A mass spectrometer and an Agilent Technologies 7693 Autosampler using helium as carrier gas (flow rate: 1.8 mL/min).

¹⁵⁸a) S. Mahajan, I. P. Singh, *Magn. Reson. Chem.* **2013**, *51*, 76–81; b) T. Schoenberger, *Anal. Bioanal. Chem.* **2012**, *403*, 247–254.

4.1.4 Solutions, Bases and Catalysts

4.1.4.1 Preparation of a ZnCl₂ solution

A ZnCl₂ solution (1.0 M in THF) was prepared by drying ZnCl₂ (136.3 g, 1 mol) with a heatgun (600 °C, 5 min) and in a Schlenk-flask under vacuum at 140 °C for 5 h. After cooling, dry THF (100 mL) was added and stirring was continued until all salts were dissolved (12 h).¹⁵⁹

4.1.4.2 Synthesis of TMPZnCl · LiCl base

A pre-dried ($2 \cdot 10^{-2}$ mbar, heat-gun) and argon flushed 250 mL Schlenk flask, equipped with a magnetic stirring bar and a septum, was charged with 2,2,6,6-tetramethylpiperidine (3.38 mL, 20.0 mmol, 1.0 eq.) dissolved in THF (20 mL). This solution was cooled to – 40 °C and *n*-BuLi (1.58 M in hexane, 12.7 mL, 20.0 mmol, 1.0 eq.) was dropwise added. After the addition was complete, the reaction mixture was allowed to warm up to – 10 °C for 1 h. ZnCl₂ (1.0 M in THF, 22 mL, 22 mmol, 1.1 eq.) was dropwise added and the resulting solution was stirred for 30 min at – 10 °C and then for 30 min at 25 °C. The solvents were then removed under vacuum affording a yellowish solid. Freshly distilled THF was then slowly added under vigorous stirring until the salts were completely dissolved. The TMPZnCl · LiCl solution was titrated prior to use at 25 °C with iodine as indicator.⁶⁰

4.1.4.3 Synthesis of Pd-PEPPSI-IPr catalyst

A pre-dried ($2 \cdot 10^{-2}$ mbar, heat-gun) and argon flushed 10 mL Schlenk flask, equipped with a magnetic stirring bar and a septum, was charged with Palladium(II)chloride (177 mg, 1.00 mmol, 1.0 eq.) and IPrHCl (425 mg, 1.00 mmol, 1.0 eq.) in acetone (4 mL) and stirred for one day at room temperature, providing a dark-red solution. K₂CO₃ (207 mg, 1.50 mmol, 1.5 eq.) and 3-Cl-pyridine (240 µL, 287 mg, 2.52 mmol, 2.5 eq.) were added and the orange suspension was stirred for one day at 40 °C. After cooling to room temperature, the orange suspension was diluted with DCM (4 mL), passed through a short pad of silica gel eluting with DCM until the product was completely recovered. After removing the solvent under reduced pressure (40 °C, 10 mbar), the remaining solid was washed with pentane (3 x 10 mL) and dried under vacuum ($2 \cdot 10^{-2}$). A pale-yellow solid (657 mg, 97 %) was obtained. The analytical data matched those reported in the literature.⁶⁷

¹H-NMR (400 MHz, CDCl₃): δ = 1.12 (d, *J* = 6.9 Hz, 12H), 1.48 (d, *J* = 6.6 Hz, 12H), 3.16 (hept, *J* = 6.8 Hz, 4H), 7.07 (ddd, *J* = 0.7, 5.5, 8.2 Hz, 1H), 7.14 (s, 2H), 7.35 (d, *J* = 7.7 Hz, 4H), 7.48 – 7.56 (m, 2H), 7.55 (ddd, *J* = 1.4, 2.3, 8.2 Hz, 1H), 8.50 – 8.55 (m, 1H), 8.60 (dd, *J* = 0.6, 2.4 Hz, 2H).

¹³C-NMR (100 MHz, CDCl₃): δ = 23.22, 26.31, 28.74, 124.04, 124.32, 125.13, 130.32, 131.98, 134.99, 135.81, 137.41, 146.65, 149.40, 150.45, 153.44.

¹⁵⁹Castelló-Micó, A.; Nafe, J.; Higashida, K.; Karaghiosoff, K.; Gingras, M.; Knochel, P. *Org. Lett.* **2017**, *19*, 360–363.

4.2. Experimental Data to Chapter 1

4.2.1 General Procedures

4.2.1.1 General Procedure 1.1 for Synthesis of Pyrroles

A round-bottom flask, equipped with a magnetic stirring bar, was charged with hexane-2,5-dione (1.0 eq.) and the corresponding amine (1.0 eq.) and the reaction mixture was stirred for the indicated time at room temperature. After the reaction was complete and completed evaporation of the byproduct water by letting the reaction flask stand over night the product was placed under vacuum to remove traces of water.⁵³

4.2.1.2 General Procedure 1.2 for Synthesis of Sulfonium Salts

A pre-dried ($2 \cdot 10^{-2}$ mbar, heat-gun) and argon flushed round-bottom flask, equipped with a magnetic stirring bar and a septum, was charged with the corresponding sulfoxide (1.1 eq.) and trifluoromethanesulfonic anhydride (1.1 eq.) under argon in DCM (1 ml/mmol) at -50 °C and it was stirred for 10 min. The corresponding nitrogen heterocycle (1.0 eq.) was added portion wise and the reaction mixture was stirred for 30 min at -50 °C. After warming to room temperature an equal amount of conc. NaHCO_3 -solution was added carefully. The organic phase was separated and washed two times with a saturated, aqueous solution of NaCl and the solvent was removed under reduced pressure. The resulting resin was precipitated by addition of Et_2O . Removing the solvent under reduced pressure afforded the corresponding sulfonium salt.

4.2.1.3 General Procedure 1.3 for Synthesis of Aryl Sulfonates

This procedure was adapted from LEI and coworkers.⁷² An aqueous sodium hydroxide solution (15 %, 3.3 eq.) was added to a solution of a phenol (1.0 eq.) in THF. At 0 °C, a solution of TsCl (1.2 eq.) in THF was added dropwise and the suspension was stirred for 24 h at room temperature. The reaction mixture was transferred with EtOAc (5 mL/mmol) to a separatory funnel and the phases were separated. The organic phase was washed with water (2 x 5 mL/mmol) and a saturated aqueous solution of NaCl (5 mL/mmol), dried over MgSO_4 , filtered and the solvent was removed under reduced pressure (50 °C, 10 mbar). Washing with hexanes or purification by silica gel flash column chromatography and drying under reduced pressure ($<1.0 \cdot 10^{-1}$ mbar) afforded the pure product.

4.2.1.4 General Procedure 1.4 for Chlorination of Pyrroles

This procedure was adapted from SAMANTA and coworkers.⁵⁸ A pre-dried ($2 \cdot 10^{-2}$ mbar, heat-gun) and argon flushed Schlenk tube, equipped with a magnetic stirring bar and a septum, was charged with the corresponding pyrrole (1.0 eq.) and 2,4,6-trimethylaniline (0.1 eq.) in DCM (1 ml/mmol). *N*-chlorosuccinimide (1.2 eq.) was added portion wise and it was stirred at r.t. for 2 h. The reaction was monitored by thin layer chromatography. The crude reaction mixture was concentrated. Purification by silica gel flash column chromatography and drying under reduced pressure ($<1.0 \cdot 10^{-1}$ mbar) afforded the pure product.

4.2.1.5 General Procedure 1.5 for Negishi Couplings via Transmetalation of Pyrrolyl Halides

This procedure was adapted from FÜRSTNER and coworkers.¹⁶⁰ A pre-dried ($2 \cdot 10^{-2}$ mbar, heat-gun) and argon flushed Schlenk tube, equipped with a magnetic stirring bar and a septum, was charged with 3-bromo-2,5-dimethyl-1-phenylpyrrole (125 mg, 0.5 mmol, 1.0 eq.) in degassed (!) THF (1 mL). This light-yellow solution was then cooled to -78 °C and *n*-BuLi was added (0.55 mmol, 1.1 eq.). After stirring at -78 °C for 30 minutes a ZnCl₂-solution (0.6 mmol, 1.2 eq, 1 M)) was added and the colorless mixture was allowed to warm to room temperature and it was stirred for 1 h. After that, the corresponding catalyst (0.05 eq.) and electrophile (1.2 eq.) were added and it was stirred at the indicated temperature for the indicated time. After completion, the reaction was cooled to room temperature and quenched with NH₄Cl (5 mL). The aqueous phase was extracted with diethylether (10 mL and 3 x 5 mL). The combined organic phases were washed with a saturated aqueous solution of NH₄Cl (2 x 20 mL) and NaCl (20 mL), dried over Na₂SO₄, filtered and the solvent was removed under reduced pressure (40 °C, 600 mbar for volatile products, 200 mbar for non-volatile ones). The crude product was analyzed by qNMR using either 1,1,2,2-tetrachloroethane (50.0 µL, 473.6 µmol) or trichloroethene (200 µL, 2.22 mmol) as internal standard.

4.2.1.6 General Procedure 1.6 for Pyrrole and Indole C–H Arylation

After completed zincation of the aryl tosylate the stirring was stopped and the supernatant solution was transferred dropwise into a pre-dried ($2 \cdot 10^{-2}$ mbar, heat-gun) and argon flushed Schlenk tube charged with the corresponding sulfonium salt, catalyst and co-solvent. The reaction mixture was stirred for the indicated time at the indicated temperature. After completion, the reaction was cooled to room temperature and quenched with HCl (1 M, 5 mL). The reaction mixture was extracted with Et₂O (3 x 10 mL), washed with a saturated aqueous solution of NH₄Cl (1 mL/mmol) and NaCl (1 mL/mmol), dried over MgSO₄ and filtered. The solvent was removed under reduced pressure and the crude product mixture was analyzed by qNMR using either 1,1,2,2-tetrachloroethane (50.0 µL, 473.6 µmol) or trichloroethene (200 µL, 2.22 mmol) as internal standard. For isolation, the sample was purified *via* column chromatography.

4.2.1.7 General Procedure 1.7 for Caffeine Arylation with Pyrrolyl Halides

A pre-dried ($2 \cdot 10^{-2}$ mbar, heat-gun) and argon flushed Schlenk tube, equipped with a magnetic stirring bar and a septum, was charged with caffeine (78 mg, 0.4 mmol, 1.0 eq.) and 3-bromo-2,5-dimethyl-1-phenylpyrrole (1.5 – 2.0 eq.), the corresponding base (0.8 mmol, 2.0 eq.), catalysator (20 µmol, 0.05 eq.), and additive (40 µmol, 0.1 eq.). The walls were rinsed with solvent (1 – 2 mL). After stirring for 10 minutes at room temperature the reaction mixture was heated to the indicated temperature and stirred for 20 hours. The mixture was cooled to room temperature, diluted with DCM (5 mL), filtered over a silica plug and washed with DCM. The solvent was removed under reduced pressure and the crude product mixture was analyzed by qNMR using either 1,1,2,2-tetrachloroethane (50.0 µL, 473.6 µmol) or trichloroethene (200 µL, 2.22 mmol) as internal standard.

¹⁶⁰Fürstner, A.; Weintritt, H. *J. Am. Chem. Soc.* **1998**, *120*, 2817–2825.

4.2.1.8 General Procedure 1.8 for Pyrrole Arylation with Aryl Tosylates

A pre-dried ($2 \cdot 10^{-2}$ mbar, heat-gun) and argon flushed Schlenk tube, equipped with a magnetic stirring bar and a septum, was charged with 2,5-dimethyl-1-phenyl-1*H*-pyrrole (86 mg, 0.5 mmol, 1.0 eq.), the corresponding aryl tosylate (1.2 eq.), base (1.5 eq.), pre-catalyst (0.05 eq.) and ligand X-Phos (23.8 mg, 50 μ mol, 0.1 eq.) in a mixture of DMF and *t*BuOH (2:1, 3 mL). After stirring for 20 h at 100 °C the reaction mixture was cooled to room temperature and extracted with Et₂O (3 x 10 mL), washed with a saturated aqueous solution of NH₄Cl (1 mL/mmol) and NaCl (1 mL/mmol), dried over MgSO₄ and filtered. The solvent was removed under reduced pressure (50 °C, 10 mbar). The crude product mixture was analyzed by qNMR using either 1,1,2,2-tetrachloroethane (50.0 μ L, 473.6 μ mol) or trichloroethene (200 μ L, 2.22 mmol) as internal standard, and by GCMS.

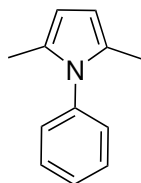
4.2.1.9 General Procedure 1.9 for Pyrrole Amination

A pre-dried ($2 \cdot 10^{-2}$ mbar, heat-gun) and argon flushed Schlenk tube, equipped with a magnetic stirring bar and a septum, was charged with 3-bromo-2,5-dimethyl-1-phenyl-1*H*-pyrrole (**B1**, 0.5 mmol, 125 mg, 1.0 eq.), 1-methylpiperazine (0.6 mmol, 60.1 mg, 1.2 eq.), the indicated catalyst, additive, base and toluene (5 mL) and it was stirred at 100 °C for 9 h. After cooling to room temperature the reaction mixture was diluted with Et₂O (5 mL) and washed with brine (10 mL). The organic phase was separated, dried over MgSO₄, filtered and the solvent was removed under reduced pressure (50 °C, 10 mbar). The crude product mixture was analyzed by qNMR using either 1,1,2,2-tetrachloroethane (50.0 μ L, 473.6 μ mol) or trichloroethene (200 μ L, 2.22 mmol) as internal standard, and by GCMS.

4.2.2 Isolated Compounds and Analytical Data

4.2.2.1 Synthesis of Pyrrole Precursors

2,5-Dimethyl-1-phenyl-1*H*-pyrrole (**S1**)



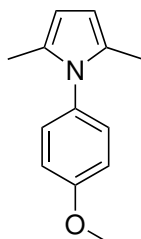
According to general procedure 1.1 (see subsection 4.2.1.1) the reaction of hexane-2,5-dione (11.7 mL, 100 mmol, 1.0 eq.) with aniline (9.1 mL, 100 mmol, 1.0 eq.) provided **S1** (99 %, 16.93 g, 99 mmol) in 72 h as red solid. The analytical data matched those reported in the literature.⁵³

¹H-NMR (400 MHz, CDCl₃): δ = 2.03 (s, 6H), 5.90 (s, 2H), 7.17 – 7.25 (m, 2H), 7.34 – 7.50 (m, 3H).

¹³C-NMR (100 MHz, CDCl₃): δ = 13.02, 105.62, 127.63, 128.26, 128.81, 129.04, 139.00.

R_f = 0.4 (hexane).

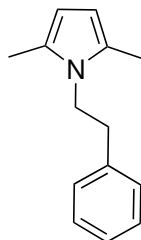
1-(4-Methoxyphenyl)-2,5-dimethyl-1*H*-pyrrole (**S2**)



According to general procedure 1.1 (see subsection 4.2.1.1) the reaction of hexane-2,5-dione (11.7 mL, 100 mmol, 1.0 eq.) with 4-methoxyaniline (11.5 mL, 100 mmol, 1.0 eq.) provided **S2** (97 %, 19.53 g, 97 mmol) in 24 h as orange solid. The analytical data matched those reported in the literature.⁵³

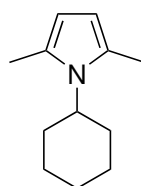
¹H-NMR (400 MHz, CDCl₃): δ = 2.01 (s, 6H), 3.86 (s, 3H), 5.88 (s, 2H), 6.90 – 7.00 (m, 2H), 7.08 – 7.17 (m, 2H).

¹³C-NMR (100 MHz, CDCl₃): δ = 12.95, 55.46, 105.26, 114.20, 129.03, 129.23, 131.78, 158.87.

2,5-Dimethyl-1-phenethyl-1*H*-pyrrole (S3)

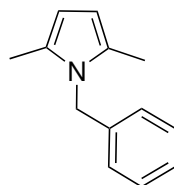
According to general procedure 1.1 (see subsection 4.2.1.1) the reaction of hexane-2,5-dione (1.17 mL, 10.0 mmol, 1.0 eq.) with 2-phenylethan-1-amine (1.26 mL, 10.0 mmol, 1.0 eq.) provided **S3** (99 %, 1.99 g, 9.9 mmol) in 24 h as red oil. The analytical data matched those reported in the literature.⁵³

¹H-NMR (400 MHz, CDCl₃): δ = 2.14 (s, 6H), 2.85 – 2.91 (t, 2H), 3.91 – 3.98 (t, 2H), 5.77 (s, 2H), 7.10 (dd, J = 1.8, 6.9 Hz, 2H), 7.20 – 7.33 (m, 3H).

1-Cyclohexyl-2,5-dimethyl-1*H*-pyrrole (S4)

According to general procedure 1.1 (see subsection 4.2.1.1) the reaction of hexane-2,5-dione (1.17 mL, 10.0 mmol, 1.0 eq.) with cyclohexylamine (1.15 mL, 10.0 mmol, 1.0 eq.) provided **S4** (95 %, 1.69 g, 9.53 mmol) in 24 h as dark brown oil. The analytical data matched those reported in the literature.⁵³

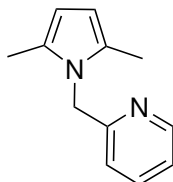
¹H-NMR (400 MHz, CDCl₃): δ = 1.07 – 1.30 (m, 2H), 1.79 – 1.98 (m, 8H), 2.29 (s, 6H), 3.89 (tt, J = 3.9, 11.7 Hz, 1H), 5.73 (s, 2H).

1-Benzyl-2,5-dimethyl-1*H*-pyrrole (S5)

According to general procedure 1.1 (see subsection 4.2.1.1) the reaction of hexane-2,5-dione (1.17 mL, 10.0 mmol, 1.0 eq.) with phenylmethanamine (1.09 mL, 10.0 mmol, 1.0 eq.) provided **S5** (99 %, 1.85 g, 10.0 mmol) in 24 h as light yellow solid. The analytical data matched those reported in the literature.⁵³

¹H-NMR (400 MHz, CDCl₃): δ = 2.14 (s, 6H), 5.01 (s, 2H), 5.85 (s, 2H), 6.86 – 6.91 (m, 2H), 7.19 – 7.32 (m, 3H).

2-((2,5-Dimethyl-1*H*-pyrrol-1-yl)methyl)pyridine (S6)

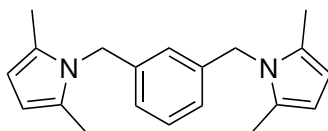


According to general procedure 1.1 (see subsection 4.2.1.1) the reaction of hexane-2,5-dione (1.17 mL, 10.0 mmol, 1.0 eq.) with pyridin-2-ylmethanamine (1.03 mL, 10.0 mmol, 1.0 eq.) provided **S6** (99 %, 1.86 g, 9.9 mmol) in 24 h as dark yellow solid. The analytical data matched those reported in the literature.⁵³

¹H-NMR (400 MHz, CDCl₃): δ = 2.14 (s, 6H), 5.12 (s, 2H), 5.88 (s, 2H), 6.43 (d, J = 7.9 Hz, 1H), 7.16 (dd, J = 4.8, 7.5 Hz, 1H), 7.58 (td, J = 1.8, 7.7 Hz, 1H), 8.54 – 8.59 (m, 1H).

¹³C-NMR (100 MHz, CDCl₃): δ = 12.37, 48.85, 105.80, 119.86, 122.06, 127.89, 137.22, 149.30, 158.62.

1,3-Bis((2,5-dimethyl-1*H*-pyrrol-1-yl)methyl)benzene (S7)

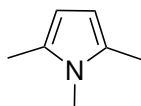


According to general procedure 1.1 (see subsection 4.2.1.1) the reaction of hexane-2,5-dione (2.35 mL, 20.0 mmol, 2.0 eq.) with 1,3-phenylenedimethanamine (1.32 mL, 10.0 mmol, 1.0 eq.) provided **S7** (94 %, 2.74 g, 9.4 mmol) in 48 h as ochre solid. The analytical data matched those reported in the literature.⁵³

¹H-NMR (400 MHz, CDCl₃): δ = 2.11 (s, 12H), 4.94 (s, 4H), 5.84 (s, 4H), 6.53 (td, J = 0.9, 1.8 Hz, 1H), 6.68 (ddt, J = 0.9, 1.7, 7.6 Hz, 2H), 7.19 (t, J = 7.7 Hz, 1H).

¹³C-NMR (100 MHz, CDCl₃): δ = 12.44, 46.67, 105.49, 123.12, 124.43, 127.90, 129.26, 139.13.

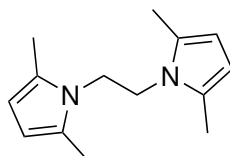
1,2,5-Trimethyl-1*H*-pyrrole (S8)



According to general procedure 1.1 (see subsection 4.2.1.1) the reaction of hexane-2,5-dione (1.17 mL, 10.0 mmol, 1.0 eq.) with methylamine (40 %-sol., 777 mg, 10.0 mmol, 1.0 eq.) provided **S8** (49 %, 530 mg, 4.85 mmol) in 24 h as brown oil. The analytical data matched those reported in the literature.⁵³

¹H-NMR (400 MHz, CDCl₃): δ = 2.20 (s, 6H), 3.31 (s, 3H), 5.77 (s, 2H).

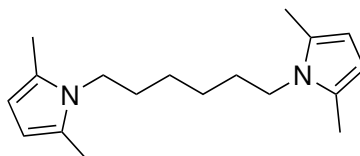
1,2-Bis(2,5-dimethyl-1*H*-pyrrol-1-yl)ethane (**S9**)



According to general procedure 1.1 (see subsection 4.2.1.1) the reaction of hexane-2,5-dione (2.35 mL, 20.0 mmol, 2.0 eq.) with ethane-1,2-diamine (0.67 mL, 10.0 mmol, 1.0 eq.) provided **S9** (99 %, 2.16 g, 9.9 mmol) in 24 h as light yellow solid. The analytical data matched those reported in the literature.⁵³

¹H-NMR (400 MHz, CDCl₃): δ = 2.01 (s, 12H), 3.93 (s, 4H), 5.75 (s, 4H).

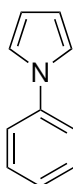
1,6-Bis(2,5-dimethyl-1*H*-pyrrol-1-yl)hexane (**S10**)



According to general procedure 1.1 (see subsection 4.2.1.1) the reaction of hexane-2,5-dione (2.35 mL, 20.0 mmol, 2.0 eq.) with hexane-1,6-diamine (1.31 mL, 10.0 mmol, 1.0 eq.) provided **S10** (99 %, 2.72 g, 9.9 mmol,) in 48 h as light grey solid. The analytical data matched those reported in the literature.⁵³

¹H-NMR (400 MHz, CDCl₃): δ = 1.36 (p, J = 3.6 Hz, 4H), 1.54 – 1.59 (m, 5H), 2.20 (s, 12H), 3.66 – 3.74 (m, 4H), 5.76 (s, 4H).

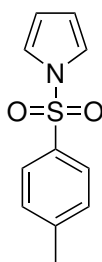
1-Phenyl-1*H*-pyrrole (**S17**)



According to a procedure from AZIZI⁵⁴ a round-bottom flask was charged with 2,5-dimethoxytetrahydrofuran (1.30 mL, 10.0 mmol, 1.0 eq.), aniline (1.02 mL, 10.0 mmol, 1.0 eq.) and water (20 mL) and it was heated to 60 °C. FeCl₃ (32.4 mg, 0.20 mmol, 0.02 eq.) was added and it was stirred for 4 h. The reaction mixture was diluted with ethyl acetate (20 mL) and filtered. The organic phase was separated and the solvent was removed under reduced pressure yielding **S17** (96 %, 1.37 g, 9.60 mmol) as dark brown solid. The analytical data matched those reported in the literature.

¹H-NMR (400 MHz, CDCl₃): δ = 6.35 (t, J = 2.2 Hz, 2H), 7.10 (t, J = 2.1 Hz, 2H), 7.21 – 7.27 (m, 1H), 7.37 – 7.43 (m, 3H), 7.41 – 7.46 (m, 1H).

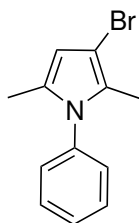
1-Tosyl-1*H*-pyrrole (**S18**)



According to a procedure from ABID⁵⁵ a round-bottom flask was charged with 2,5-dimethoxytetrahydrofuran (1.30 mL, 10.0 mmol, 1.0 eq.), aniline (1.02 mL, 10.0 mmol, 1.0 eq.) and it was cooled to 0 °C. Then, trifluoromethanesulfonic acid (0.22 mL, 0.25 mmol, 0.05 eq.) was added dropwise and it was stirred for 2 h. The reaction mixture was diluted with water (20 mL) and extracted with DCM. The organic phase was separated and the solvent was removed under reduced pressure. Purification *via* silica gel flash column chromatography (hexane → hexane/EtOAc 9:1) yielded **S18** as a white solid (55 %, 610 mg, 2.76 mmol). The analytical data matched those reported in the literature.

¹H-NMR (400 MHz, CDCl₃): δ = 2.40 (s, 3H), 6.25 – 6.31 (m, 2H), 7.12 – 7.18 (m, 2H), 7.27 – 7.31 (m, 2H), 7.70 – 7.79 (m, 2H).

3-Bromo-2,5-dimethyl-1-phenyl-1*H*-pyrrole (**B1**)



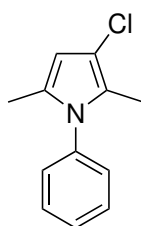
A pre-dried ($2 \cdot 10^{-2}$ mbar, heat-gun) Schlenk flask was charged with 2,5-dimethyl-1-phenyl-1*H*-pyrrole (3.42 g, 20.0 mmol, 1.0 eq.) in THF (20 mL) and cooled to – 78 °C. *N*-bromosuccinimide (3.56 g, 20.0 mmol, 1.0 eq., solved in THF (10 mL)) was added via dropping funnel and it was stirred for 1 h. After warming to room temperature a

saturated, aqueous solution of NaHCO_3 (20 mL) was added and the mixture was extracted with EtOAc (3 x 20 mL). The combined organic phases were washed with brine, dried over Na_2SO_4 and the solvent was removed under reduced pressure. Purification *via* silica gel flash column chromatography (hexane) yielded **B1** as a pale yellow resin (82 %, 4.12 g, 16.5 mmol).

$^1\text{H-NMR}$ (400 MHz, CDCl_3): $\delta = 1.99$ (s, 6H), 5.97 (s, 1H), 7.17 (d, $J = 1.9$ Hz, 2H), 7.38 – 7.45 (m, 1H), 7.43 – 7.51 (m, 2H).

GC-MS (EI, 70 eV) calcd. m/z for $\text{C}_{12}\text{H}_{12}\text{BrN}$: 249.0; found: 249.0.

3-Chloro-2,5-dimethyl-1-phenyl-1*H*-pyrrole (**C1**)

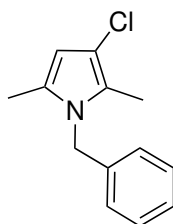


According to general procedure 1.4 (see subsection 4.2.1.4) the reaction of 2,5-dimethyl-1-phenyl-1*H*-pyrrole (**S1**, 343 mg, 2.00 mmol, 1.0 eq.) with *N*-chlorosuccinimide (343 mg, 2.40 mmol, 1.2 eq.) and 2,4,6-trimethylaniline (28 μL , 0.2 mmol, 0.1 eq.) provided **C1** (29 %, 118 mg, 0.57 mmol) as orange oil after purification *via* silica gel flash column chromatography (hexane).

$^1\text{H-NMR}$ (400 MHz, CDCl_3): $\delta = 1.96 - 2.01$ (m, 6H), 5.91 (s, 1H), 7.13 – 7.22 (m, 2H), 7.37 – 7.45 (m, 1H), 7.46 (dd, $J = 6.6, 8.2$ Hz, 2H).

GC-MS (EI, 70 eV) calcd. m/z for $\text{C}_{12}\text{H}_{12}\text{ClN}$: 205.0; found: 205.1.

1-Benzyl-3-chloro-2,5-dimethyl-1*H*pyrrole (**C2**)

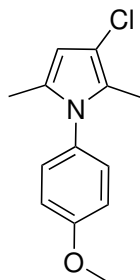


According to general procedure 1.4 (see subsection 4.2.1.4) the reaction of 1-benzyl-2,5-dimethyl-1*H*-pyrrole (**S5**, 926 mg, 5.00 mmol, 1.0 eq.) with *N*-chlorosuccinimide (801 mg, 6.00 mmol, 1.2 eq.) and 2,4,6-trimethylaniline (70 μL , 0.50 mmol, 0.1 eq.) provided **C2** (27 %, 294 mg, 1.86 mmol) as orange oil after purification *via* silica gel flash column chromatography (hexane \rightarrow hexane/EtOAc 9:1).

¹H-NMR (400 MHz, CDCl₃): δ = 2.09 (d, J = 6.4 Hz, 6H), 4.98 (s, 2H), 5.87 (d, J = 1.0 Hz, 1H), 6.85 – 6.92 (m, 2H), 7.21 – 7.34 (m, 3H).

GC-MS (EI, 70 eV) calcd. m/z for C₁₃H₁₄ClN: 219.1; found: 219.1.

3-Chloro-1-(4-methoxyphenyl)-2,5-dimethyl-1*H*pyrrole (**C3**)



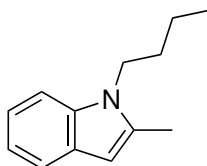
According to general procedure 1.4 (see subsection 4.2.1.4) the reaction of 1-(4-methoxyphenyl)-2,5-dimethyl-1*H*-pyrrole (**S2**, 1.01 g, 5.00 mmol, 1.0 eq.) with *N*-chlorosuccinimide (801 mg, 6.00 mmol, 1.2 eq.) and 2,4,6-trimethylaniline (70 μ L, 0.50 mmol, 0.1 eq.) provided **C3** (25 %, 291 mg, 1.23 mmol) as orange oil after purification *via* silica gel flash column chromatography (hexane).

¹H-NMR (400 MHz, CDCl₃): δ = 1.94 – 2.04 (m, 6H), 3.86 (s, 3H), 5.86 – 5.91 (m, 1H), 6.92 – 7.00 (m, 2H), 7.05 – 7.17 (m, 2H).

GC-MS (EI, 70 eV) calcd. m/z for C₁₃H₁₄ClNO: 235.1; found: 235.1.

4.2.2.2 Synthesis of Indole Precursors

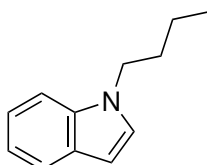
1-Butyl-2-methyl-1*H*-indole (S21)



A round-bottom flask was charged with 2-methyl-1*H*-indole (2.62 g, 20.0 mmol, 1.0 eq.), 1-bromobutane (2.74 g, 20.0 mmol, 1.0 eq.), NaOH (1.60 g, 40.0 mmol, 2.0 eq.) in DMSO (40 mL) and it was stirred at room temperature under nitrogen atmosphere for 2.5 h. The reaction mixture was diluted with ethyl acetate (120 mL) and washed with water (4 x 120 mL). The organic phase was dried over anhydrous sodium sulfate, filtered and the solvent was removed *in vacuo* yielding **S21** as brown oil (57 %, 2.14 g).

¹H-NMR (400 MHz, CDCl₃): δ = 0.94 (td, *J* = 1.6, 7.3 Hz, 3H), 1.34 – 1.42 (m, 2H), 1.72 (tt, *J* = 6.6, 7.7 Hz, 2H), 2.42 (d, *J* = 1.9 Hz, 3H), 4.05 (t, *J* = 7.5 Hz, 2H), 6.22 (d, *J* = 3.3 Hz, 1H), 7.04 (td, *J* = 1.2, 7.5 Hz, 1H), 7.12 (ddd, *J* = 1.3, 7.0, 8.4 Hz, 1H), 7.26 (d, *J* = 8.1 Hz, 1H), 7.48 – 7.53 (m, 1H).

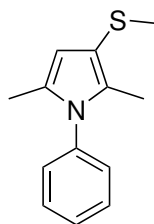
1-Butyl-1*H*-indole (S22)



A round-bottom flask was charged with 2-methyl-1*H*-indole (2.34 g, 20.0 mmol, 1.0 eq.), 1-bromobutane (2.74 g, 20.0 mmol, 1.0 eq.), NaOH (1.60 g, 40.0 mmol, 2.0 eq.) in DMSO (40 mL) and it was stirred at room temperature under nitrogen atmosphere for 2.5 h. The reaction mixture was diluted with ethyl acetate (120 mL) and washed with water (4 x 120 mL). The aqueous phase was extracted with ethyl acetate (2 x 120 mL) and the combined organic phases were dried over anhydrous sodium sulfate. After filtration and evaporation of the solvents *in vacuo* the crude product was redissolved in ethyl acetate and extracted with water (3 x 100 mL) to remove the remaining DMSO. The organic phase was dried over anhydrous sodium sulfate, filtered and the solvent was removed *in vacuo* yielding **S22** as brown oil (96 %, 3.32 g).

¹H-NMR (400 MHz, CDCl₃): δ = 0.93 (t, *J* = 7.4 Hz, 3H), 1.29 – 1.40 (m, 2H), 1.77 – 1.87 (m, 2H), 4.12 (t, *J* = 7.1 Hz, 2H), 6.48 (dd, *J* = 0.9, 3.2 Hz, 1H), 7.05 – 7.15 (m, 2H), 7.20 (ddd, *J* = 1.2, 7.0, 8.2 Hz, 1H), 7.34 (dq, *J* = 0.9, 8.1 Hz, 1H), 7.62 (dt, *J* = 1.0, 7.8 Hz, 1H).

4.2.2.3 Synthesis of Sulfonium Salts

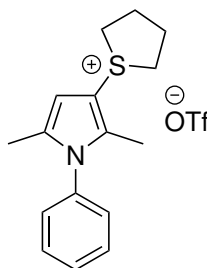
2,5-Dimethyl-3-(methylthio)-1-phenyl-1*H*-pyrrole (**A2**)

According to general procedure 1.2 (see subsection 4.2.1.2) 2,5-dimethyl-1-phenyl-1*H*-pyrrole (**S1**, 8.56 g, 50.0 mmol, 1.0 eq.) was allowed to react with dimethyl sulfoxide (3.91 mL, 55.0 mmol, 1.1 eq.) and trimethylsilyl chloride (6.98 mL, 55.0 mmol, 1.1 eq.) yielding the demethylated side product **A2** as a purple solid (67 %, 9.01 g).

¹H-NMR (400 MHz, CDCl₃): δ = 2.02 (s, 3H), 2.18 (s, 3H), 3.51 (s, 3H), 6.51 (s, 1H), 7.19 (dt, J = 2.1, 7.1 Hz, 2H), 7.54 (dd, J = 2.0, 5.1 Hz, 3H).

¹³C-NMR (100 MHz, CDCl₃): δ = 11.50, 12.90, 32.10, 98.68, 104.08, 127.71, 129.55, 129.89, 134.31, 136.45, 174.08.

HRMS (EI, 70 eV) m/z calc. for [C₁₃H₁₅NS]⁺: 217.0925, found: 217.0920.

1-(2,5-Dimethyl-1-phenyl-1*H*-pyrrol-3-yl)tetrahydro-1*H*-thiophen-1-ium triflate (**A3**)

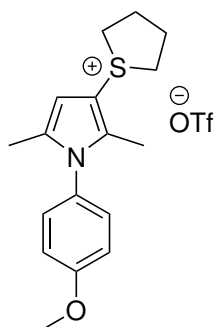
According to general procedure 1.2 (see subsection 4.2.1.2) 2,5-dimethyl-1-phenyl-1*H*-pyrrole (**S1**, 2.68 g, 15.0 mmol, 1.0 eq.) was allowed to react with tetrahydrothiophene 1-oxide (1.47 mL, 16.5 mmol, 1.1 eq.) and trifluoromethanesulfonic anhydride (2.78 mL, 16.5 mmol, 1.1 eq.) yielding **A3** as an ochre solid (83 %, 5.11 g).

¹H-NMR (400 MHz, CDCl₃): δ = 2.01 (s, 3H), 2.20 (s, 3H), 2.48 – 2.63 (m, 4H), 3.35 (dt, J = 6.1, 12.1 Hz, 2H), 4.12 (dt, J = 6.7, 12.9 Hz, 2H), 6.11 (d, J = 1.2 Hz, 1H), 7.14 – 7.22 (m, 2H), 7.48 – 7.59 (m, 3H).

¹³C-NMR (100 MHz, CDCl₃): δ = 11.43, 12.81, 29.07, 49.66, 99.31, 104.02, 122.43, 127.69, 129.61, 129.94, 134.70, 136.30, 137.88.

HRMS (EI, 70 eV) m/z calc. for [C₁₆H₂₀NS]⁺: 258.1311, found: 258.1356.

1-(1-(4-Methoxyphenyl)-2,5-dimethyl-1*H*-pyrrol-3-yl)tetrahydro-1*H*-thiophen-1-ium triflate (A4)



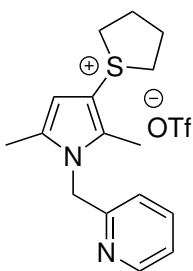
According to general procedure 1.2 (see subsection 4.2.1.2) 1-(4-methoxyphenyl)-2,5-dimethyl-1*H*-pyrrole (**S2**) 3.02 g, 15.0 mmol, 1.0 eq.) was allowed to react with tetrahydrothiophene 1-oxide (1.47 mL, 16.5 mmol, 1.1 eq.) and trifluoromethanesulfonic anhydride (2.78 mL, 16.5 mmol, 1.1 eq.) yielding **A4** as an off-white solid (67 %, 4.34 g).

¹H-NMR (400 MHz, CDCl₃): δ = 1.99 (s, 3H), 2.19 (s, 3H), 2.54 (dt, J = 6.6, 11.8 Hz, 4H), 3.29 – 3.39 (m, 2H), 3.88 (s, 3H), 4.05 – 4.15 (m, 2H), 6.09 (s, 1H), 7.02 (d, J = 8.9 Hz, 2H), 7.09 (d, J = 8.8 Hz, 2H).

¹³C-NMR (100 MHz, CDCl₃): δ = 11.43, 12.80, 29.08, 49.67, 55.63, 99.00, 103.66, 115.03, 119.24, 122.42, 128.75, 135.01, 138.34, 160.19.

HRMS (EI, 70 eV) m/z calc. for [C₁₈H₂₂F₃NO₄S₂]⁺: 437.0942, found: 437.0921.

1-(2,5-Dimethyl-1-(pyridin-2-ylmethyl)-1*H*-pyrrol-3-yl)tetrahydro-1*H*-thiophen-1-ium triflate (A5)



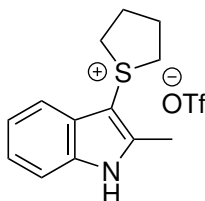
According to general procedure 1.2 (see subsection 4.2.1.2) 2-((2,5-dimethyl-1*H*-pyrrol-1-yl)methyl)pyridine (**S6**, 2.79 g, 15.0 mmol, 1.0 eq.) was allowed to react with tetrahydrothiophene 1-oxide (1.47 mL, 16.5 mmol, 1.1 eq.) and trifluoromethanesulfonic anhydride (2.78 mL, 16.5 mmol, 1.1 eq.) yielding **A5** as a red solid (80 %, 5.06 g). Caution: The product is soluble in H₂O, so the crude product was only washed with Et₂O.

¹H-NMR (400 MHz, CDCl₃): δ = 2.10 – 2.21 (m, 3H), 2.35 (s, 4H), 2.28 – 2.41 (m, 2H), 2.60 (dddd, J = 3.9, 6.0, 8.6, 12.7 Hz, 2H), 3.47 (dt, J = 6.9, 13.3 Hz, 2H), 3.81 –

3.92 (m, 2H), 5.64 (s, 2H), 6.41 (d, $J = 1.2$ Hz, 1H), 7.31 (d, $J = 8.1$ Hz, 1H), 8.03 (ddd, $J = 1.2, 5.9, 7.5$ Hz, 1H), 8.56 (td, $J = 1.7, 8.0$ Hz, 1H), 8.81 (dd, $J = 1.6, 6.0$ Hz, 1H).

HRMS (EI, 70 eV) m/z calc. for $[C_{17}H_{21}F_3N_2O_3S_2]^+$: 422.0946, found: 422.9659.

1-(2-Methyl-1*H*-indol-3-yl)tetrahydro-1*H*-thiophen-1-ium triflate (A6)

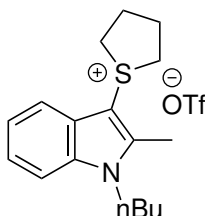


According to general procedure 1.2 (see subsection 4.2.1.2) 2-methyl-1*H*-indole (1.31 g, 10.0 mmol, 1.0 eq.) was allowed to react with tetrahydrothiophene 1-oxide (0.98 mL, 11.0 mmol, 1.1 eq.) and trifluoromethanesulfonic anhydride (1.85 mL, 11.0 mmol, 1.1 eq.) yielding **A6** as a dark purple oil (37 %, 527 mg).

¹H-NMR (400 MHz, CDCl₃): $\delta = 2.33$ (dtdd, $J = 2.5, 4.7, 10.1, 12.4$ Hz, 2H), 2.63 (s, 3H), 2.59 – 2.72 (m, 2H), 3.67 (dt, $J = 7.3, 12.8$ Hz, 2H), 3.91 (dt, $J = 6.6, 12.9$ Hz, 2H), 7.23 – 7.35 (m, 2H), 7.55 (d, $J = 8.0$ Hz, 1H), 7.65 (d, $J = 7.9$ Hz, 1H), 12.49 (s, 1H).

HRMS (EI, 70 eV) m/z calc. for $[C_{14}H_{16}F_3NO_3S_2]^+$: 367.0524, found: 367.0514.

1-(1-Butyl-2-methyl-1*H*-indol-3-yl)tetrahydro-1*H*-thiophen-1-ium triflate (A7)

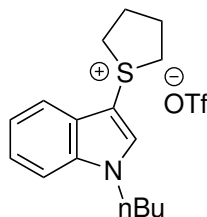


According to general procedure 1.2 (see subsection 4.2.1.2) 1-butyl-2-methyl-1*H*-indole (**S21**, 1.87 g, 10.0 mmol, 1.0 eq.) was allowed to react with tetrahydrothiophene 1-oxide (0.98 mL, 11.0 mmol, 1.1 eq.) and trifluoromethanesulfonic anhydride (1.85 mL, 11.0 mmol, 1.1 eq.) yielding **A3** as a purple solid (46 %, 1.96 g).

¹H-NMR (400 MHz, CDCl₃): $\delta = 0.99$ (t, $J = 7.4$ Hz, 3H), 1.42 (dq, $J = 7.4, 14.8$ Hz, 2H), 1.77 (m, $J = 7.6$ Hz, 2H), 2.55 – 2.68 (m, 2H), 2.74 (s, 5H), 3.56 – 3.67 (m, 2H), 4.07 – 4.20 (m, 4H), 7.32 (ddd, $J = 1.1, 7.2, 8.0$ Hz, 1H), 7.35 – 7.42 (m, 1H), 7.47 (d, $J = 8.3$ Hz, 1H), 7.51 (d, $J = 7.9$ Hz, 1H).

¹³C-NMR (100 MHz, CDCl₃): $\delta = 11.58, 13.69, 20.20, 29.70, 31.57, 44.45, 45.45, 88.53, 111.81, 117.07, 119.20, 122.87, 123.05, 124.15, 137.71, 147.96$.

HRMS (EI, 70 eV) m/z calc. for $[C_{18}H_{24}F_3NO_3S_2]^+$: 423.1150, found: 423.1144.

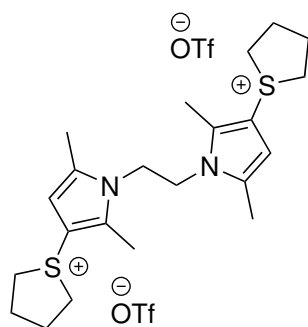
1-(1-Butyl-1*H*-indol-3-yl)tetrahydro-1*H*-thiophen-1-ium triflate (**A8**)

According to general procedure 1.2 (see subsection 4.2.1.2) 1-butyl-1*H*-indole (**S22**, 1.73 g, 10.0 mmol, 1.0 eq.) was allowed to react with tetrahydrothiophene 1-oxide (0.98 mL, 11.0 mmol, 1.1 eq.) and trifluoromethanesulfonic anhydride (1.85 mL, 11.0 mmol, 1.1 eq.) yielding **A8** as a pale yellow solid (61 %, 1.25 g).

¹H-NMR (400 MHz, CDCl₃): δ = 0.95 (td, J = 0.9, 7.4 Hz, 3H), 1.37 (m, J = 7.4 Hz, 2H), 1.87 (m, J = 7.5 Hz, 2H), 2.44 – 2.55 (m, 2H), 2.71 – 2.82 (m, 2H), 3.61 – 3.70 (m, 2H), 4.05 (dt, J = 6.6, 13.0 Hz, 2H), 4.27 (t, J = 7.4 Hz, 2H), 7.31 – 7.37 (m, 1H), 7.40 (tt, J = 1.3, 8.4 Hz, 1H), 7.50 (dd, J = 0.9, 8.3 Hz, 1H), 7.66 (dd, J = 1.1, 8.0 Hz, 1H), 8.25 – 8.30 (m, 1H).

¹³C-NMR (100 MHz, CDCl₃): δ = 13.56, 20.00, 29.05, 31.84, 47.64, 48.26, 91.48, 111.84, 117.66, 122.98, 124.39, 125.44, 135.73, 137.03.

HRMS (EI, 70 eV) m/z calc. for [C₁₆H₂₂NS]⁺: 260.1467, found: 260.1457.

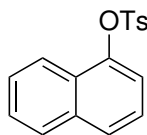
1,1'-(Ethane-1,2-diylbis(2,5-dimethyl-1*H*-pyrrole-1,3-diyl))bis(tetrahydro-1*H*-thiophen-1-ium) triflate (**A9**)

According to general procedure 1.2 (see subsection 4.2.1.2) 1,2-bis(2,5-dimethyl-1*H*-pyrrol-1-yl)ethane (**S9**, 1.08 g, 5.0 mmol, 1.0 eq.) was allowed to react with tetrahydrothiophene 1-oxide (0.98 mL, 11.0 mmol, 2.2 eq.) and trifluoromethanesulfonic anhydride (1.85 mL, 11.0 mmol, 2.2 eq.) yielding **A9** as a brown solid (13 %, 450 mg).

¹H-NMR (400 MHz, CDCl₃): δ = 1.92 (s, 6H), 2.12 (s, 6H), 2.21 (qd, J = 4.6, 9.7 Hz, 4H), 2.41 (dtd, J = 4.1, 6.1, 13.0 Hz, 4H), 3.23 (dt, J = 6.4, 12.6 Hz, 4H), 3.83 (dt, J = 7.0, 12.4 Hz, 4H), 4.17 (s, 4H), 6.29 (d, J = 1.2 Hz, 2H).

4.2.2.4 Synthesis of Aryl Sulfonates

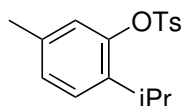
Naphthalen-1-yl 4-methylbenzenesulfonate (T1)



According to general procedure 1.3 (see subsection 4.2.1.3) tosylation of naphthalen-1-ol (14.4 g, 100 mmol, 1.0 eq.) afforded the product as an off-white solid (29.83 g, 99 %).

¹H-NMR (400 MHz, CDCl₃): δ = 2.41 (s, 3H), 7.20 (dd, J = 1.1, 7.6 Hz, 1H), 7.24 – 7.30 (m, 2H), 7.33 – 7.39 (m, 1H), 7.39 – 7.50 (m, 2H), 7.70 – 7.76 (m, 1H), 7.76 – 7.83 (m, 3H), 7.87 – 7.93 (m, 1H).

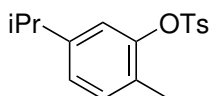
2-Isopropyl-5-methylphenyl 4-methylbenzenesulfonate (T8)



According to general procedure 1.3 (see subsection 4.2.1.3) tosylation of 2-isopropyl-5-methylphenol (1.50 g, 10.0 mmol, 1.0 eq.) afforded the product as an off-white solid (2.99 g, 98 %).

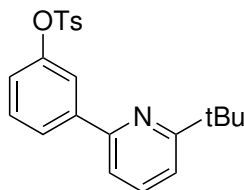
¹H-NMR (400 MHz, CDCl₃): δ = 1.01 (d, J = 6.9 Hz, 6H), 2.26 (s, 3H), 2.45 (s, 3H), 3.01 (hept, J = 6.9 Hz, 1H), 6.89 (d, J = 1.7 Hz, 1H), 7.02 (dd, J = 1.8, 8.0 Hz, 1H), 7.12 (d, J = 7.9 Hz, 1H), 7.32 (d, J = 8.1 Hz, 2H), 7.73 – 7.79 (m, 2H).

5-Isopropyl-2-methylphenyl 4-methylbenzenesulfonate (T9)



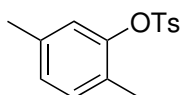
According to general procedure 1.3 (see subsection 4.2.1.3) tosylation of 5-isopropyl-2-methylphenol (1.50 g, 10.0 mmol, 1.0 eq.) afforded the product as an off-white solid (2.97 g, 97 %).

¹H-NMR (400 MHz, CDCl₃): δ = 1.12 (d, J = 6.9 Hz, 6H), 2.08 (s, 3H), 2.45 (s, 3H), 2.78 (hept, J = 6.9 Hz, 1H), 6.71 (d, J = 1.8 Hz, 1H), 6.99 (dd, J = 1.9, 7.8 Hz, 1H), 7.04 – 7.10 (m, 1H), 7.29 – 7.36 (m, 2H), 7.70 – 7.78 (m, 2H).

3-(6-(Tert-Butyl)pyridin-2-yl)phenyl 4-methylbenzenesulfonate (T13)

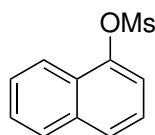
According to general procedure 1.3 (see subsection 4.2.1.3) tosylation of 3-(6-(tert-butyl)pyridin-2-yl)phenol (682 mg, 3.0 mmol, 1.0 eq.) afforded the product as a yellow oil (0.99 g, 87 %).

¹H-NMR (400 MHz, CDCl₃): δ = 1.36 (s, 9H), 2.43 (s, 3H), 7.05 (ddd, J = 1.0, 2.4, 8.2 Hz, 1H), 7.24 – 7.41 (m, 5H), 7.43 (dd, J = 0.9, 7.8 Hz, 1H), 7.64 (t, J = 7.8 Hz, 1H), 7.69 (t, J = 2.1 Hz, 1H), 7.77 (s, 1H), 7.95 (dt, J = 1.3, 7.9 Hz, 1H).

2,5-Dimethylphenyl 4-methylbenzenesulfonate (T16)

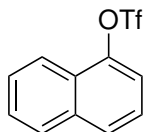
According to general procedure 1.3 (see subsection 4.2.1.3) tosylation of 2,5-dimethylphenol (1.22 g, 10.0 mmol, 1.0 eq.) afforded the product as an off-white solid (2.70 g, 98 %).

¹H-NMR (400 MHz, CDCl₃): δ = 1.98 (s, 3H), 2.26 (s, 3H), 2.45 (s, 3H), 6.87 (d, J = 1.7 Hz, 1H), 6.95 (dd, J = 1.7, 7.9 Hz, 1H), 7.02 (d, J = 7.8 Hz, 1H), 7.28 – 7.35 (m, 2H), 7.71 – 7.78 (m, 2H).

Naphthalene-1-yl methanesulfonate (T17)

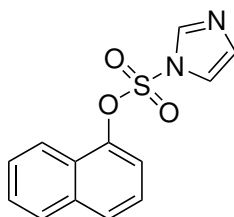
A solution of 1-naphthol (720 mg, 5.00 mmol, 1.0 eq.) and triethylamine (1.39 mL, 10.0 mmol, 2.0 eq.) in EtOAc (15 mL) was cooled to 0 °C in an ice bath. Methanesulfonyl chloride (0.51 mL, 6.50 mmol, 1.3 eq.) was added dropwise, the ice bath was removed, and the reaction mixture was continued to stir for 10 min. H₂O (10 mL) was added, the two phases were separated, the organic layer was washed with H₂O (5 mL), conc. NH₄Cl-solution (10 mL) and brine (10 mL) and dried over MgSO₄. Evaporation of the solvents yielded **T17** as a yellow-brown crystalline solid (1.00 g, 90 %).

¹H-NMR (400 MHz, CDCl₃): δ = 3.22 (s, 3H), 7.48 (t, J = 7.9 Hz, 1H), 7.51 – 7.64 (m, 3H), 7.82 (dt, J = 1.1, 8.1 Hz, 1H), 7.88 – 7.92 (m, 1H), 8.14 (dq, J = 1.0, 8.8 Hz, 1H). The analytical data matched those reported in literature.⁷²

Naphthalene-1-yl trifluoromethanesulfonate (T18)

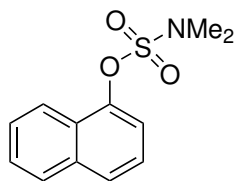
To a solution of 1-naphthol (721 mg, 5.00 mmol, 1.0 eq.) in DCM (20 mL) was added pyridine (0.81 mL, 10.0 mmol, 2.0 eq.) and the mixture was cooled to 0 °C with an ice bath. After cooling triflic anhydride (1.01 mL, 6.0 mmol, 1.2 eq.) was added dropwise at 0 °C, the ice bath was removed, and the reaction mixture was continued to stir for 10 min. Et₂O (10 mL) was added and the reaction was quenched by the addition of aq. HCl (10 mL, 10 %). The phases were separated, the organic layer was washed with NaHCO₃ (20 mL), brine and dried over Na₂SO₄. Evaporation of the solvents yielded **T18** as a brown viscous oil (1.2 g, 85 %).

¹H-NMR (400 MHz, CDCl₃): δ = 7.44 – 7.54 (m, 2H), 7.57 – 7.69 (m, 2H), 7.84 – 7.95 (m, 2H), 8.09 (dd, J = 1.2, 8.3 Hz, 1H). The analytical data matched those reported in literature.⁷⁴

Naphthalene-1-yl 1*H*-imidazole-1-sulfonate (T19)

A suspension of 1-naphthol (364 mg, 2.52 mmol, 1.0 eq.), 1,1'-sulfonyldiimidazole (1.00 g, 5.12 mmol, 2.0 eq.) and Cs₂CO₃ (411 mg, 1.26 mmol, 0.5 eq.) in THF (35 mL) was stirred for 24 hours at room temperature. The solvent of the greenish suspension was removed under reduced pressure (45 °C, 320 mbar). After cooling to 0 °C, EtOAc (20 mL) and a saturated aqueous solution of NH₄Cl (15 mL) was added, yielding an orange-yellow two-phase mixture. The phases were separated and the aqueous phase was extracted with EtOAc (2 x 40 mL). The organic phase was washed with water (50 mL) and a saturated aqueous solution of NaCl (40 mL), dried over Na₂SO₄, filtered and the solvent was removed under reduced pressure (45 °C, 100 mbar). Purification by column chromatography (hexane/EtOAc 2:1) afforded a pinkish, crystalline solid (585 mg, 83 %).

¹H-NMR (400 MHz, CDCl₃): δ = 7.02 (dd, J = 1.0, 7.7 Hz, 1H), 7.13 (dd, J = 0.8, 1.6 Hz, 1H), 7.32 (t, J = 1.5 Hz, 1H), 7.43 (t, J = 8.0 Hz, 1H), 7.53 – 7.62 (m, 2H), 7.78 – 7.85 (m, 4H). The analytical data matched those reported in literature.⁷⁵

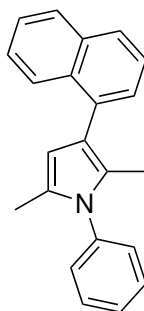
Naphthalene-1-yl dimethylsulfamate (T20)

1-Naphthol (1.44 g, 10.0 mmol, 2.0 eq.) and benzyltriethylammonium chloride (45.8 mg, 201 μmol , 4 mol%) were added to a 25 mL round-bottom flask. The flask was sealed with a septum, evacuated and backfilled with argon three times. Toluene (2.5 mL) and aqueous sodium hydroxide (30 %, 2.5 mL) were added and the mixture was stirred at r.t. A solution of dimethylsulfamoyl chloride (0.53 mL, 5.00 mmol, 1.0 eq.) in toluene (2.5 mL) was added dropwise and the yellowish-green two-phase system was stirred for 7 hours at 50 °C. The reaction mixture was transferred with Et₂O (15 mL) to a separatory funnel leading to a three-phase system. To further decrease polarity, hexanes (10 mL) were added and phases were separated. The organic phase was washed with aqueous sodium hydroxide (2 M, 20 mL), water (3 x 20 mL) and a saturated aqueous solution of NaCl (20 mL), dried over MgSO₄, filtered and the solvent was removed under reduced pressure (45 °C, 25 mbar). The yellowish oil crystallized promptly. After pulverizing and drying under reduced pressure an off-white solid (1.07 g, 85 %) was obtained.

¹H-NMR (400 MHz, CDCl₃): δ = 3.07 (s, 6H), 7.42 – 7.62 (m, 4H), 7.73 – 7.80 (m, 1H), 7.84 – 7.91 (m, 1H), 8.14 – 8.21 (m, 1H). The analytical data matched those reported in literature.⁷⁶

4.2.2.5 Synthesis of Pyrrole Coupling Products

2,5-Dimethyl-3-(naphthalen-1-yl)-1-phenyl-1*H*-pyrrole (P1)



According to general procedure 1.6 (see subsection 4.2.1.6) pyrrole sulfonium salt **A3** (407.5 mg, 1.0 mmol, 1.0 eq.) was allowed to react with the zincated aryl tosylate **T1** (596.7 mg, 2.0 mmol, 2.0 eq.), catalyst PEPPSI-IPr (2 mol%, 13.6 mg) in equal amounts of THF and DMF at 60 °C for 20 h. Purification via column chromatography (hexane → hexane/DCM 8:2) yielded **P1** as a colorless resin (89 %, 261 mg).

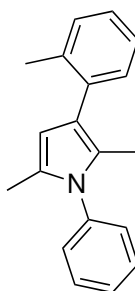
TLC: R_f 0.3 (hexane/DCM 8:2).

¹H-NMR (400 MHz, CDCl₃): δ = 1.94 (s, 3H), 2.14 (s, 3H), 6.15 (s, 1H), 7.30 – 7.38 (m, 2H), 7.36 – 7.55 (m, 7H), 7.77 (d, J = 7.8 Hz, 1H), 7.82 – 7.92 (m, 1H), 8.11 – 8.21 (m, 1H).

¹³C-NMR (100 MHz, CDCl₃): δ = 11.98, 12.97, 108.94, 119.31, 125.40, 125.42, 125.46, 126.34, 127.03, 127.59, 127.72, 128.03, 128.15, 128.43, 129.13, 129.30, 132.71, 133.94, 135.48, 139.12.

HRMS (EI, 70 eV) m/z calc. for [C₂₂H₁₉N]⁺: 297.1517, found: 297.1506.

2,5-Dimethyl-1-phenyl-3-(*o*-tolyl)-1*H*-pyrrole (P2)



According to general procedure 1.6 (see subsection 4.2.1.6) pyrrole sulfonium salt **A3** (407.5 mg, 1.0 mmol, 1.0 eq.) was allowed to react with the zincated aryl tosylate **T2** (524.7 mg, 2.0 mmol, 2.0 eq.), catalyst PEPPSI-IPr (2 mol%, 13.6 mg) in equal amounts of THF and DMF at 60 °C for 20 h. Purification via column chromatography (hexane → hexane/DCM 8:2) yielded **P2** as an orange solid (79 %, 207 mg).

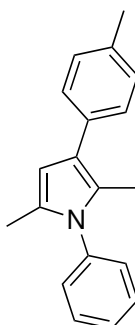
TLC: R_f 0.3 (hexane/DCM 8:2).

$^1\text{H-NMR}$ (400 MHz, CDCl_3): δ = 1.91 (s, 3H), 2.08 (s, 3H), 2.33 (s, 3H), 5.96 (q, J = 0.9 Hz, 1H), 7.15 – 7.20 (m, 2H), 7.22 – 7.31 (m, 5H), 7.36 – 7.43 (m, 1H), 7.44 – 7.51 (m, 2H).

$^{13}\text{C-NMR}$ (100 MHz, CDCl_3): δ = 11.79, 12.93, 20.62, 107.96, 120.33, 123.46, 125.26, 125.38, 126.04, 127.18, 127.58, 128.33, 128.37, 129.03, 129.96, 130.85, 136.81.

HRMS (EI, 70 eV) m/z calc. for $[\text{C}_{19}\text{H}_{19}\text{N}]^+$: 261.1517, found: 261.1512.

2,5-Dimethyl-1-phenyl-3-(*p*-tolyl)-1*H*-pyrrole (**P3**)



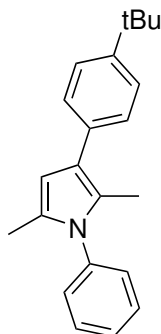
According to general procedure 1.6 (see subsection 4.2.1.6) pyrrole sulfonium salt **A3** (407.5 mg, 1.0 mmol, 1.0 eq.) was allowed to react with the zincated aryl tosylate **T3** (524.7 mg, 2.0 mmol, 2.0 eq.), catalyst PEPPSI-IPr (2 mol%, 13.6 mg) in equal amounts of THF and DMF at 60 °C for 20 h. Purification via column chromatography (hexane → hexane/DCM 8:2) yielded **P3** as an ochre solid (70 %, 183 mg).

TLC: R_f 0.3 (hexane/DCM 8:2).

$^1\text{H-NMR}$ (400 MHz, CDCl_3): δ = 2.07 (s, 3H), 2.14 (s, 3H), 2.35 (s, 3H), 6.14 (s, 1H), 7.18 (d, J = 7.9 Hz, 2H), 7.21 – 7.29 (m, 2H), 7.32 – 7.42 (m, 3H), 7.44 (dd, J = 6.8, 8.3 Hz, 2H).

$^{13}\text{C-NMR}$ (100 MHz, CDCl_3): δ = 12.35, 13.02, 21.25, 106.75, 121.17, 124.96, 127.88, 127.91, 128.54, 128.57, 129.17, 129.24, 134.56, 134.59, 139.04.

HRMS (EI, 70 eV) m/z calc. for $[\text{C}_{19}\text{H}_{19}\text{N}]^+$: 261.1517, found: 261.1504.

3-(4-(Tert-butyl)phenyl)-2,5-dimethyl-1-phenyl-1H-pyrrole (P4)

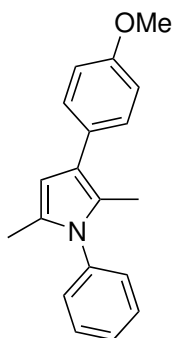
According to general procedure 1.6 (see subsection 4.2.1.6) pyrrole sulfonium salt **A3** (407.5 mg, 1.0 mmol, 1.0 eq.) was allowed to react with the zincated aryl tosylate **T4** (608.8 mg, 2.0 mmol, 2.0 eq.), catalyst PEPPSI-IPr (2 mol%, 13.6 mg) in equal amounts of THF and DMF at 60 °C for 20 h. Purification via column chromatography (hexane → hexane/DCM 7:3) yielded **P4** as an orange solid (81 %, 246 mg).

TLC: R_f 0.4 (hexane/DCM 8:2).

$^1\text{H-NMR}$ (400 MHz, CDCl_3): δ = 1.35 (s, 9H), 2.07 (s, 3H), 2.14 (s, 3H), 6.13 (d, J = 1.2 Hz, 1H), 7.22 – 7.30 (m, 2H), 7.35 – 7.43 (m, 5H), 7.44 – 7.50 (m, 2H).

$^{13}\text{C-NMR}$ (100 MHz, CDCl_3): δ = 12.23, 12.89, 13.00, 31.44, 34.39, 105.60, 106.59, 120.90, 124.92, 125.16, 127.48, 127.69, 128.23, 128.38, 128.41, 129.01, 129.07, 134.40, 138.92, 147.68.

HRMS (EI, 70 eV) m/z calc. for $[\text{C}_{22}\text{H}_{25}\text{N}]^+$: 303.1987, found: 303.1979.

3-(4-Methoxyphenyl)-2,5-dimethyl-1-phenyl-1H-pyrrole (P5)

According to general procedure 1.6 (see subsection 4.2.1.6) pyrrole sulfonium salt **A3** (407.5 mg, 1.0 mmol, 1.0 eq.) was allowed to react with the zincated aryl tosylate **T5** (556.6 mg, 2.0 mmol, 2.0 eq.), catalyst PEPPSI-IPr (2 mol%, 13.6 mg) in equal amounts of THF and DMF at 60 °C for 20 h. Purification via column chromatography (hexane → hexane/DCM 1:1) yielded **P5** as an off-white solid (89 %, 247 mg).

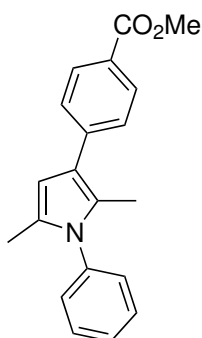
TLC: R_f 0.3 (hexane/DCM 1:1).

¹H-NMR (400 MHz, CDCl₃): δ = 2.07 (s, 3H), 2.12 (s, 3H), 3.83 (s, 3H), 6.10 (s, 1H), 6.91 – 6.95 (m, 2H), 7.25 – 7.29 (m, 2H), 7.35 – 7.38 (m, 2H), 7.39 (s, 2H), 7.48 (d, J = 1.8 Hz, 1H).

¹³C-NMR (100 MHz, CDCl₃): δ = 12.13, 12.86, 55.26, 106.48, 113.77, 120.65, 124.54, 127.72, 128.39, 128.41, 128.87, 129.09, 129.94, 138.90, 157.34.

HRMS (EI, 70 eV) m/z calc. for [C₁₉H₁₉NO]⁺: 277.1467, found: 277.1465.

Methyl 4-(2,5-dimethyl-1-phenyl-1*H*-pyrrol-3-yl)benzoate (**P6**)



According to general procedure 1.6 (see subsection 4.2.1.6) pyrrole sulfonium salt **A3** (407.5 mg, 1.0 mmol, 1.0 eq.) was allowed to react with the zincated aryl tosylate **T6** (612.7 mg, 2.0 mmol, 2.0 eq.), catalyst PEPPSI-IPr (2 mol%, 13.6 mg) in equal amounts of THF and DMF at 60 °C for 20 h. Purification via column chromatography (hexane → hexane/DCM 3:7) yielded **P6** as an ochre solid (65 %, 198 mg).

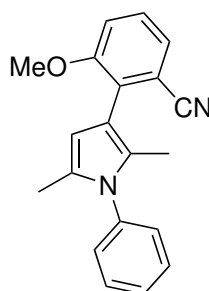
TLC: R_f 0.3 (hexane/DCM 4:6).

¹H-NMR (400 MHz, CDCl₃): δ = 2.07 (s, 3H), 2.17 (s, 3H), 3.92 (s, 3H), 6.20 (s, 1H), 7.22 – 7.30 (m, 2H), 7.41 – 7.46 (m, 1H), 7.47 – 7.53 (m, 4H), 8.01 – 8.06 (m, 2H).

¹³C-NMR (100 MHz, CDCl₃): δ = 12.54, 12.85, 51.92, 106.35, 120.17, 126.34, 127.16, 128.06, 128.08, 128.36, 129.26, 129.55, 129.76, 138.52, 142.20, 167.34.

HRMS (EI, 70 eV) m/z calc. for [C₂₀H₁₉NO₂]⁺: 305.1416, found: 305.1411.

2-(2,5-Dimethyl-1-phenyl-1*H*-pyrrol-3-yl)-3-methoxybenzonitrile (**P7**)



According to general procedure 1.6 (see subsection 4.2.1.6) pyrrole sulfonium salt **A3** (407.5 mg, 1.0 mmol, 1.0 eq.) was allowed to react with the zincated aryl tosylate **T7** (612.7 mg, 2.0 mmol, 2.0 eq.), catalyst PEPPSI-IPr (2 mol%, 13.6 mg) in equal amounts of THF and DMF at 60 °C for 20 h. Purification via column chromatography (hexane → hexane/DCM 4:6) yielded **P7** as a beige solid (41 %, 124 mg).

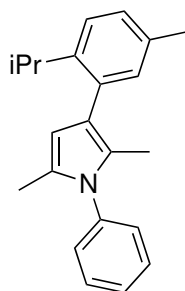
TLC: R_f 0.3 (hexane/DCM 4:6).

$^1\text{H-NMR}$ (400 MHz, CDCl_3): δ = 1.94 (s, 3H), 2.07 (s, 3H), 3.86 (s, 3H), 6.12 (s, 1H), 7.12 (dd, J = 2.8, 6.7 Hz, 1H), 7.26 – 7.34 (m, 4H), 7.37 – 7.43 (m, 1H), 7.47 (t, J = 7.4 Hz, 2H).

$^{13}\text{C-NMR}$ (100 MHz, CDCl_3): δ = 12.63, 13.04, 55.89, 108.14, 113.05, 114.59, 114.67, 119.29, 124.98, 127.55, 127.76, 128.00, 128.23, 128.43, 129.07, 130.74, 138.81, 157.41.

HRMS (EI, 70 eV) m/z calc. for $[\text{C}_{20}\text{H}_{18}\text{N}_2\text{O}]^+$: 302.1419, found: 302.1415.

3-(2-Isopropyl-5-methylphenyl)-2,5-dimethyl-1-phenyl-1*H*-pyrrole (**P8**)



According to general procedure 1.6 (see subsection 4.2.1.6) pyrrole sulfonium salt **A3** (407.5 mg, 1.0 mmol, 1.0 eq.) was allowed to react with the zincated aryl tosylate **T8** (608.9 mg, 2.0 mmol, 2.0 eq.), catalyst PEPPSI-IPr (2 mol%, 13.6 mg) in equal amounts of THF and DMF at 60 °C for 20 h. Purification via column chromatography (hexane → hexane/DCM 8:2) yielded **P8** as an orange solid (60 %, 183 mg).

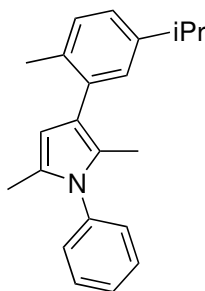
TLC: R_f 0.3 (hexane/DCM 9:1).

$^1\text{H-NMR}$ (400 MHz, CDCl_3): δ = 1.17 (d, J = 6.9 Hz, 6H), 1.89 (s, 3H), 2.08 (s, 3H), 2.32 (s, 3H), 3.24 (hept, J = 6.9 Hz, 1H), 5.91 (d, J = 1.2 Hz, 1H), 7.04 (d, J = 1.9 Hz, 1H), 7.09 (dd, J = 2.0, 7.9 Hz, 1H), 7.25 (d, J = 5.4 Hz, 1H), 7.29 (dd, J = 1.4, 8.1 Hz, 2H), 7.37 – 7.43 (m, 1H), 7.47 (dd, J = 6.8, 8.3 Hz, 2H).

$^{13}\text{C-NMR}$ (100 MHz, CDCl_3): δ = 11.60, 12.95, 20.92, 24.36, 29.22, 108.27, 120.52, 125.11, 125.33, 127.35, 127.44, 127.51, 128.39, 128.99, 131.96, 134.27, 135.88, 139.24, 145.07.

HRMS (EI, 70 eV) m/z calc. for $[\text{C}_{22}\text{H}_{25}\text{N}]^+$: 303.1987, found: 303.1992.

3-(5-Isopropyl-2-methylphenyl)-2,5-dimethyl-1-phenyl-1*H*-pyrrole (**P9**)



According to general procedure 1.6 (see subsection 4.2.1.6) pyrrole sulfonium salt **A3** (407.5 mg, 1.0 mmol, 1.0 eq.) was allowed to react with the zincated aryl tosylate **T9** (608.9 mg, 2.0 mmol, 2.0 eq.), catalyst PEPPSI-IPr (2 mol%, 13.6 mg) in equal amounts of THF and DMF at 60 °C for 20 h. Purification via column chromatography (hexane → hexane/EtOAc 98:2) yielded **P9** as an orange solid (67 %, 202 mg).

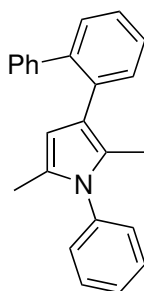
TLC: R_f 0.3 (hexane/EtOAc 98:2).

$^1\text{H-NMR}$ (400 MHz, CDCl_3): δ = 1.17 (d, J = 6.9 Hz, 6H), 1.89 (s, 3H), 2.08 (s, 3H), 2.32 (s, 3H), 3.24 (hept, J = 6.9 Hz, 1H), 5.91 (d, J = 1.2 Hz, 1H), 7.04 (d, J = 1.9 Hz, 1H), 7.09 (dd, J = 2.0, 7.9 Hz, 1H), 7.25 (d, J = 5.4 Hz, 1H), 7.29 (dd, J = 1.4, 8.1 Hz, 2H), 7.37 – 7.43 (m, 1H), 7.47 (dd, J = 6.8, 8.3 Hz, 2H).

$^{13}\text{C-NMR}$ (100 MHz, CDCl_3): δ = 11.60, 12.95, 20.92, 24.36, 29.22, 108.27, 120.52, 125.11, 125.33, 127.35, 127.44, 127.51, 128.39, 128.99, 131.96, 134.27, 135.88, 139.24, 145.07.

HRMS (EI, 70 eV) m/z calc. for $[\text{C}_{22}\text{H}_{25}\text{N}]^+$: 303.1987, found: 303.1976.

3-([1,1'-Biphenyl]-2-yl)-2,5-dimethyl-1-phenyl-1*H*-pyrrole (**P10**)



According to general procedure 1.6 (see subsection 4.2.1.6) pyrrole sulfonium salt **A3** (407.5 mg, 1.0 mmol, 1.0 eq.) was allowed to react with the zincated aryl tosylate **T10** (648.8 mg, 2.0 mmol, 2.0 eq.), catalyst PEPPSI-IPr (2 mol%, 13.6 mg) in equal amounts of THF and DMF at 60 °C for 20 h. Purification via column chromatography (hexane → hexane/DCM 9:1) yielded **P10** as a yellow resin (69 %, 224 mg).

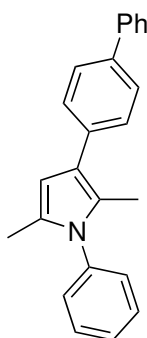
TLC: R_f 0.3 (hexane/DCM 9:1).

¹H-NMR (400 MHz, CDCl₃): δ = 1.35 (s, 3H), 2.01 (s, 3H), 5.89 (s, 1H), 6.99 – 7.07 (m, 2H), 7.16 – 7.50 (m, 12H).

¹³C-NMR (100 MHz, CDCl₃): δ = 11.54, 12.96, 108.36, 120.22, 125.63, 126.06, 126.45, 127.07, 127.16, 127.51, 127.60, 127.90, 128.28, 128.97, 129.58, 129.85, 130.09, 131.54, 136.03, 139.04, 141.11, 142.73.

HRMS (EI, 70 eV) m/z calc. for [C₂₂H₂₁N]⁺: 323.1674, found: 323.1662.

3-([1,1'-Biphenyl]-4-yl)-2,5-dimethyl-1-phenyl-1*H*-pyrrole (P11)



According to general procedure 1.6 (see subsection 4.2.1.6) pyrrole sulfonium salt **A3** (407.5 mg, 1.0 mmol, 1.0 eq.) was allowed to react with the zincated aryl tosylate **T11** (648.8 mg, 2.0 mmol, 2.0 eq.), catalyst PEPPSI-IPr (2 mol%, 13.6 mg) in equal amounts of THF and DMF at 60 °C for 20 h. Purification via column chromatography (hexane → hexane/DCM 7:3) yielded **P11** as a yellow resin (62 %, 199 mg).

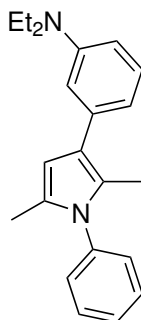
TLC: R_f 0.3 (hexane/DCM 8:2).

¹H-NMR (400 MHz, CDCl₃): δ = 2.09 (s, 3H), 2.19 (s, 3H), 6.19 (s, 1H), 7.27 – 7.35 (m, 3H), 7.40 – 7.54 (m, 8H), 7.58 – 7.68 (m, 4H).

¹³C-NMR (100 MHz, CDCl₃): δ = 12.37, 12.90, 106.48, 120.61, 125.34, 126.88, 126.90, 127.01, 127.86, 128.09, 128.42, 128.71, 128.77, 129.16, 136.43, 137.67, 138.81, 141.17.

HRMS (EI, 70 eV) m/z calc. for [C₂₄H₂₁N]⁺: 323.1674, found: 323.1668.

3-(2,5-Dimethyl-1-phenyl-1*H*-pyrrol-3-yl)-*N,N*-diethylaniline (P12)



According to general procedure 1.6 (see subsection 4.2.1.6) pyrrole sulfonium salt **A3** (407.5 mg, 1.0 mmol, 1.0 eq.) was allowed to react with the zincated aryl tosylate **T12** (638.8 mg, 2.0 mmol, 2.0 eq.), catalyst PEPPSI-IPr (2 mol%, 13.6 mg) in equal amounts of THF and DMF at 60 °C for 20 h. Purification via column chromatography (hexane → hexane/EtOAc 95:5) yielded **P12** as a yellow oil (41 %, 130 mg).

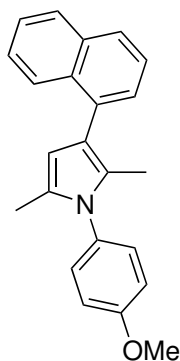
TLC: R_f 0.3 (hexane/EtOAc 95:5).

$^1\text{H-NMR}$ (400 MHz, CDCl_3): δ = 1.18 (t, J = 7.0 Hz, 6H), 2.07 (s, 3H), 2.16 (s, 3H), 3.38 (q, J = 7.0 Hz, 4H), 6.14 (d, J = 1.1 Hz, 1H), 6.53 – 6.61 (m, 1H), 6.71 – 6.79 (m, 2H), 7.21 (dd, J = 7.5, 8.3 Hz, 1H), 7.25 – 7.32 (m, 2H), 7.37 – 7.43 (m, 1H), 7.43 – 7.52 (m, 2H).

$^{13}\text{C-NMR}$ (100 MHz, CDCl_3): δ = 12.28, 12.79, 22.47, 27.96, 44.45, 106.82, 109.19, 111.92, 115.83, 122.15, 124.97, 127.69, 128.27, 128.46, 129.05, 129.07, 138.25, 139.00, 147.91.

HRMS (EI, 70 eV) m/z calc. for $[\text{C}_{22}\text{H}_{26}\text{N}_2]^+$: 318.2096, found: 318.2087.

1-(4-Methoxyphenyl)-2,5-dimethyl-3-(naphthalen-1-yl)-1*H*-pyrrole (**P13**)



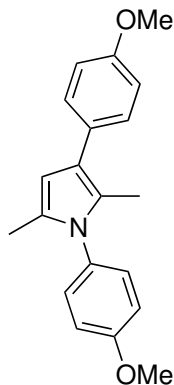
According to general procedure 1.6 (see subsection 4.2.1.6) pyrrole sulfonium salt **A4** (437.5 mg, 1.0 mmol, 1.0 eq.) was allowed to react with zincated aryl tosylate **T1** (596.7 mg, 2.0 mmol, 2.0 eq.), catalyst PEPPSI-IPr (2 mol%, 13.6 mg) in equal amounts of THF and DMF at 60 °C for 20 h. Purification via column chromatography (hexane → hexane/EtOAc 95:5) yielded **P13** as an orange resin (87 %, 284 mg).

TLC: R_f 0.3 (hexane/EtOAc 95:5).

$^1\text{H-NMR}$ (400 MHz, CDCl_3): δ = 1.96 (s, 3H), 2.16 (s, 3H), 3.91 (s, 3H), 6.17 (d, J = 1.2 Hz, 1H), 7.02 – 7.07 (m, 2H), 7.28 – 7.32 (m, 2H), 7.45 – 7.56 (m, 5H), 7.80 (dd, J = 1.4, 7.9 Hz, 1H), 7.88 – 7.93 (m, 1H), 8.16 – 8.24 (m, 1H).

$^{13}\text{C-NMR}$ (100 MHz, CDCl_3): δ = 11.92, 12.92, 55.50, 108.56, 114.28, 118.97, 125.36, 125.40, 125.45, 126.26, 126.61, 127.05, 127.55, 128.13, 128.27, 129.41, 131.89, 132.70, 133.94, 135.59, 158.95.

HRMS (EI, 70 eV) m/z calc. for $[\text{C}_{23}\text{H}_{21}\text{NO}]^+$: 327.1623, found: 327.1748.

1,3-Bis(4-methoxyphenyl)-2,5-dimethyl-1*H*-pyrrole (P14)

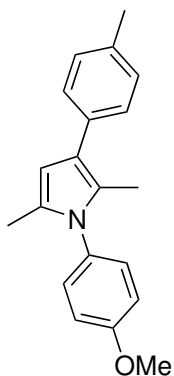
According to general procedure 1.6 (see subsection 4.2.1.6) pyrrole sulfonium salt **A4** (437.5 mg, 1.0 mmol, 1.0 eq.) was allowed to react with the zincated aryl tosylate **T5** (556.6 mg, 2.0 mmol, 2.0 eq.), catalyst PEPPSI-IPr (2 mol%, 13.6 mg) in equal amounts of THF and DMF at 60 °C for 20 h. Purification via column chromatography (hexane → hexane/DCM 95:5) yielded **P14** as a light brown powder (57 %, 174 mg).

TLC: R_f 0.2 (hexane/DCM 1:1).

$^1\text{H-NMR}$ (400 MHz, CDCl_3): δ = 2.05 (s, 3H), 2.11 (s, 3H), 3.83 (s, 3H), 3.87 (s, 3H), 6.08 (s, 1H), 6.89 – 6.95 (m, 2H), 6.95 – 7.02 (m, 2H), 7.15 – 7.22 (m, 2H), 7.32 – 7.40 (m, 2H).

$^{13}\text{C-NMR}$ (100 MHz, CDCl_3): δ = 12.07, 12.82, 55.28, 55.49, 106.10, 113.77, 114.26, 120.34, 124.83, 128.69, 128.84, 129.39, 130.06, 131.70, 157.30, 158.94.

HRMS (EI, 70 eV) m/z calc. for $[\text{C}_{20}\text{H}_{21}\text{NO}_2]^+$: 307.1572, found: 307.1564.

1-(4-Methoxyphenyl)-2,5-dimethyl-3-(*p*-tolyl)-1*H*-pyrrole (P15)

According to general procedure 1.6 (see subsection 4.2.1.6) pyrrole sulfonium salt **A4** (437.5 mg, 1.0 mmol, 1.0 eq.) was allowed to react with the zincated aryl tosylate **T3** (524.7 mg, 2.0 mmol, 2.0 eq.), catalyst PEPPSI-IPr (2 mol%, 13.6 mg) in equal amounts

of THF and DMF at 60 °C for 20 h. Purification via column chromatography (hexane → hexane/DCM 7:3) yielded **P15** as a brown powder (70 %, 203 mg).

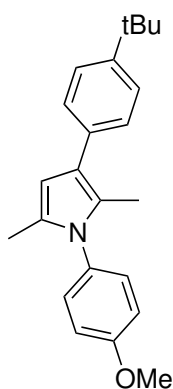
TLC: R_f 0.3 (hexane/DCM 8:2).

$^1\text{H-NMR}$ (400 MHz, CDCl_3): δ = 2.05 (s, 3H), 2.12 (s, 3H), 2.36 (s, 3H), 3.87 (s, 3H), 6.10 (s, 1H), 6.96 – 7.01 (m, 2H), 7.15 – 7.22 (m, 4H), 7.33 (d, J = 7.8 Hz, 2H).

$^{13}\text{C-NMR}$ (100 MHz, CDCl_3): δ = 12.14, 12.83, 21.10, 55.49, 106.14, 114.26, 120.65, 125.16, 127.72, 128.75, 129.00, 129.41, 131.68, 134.42, 134.48, 158.96.

HRMS (EI, 70 eV) m/z calc. for $[\text{C}_{20}\text{H}_{21}\text{NO}]^+$: 291.1623, found: 291.1610.

3-(4-(tert-Butyl)phenyl)-1-(4-methoxyphenyl)-2,5-dimethyl-1*H*-pyrrole (**P16**)



According to general procedure 1.6 (see subsection 4.2.1.6) pyrrole sulfonium salt **A4** (437.5 mg, 1.0 mmol, 1.0 eq.) was allowed to react with the zincated aryl tosylate **T4** (608.8 mg, 2.0 mmol, 2.0 eq.), catalyst PEPPSI-IPr (2 mol%, 13.6 mg) in equal amounts of THF and DMF at 60 °C for 20 h. Purification via column chromatography (hexane → hexane/DCM 8:2) yielded **P16** as a yellow powder (58 %, 195 mg).

TLC: R_f 0.3 (hexane/DCM 7:3).

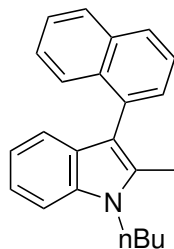
$^1\text{H-NMR}$ (400 MHz, CDCl_3): δ = 1.35 (s, 9H), 2.05 (s, 3H), 2.13 (s, 3H), 3.87 (s, 3H), 6.10 (s, 1H), 6.96 – 7.01 (m, 2H), 7.17 – 7.21 (m, 2H), 7.34 – 7.41 (m, 4H).

$^{13}\text{C-NMR}$ (100 MHz, CDCl_3): δ = 12.17, 12.85, 31.45, 34.39, 55.49, 106.21, 114.24, 120.59, 125.16, 125.22, 127.45, 128.66, 129.42, 131.72, 134.51, 147.61, 158.93.

HRMS (EI, 70 eV) m/z calc. for $[\text{C}_{23}\text{H}_{27}\text{NO}]^+$: 333.2093, found: 333.2090.

4.2.2.6 Synthesis of Indole Coupling Products

1-Butyl-2-methyl-3-(naphthalen-1-yl)-1*H*-indole (P24)



According to general procedure 1.7 (see subsection 4.2.1.7) indole sulfonium salt **A7** (423.5 mg, 1.0 mmol, 1.0 eq.) was allowed to react with the zincated aryl tosylate **T1** (596.7 mg, 2.0 mmol, 2.0 eq.), catalyst PEPPSI-IPr (2 mol%, 13.6 mg) in equal amounts of THF and DMF at 60 °C for 40 h. Purification via column chromatography (hexane → hexane/DCM 9:1) yielded **P17** as a white powder (82 %, 258 mg).

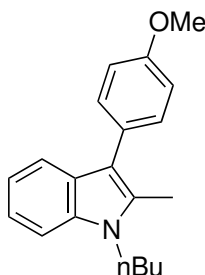
TLC: R_f 0.6 (hexane/DCM 7:3).

$^1\text{H-NMR}$ (400 MHz, CDCl_3): δ = 1.01 (t, J = 7.3 Hz, 3H), 1.47 (dt, J = 7.7, 15.2 Hz, 2H), 1.85 (p, J = 7.5 Hz, 2H), 2.30 (s, 3H), 4.20 (p, J = 7.8 Hz, 2H), 6.99 – 7.06 (m, 1H), 7.15 – 7.30 (m, 2H), 7.32 – 7.41 (m, 2H), 7.47 (ddd, J = 1.3, 7.0, 8.3 Hz, 2H), 7.55 (dd, J = 7.0, 8.1 Hz, 1H), 7.75 (d, J = 8.5 Hz, 1H), 7.86 (d, J = 8.1 Hz, 1H), 7.89 – 7.95 (m, 1H).

$^{13}\text{C-NMR}$ (100 MHz, CDCl_3): δ = 11.28, 13.94, 20.42, 32.44, 43.38, 108.94, 112.23, 119.23, 119.33, 120.76, 125.49, 125.54, 126.64, 126.90, 126.98, 128.18, 128.56, 128.77, 133.10, 133.42, 133.95, 134.08, 135.91.

HRMS (EI, 70 eV) m/z calc. for $[\text{C}_{23}\text{H}_{23}\text{N}]^+$: 313.1830, found: 313.1801.

1-Butyl-3-(4-methoxyphenyl)-2-methyl-1*H*-indole (P25)



According to general procedure 1.7 (see subsection 4.2.1.7) indole sulfonium salt **A7** (423.5 mg, 1.0 mmol, 1.0 eq.) was allowed to react with the zincated aryl tosylate **T5** (556.6 mg, 2.0 mmol, 2.0 eq.), catalyst PEPPSI-IPr (2 mol%, 13.6 mg) in equal amounts of THF and DMF at 60 °C for 40 h. Purification via column chromatography (hexane → hexane/DCM 9:1) yielded **P18** as a yellow oil (78 %, 207 mg).

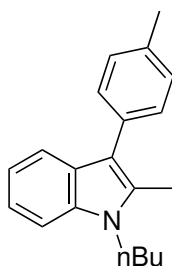
TLC: R_f 0.4 (hexane/DCM 7:3).

$^1\text{H-NMR}$ (400 MHz, CDCl_3): δ = 0.98 (t, J = 7.3 Hz, 3H), 1.43 (hept, J = 7.4 Hz, 2H), 1.78 (tt, J = 6.3, 7.8 Hz, 2H), 2.46 (s, 3H), 3.87 (s, 3H), 4.08 – 4.16 (m, 2H), 6.98 – 7.04 (m, 2H), 7.08 (ddd, J = 1.0, 7.0, 7.9 Hz, 1H), 7.18 (td, J = 1.2, 7.5 Hz, 1H), 7.32 (d, J = 8.1 Hz, 1H), 7.37 – 7.44 (m, 2H), 7.57 – 7.65 (m, 1H).

$^{13}\text{C-NMR}$ (100 MHz, CDCl_3): δ = 11.00, 13.91, 20.39, 32.41, 43.23, 55.32, 108.93, 113.62, 113.92, 118.70, 119.33, 120.86, 127.32, 128.21, 130.80, 132.51, 135.88, 157.74.

HRMS (EI, 70 eV) m/z calc. for $[\text{C}_{20}\text{H}_{23}\text{NO}]^+$: 293.1780, found: 293.1779.

1-Butyl-2-methyl-3-(*p*-tolyl)-1*H*-indole (P26)



According to general procedure 1.7 (see subsection 4.2.1.7) indole sulfonium salt **A7** (423.5 mg, 1.0 mmol, 1.0 eq.) was allowed to react with the zincated aryl tosylate **T3** (524.7 mg, 2.0 mmol, 2.0 eq.), catalyst PEPPSI-IPr (2 mol%, 13.6 mg) in equal amounts of THF and DMF at 60 °C for 40 h. Purification via column chromatography (hexane → hexane/DCM 9:1) yielded **P19** as a colorless oil (80 %, 221 mg).

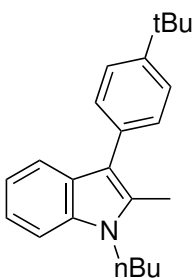
TLC: R_f 0.3 (hexane/DCM 7:3).

$^1\text{H-NMR}$ (400 MHz, CDCl_3): δ = 0.97 (t, J = 7.3 Hz, 3H), 1.38 – 1.49 (m, 2H), 1.73 – 1.82 (m, 2H), 2.41 (s, 3H), 2.47 (s, 3H), 4.08 – 4.16 (m, 2H), 7.08 (ddd, J = 1.0, 7.0, 8.0 Hz, 1H), 7.17 (ddd, J = 1.2, 7.0, 8.1 Hz, 1H), 7.27 (d, J = 7.8 Hz, 2H), 7.31 (d, J = 8.1 Hz, 1H), 7.35 – 7.42 (m, 2H), 7.64 (dd, J = 1.1, 7.8 Hz, 1H).

$^{13}\text{C-NMR}$ (100 MHz, CDCl_3): δ = 11.06, 13.93, 20.41, 21.23, 32.41, 43.24, 108.96, 113.93, 118.80, 119.39, 120.90, 127.23, 129.16, 129.66, 132.67, 132.83, 135.16, 135.95.

HRMS (EI, 70 eV) m/z calc. for $[\text{C}_{20}\text{H}_{23}\text{N}]^+$: 277.1830, found: 277.1823.

1-Butyl-3-(4-(*tert*-butyl)phenyl)-2-methyl-1*H*-indole (P27)



According to general procedure 1.7 (see subsection 4.2.1.7) indole sulfonium salt **A7** (423.5 mg, 1.0 mmol, 1.0 eq.) was allowed to react with the zincated aryl tosylate **T4** (739 mg, 2.0 mmol, 2.0 eq.), catalyst PEPPSI-IPr (2 mol%, 13.6 mg) in equal amounts of THF and DMF at 60 °C for 20 h. Purification via column chromatography (hexane → hexane/DCM 7:3) yielded **P26** as a white powder (76 %, 241 mg).

TLC: R_f 0.4 (hexane/DCM 7:3).

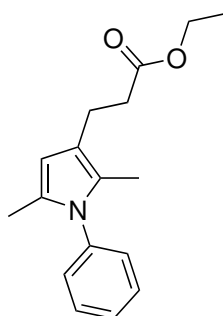
$^1\text{H-NMR}$ (400 MHz, CDCl_3): δ = 0.98 (t, J = 7.3 Hz, 3H), 1.38 (s, 9H), 1.41 – 1.49 (m, 2H), 1.78 (tt, J = 6.5, 7.9 Hz, 2H), 2.49 (s, 3H), 4.07 – 4.17 (m, 2H), 7.08 (t, J = 7.4 Hz, 1H), 7.18 (td, J = 1.3, 7.6 Hz, 1H), 7.31 (d, J = 8.1 Hz, 1H), 7.39 – 7.50 (m, 4H), 7.68 (d, J = 7.9 Hz, 1H).

$^{13}\text{C-NMR}$ (100 MHz, CDCl_3): δ = 11.14, 13.92, 20.40, 31.48, 32.39, 34.52, 43.23, 108.93, 113.86, 118.94, 119.33, 120.85, 125.31, 127.24, 129.32, 132.74, 132.82, 135.96, 148.28.

HRMS (EI, 70 eV) m/z calc. for $[\text{C}_{23}\text{H}_{29}\text{N}]^+$: 319.2300, found: 319.2288.

4.2.2.7 Synthesis of Propionic Acid Coupling Products

Ethyl 3-(2,5-dimethyl-1-phenyl-1*H*-pyrrol-3-yl)propanoate (**P36**)



According to general procedure 1.6 (see subsection 4.2.1.6) pyrrole sulfonium salt **A3** (437.5 mg, 1.0 mmol, 1.0 eq.) was allowed to react with the zincated 3-bromopropanoate **Z1** (739 mg, 3.0 mmol, 3.0 eq.), catalyst PEPPSI-IPr (2 mol%, 13.6 mg) in equal amounts of THF and DMF at 60 °C for 20 h. Purification via column chromatography (hexane → hexane/DCM 8:2) yielded **P35** as yellow oil (86 %, 232 mg).

TLC: R_f 0.3 (hexane/DCM 8:2).

$^1\text{H-NMR}$ (400 MHz, CDCl_3): δ = 0.91 (t, J = 7.3 Hz, 3H), 1.35 – 1.52 (m, 2H), 1.51 – 1.65 (m, 2H), 2.00 (s, 3H), 2.07 (s, 3H), 2.54 – 2.72 (m, 2H), 6.00 (d, J = 1.1 Hz, 1H), 7.14 – 7.23 (m, 2H), 7.34 – 7.44 (m, 1H), 7.41 – 7.52 (m, 2H).

$^{13}\text{C-NMR}$ (100 MHz, CDCl_3): δ = 11.31, 12.80, 13.78, 21.84, 31.89, 36.97, 108.59, 111.29, 127.87, 128.15, 128.38, 129.13, 129.15, 132.31, 138.92.

4.3. Experimental Data to Chapter 2

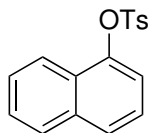
4.3.1 General Procedures

4.3.1.1 General Procedure 2.1 for Catalytic Zincation of Aryl Tosylates followed by Iodolysis

A pre-dried ($2 \cdot 10^{-2}$ mbar, heat-gun) and argon flushed Schlenk tube, equipped with a magnetic stirring bar and a septum, was charged with zinc powder (262 mg, 4.00 mmol, 4.0 eq.) which was dried under vacuum ($2 \cdot 10^{-2}$ mbar) and stirring with a heat-gun. 1,2-Dibromoethane (98 %, 17.6 μ L, 37.6 mg, 200 μ mol, 0.2 eq.) was added and the walls were rinsed with dry DMF (1 mL). After stirring at 60 °C for 20 min the reaction mixture was cooled down to room temperature for 5 min in a water bath. NiCl₂(dme) (11.0 mg, 50.0 μ mol, 5 mol%) and IPr-MeDAD (*N,N*-bis(2,6-diisopropylphenyl)butane-2,3-diimine), 40.5 mg, 100 μ mol, 10 mol%) were added and the walls were rinsed with dry DMF (1 mL). The brownish-green suspension was stirred for 30 min at room temperature. Finally, the aryl tosylate (1.00 mmol, 1.0 eq.) was added, the walls were rinsed with dry DMF (1 mL) and the reaction mixture was stirred for 20 h at room temperature. Then it was cooled to 0 °C before adding iodine (1.02 g, 4.00 mmol, 4.0 eq.) and stirring for ten minutes at 0 °C. A saturated aqueous solution of NH₄Cl (10 mL) and solid sodium sulfite (approx. 500 mg) were added and the reaction mixture was stirred until most of the brown color faded. The aqueous phase was extracted with diethylether (10 mL and 3 x 5 mL). The combined organic phases were washed with a saturated aqueous solution of NH₄Cl (2 x 20 mL) and NaCl (20 mL), dried over Na₂SO₄, filtered and the solvent was removed under reduced pressure (40 °C, 600 mbar for volatile products, 200 mbar for non-volatile ones). The crude product was analyzed by qNMR using either 1,1,2,2-tetrachloroethane (50.0 μ L, 473.6 μ mol) or trichloroethene (200 μ L, 2.22 mmol) as internal standard.

4.3.2 Isolated Compounds and Analytical Data

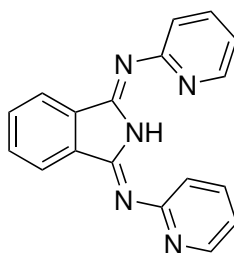
Naphthalen-1-yl 4-methylbenzenesulfonate (T1)



According to general procedure 1.3 (see subsection 4.2.1.3) tosylation of naphthalen-1-ol (14.4 g, 100 mmol, 1.0 eq.) afforded the product as an off-white solid (29.83 g, 99 %).

¹H-NMR (400 MHz, CDCl₃): δ = 2.41 (s, 3H), 7.20 (dd, J = 1.1, 7.6 Hz, 1H), 7.24 – 7.30 (m, 2H), 7.33 – 7.39 (m, 1H), 7.39 – 7.50 (m, 2H), 7.70 – 7.76 (m, 1H), 7.76 – 7.83 (m, 3H), 7.87 – 7.93 (m, 1H).

*N*¹,*N*³-Di(pyridine-2-yl)isoindoline-1,3-diimine (L8)



A 500 mL round-bottom flask, equipped with a magnetic stirring bar, was charged with phthalonitrile (12.81 g, 100 mmol, 1.0 eq.), pyridine-2-amine (19.76 g, 210 mmol, 2.1 eq.) and CaCl₂ (1.11 g, 10 mmol, 0.1 eq.) in 1-butanol (150 mL) and it was heated to 140 °C for 48 h. After cooling to room temperature, the precipitate was filtrated, washed with water and recrystallized out of ethanol and water (80 mL/20mL). The recrystallization yielded a yellow, fluffy solid (15.5 g, 51.8 mmol, 52 %).

¹H-NMR (400 MHz, CDCl₃): δ = 7.12 (ddd, J = 1.1, 4.9, 7.3 Hz, 1H), 7.46 (d, J = 8.0 Hz, 1H), 7.62 – 7.69 (m, 1H), 7.73 – 7.80 (m, 2H), 7.80 – 7.86 (m, 1H), 8.08 (dt, J = 3.4, 5.6 Hz, 1H), 8.62 (dd, J = 2.0, 4.8 Hz, 1H).

4.4. Experimental Data to Chapter 3

4.4.1 General Procedures

4.4.1.1 General Procedure 3.1 for Reductive Cross-Electrophile-Coupling

A pre-dried ($2 \cdot 10^{-2}$ mbar, heat-gun) and argon flushed Schlenk tube, equipped with a magnetic stirring bar and a septum, was charged with zinc powder (262 mg, 4.00 mmol, 4.0 eq.) which was dried under vacuum ($2 \cdot 10^{-2}$ mbar mbar) and stirring with a heat-gun. 1,2-Dibromoethane (98 %, 17.6 μ L, 37.6 mg, 200 μ mol, 0.2 eq.) was added and the walls were rinsed with the corresponding solvent (1 mL). After stirring at 60 °C for 20 min the reaction mixture was cooled down to room temperature for 5 min in a water bath. NiCl₂(dme) (11.0 mg, 50.0 μ mol, 5 mol%), the corresponding ligand (100 μ mol, 10 mol%), second catalyst (50.0 μ mol, 5 mol%), additive, tosylate (1.0 mmol, 1.0 eq.) and bromide (1.0 – 2.0 mmol, 1.0 – 2.0 eq.) were added and the reaction mixture was stirred at the indicated temperature for the indicated time. After cooling to room temperature the reaction mixture was diluted with Et₂O (10 mL) and washed with brine (10 mL). The aqueous phase was extracted with Et₂O (10 mL and 3 x 5 mL). The combined organic phases were washed with a saturated aqueous solution of NH₄Cl (2 x 20 mL) and NaCl (20 mL), dried over Na₂SO₄, filtered and the solvent was removed under reduced pressure (40 °C, 600 mbar for volatile products, 200 mbar for non-volatile ones). The crude product was analyzed by qNMR using either 1,1,2,2-tetrachloroethane (50.0 μ L, 473.6 μ mol) as internal standard.

4.5. NMR Spectra

2,5-Dimethyl-1-phenyl-1*H*-pyrrole (S1)

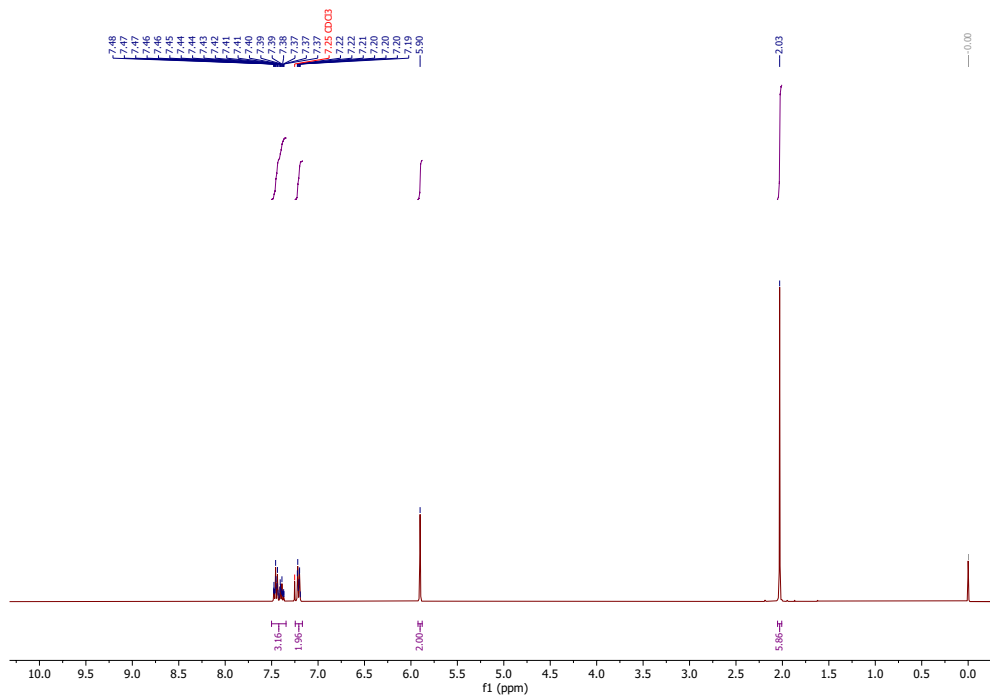


Figure 4.1: $^1\text{H-NMR}$ spectrum of S1.

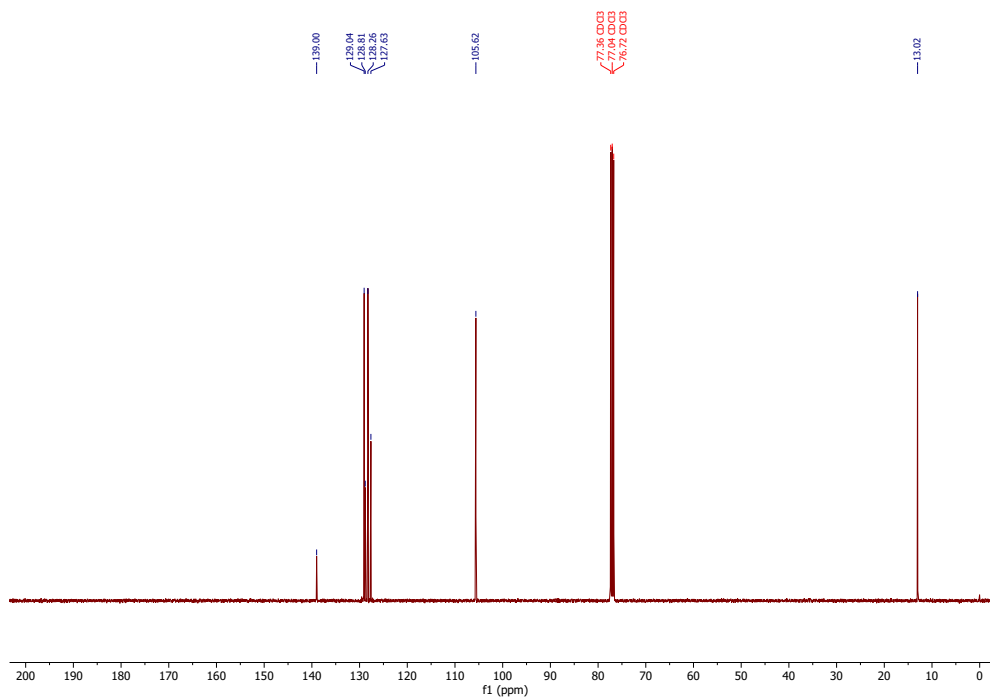
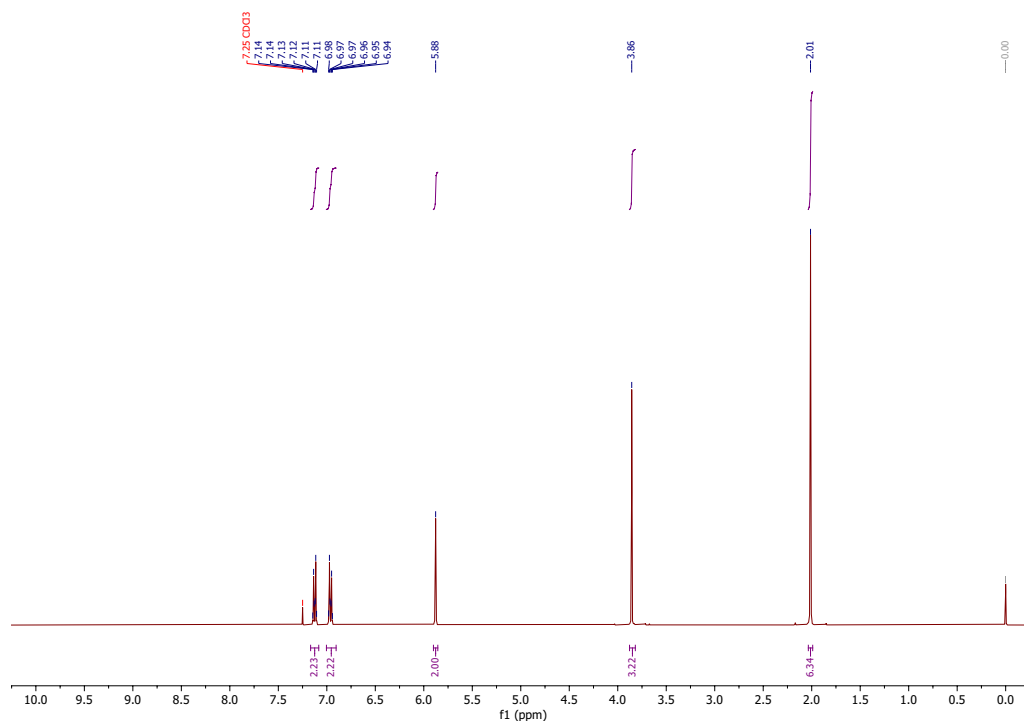
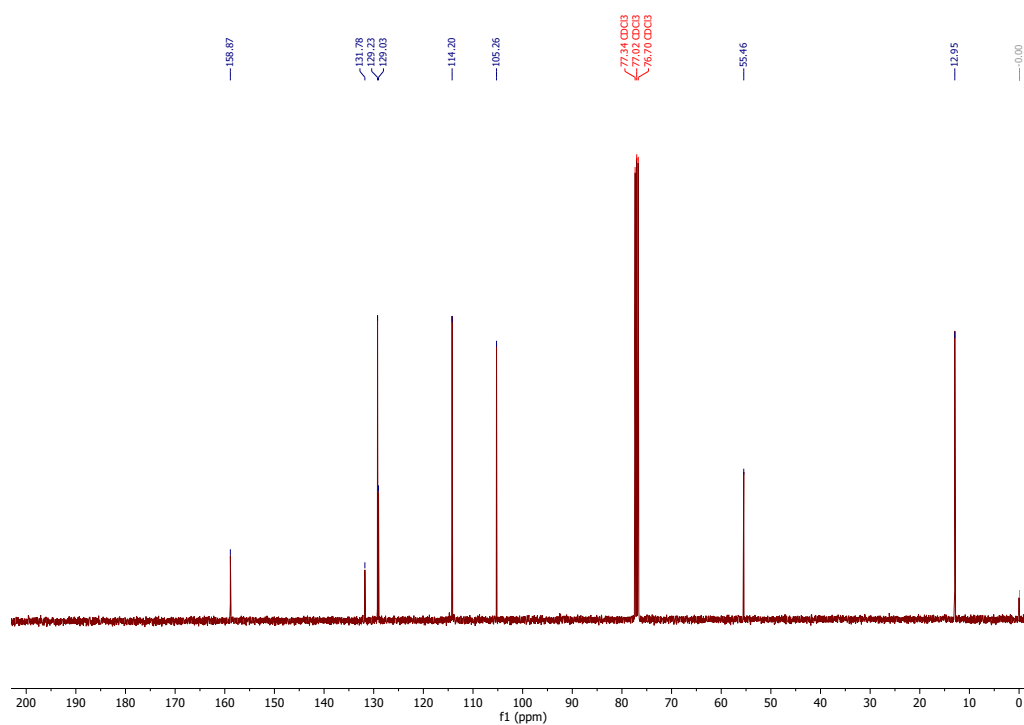
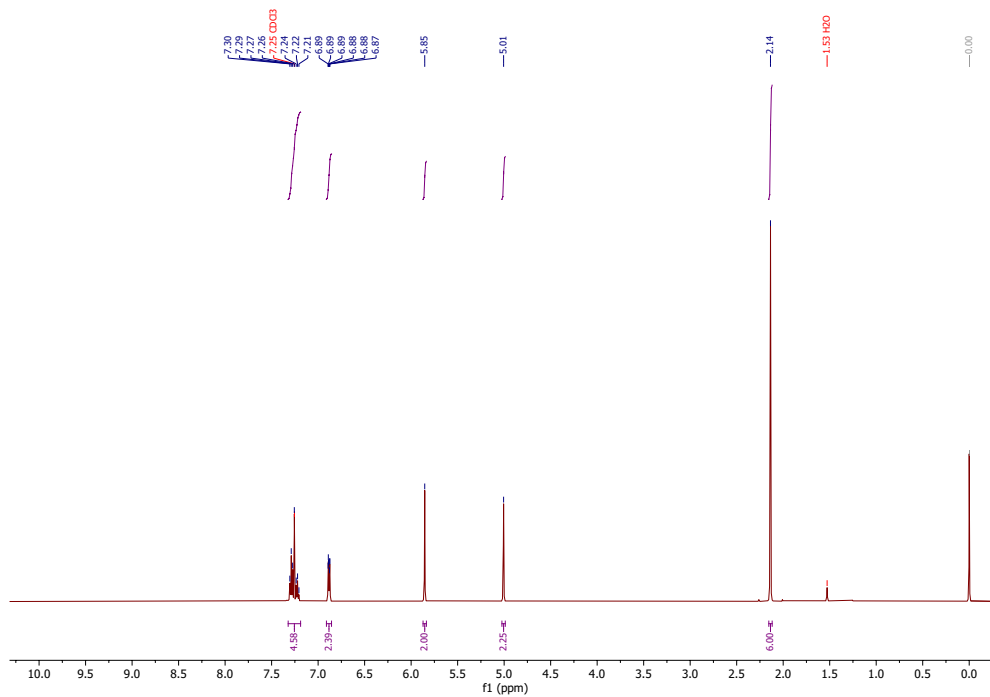
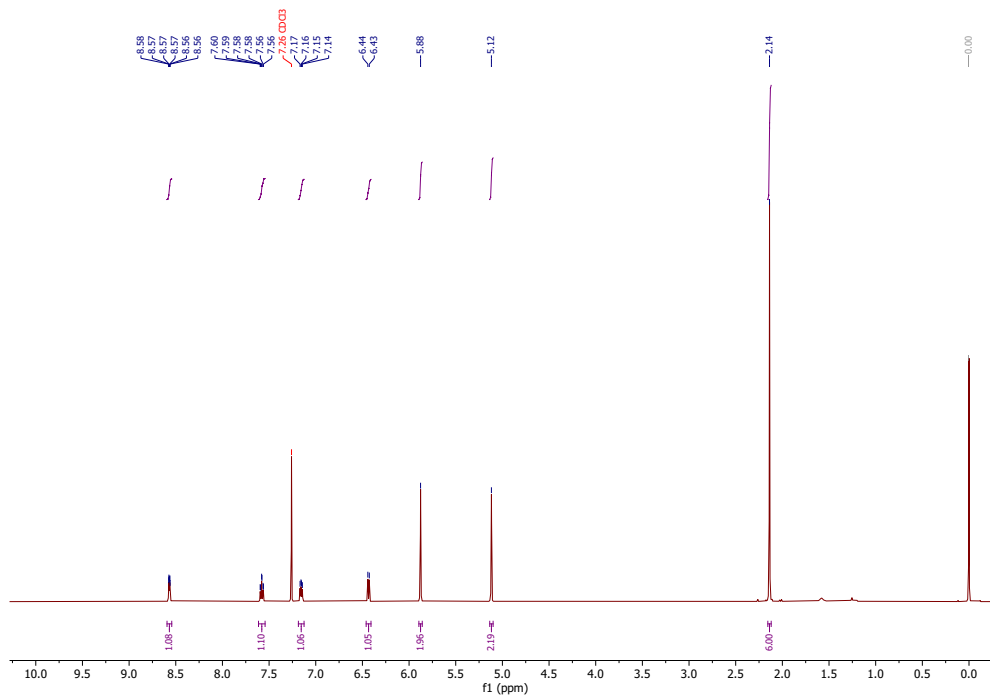


Figure 4.2: $^{13}\text{C-NMR}$ spectrum of S1.

1-(4-Methoxyphenyl)-2,5-dimethyl-1*H*-pyrrole (S2)Figure 4.3: ¹H-NMR spectrum of S2.Figure 4.4: ¹³C-NMR spectrum of S2.

1-Benzyl-2,5-dimethyl-1*H*-pyrrole (S5)Figure 4.7: ^1H -NMR spectrum of S5.2-((2,5-Dimethyl-1*H*-pyrrol-1-yl)methyl)pyridine (S6)Figure 4.8: ^1H -NMR spectrum of S6.

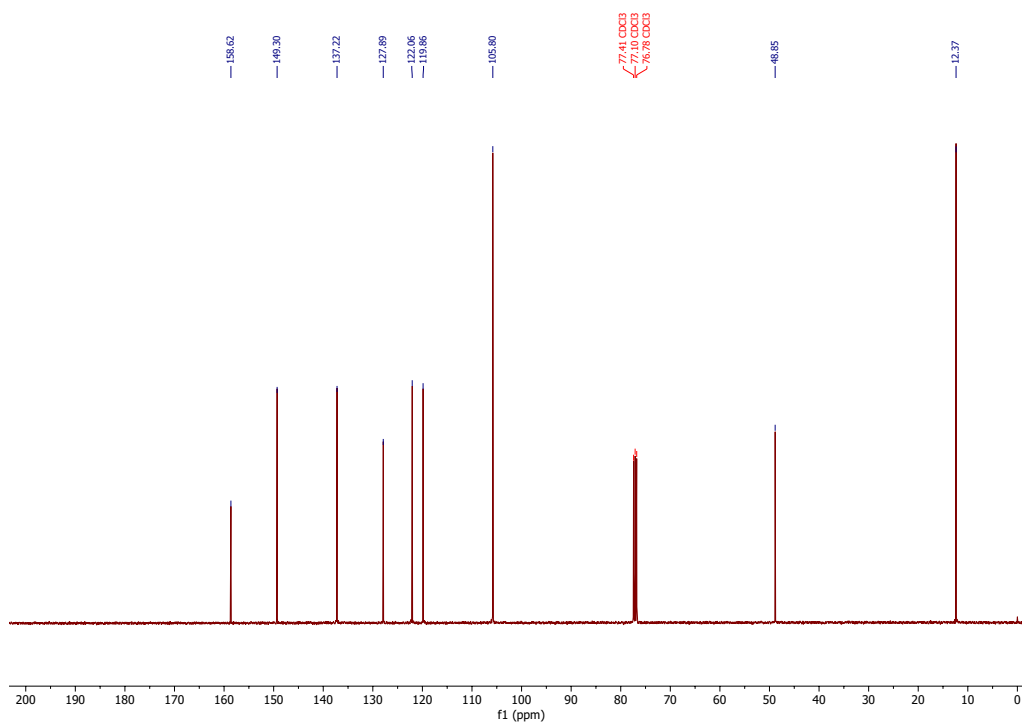


Figure 4.9: ¹³C-NMR spectrum of **S6**.

1,3-Bis((2,5-dimethyl-1*H*-pyrrol-1-yl)methyl)benzene (S7**)**

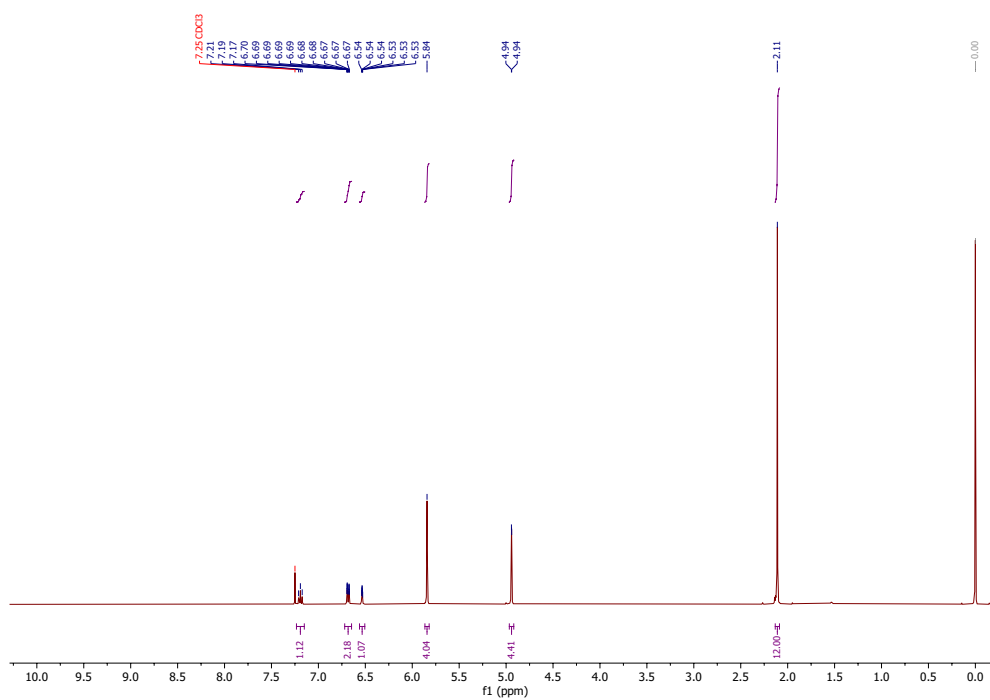


Figure 4.10: ¹H-NMR spectrum of **S7**.

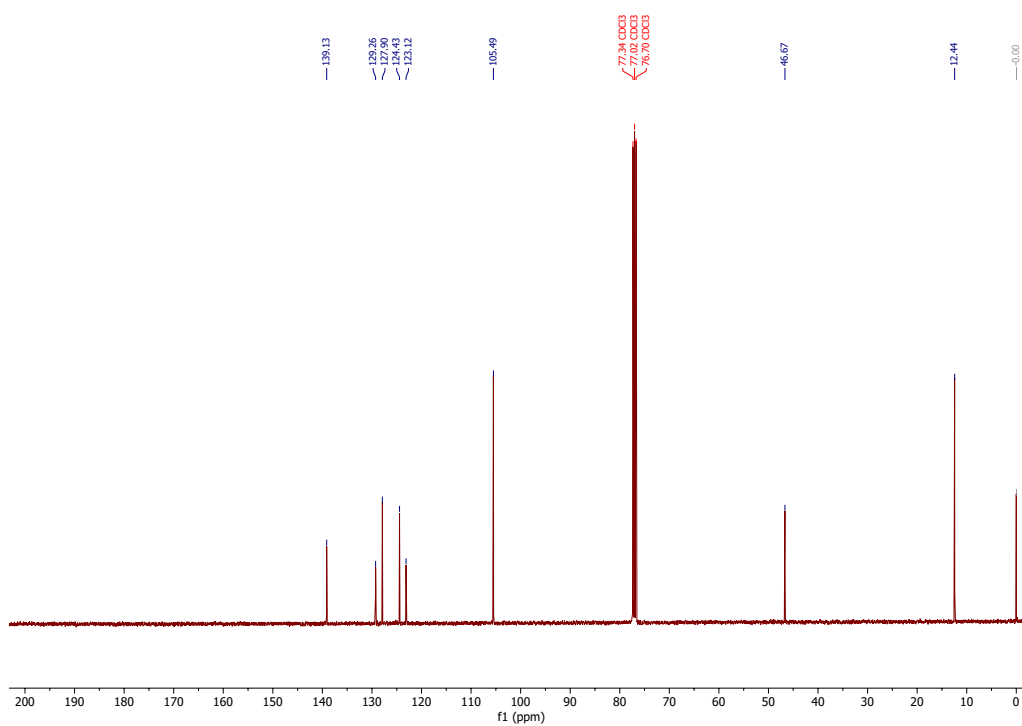


Figure 4.11: ^{13}C -NMR spectrum of **S7**.

1,2,5-Trimethyl-1*H*-pyrrole (**S8**)

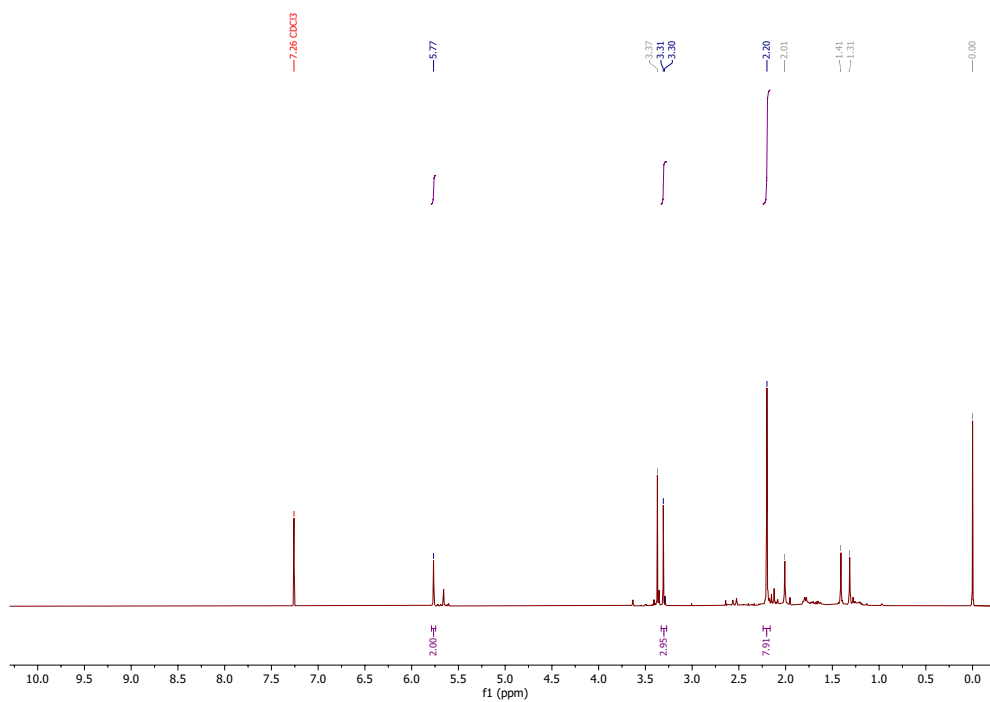
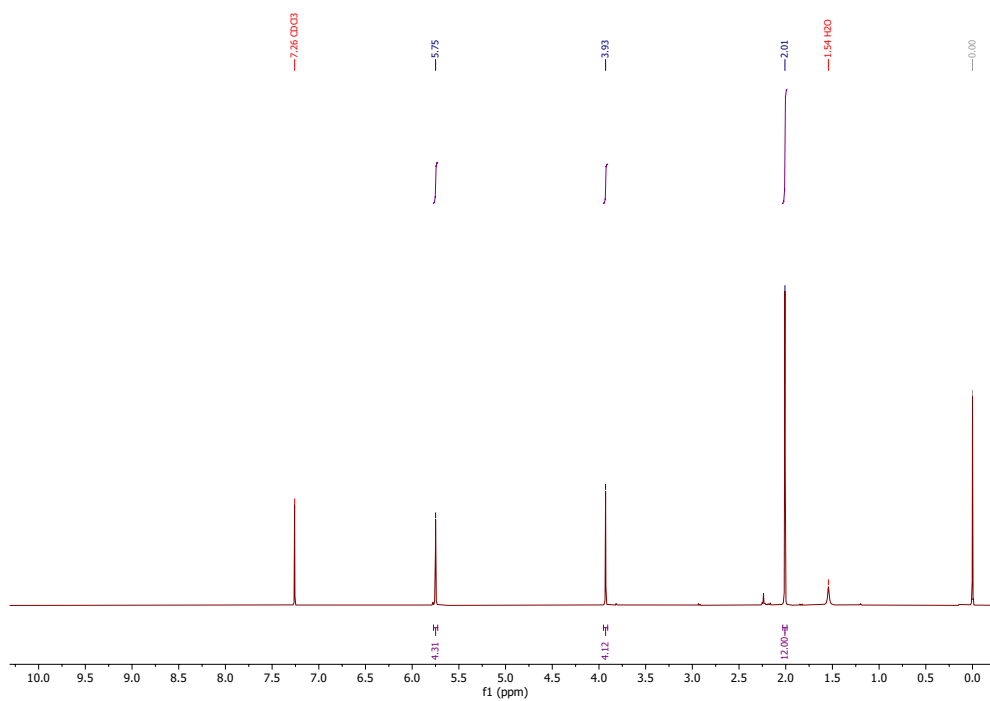
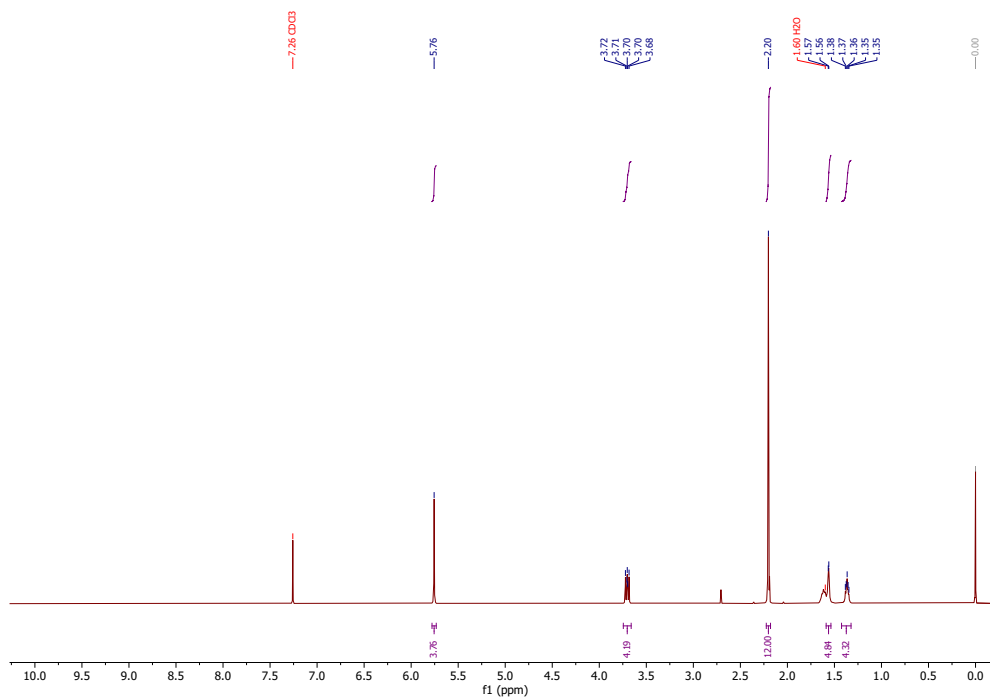


Figure 4.12: ^1H -NMR spectrum of **S8**.

1,2-Bis(2,5-dimethyl-1*H*-pyrrol-1-yl)ethane (S9)Figure 4.13: ^1H -NMR spectrum of S9.1,6-Bis(2,5-dimethyl-1*H*-pyrrol-1-yl)hexane (S10)Figure 4.14: ^1H -NMR spectrum of S10.

1-Phenyl-1*H*-pyrrole (S17)

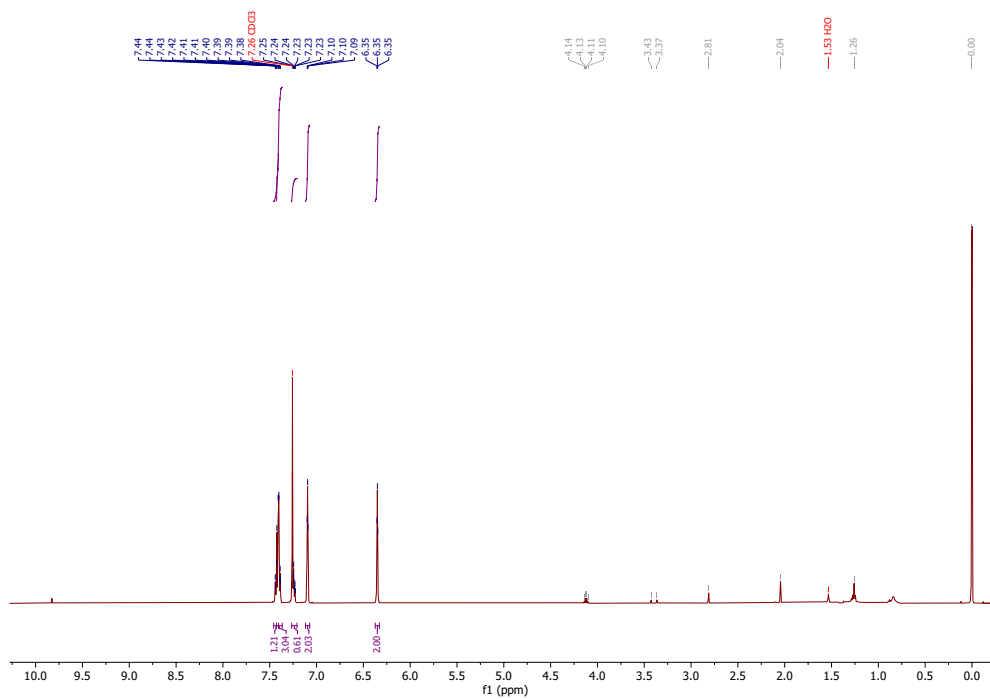


Figure 4.15: ¹H-NMR spectrum of S17.

1-Tosyl-1*H*-pyrrole (S18)

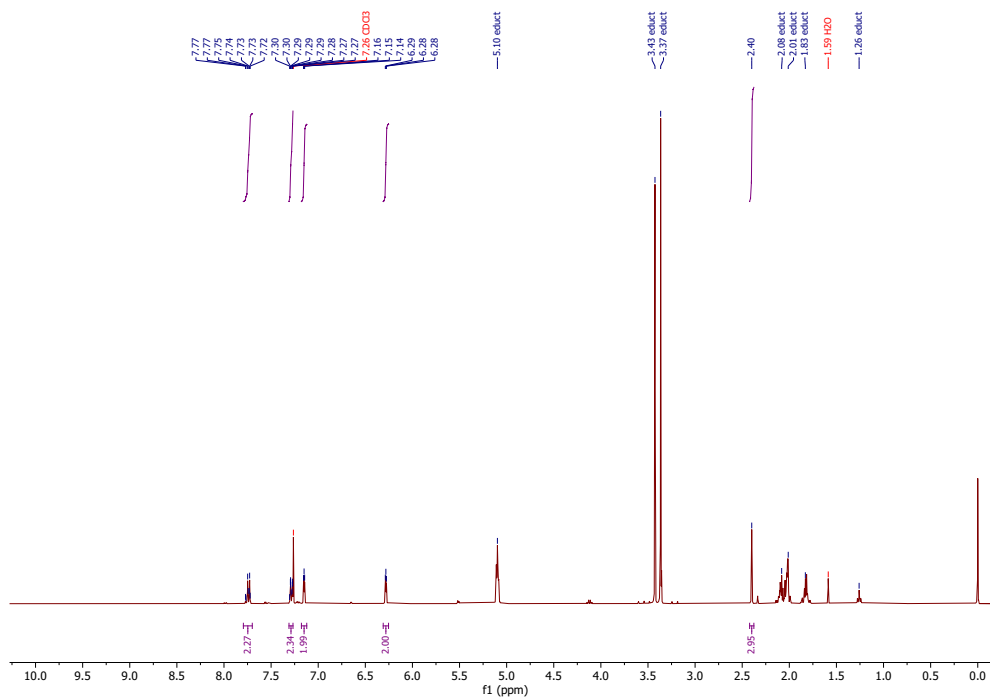
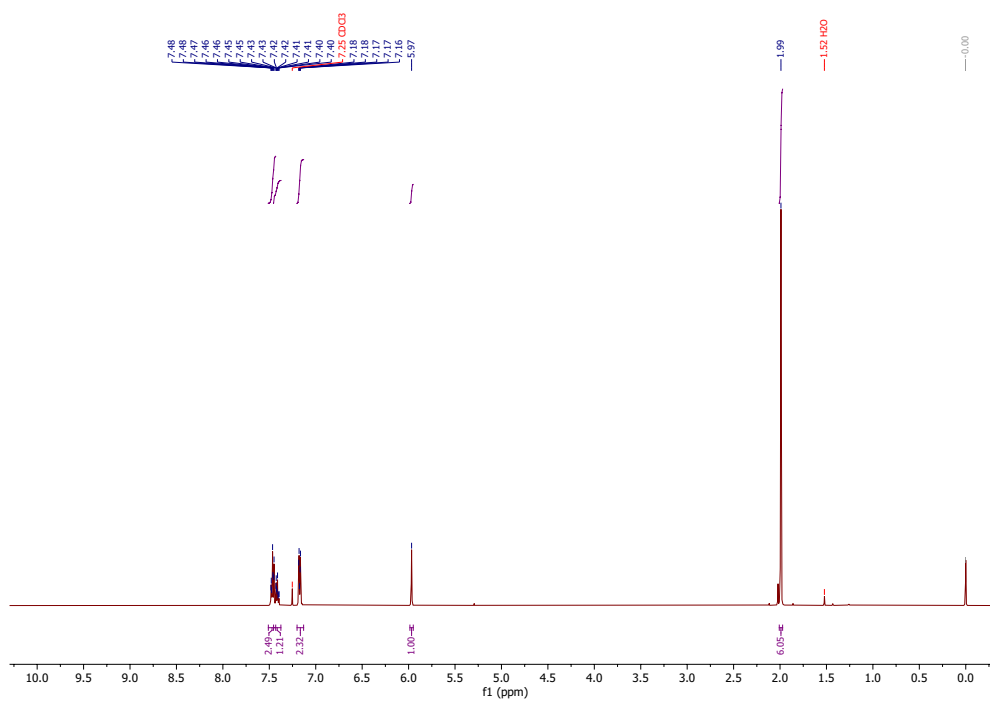
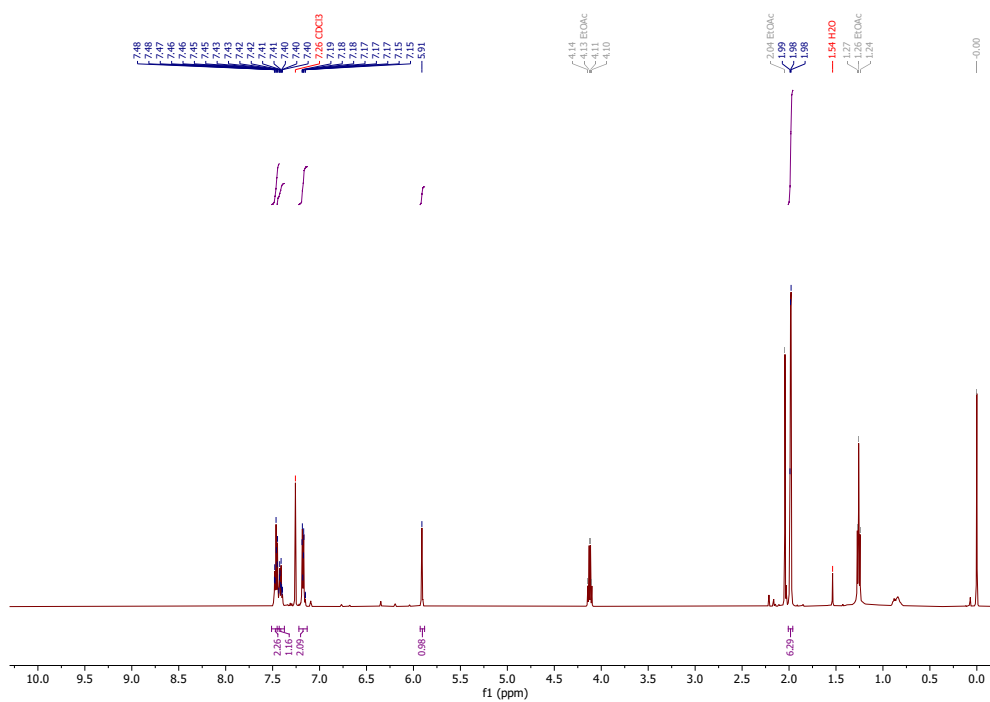
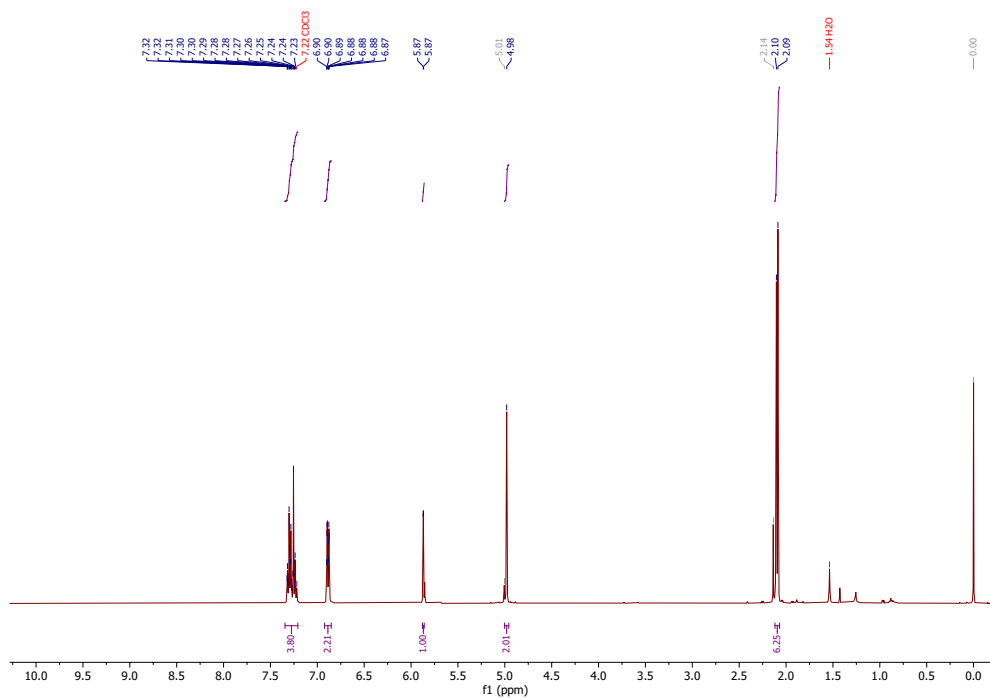
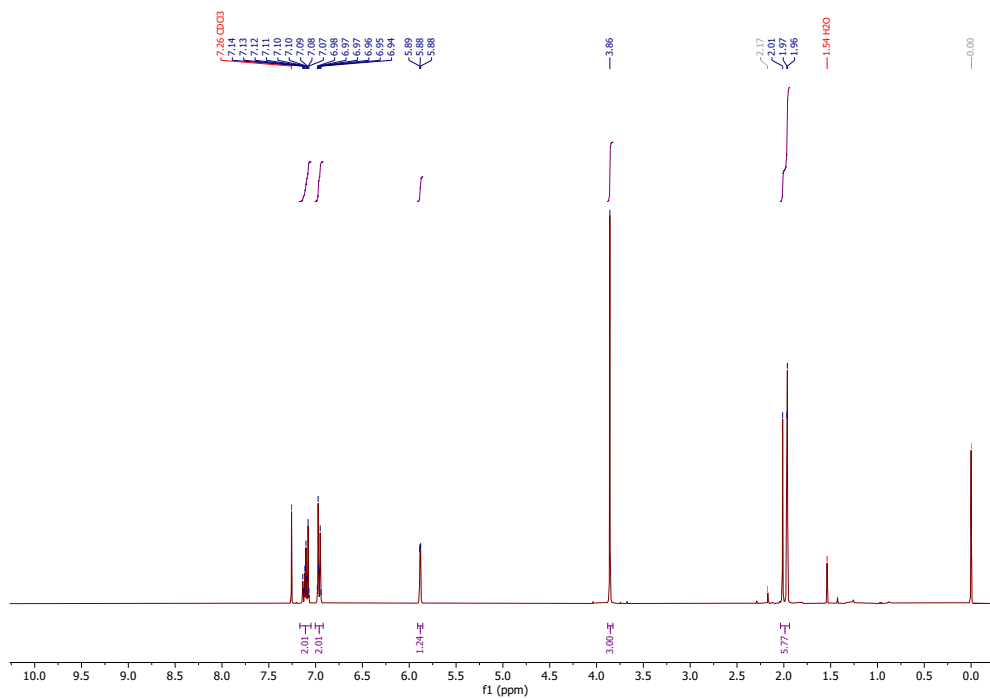


Figure 4.16: ¹H-NMR spectrum of S19.

3-Bromo-2,5-dimethyl-1-phenyl-1*H*-pyrrole (B1)Figure 4.17: ¹H-NMR spectrum of B1.3-Chloro-2,5-dimethyl-1-phenyl-1*H*-pyrrole (C1)

1-Benzyl-3-chloro-2,5-dimethyl-1*H*pyrrole (C2)Figure 4.19: ¹H-NMR spectrum of C2.3-Chloro-1-(4-methoxyphenyl)-2,5-dimethyl-1*H*pyrrole (C3)Figure 4.20: ¹H-NMR spectrum of C3.

1-Butyl-2-methyl-1*H*-indole (S21)

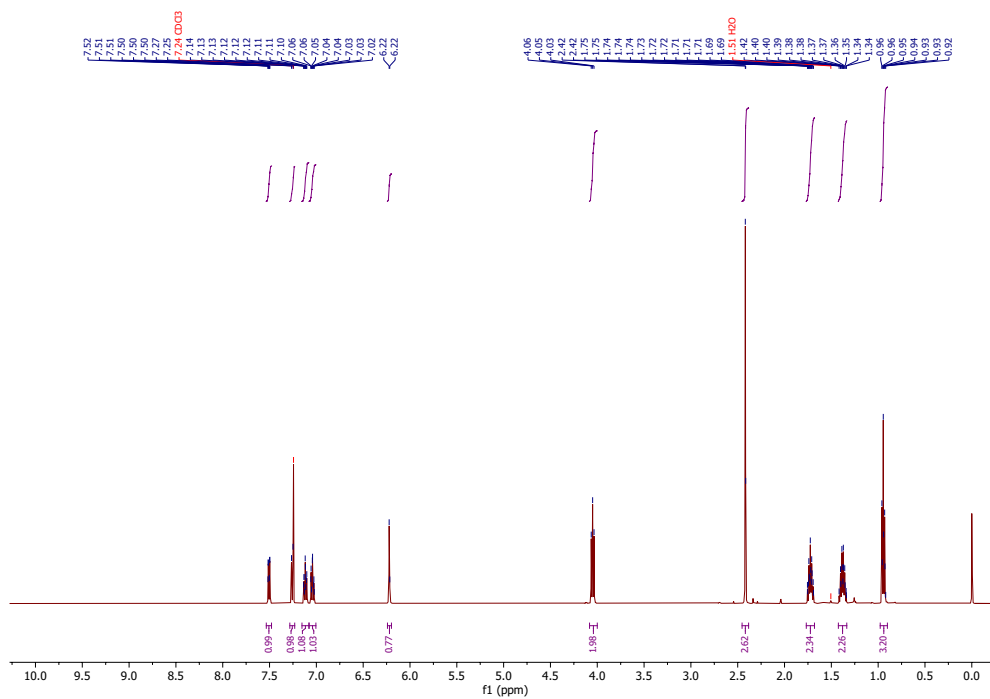


Figure 4.21: ¹H-NMR spectrum of S21.

1-Butyl-1*H*-indole (S22)

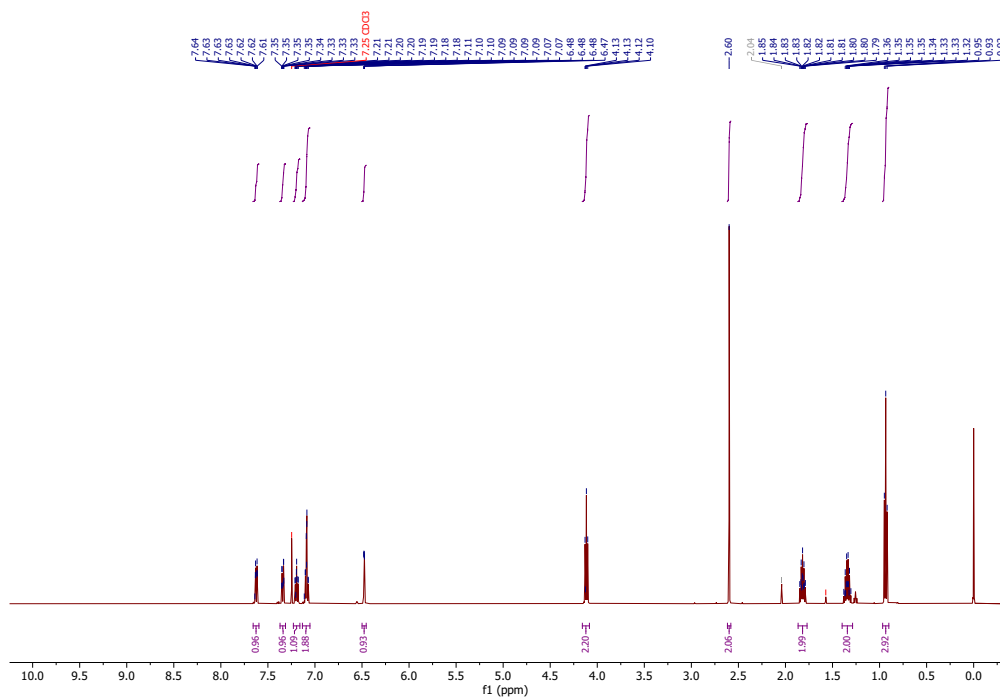
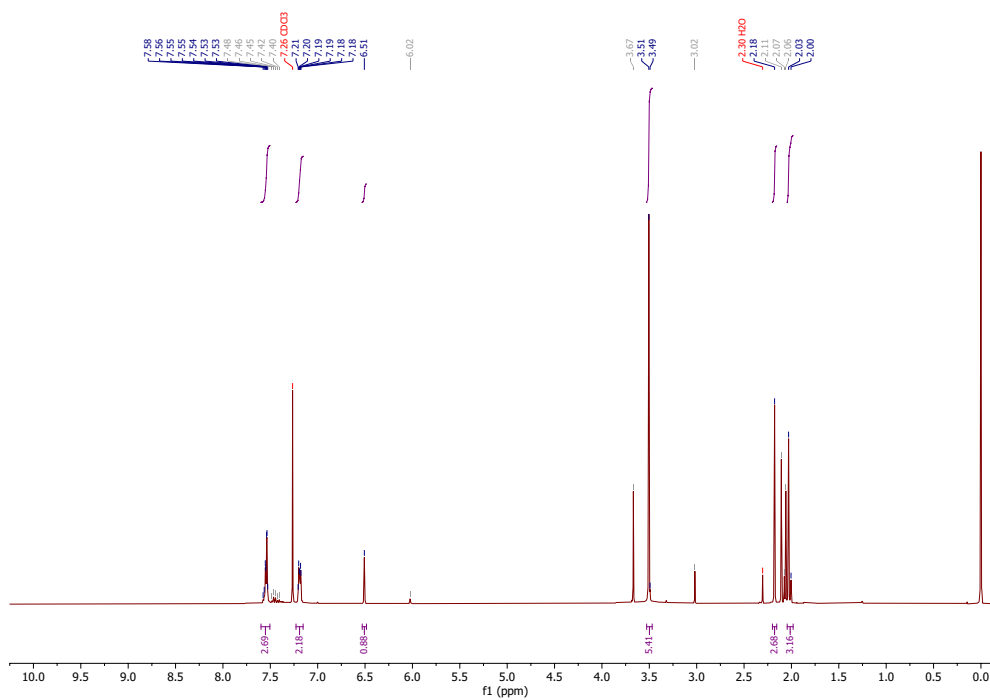
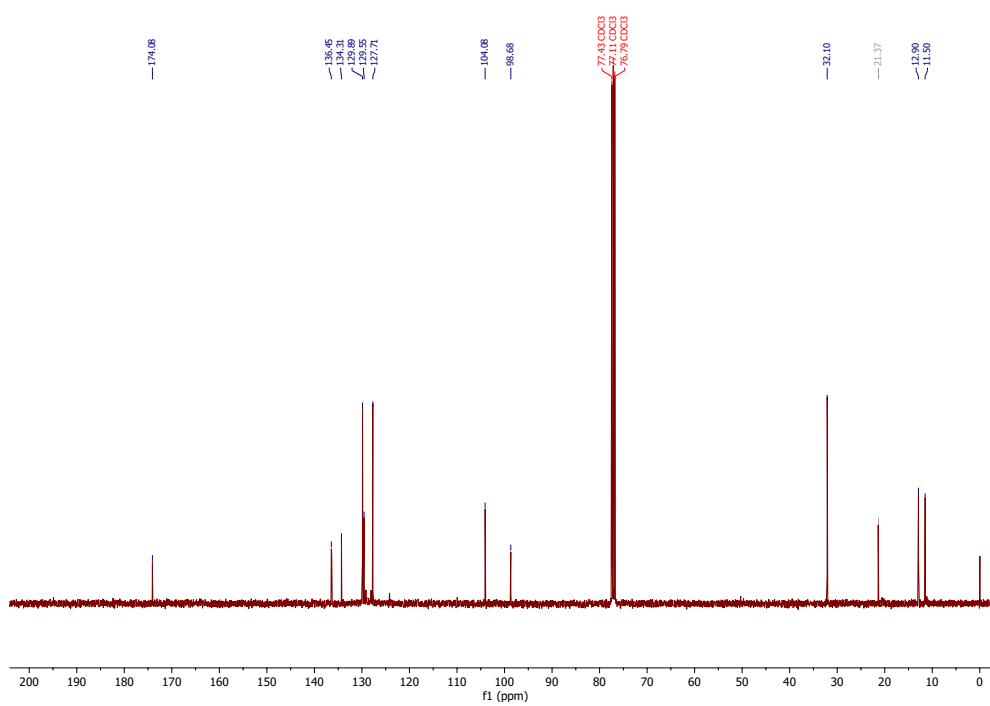
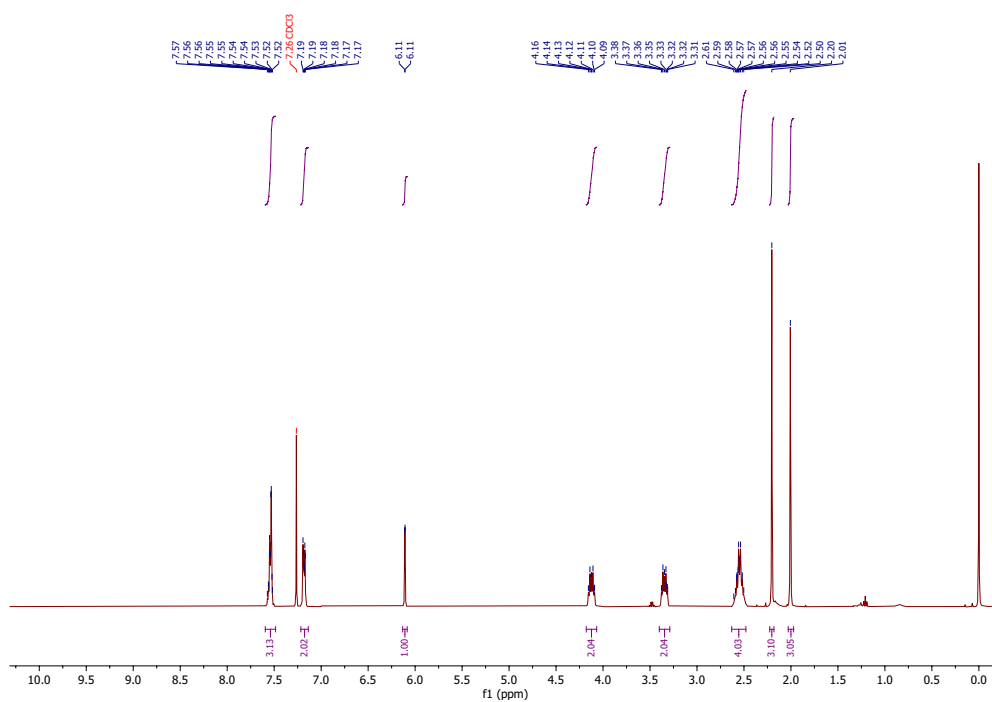
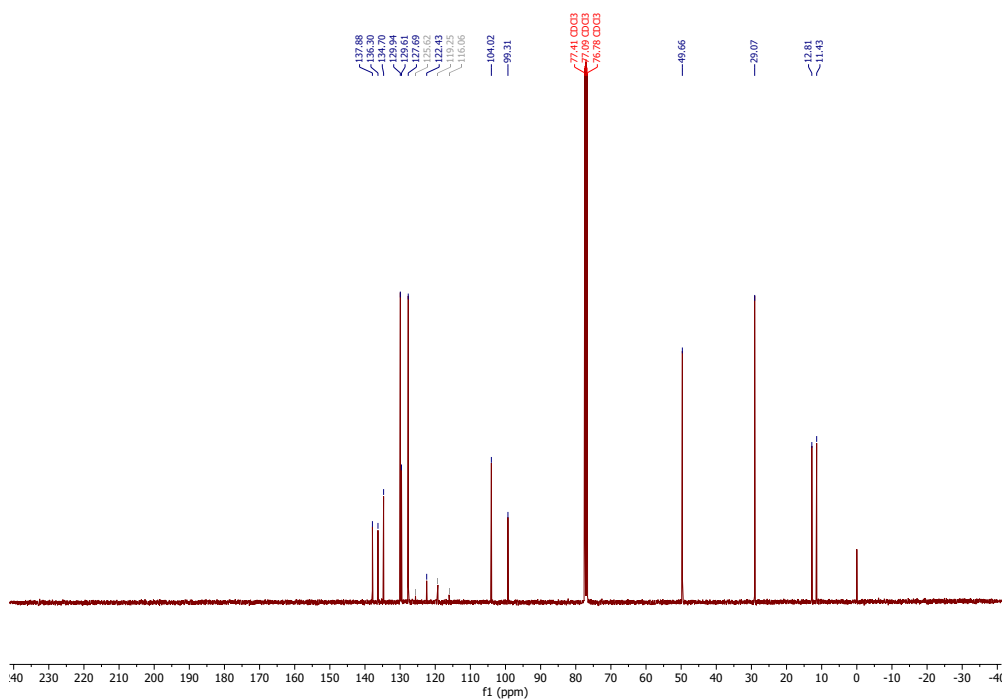
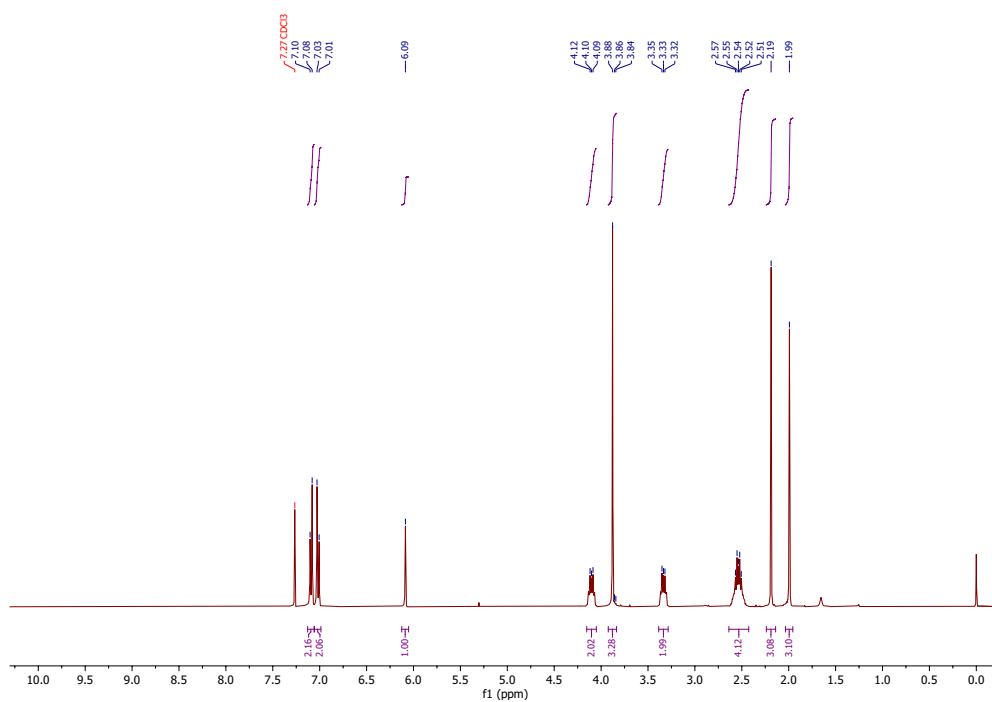
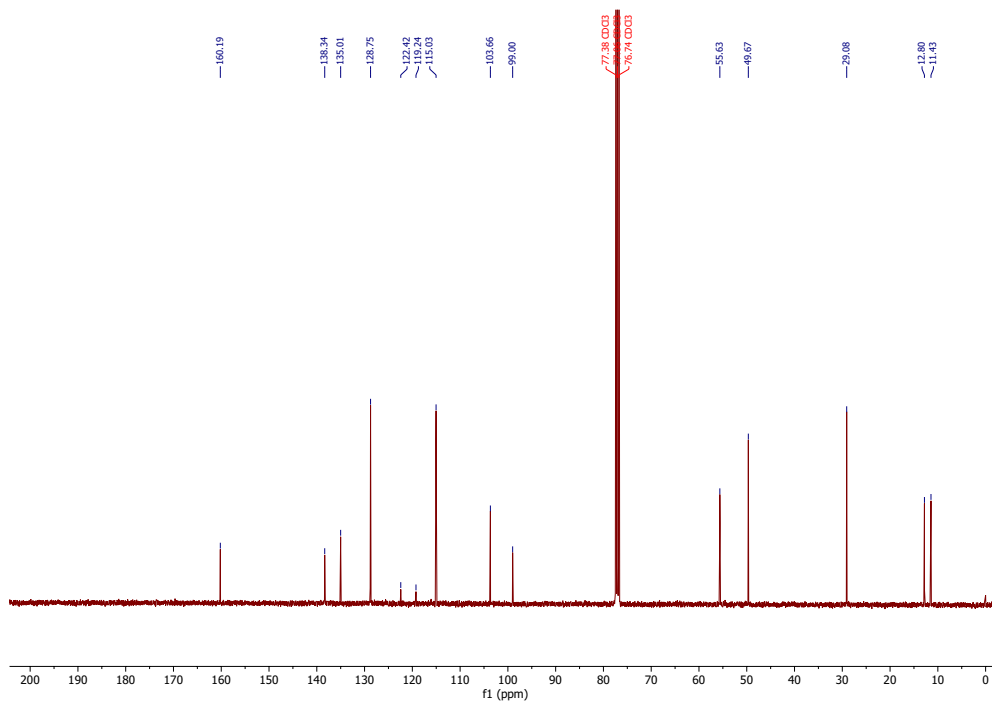
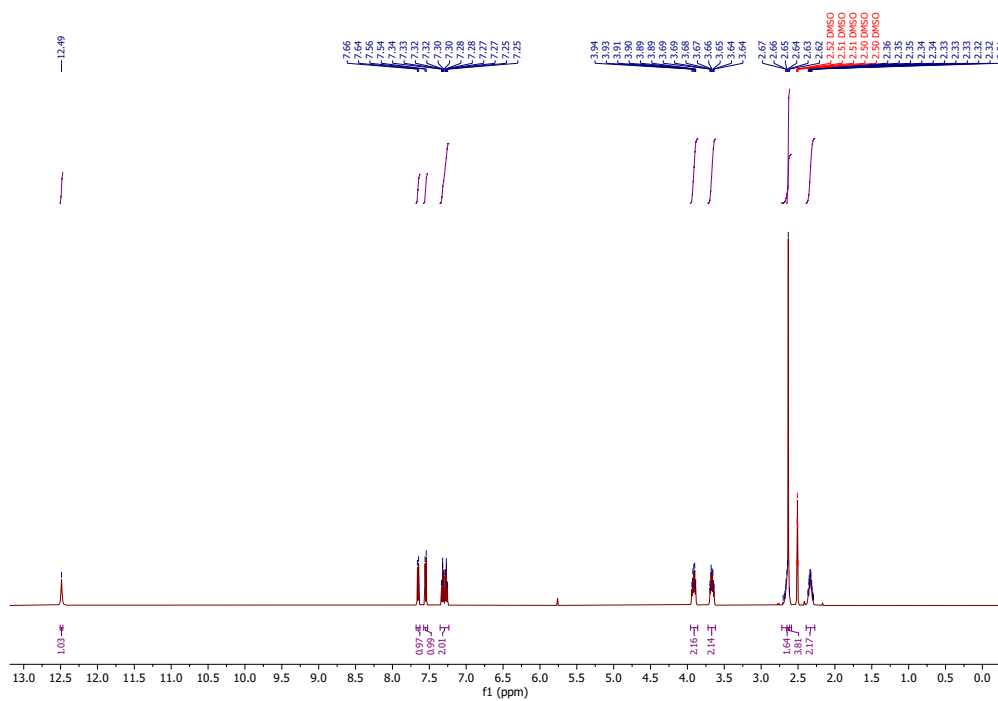
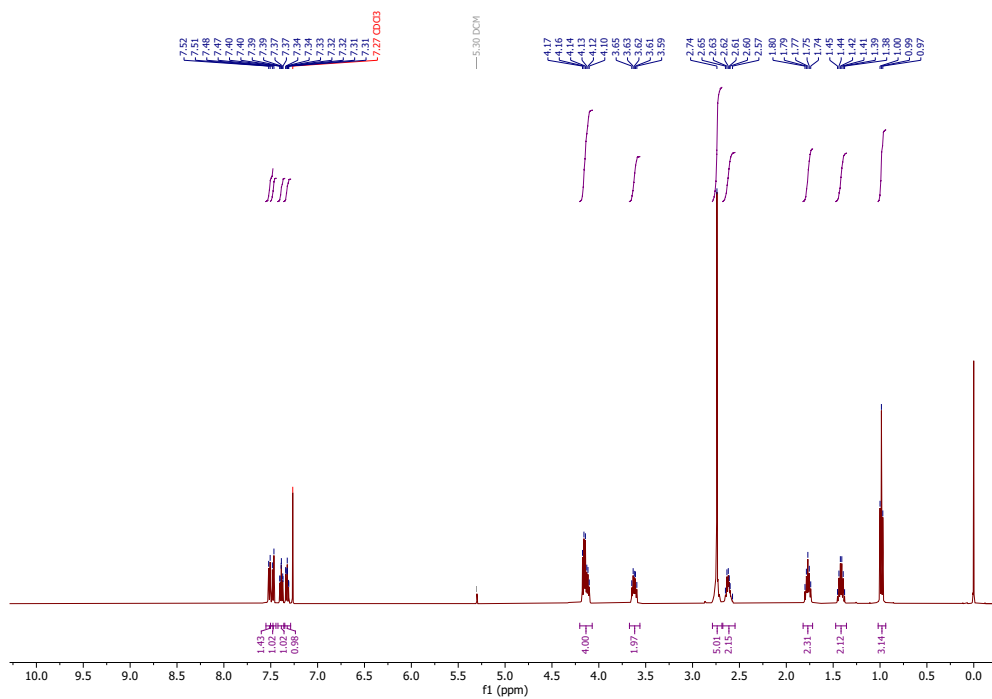


Figure 4.22: ¹H-NMR spectrum of S22.

2,5-Dimethyl-3-(methylthio)-1-phenyl-1*H*-pyrrole (A2)Figure 4.23: ¹H-NMR spectrum of A2.Figure 4.24: ¹³C-NMR spectrum of A2.

1-(2,5-Dimethyl-1-phenyl-1*H*-pyrrol-3-yl)tetrahydro-1*H*-thiophen-1-ium triflate (A3)Figure 4.25: ^1H -NMR spectrum of **A3**.Figure 4.26: ^{13}C -NMR spectrum of **A3**.

1-(1-(4-Methoxyphenyl)-2,5-dimethyl-1*H*-pyrrol-3-yl)tetrahydro-1*H*-thiophen-1-ium triflate (A4)**Figure 4.27:** ¹H-NMR spectrum of A4.**Figure 4.28:** ¹³C-NMR spectrum of A4.

1-(2-Methyl-1*H*-indol-3-yl)tetrahydro-1*H*-thiophen-1-ium triflate (A6)Figure 4.30: ^1H -NMR spectrum of A6.1-(1-Butyl-2-methyl-1*H*-indol-3-yl)tetrahydro-1*H*-thiophen-1-ium triflate (A7)Figure 4.31: ^1H -NMR spectrum of A7.

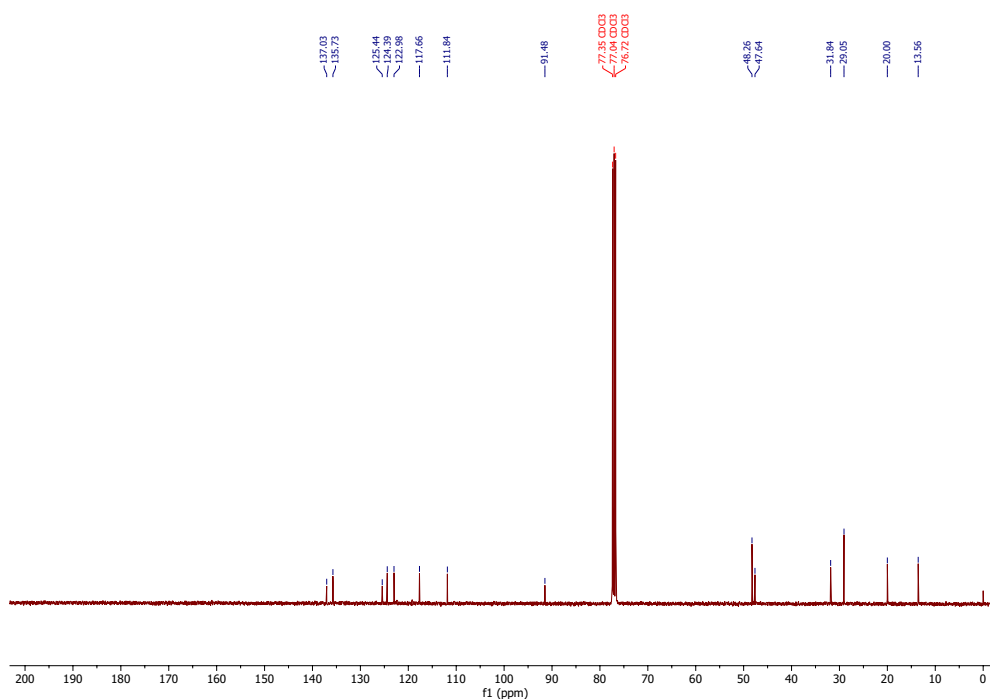


Figure 4.34: ^{13}C -NMR spectrum of A8.

1,1'-(Ethane-1,2-diylbis(2,5-dimethyl-1*H*-pyrrole-1,3-diyl))bis(tetrahydro-1*H*-thiophen-1-ium) triflate (A9)

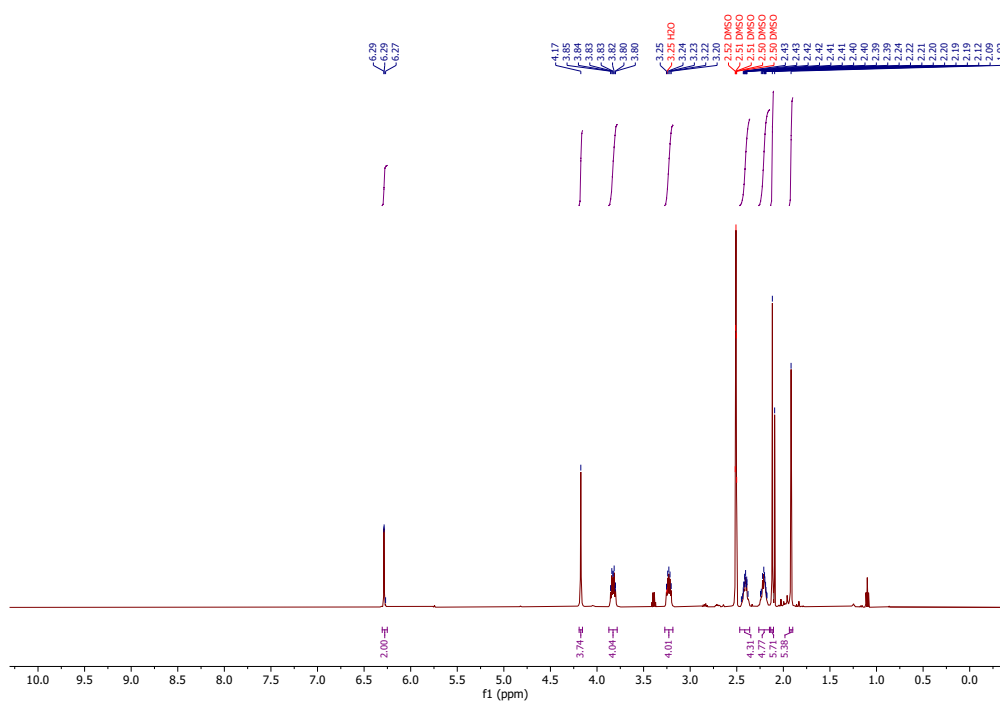
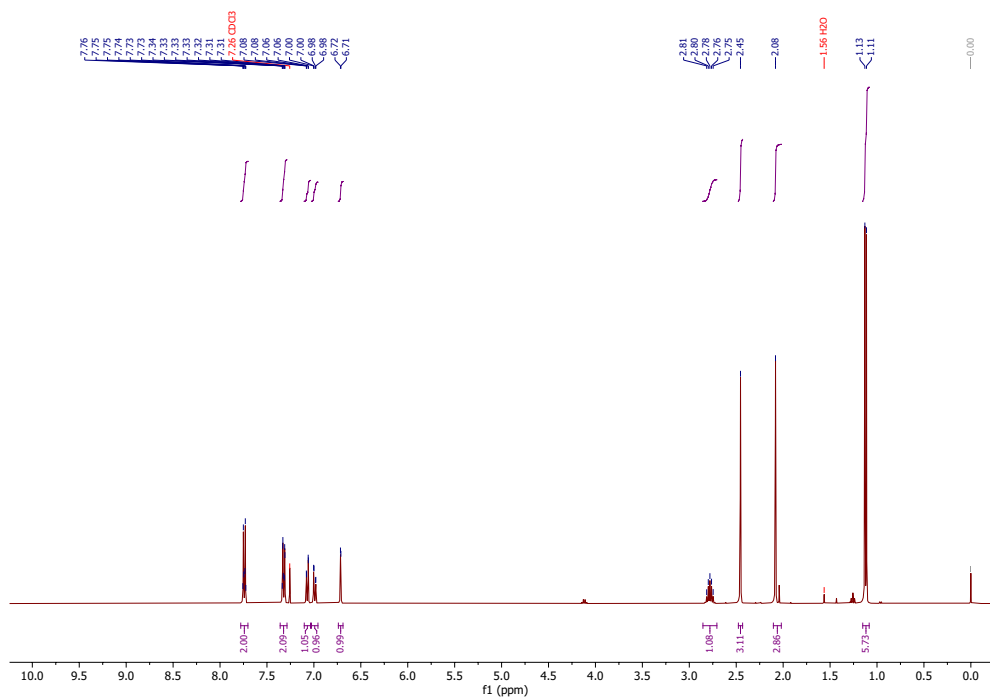
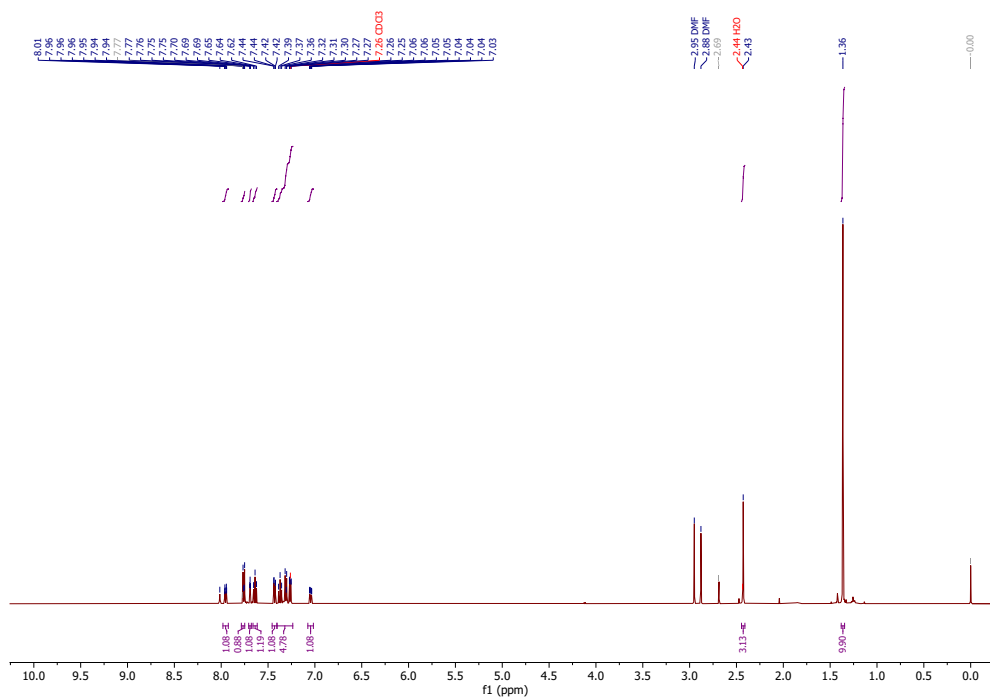


Figure 4.35: ^1H -NMR spectrum of A9.

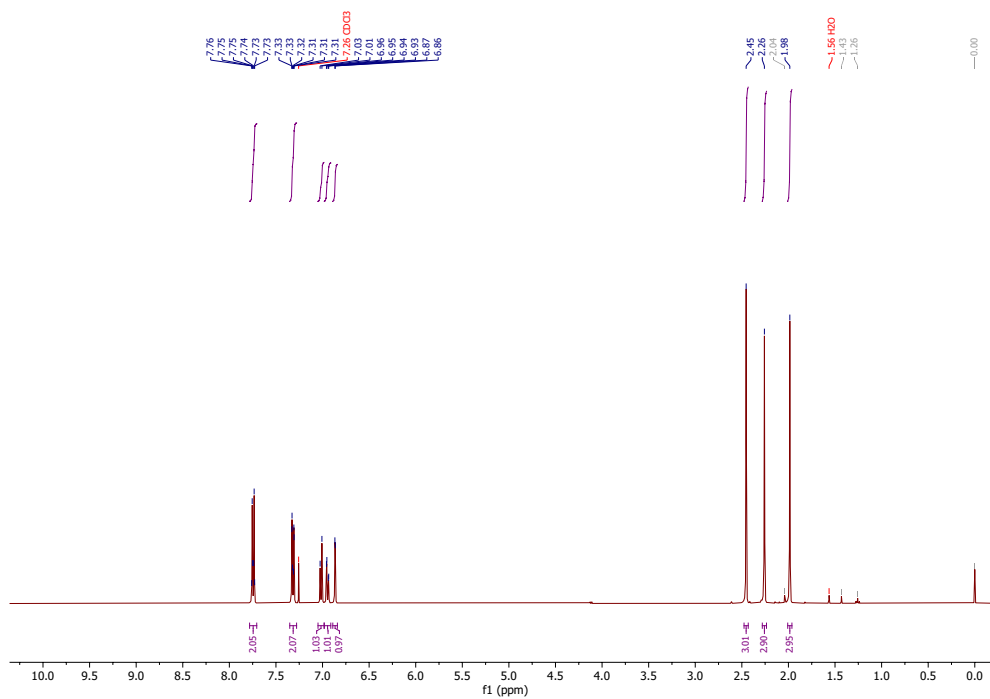
5-Isopropyl-2-methylphenyl 4-methylbenzenesulfonate (T9)

Figure 4.38: ¹H-NMR spectrum of T9.

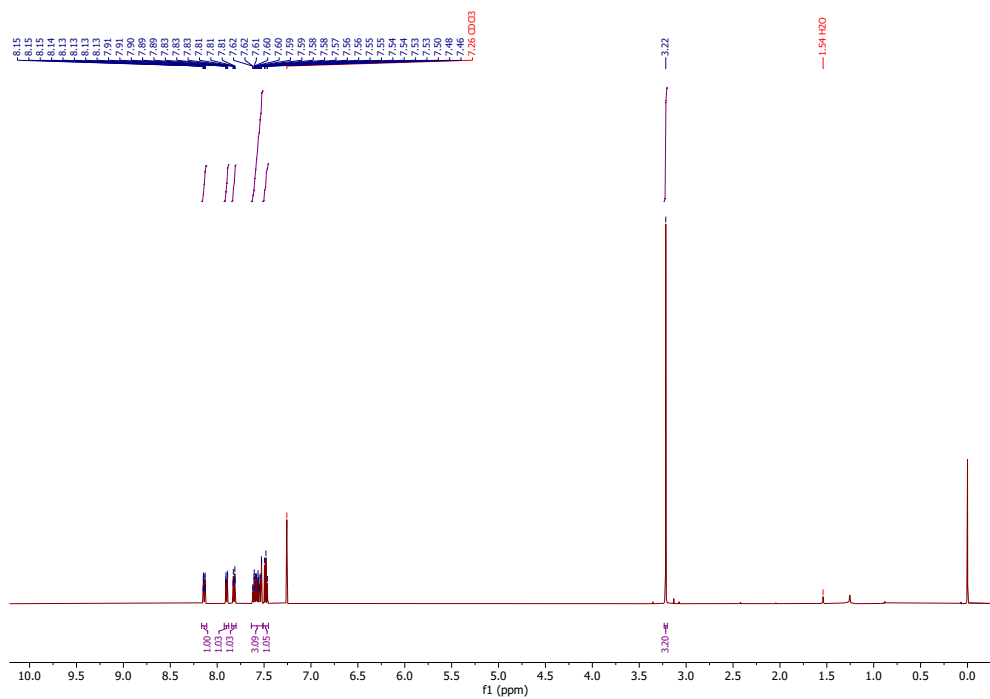
3-(6-(Tert-butyl)pyridin-2-yl)phenyl 4-methylbenzenesulfonate (T13)

Figure 4.39: ¹H-NMR spectrum of T13.

2,5-Dimethylphenyl 4-methylbenzenesulfonate (T16)

Figure 4.40: ¹H-NMR spectrum of T16.

Naphthalen-1-yl methanesulfonate (T17)

Figure 4.41: ¹H-NMR spectrum of T17.

Naphthalen-1-yl trifluoromethanesulfonate (T18)

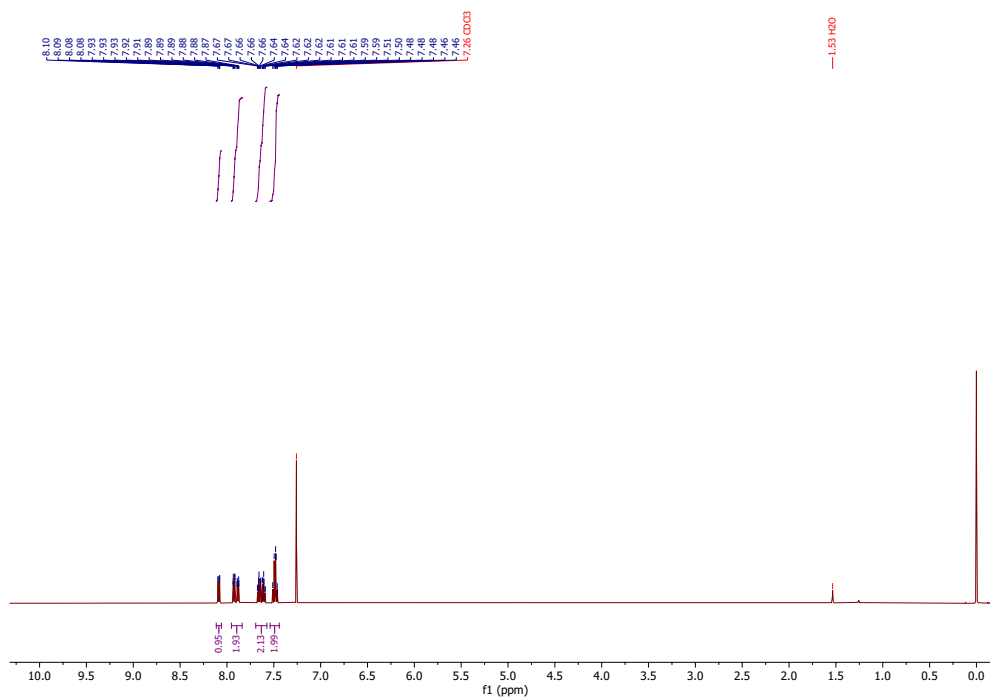


Figure 4.42: ¹H-NMR spectrum of T18.

Naphthalen-1-yl 1*H*-imidazole-1-sulfonate (T19)

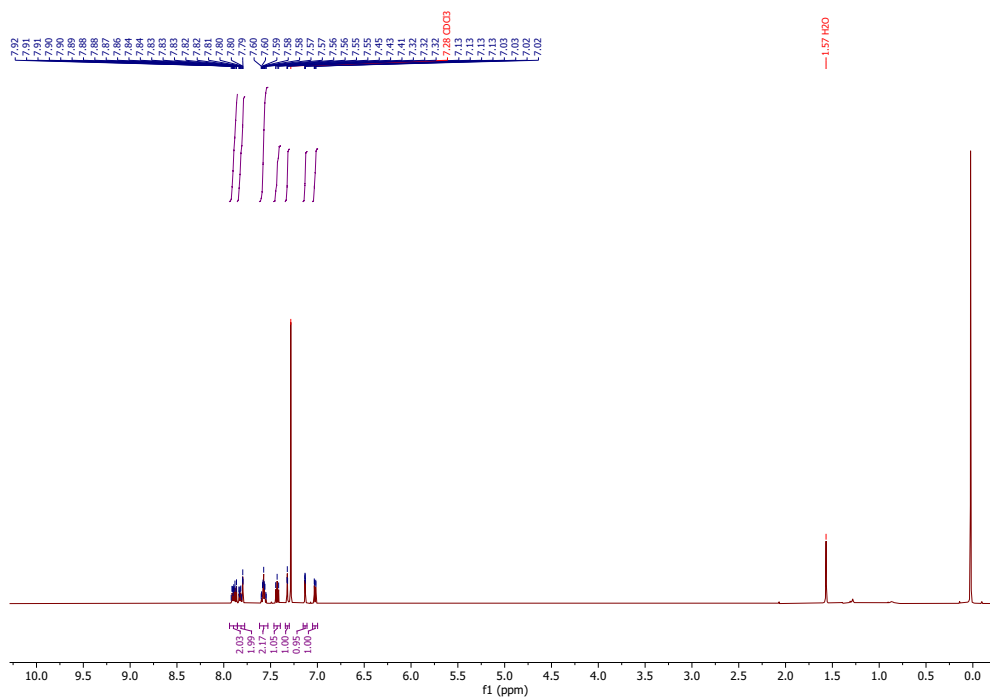
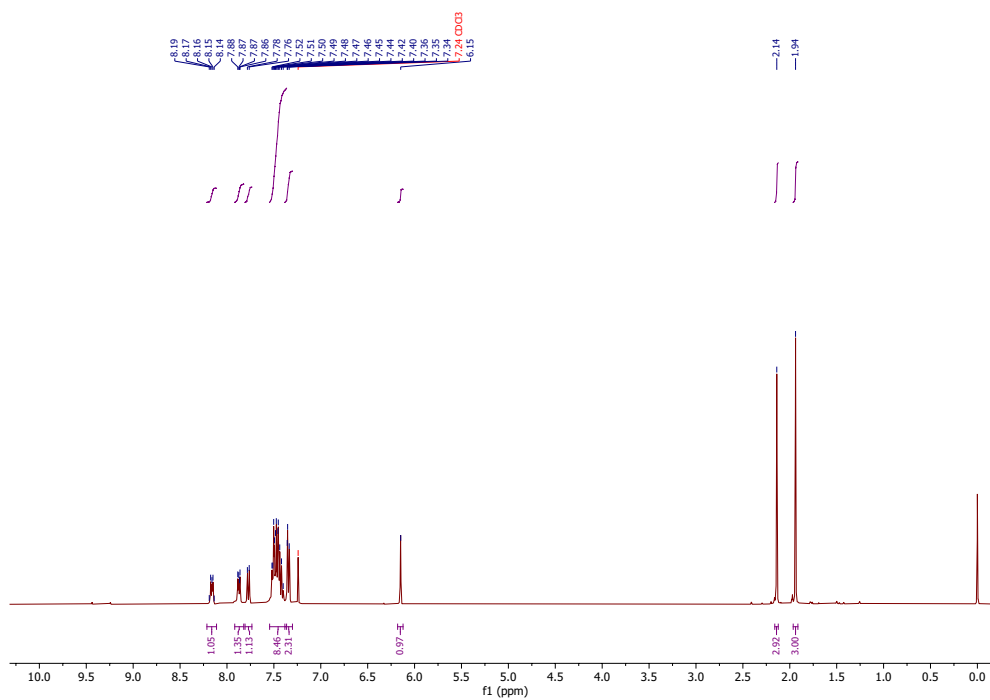
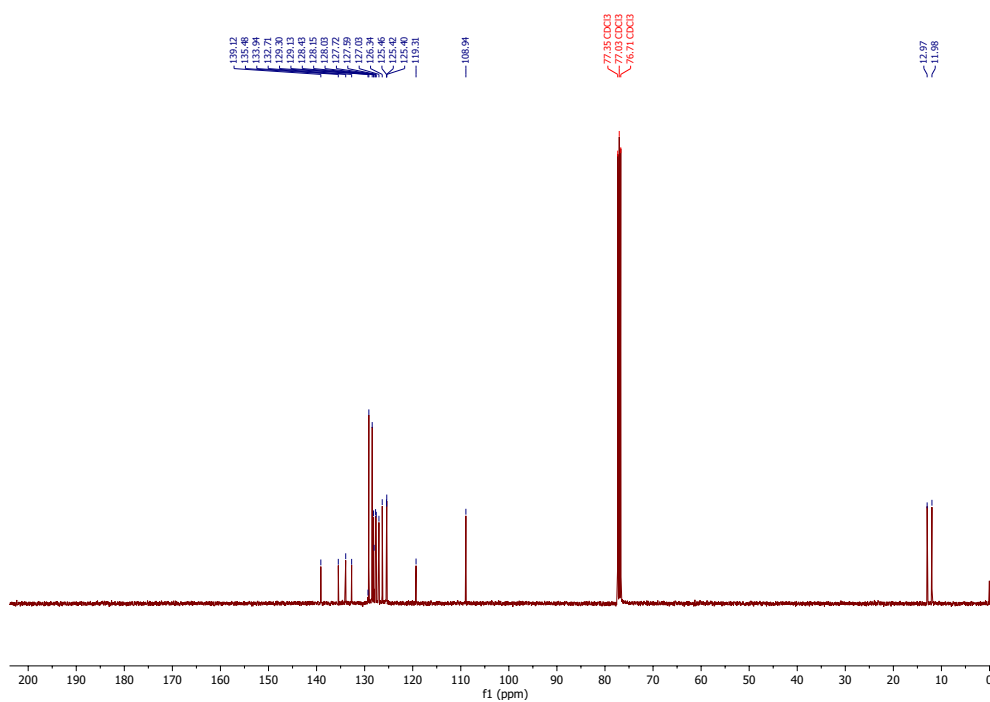
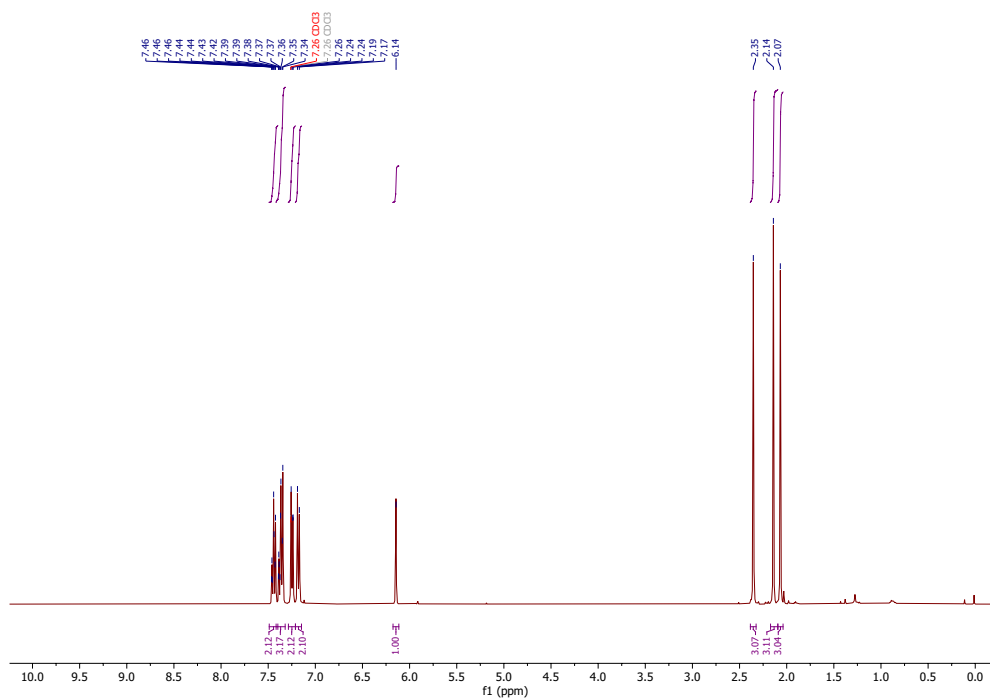
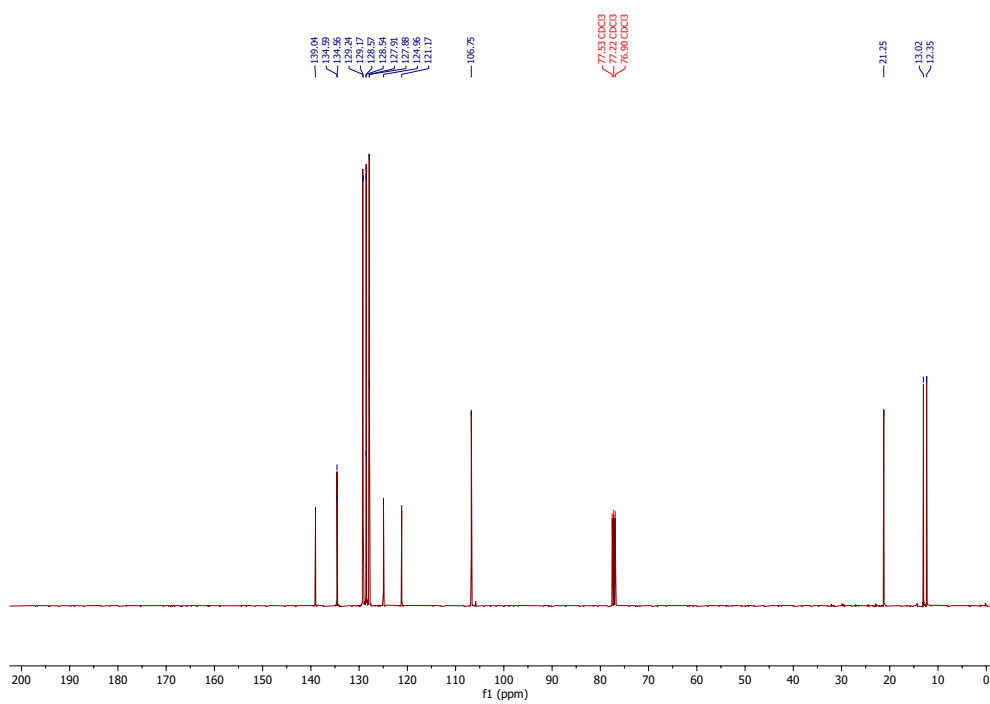
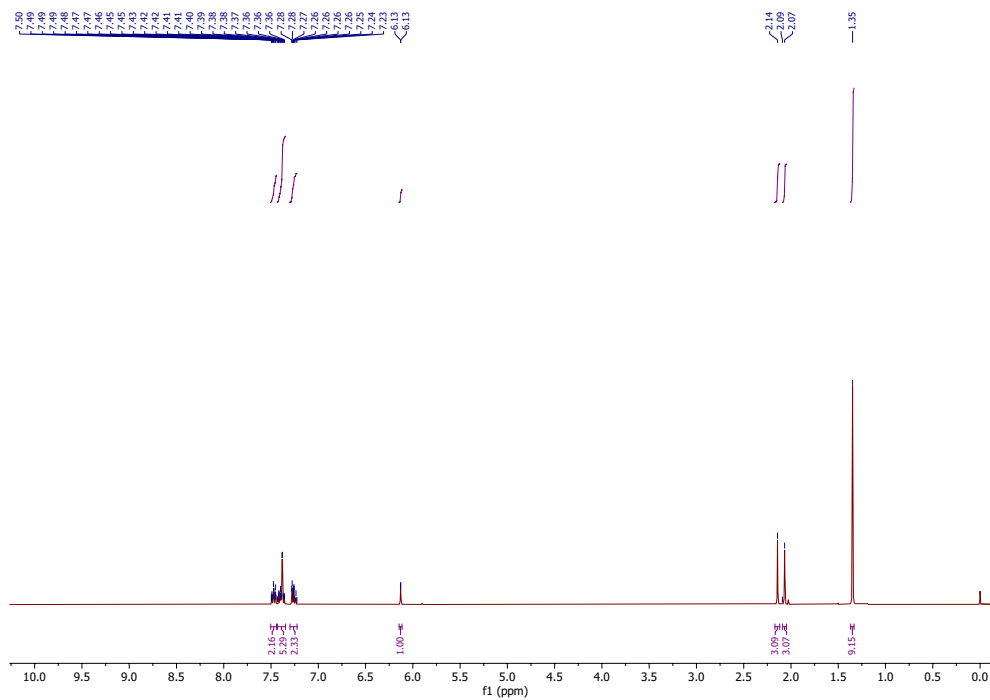
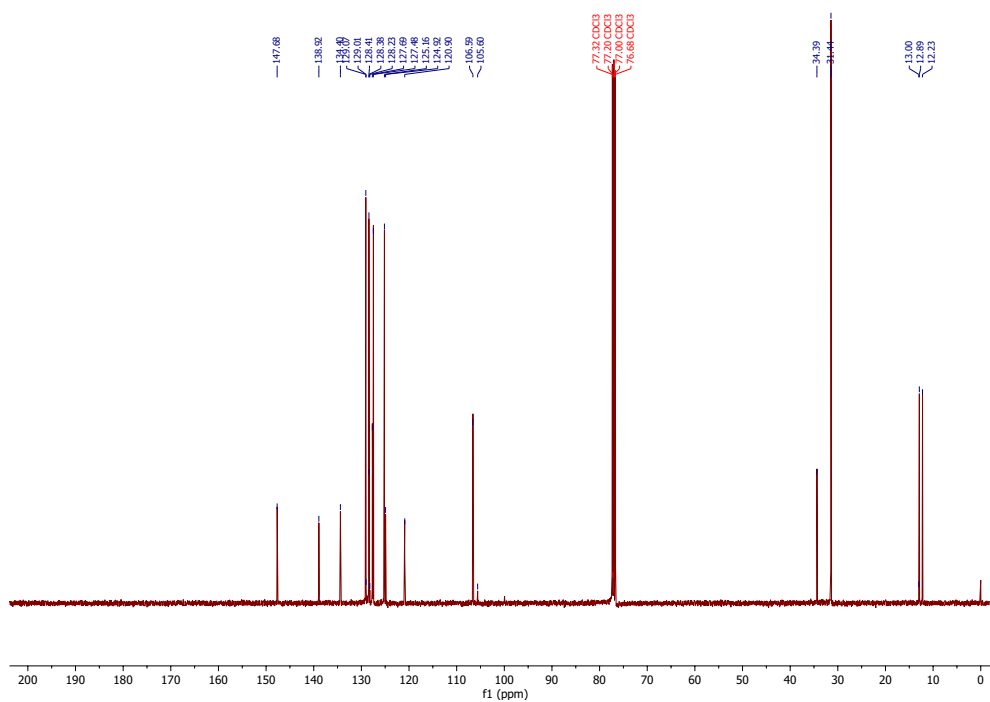
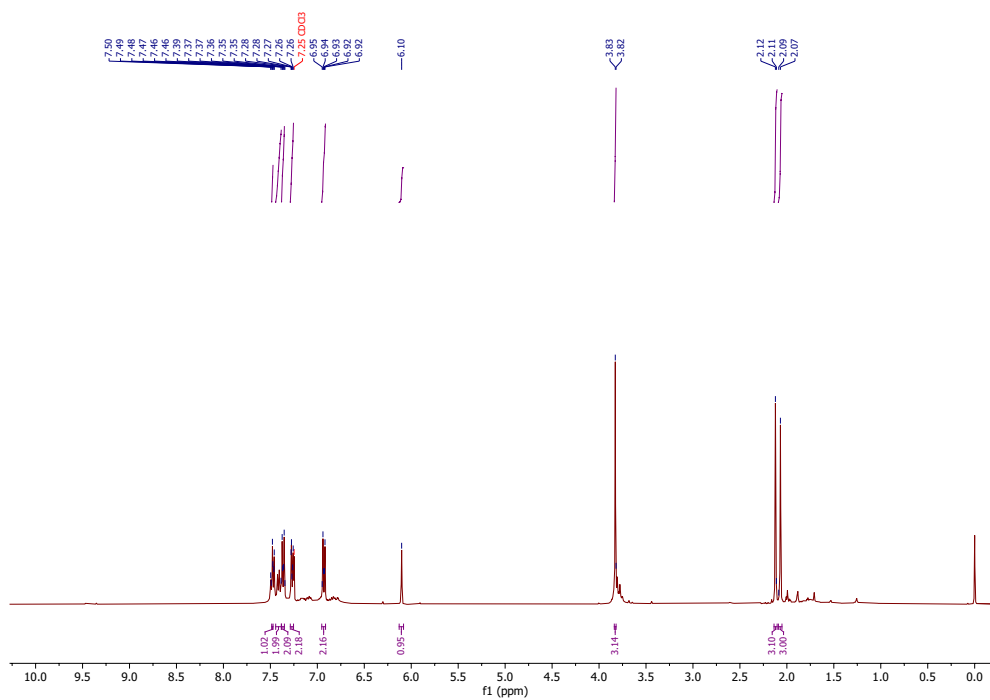
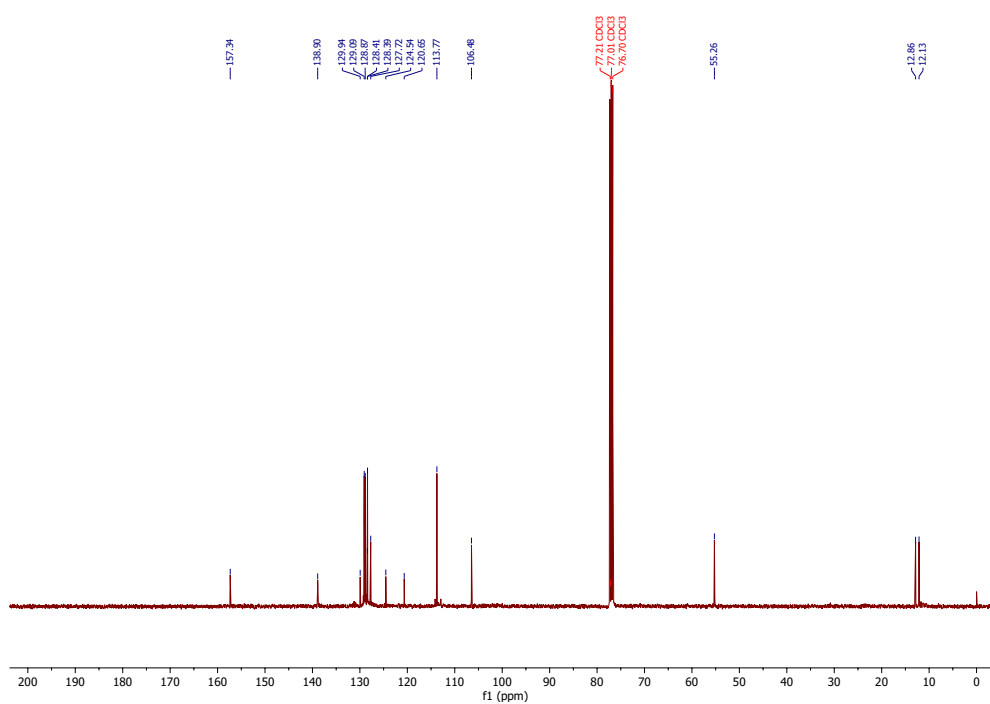


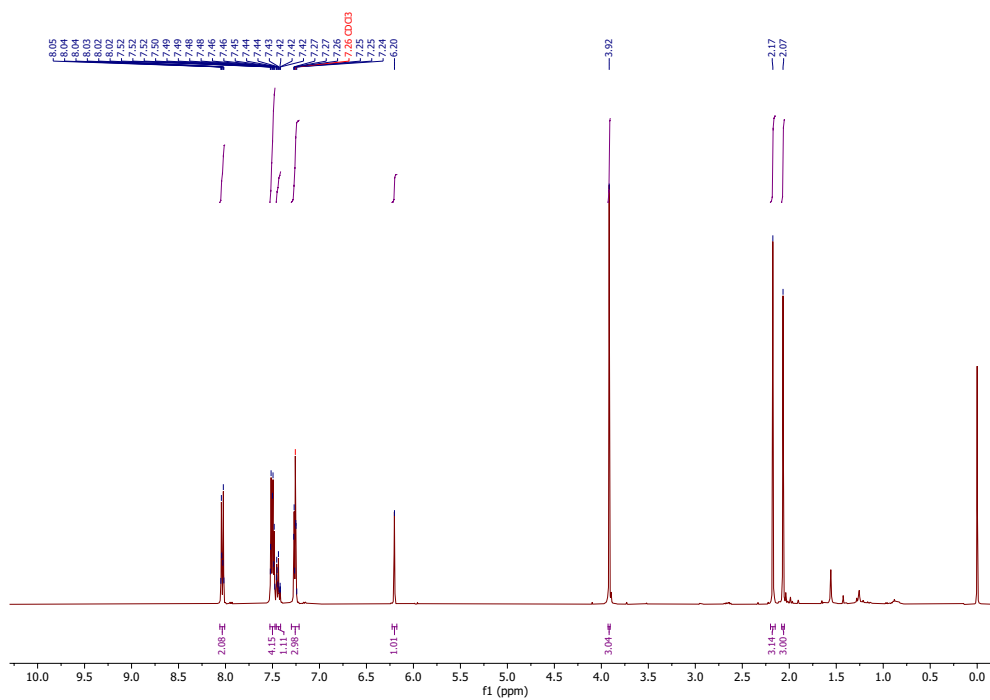
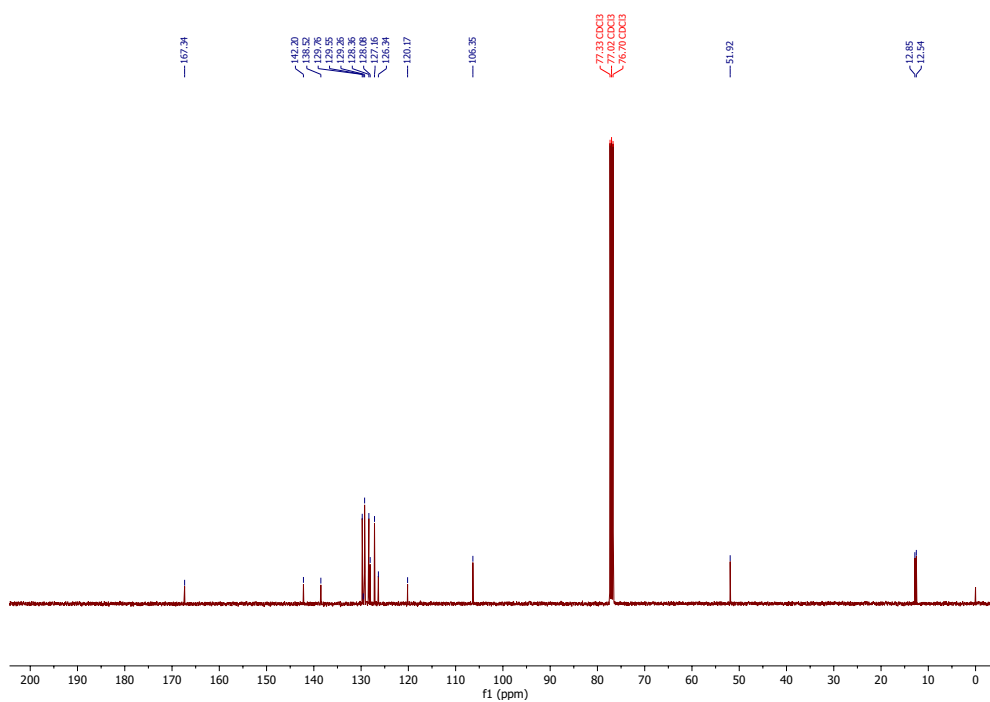
Figure 4.43: ¹H-NMR spectrum of T19.

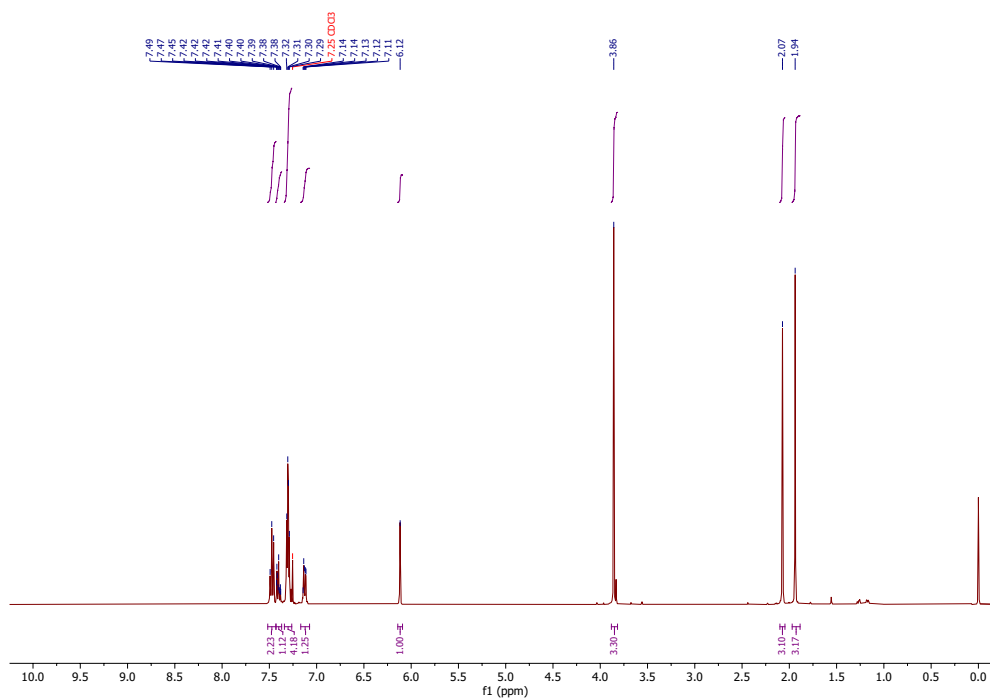
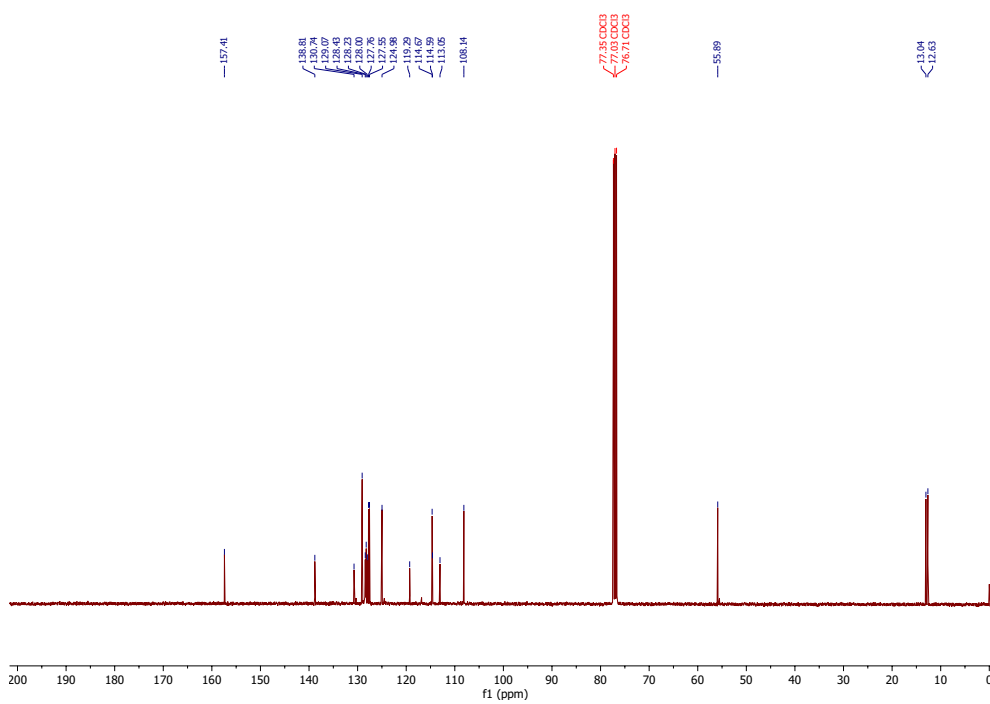
2,5-Dimethyl-3-(naphthalen-1-yl)-1-phenyl-1*H*-pyrrole (P1)Figure 4.46: ¹H-NMR spectrum of P1.Figure 4.47: ¹³C-NMR spectrum of P1.

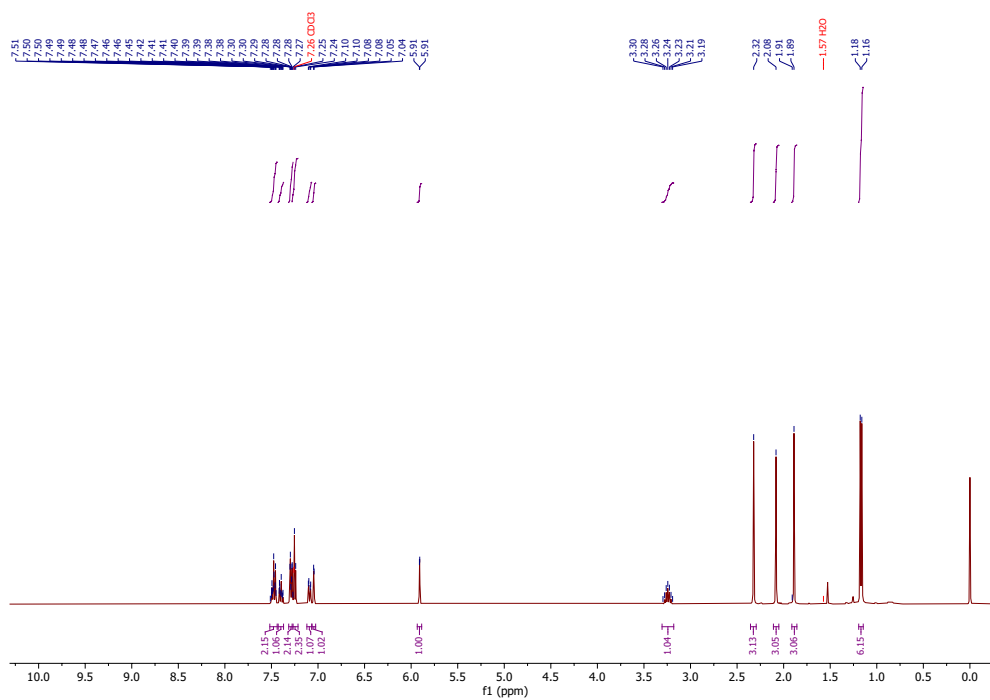
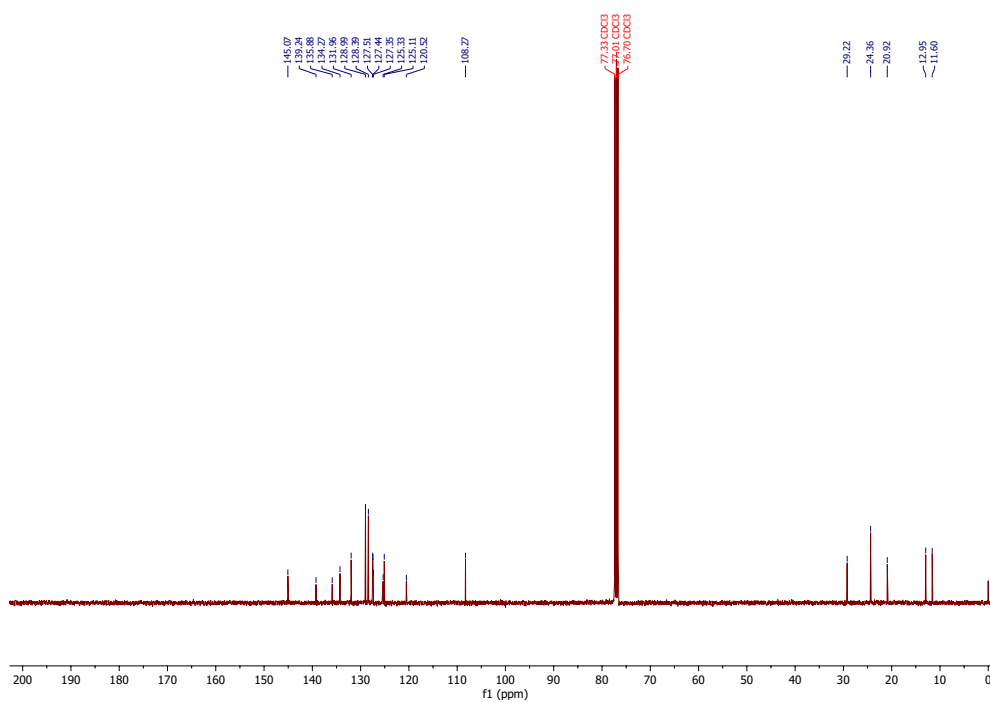
2,5-Dimethyl-1-phenyl-3-(p-tolyl)-1*H*-pyrrole (P3)Figure 4.50: ¹H-NMR spectrum of P3.Figure 4.51: ¹³C-NMR spectrum of P3.

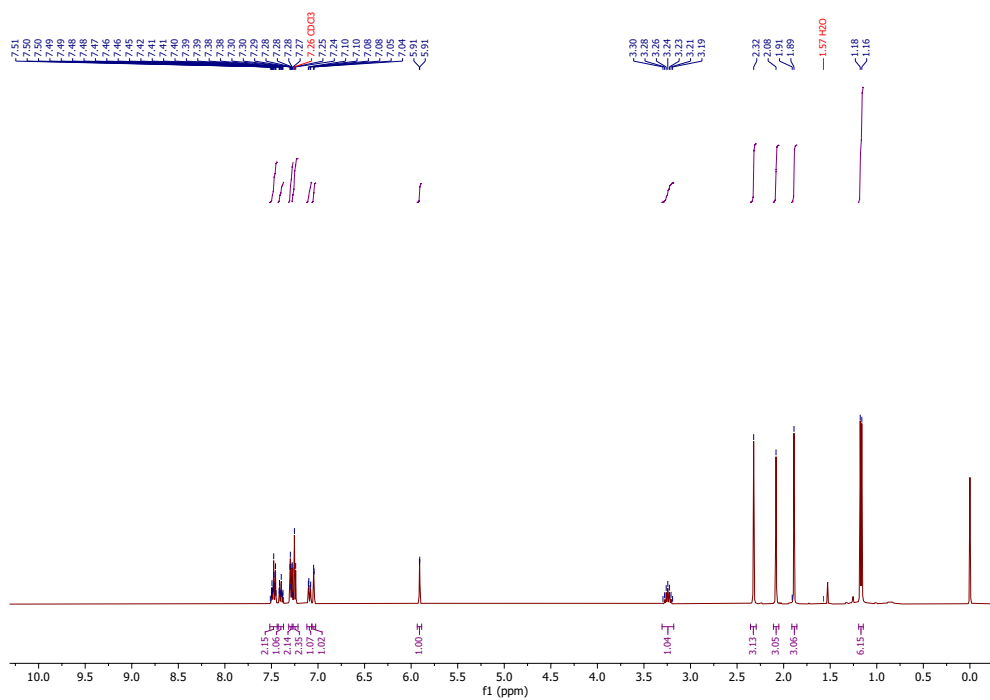
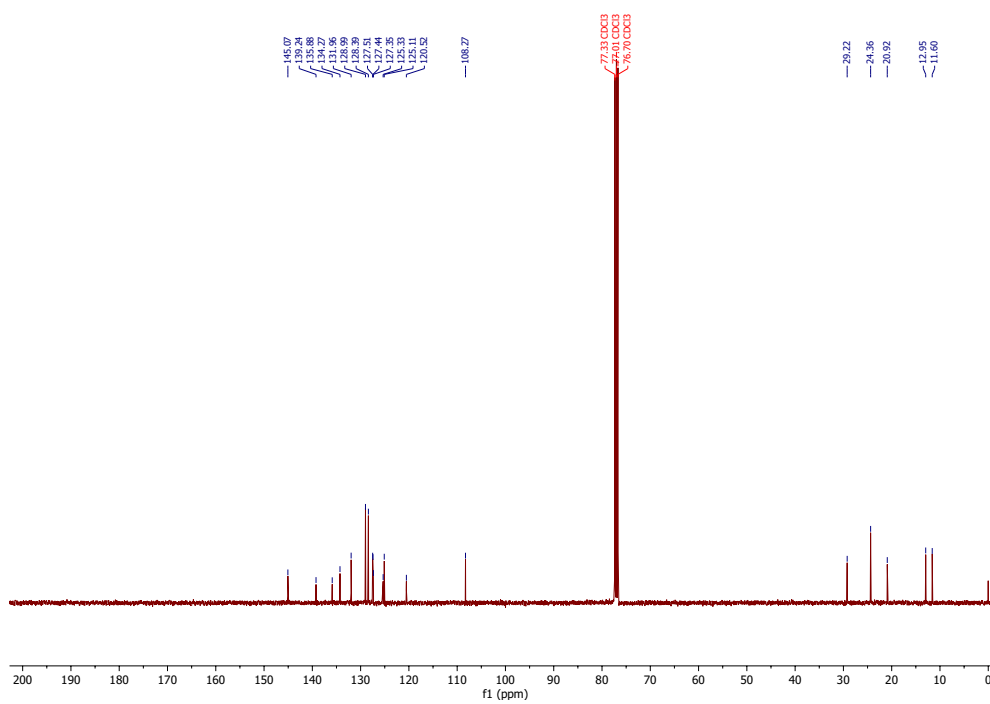
3-(4-(Tert-butyl)phenyl)-2,5-dimethyl-1-phenyl-1*H*-pyrrole (P4)Figure 4.52: $^1\text{H-NMR}$ spectrum of P4.Figure 4.53: $^{13}\text{C-NMR}$ spectrum of P4.

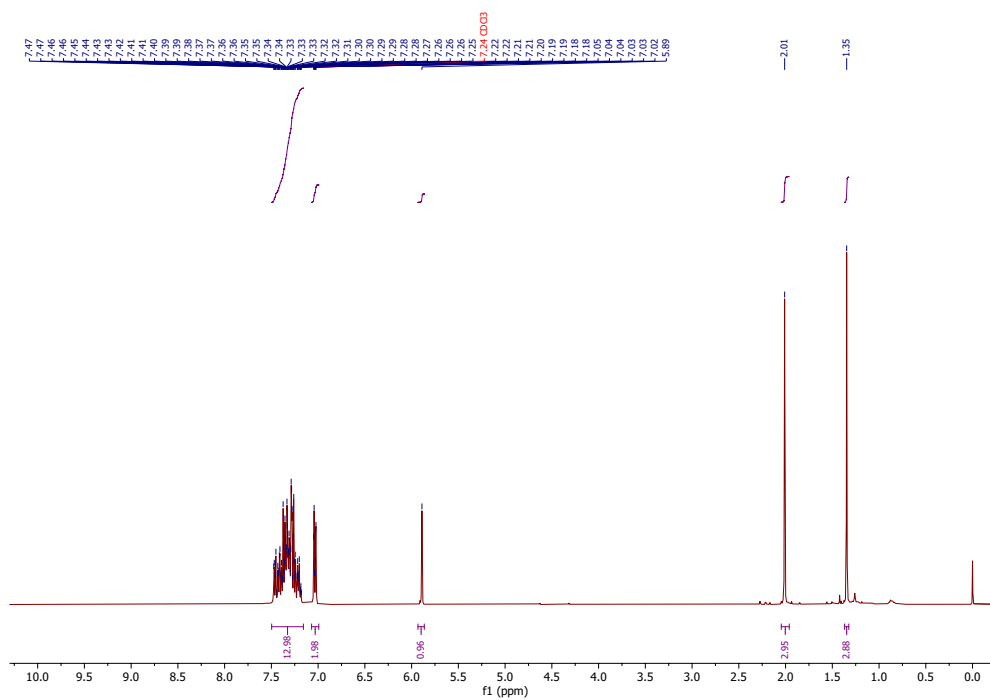
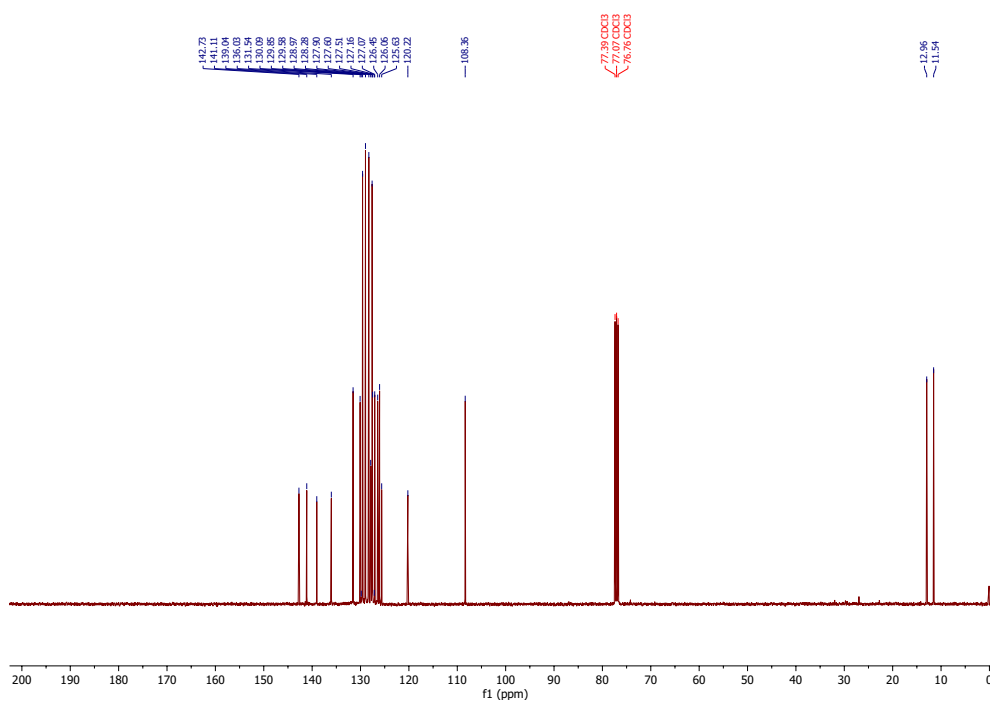
3-(4-Methoxyphenyl)-2,5-dimethyl-1-phenyl-1*H*-pyrrole (P5)Figure 4.54: ¹H-NMR spectrum of P5.Figure 4.55: ¹³C-NMR spectrum of P5.

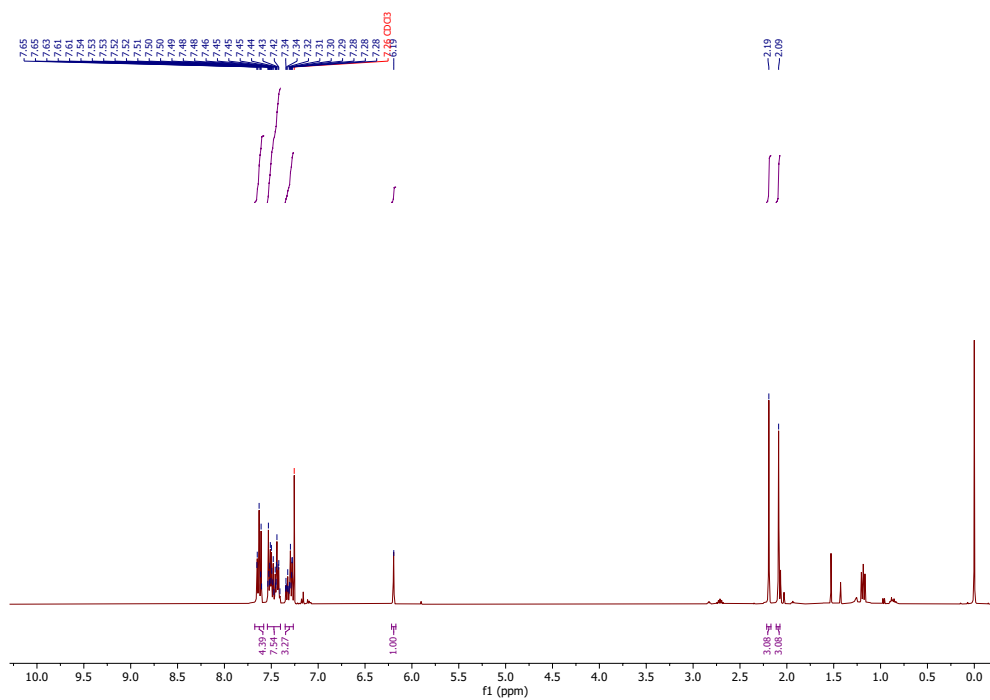
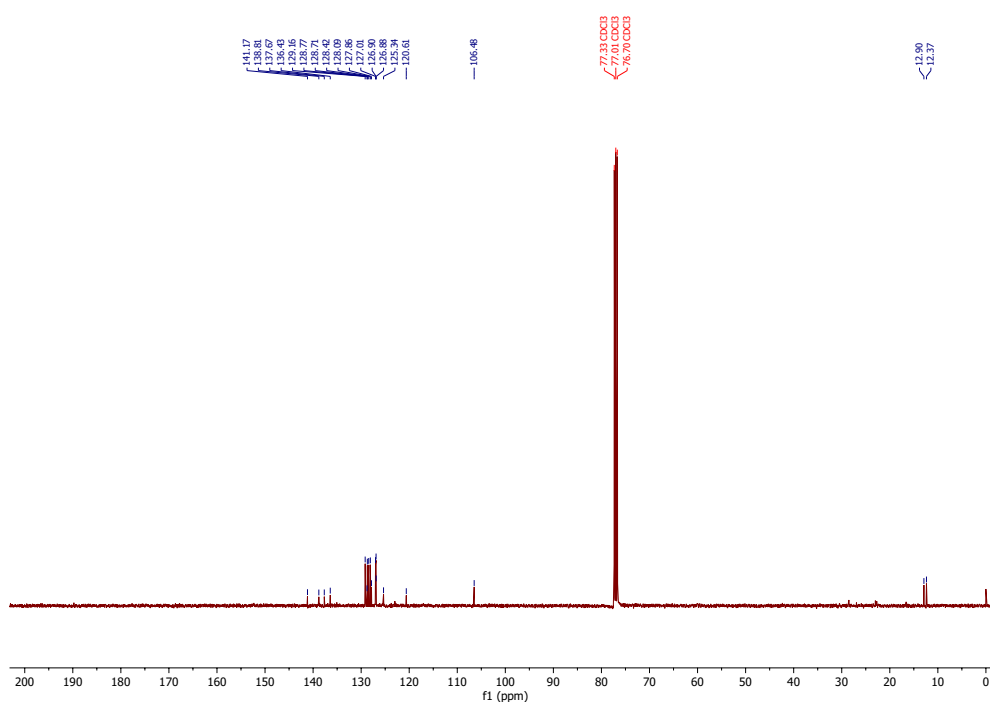
Methyl 4-(2,5-dimethyl-1-phenyl-1*H*-pyrrol-3-yl)benzoate (P6)Figure 4.56: ¹H-NMR spectrum of P6.Figure 4.57: ¹³C-NMR spectrum of P6.

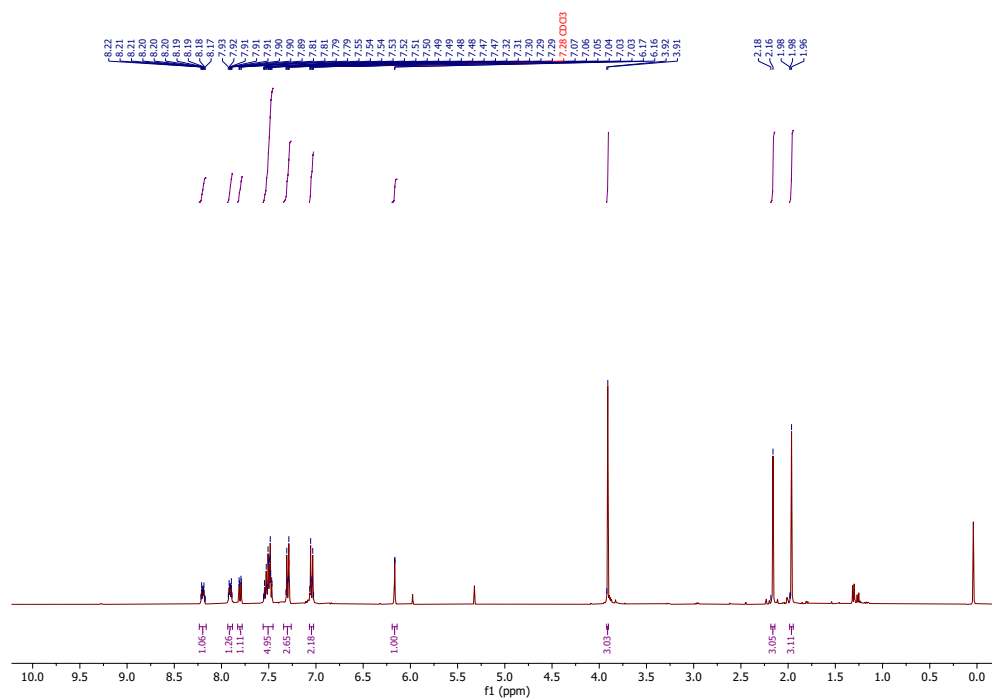
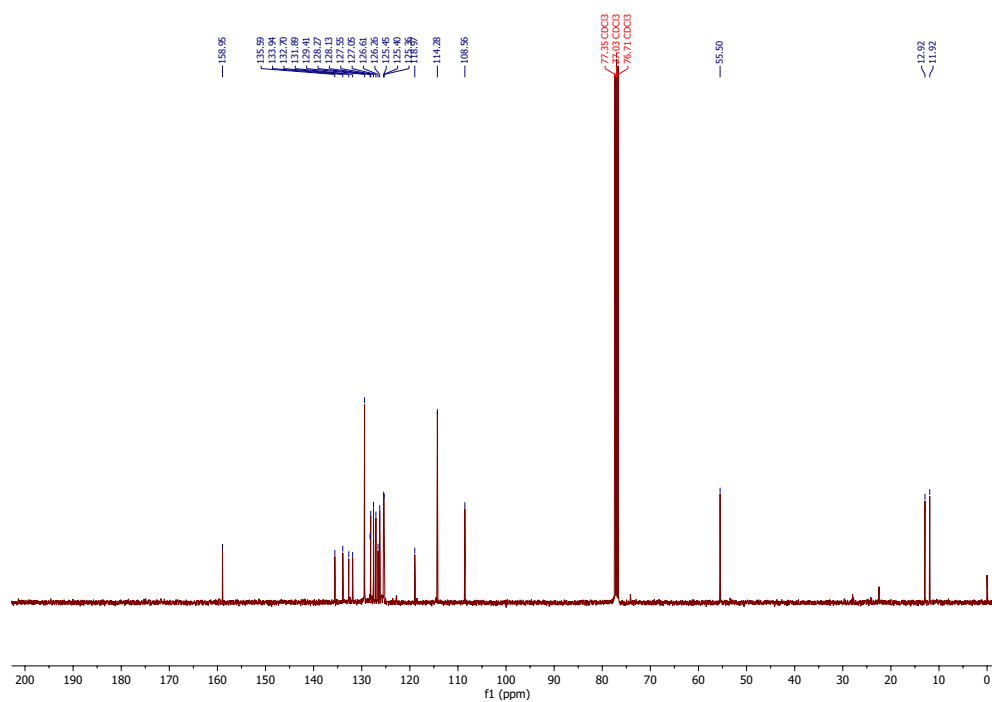
2-(2,5-Dimethyl-1-phenyl-1*H*-pyrrol-3-yl)-3-methoxybenzonitrile (P7)Figure 4.58: ¹H-NMR spectrum of P7.Figure 4.59: ¹³C-NMR spectrum of P7.

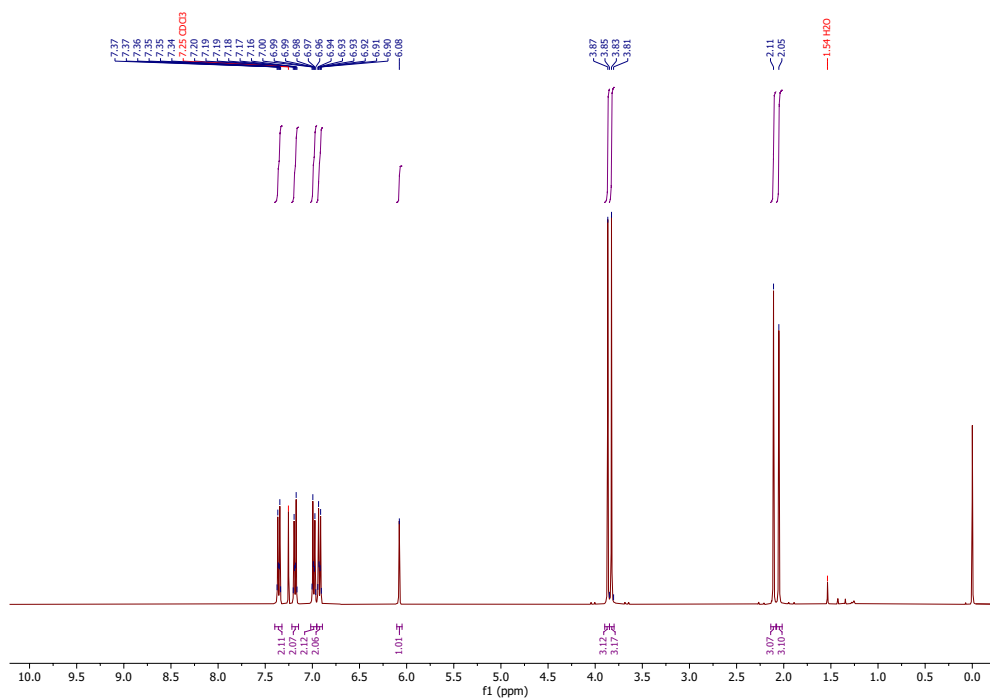
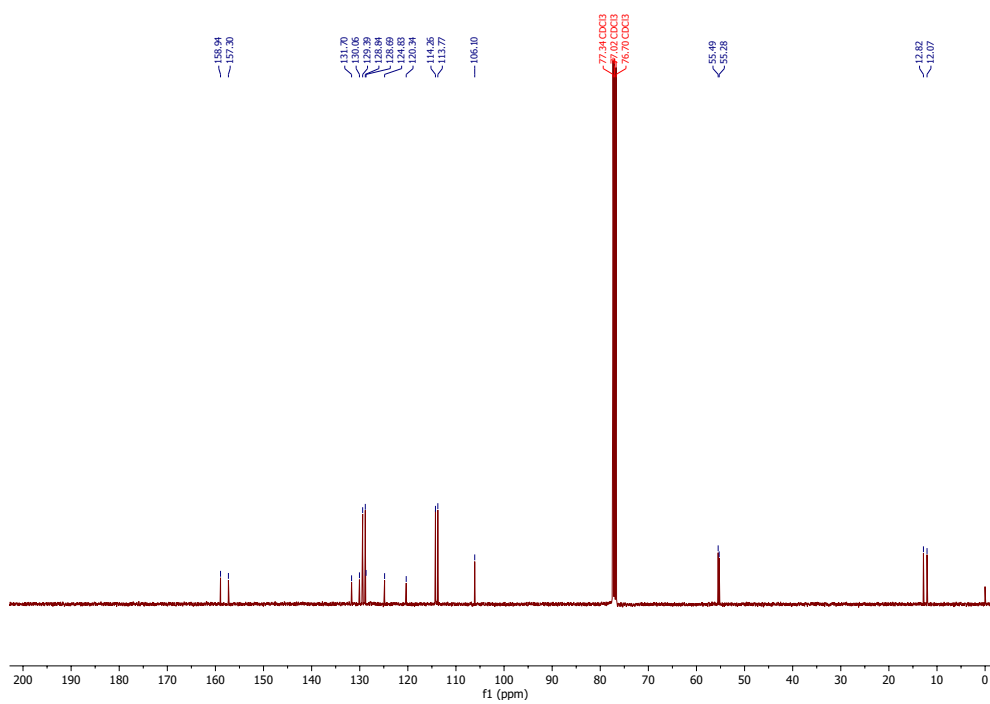
3-(2-Isopropyl-5-methylphenyl)-2,5-dimethyl-1-phenyl-1*H*-pyrrole (P8)Figure 4.60: ¹H-NMR spectrum of P8.Figure 4.61: ¹³C-NMR spectrum of P8.

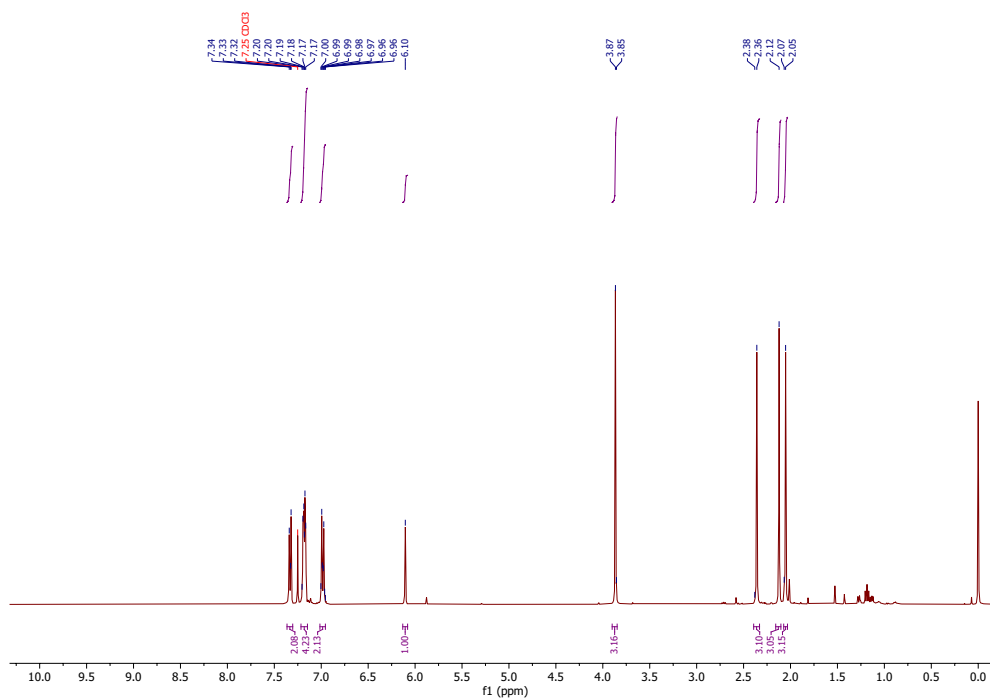
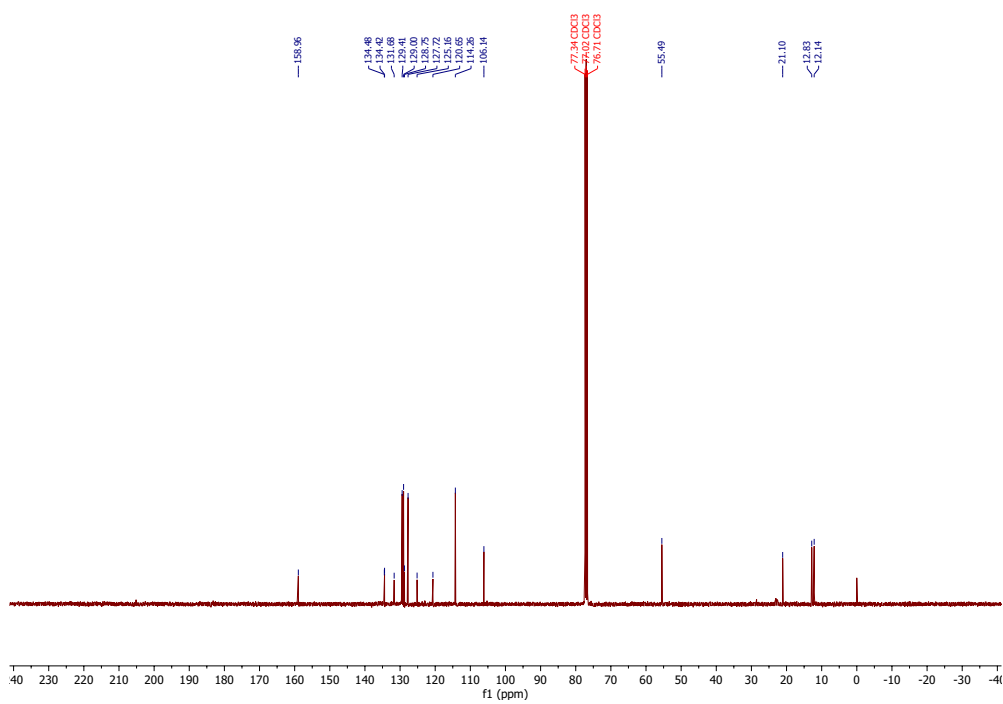
3-(5-Isopropyl-2-methylphenyl)-2,5-dimethyl-1-phenyl-1*H*-pyrrole (P9)Figure 4.62: ¹H-NMR spectrum of P9.Figure 4.63: ¹³C-NMR spectrum of P9.

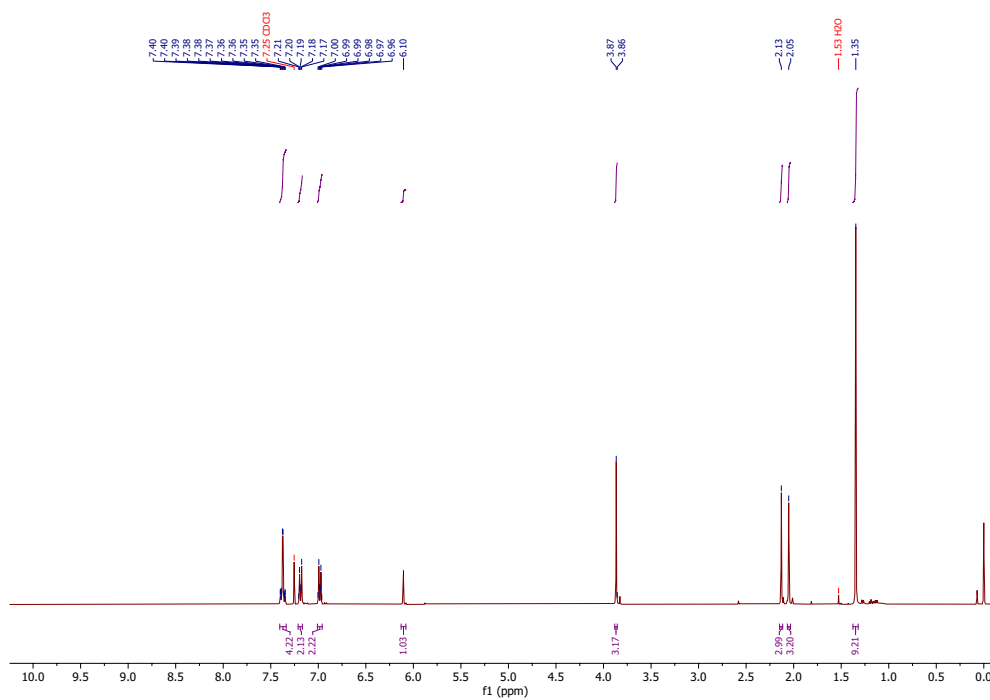
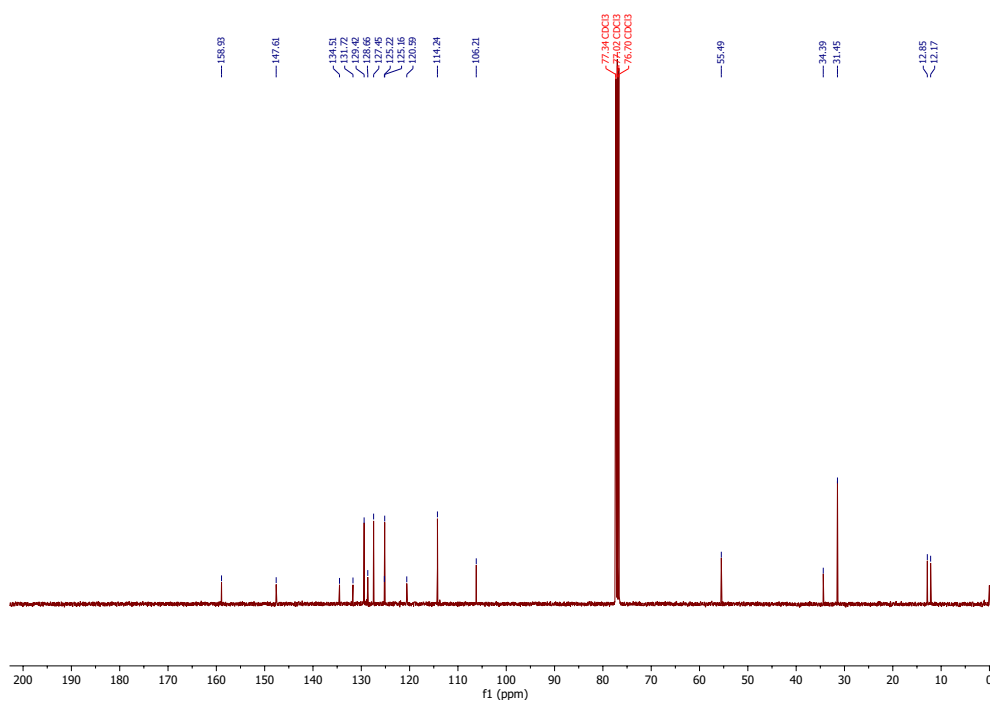
3-([1,1'-Biphenyl]-2-yl)-2,5-dimethyl-1-phenyl-1*H*-pyrrole (P10)Figure 4.64: ¹H-NMR spectrum of P10.Figure 4.65: ¹³C-NMR spectrum of P10.

3-([1,1'-Biphenyl]-4-yl)-2,5-dimethyl-1-phenyl-1*H*-pyrrole (P11)Figure 4.66: ¹H-NMR spectrum of P11.Figure 4.67: ¹³C-NMR spectrum of P11.

1-(4-Methoxyphenyl)-2,5-dimethyl-3-(naphthalen-1-yl)-1*H*-pyrrole (P13)Figure 4.70: ¹H-NMR spectrum of P13.Figure 4.71: ¹³C-NMR spectrum of P13.

1,3-Bis(4-methoxyphenyl)-2,5-dimethyl-1*H*-pyrrole (P14)Figure 4.72: ¹H-NMR spectrum of P14.Figure 4.73: ¹³C-NMR spectrum of P14.

1-(4-Methoxyphenyl)-2,5-dimethyl-3-(p-tolyl)-1*H*-pyrrole (P15)Figure 4.74: ¹H-NMR spectrum of P15.Figure 4.75: ¹³C-NMR spectrum of P15.

3-(4-(Tert-butyl)phenyl)-1-(4-methoxyphenyl)-2,5-dimethyl-1*H*-pyrrole (P16)Figure 4.76: ¹H-NMR spectrum of P16.Figure 4.77: ¹³C-NMR spectrum of P16.

1-Butyl-3-(4-methoxyphenyl)-2-methyl-1*H*-indole (P25)

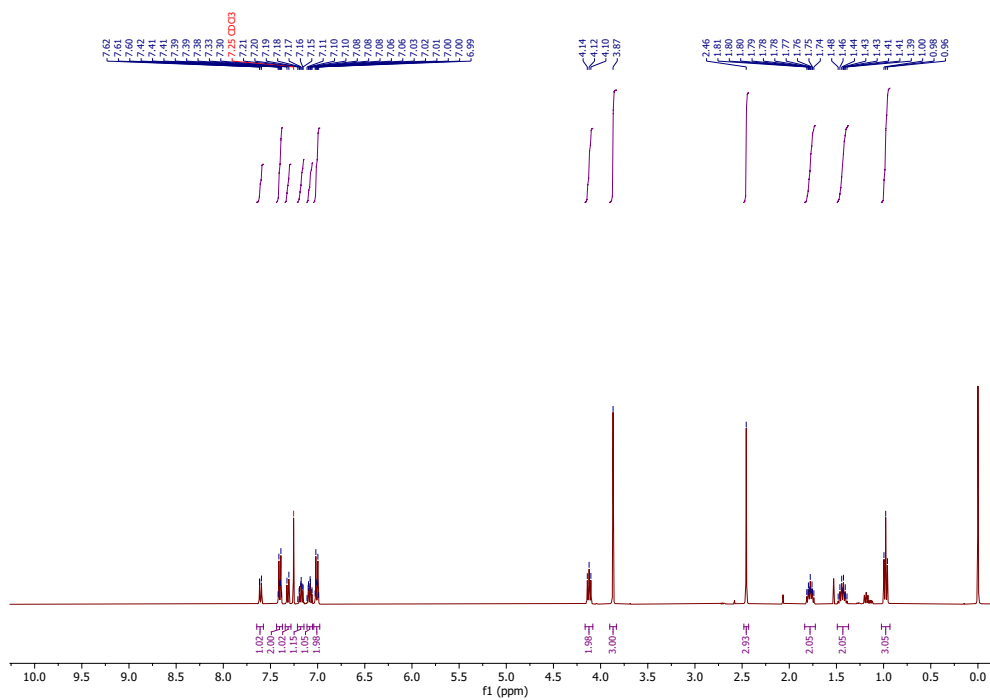


Figure 4.80: ¹H-NMR spectrum of P24.

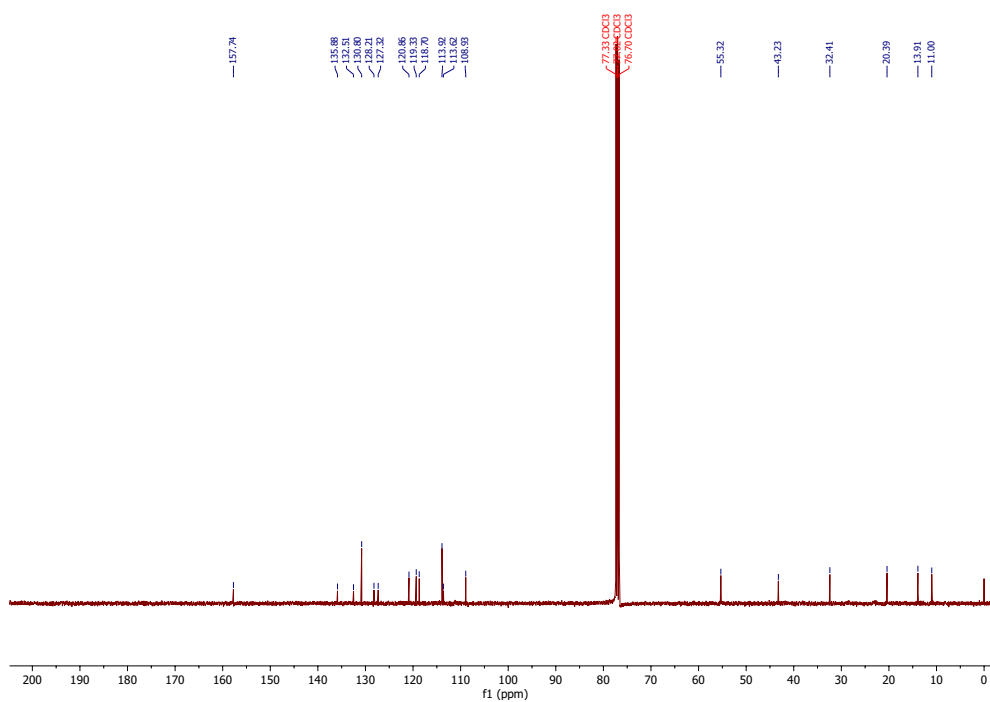
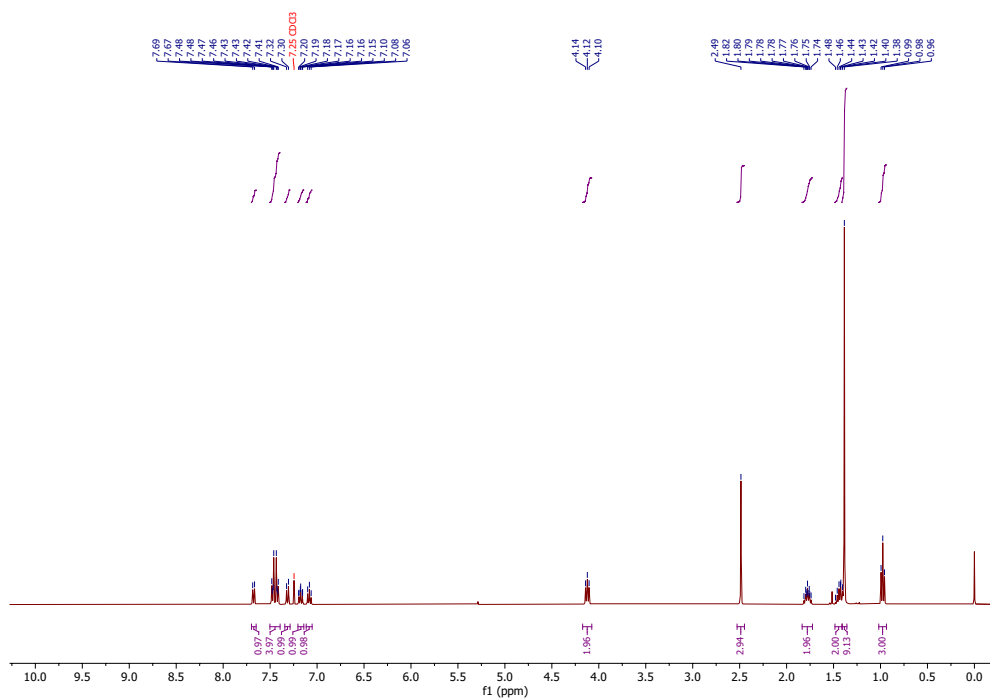
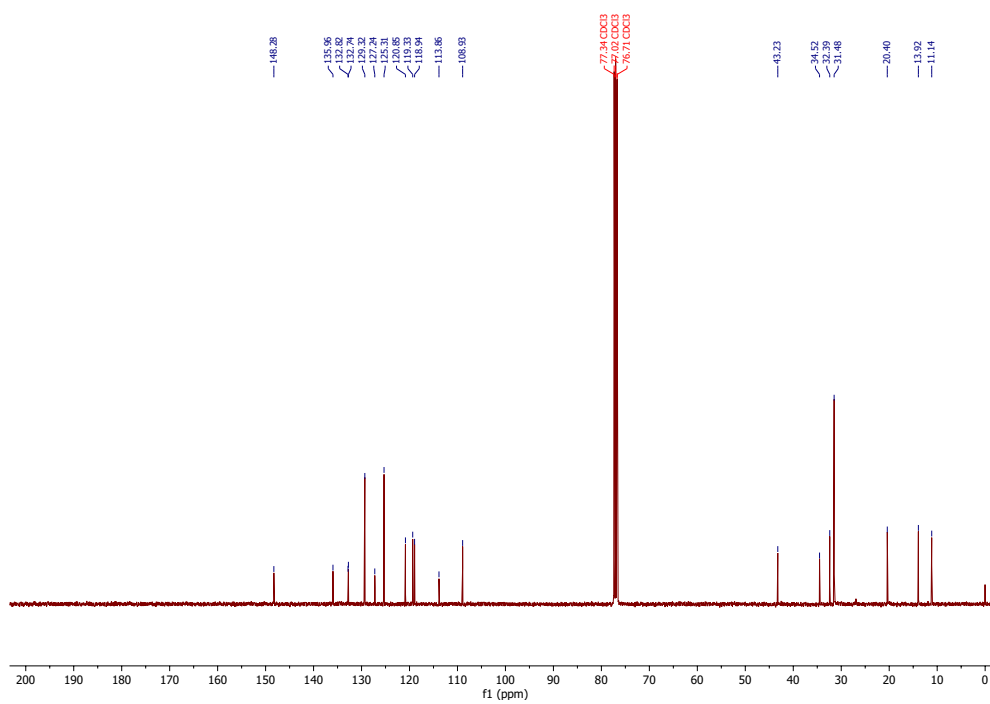
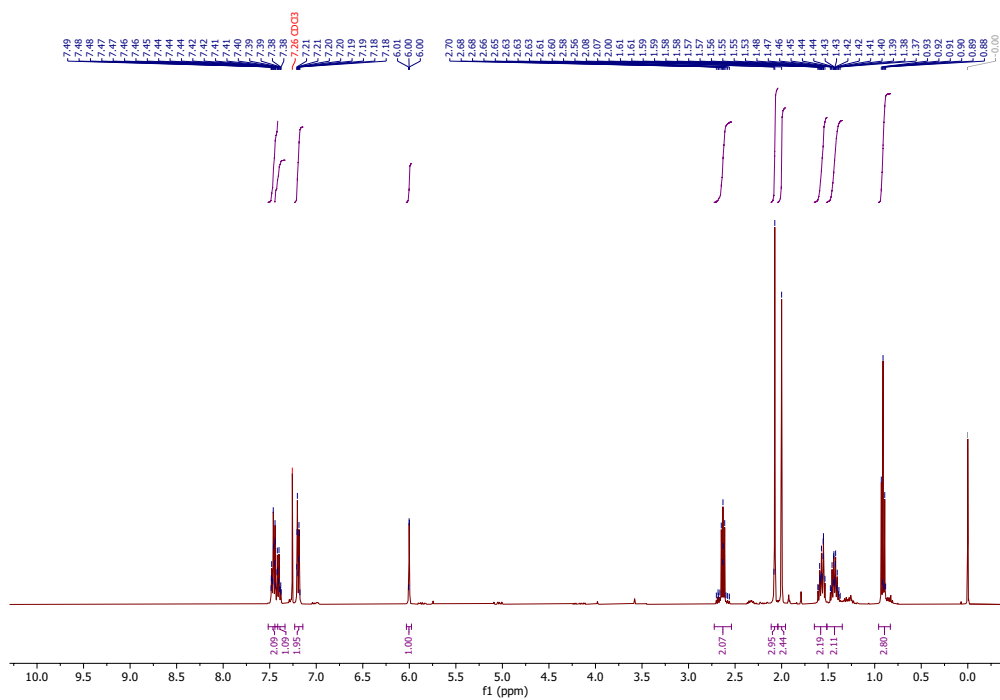
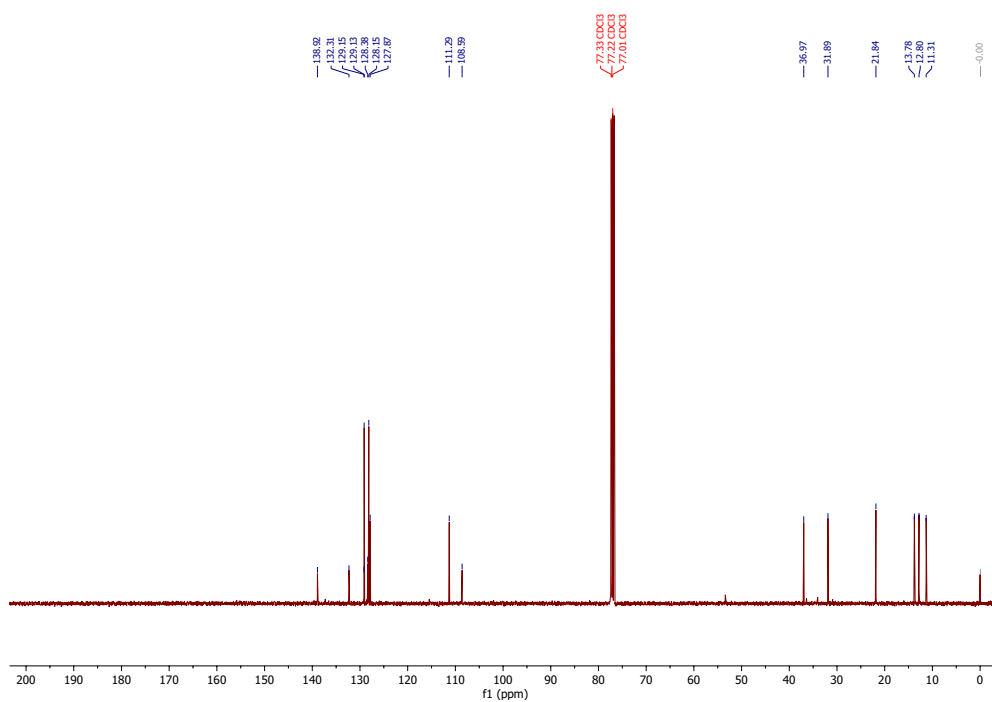


Figure 4.81: ¹³C-NMR spectrum of P24.

1-Butyl-3-(4-(tert-butyl)phenyl)-2-methyl-1*H*-indole (P27)Figure 4.84: ¹H-NMR spectrum of P26.Figure 4.85: ¹³C-NMR spectrum of P26.

Ethyl 3-(2,5-dimethyl-1-phenyl-1*H*-pyrrol-3-yl)propanoate (P36)Figure 4.86: ¹H-NMR spectrum of P36.Figure 4.87: ¹³C-NMR spectrum of P36.

5. Appendix

List of Schemes

1.1	The Knorr pyrrole synthesis.	5
1.2	The Paal Knorr synthesis.	5
1.3	The Hantzsch pyrrole synthesis.	6
1.4	The VAN LEUSEN pyrrole synthesis.	7
1.5	The Barton-Zard pyrrole synthesis.	7
1.6	Exemplary bromination of a pyrrole.	8
1.7	HECK cross-coupling of a halogenated pyrrole.	8
1.8	KUMADA cross-coupling of a brominated pyrrole.	9
1.9	NEGISHI cross-coupling of an iodinated pyrrole.	9
1.10	STILLE cross-coupling of an iodinated pyrrole.	9
1.11	Suzuki cross-coupling of a pyrrolyl triflate.	10
1.12	Synthesis of β -nicotyrine.	10
1.13	N-Arylation of a pyrrole.	10
1.14	Synthesis of alkenyl sulfonium salts and subsequent NEGISHI coupling.	11
1.15	Synthesis of azulene sulfonium salts and subsequent SUZUKI coupling.	11
1.16	C–N coupling of tetrafluorothiantrene sulfonium salts.	12
1.17	Synthesis of pyrrolyl and indolyl sulfonium salts. R = Me, (CH ₂) ₄	12
1.18	Synthesis of pyrroles.	13
1.19	Halogenation of pyrroles.	13
1.20	Coupling reactions of pyrrolyl halides.	13
1.21	Synthesis of azole sulfonium salts.	14
1.22	Coupling reactions of azole sulfonium salts.	14
1.23	C–H arylation reaction of caffeine with a pyrrolyl electrophile.	14
1.24	Synthesis of various pyrrole derivatives from hexane-2,5-dione and the corresponding amine. Yields from isolated products.	15
1.25	Failed synthesis attempts of various pyrrole derivatives from hexane-2,5-dione and the corresponding amine.	16
1.26	Synthesis of 1-phenyl-1 <i>H</i> -pyrrole S17 via the CLAUSON-KAAS reaction.	17
1.27	Synthesis of 1-tosyl-1 <i>H</i> -pyrrole S18 via the CLAUSON-KAAS reaction.	17
1.28	Bromination of pyrrole S1	19
1.29	Chlorination reactions of various pyrroles. Yields are for isolated products.	20
1.30	Iodination of pyrrole S1	21
1.31	Iodination of pyrrole S1 via initial metalation. Yield determined by GC analysis.	21

1.32	Attempted NEGISHI cross-coupling reaction of pyrrole B1 <i>via</i> lithiation and transmetalation with pyrrole B1 . Analytical yield was determined by qNMR-analysis.	25
1.33	Negishi cross-coupling reaction of pyrrole B1 <i>via</i> lithiation and transmetalation with aryl tosylate T5 . Analytical yield was determined by qNMR-analysis.	25
1.34	Attempted synthesis of pyrrole sulfonium salt A1 , returning thioether side product A2 . Yields refer to isolated products.	26
1.35	Synthesis of pyrrole sulfonium salt A3 . Yield refers to isolated product. . .	26
1.36	Synthesis of pyrrole sulfonium salt A4 . Yield refers to isolated product. . .	27
1.37	Synthesis of pyrrole sulfonium salt A5 . Yield refers to isolated product. . .	27
1.38	Synthesis of indole sulfonium salt A6 . Yield refers to isolated product. . .	27
1.39	Synthesis of <i>N</i> -butyl indoles S21 and S22 . Yields refer to isolated products.	28
1.40	Synthesis of <i>N</i> -butyl indole sulfonium salts A7 and A8 . Yields refer to isolated products.	28
1.41	Synthesis of dipyrrole bis-sulfonium salt A9 . Yield refers to isolated product.	29
1.42	Attempted synthesis of dipyrrole bis-sulfonium sulfonium salt A10	29
1.43	Synthesis of aryl tosylates by the LEI procedure. Yields refer to isolated product.	39
1.44	Synthesis of naphthalene-1-yl methanesulfonate T17 . Yield refers to isolated product.	39
1.45	Synthesis of naphthalene-1-yl trifluoromethanesulfonate T18 . Yield refers to isolated product.	40
1.46	Synthesis of naphthalene-1-yl 1 <i>H</i> -imidazole-1-sulfonate T19 . Yield refers to isolated product.	40
1.47	Synthesis of naphthalene-1-yl dimethylsulfamate T20 . Yield refers to isolated product.	40
1.48	NEGISHI cross-coupling reactions of pyrrole sulfonium salt A3 . Yields refers to isolated products.	41
1.49	NEGISHI cross-coupling reactions of pyrrole sulfonium salt A3 . Yields refers to isolated products.	42
1.50	NEGISHI cross-coupling reactions of pyrrole sulfonium salt A4 . Yields refers to isolated products.	43
1.51	Unsuccessful NEGISHI cross-coupling reactions of pyrrole sulfonium salt A3 . Yields were determined by qNMR-analysis.	44
1.52	NEGISHI cross-coupling reactions of pyrrole sulfonium salt A5 . Yields were determined by qNMR-analysis.	45
1.53	NEGISHI cross-coupling reactions of indoles. Yields from isolated products.	46
1.54	NEGISHI cross-coupling reactions of indole sulfonium salt A8 . Yields were determined by qNMR-analysis.	47
1.55	NEGISHI cross-coupling reactions of pyrrole sulfonium salt A3 with catalytically zincated aryl sulfonates obtained from various aryl sulfonates. Yields were determined by qNMR-analysis.	48
1.56	NEGISHI cross-coupling reaction of pyrrole sulfonium salt A3 with zincated ethyl 3-bromopropanoate Z1 . Yield refers to isolated product.	49

1.57	Attempted NEGISHI cross-coupling reaction of pyrrole sulfonium salt A3 with vinylzinc reagent Z2 . Yield determined by qNMR-analysis.	49
1.58	Attempted Arylation of pyrrole S1 with aryl tosylates. Yields determined by qNMR-analysis.	53
1.59	General access route to substituted pyrroles P <i>via</i> synthesis of S1 from hexane-2,5-dione (1a) and aniline (1b), bromination of pyrrole S1 and halogen-metal exchange, transmetalation and NEGISHI coupling of B1 with aryl halides.	55
1.60	Synthesis of pyrrole and indole sulfonium salts and subsequent NEGISHI cross-coupling with catalytically zincated aryl tosylates.	56
1.61	C–H arylation of caffeine E with bromopyrrole B1	57
2.1	Preparation of organometallic reagents <i>via</i> different methods.	59
2.2	Oxidative insertion of magnesium into 3-bromophenyl <i>t</i> -butyl carbonate and subsequent trapping with 4-chlorobenzoyl chloride.	60
2.3	Oxidative insertion of organohalides in the presence of LiCl and subsequent coupling reactions.	61
2.4	Wittig’s first identified halogen-lithium exchange.	62
2.5	Preparation of functionalized arylmagnesium reagents and subsequent trapping with an electrophile; FG = F, Cl, Br, CN, CO ₂ R, OMe.	62
2.6	Magnesium insertion followed by <i>in situ</i> transmetalation to zinc and subsequent trapping with <i>t</i> BuCOCl.	63
2.7	Synthesis of TMP-derived bases.	64
2.8	Metalation with TMPMgCl · LiCl and subsequent NEGISHI cross-coupling.	64
2.9	Metalation with TMPZnCl · LiCl and subsequent NEGISHI cross-coupling.	64
2.10	Iron-catalyzed GRIGNARD formation.	65
2.11	Cobalt-catalyzed zinc insertion into aryl bromide.	65
2.12	Cobalt-catalyzed zinc insertion into an aryl iodide and subsequent NEGISHI coupling.	65
2.13	Titanium-catalyzed zinc insertion into alkyl bromides and subsequent addition to carbonyl derivatives.	66
2.14	Metal-catalyzed aluminum insertion into aryl halides and subsequent transmetalation and cross-coupling.	66
2.15	C ₆₀ -fullerene-catalyzed zinc insertion into an aryl bromide and subsequent allylation.	67
2.16	Cobalt-catalyzed conjugate addition of an activated aryl triflate to methyl vinyl ketone.	67
2.17	Cobalt-catalyzed aryl sulfonate/copper exchange reaction.	67
2.18	Nickel-catalyzed zincation of aryl tosylates.	68
2.19	Nickel-catalyzed zincation of aryl tosylates.	69
2.20	Nickel-catalyzed zincation of bromopyrrole B1 and sulfonium salt A3	70
2.21	Synthesis of aryl tosylate T1 . Yield from isolated product.	71
2.22	Synthesis of ligand L8 . Yield refers to isolated product.	71
2.23	Yields were determined by qNMR- and GCMS-analysis.	81
3.1	Comparison of conventional redox-neutral cross-couplings and reductive cross-electrophile couplings.	83

3.2	Selected examples of Ni-catalyzed reductive cross-electrophile couplings. . .	84
3.3	86
3.4	Nickel-catalyzed reductive cross-electrophile coupling of 1-naphthyltosylate with benzylbromide.	93

List of Tables

1.1	Screening of conditions for the halogenation of pyrroles. Relative yields are determined by GC-FID. S1 = substrate, X1 = monohalogenated, X2 = dihalogenated product.	18
1.2	Negishi cross-coupling reactions of pyrrole B1 <i>via</i> lithiation and transmetalation with phenyl halides.	22
1.3	Negishi cross-coupling reactions of pyrrole B1 <i>via</i> lithiation and transmetalation, with selected aryl and alkyl halides.	24
1.4	Screening of reaction conditions of the model NEGISHI coupling with Pd(OAc) ₂ as precatalyst.	30
1.5	Screening of reaction conditions of sulfonium salt NEGISHI coupling with palladium catalysts.	33
1.6	Screening of reaction conditions of sulfonium salt NEGISHI coupling with PEPPSI-IPr catalyst.	34
1.7	Screening of reaction conditions of sulfonium salt NEGISHI coupling with PEPPSI-IPr catalyst.	36
1.8	Screening of reaction conditions of NEGISHI coupling with nickel catalysts.	37
1.9	C–H arylation of caffeine E with pyrrolyl bromide B1	51
1.10	C–H arylation of caffeine E with pyrrolyl bromide B1	52
1.11	Screening of conditions for amination reaction of pyrrolyl halide B1 with <i>N</i> -methylpiperazine.	54
2.1	Electronegativity difference ($\Delta\chi$) for different carbon–metal bonds.	59
2.2	Screening of ligands for catalytic zincation.	73
2.3	Screening of ligands for catalytic zincation.	74
2.4	Screening of ligands for catalytic zincation.	75
2.5	Screening of ligands for catalytic zincation.	76
2.6	Screening of mabiq complexes for catalytic zincation.	78
2.7	Screening of various reaction conditions.	80
3.1	Reductive cross-electrophile coupling of 1-naphthyltosylate with benzylbromide.	87
3.2	Reductive cross-electrophile coupling of 1-naphthyltosylate with benzylbromide.	90
3.3	Reductive cross-electrophile coupling of 1-naphthyltosylate with aryl and alkyl bromides.	91
3.4	Reductive cross-electrophile coupling of 1-naphthyltosylate with 1-brombutane.	92

4.1	Purchased dry solvents.	94
4.2	qNMR Standards.	96

List of Figures

1.1	Dipole moment of selected five-membered, aromatic heterocycles.	2
1.2	Structure of Fe(II)-Protoporphyrin IX (Hematin).	3
1.3	Natural products of pyrroles.	3
1.4	Commercial products of pyrroles.	4
1.5	Various halogenating agents.	7
1.6	Palladium catalysts screened for reaction optimization.	32
1.7	Overview of utilized aryl tosylates for NEGISHI cross-coupling.	38
1.8	CMD-additives applied in the caffeine C–H arylation.	50
2.1	Ligand core structure for 1,4-diazadienes used in Ni-catalyzed zincation. . .	69
2.2	General structure of Mabiq and bimetallic complexes thereof. $M_1 = \text{Ni}$, Cu , Co , Fe . $M_2 = \text{Ni}$. $\text{X} = \text{OTf}$, Cl , PF_6	70
2.3	Ligands of the class of <i>N</i> -2,6-diisopropylphenyl substituted diazadienes. . .	72
2.4	Ligands of the class of pyridyl and pyrazolyl isoindolines.	74
2.5	Ligands of the class of mesitylamine derived diazadines.	75
2.6	Ligands of the class of 2,6-dihaloaryl diazadienes.	76
2.7	General structure of Mabiq and Mabiq complexes. $M^1 = \text{Ni}$, Cu , Co , Fe , $M^2 = \text{Ni}$. $\text{X} = \text{OTf}$, Cl , PF_6	77
2.8	Best ligands from the screening for catalytic zincation.	82
3.1	Ligand L1 DIPA- ^{Me} DAD.	88
3.2	Ligands used in the screening in table 3.2.	89
4.1	¹ H-NMR spectrum of S1	133
4.2	¹³ C-NMR spectrum of S1	133
4.3	¹ H-NMR spectrum of S2	134
4.4	¹³ C-NMR spectrum of S2	134
4.5	¹ H-NMR spectrum of S3	135
4.6	¹ H-NMR spectrum of S4	135
4.7	¹ H-NMR spectrum of S5	136
4.8	¹ H-NMR spectrum of S6	136
4.9	¹³ C-NMR spectrum of S6	137
4.10	¹ H-NMR spectrum of S7	137
4.11	¹³ C-NMR spectrum of S7	138
4.12	¹ H-NMR spectrum of S8	138
4.13	¹ H-NMR spectrum of S9	139

4.14	$^1\text{H-NMR}$ spectrum of S10 .	139
4.15	$^1\text{H-NMR}$ spectrum of S17 .	140
4.16	$^1\text{H-NMR}$ spectrum of S19 .	140
4.17	$^1\text{H-NMR}$ spectrum of B1 .	141
4.18	$^1\text{H-NMR}$ spectrum of C1 .	141
4.19	$^1\text{H-NMR}$ spectrum of C2 .	142
4.20	$^1\text{H-NMR}$ spectrum of C3 .	142
4.21	$^1\text{H-NMR}$ spectrum of S21 .	143
4.22	$^1\text{H-NMR}$ spectrum of S22 .	143
4.23	$^1\text{H-NMR}$ spectrum of A2 .	144
4.24	$^{13}\text{C-NMR}$ spectrum of A2 .	144
4.25	$^1\text{H-NMR}$ spectrum of A3 .	145
4.26	$^{13}\text{C-NMR}$ spectrum of A3 .	145
4.27	$^1\text{H-NMR}$ spectrum of A4 .	146
4.28	$^{13}\text{C-NMR}$ spectrum of A4 .	146
4.29	$^1\text{H-NMR}$ spectrum of A5 .	147
4.30	$^1\text{H-NMR}$ spectrum of A6 .	148
4.31	$^1\text{H-NMR}$ spectrum of A7 .	148
4.32	$^{13}\text{C-NMR}$ spectrum of A7 .	149
4.33	$^1\text{H-NMR}$ spectrum of A8 .	149
4.34	$^{13}\text{C-NMR}$ spectrum of A8 .	150
4.35	$^1\text{H-NMR}$ spectrum of A9 .	150
4.36	$^1\text{H-NMR}$ spectrum of T1 .	151
4.37	$^1\text{H-NMR}$ spectrum of T8 .	151
4.38	$^1\text{H-NMR}$ spectrum of T9 .	152
4.39	$^1\text{H-NMR}$ spectrum of T13 .	152
4.40	$^1\text{H-NMR}$ spectrum of T16 .	153
4.41	$^1\text{H-NMR}$ spectrum of T17 .	153
4.42	$^1\text{H-NMR}$ spectrum of T18 .	154
4.43	$^1\text{H-NMR}$ spectrum of T19 .	154
4.44	$^1\text{H-NMR}$ spectrum of T20 .	155
4.45	$^1\text{H-NMR}$ spectrum of L8 .	155
4.46	$^1\text{H-NMR}$ spectrum of P1 .	156
4.47	$^{13}\text{C-NMR}$ spectrum of P1 .	156
4.48	$^1\text{H-NMR}$ spectrum of P2 .	157
4.49	$^{13}\text{C-NMR}$ spectrum of P2 .	157
4.50	$^1\text{H-NMR}$ spectrum of P3 .	158
4.51	$^{13}\text{C-NMR}$ spectrum of P3 .	158
4.52	$^1\text{H-NMR}$ spectrum of P4 .	159
4.53	$^{13}\text{C-NMR}$ spectrum of P4 .	159
4.54	$^1\text{H-NMR}$ spectrum of P5 .	160
4.55	$^{13}\text{C-NMR}$ spectrum of P5 .	160
4.56	$^1\text{H-NMR}$ spectrum of P6 .	161
4.57	$^{13}\text{C-NMR}$ spectrum of P6 .	161
4.58	$^1\text{H-NMR}$ spectrum of P7 .	162
4.59	$^{13}\text{C-NMR}$ spectrum of P7 .	162

4.60	^1H -NMR spectrum of P8 .	163
4.61	^{13}C -NMR spectrum of P8 .	163
4.62	^1H -NMR spectrum of P9 .	164
4.63	^{13}C -NMR spectrum of P9 .	164
4.64	^1H -NMR spectrum of P10 .	165
4.65	^{13}C -NMR spectrum of P10 .	165
4.66	^1H -NMR spectrum of P11 .	166
4.67	^{13}C -NMR spectrum of P11 .	166
4.68	^1H -NMR spectrum of P12 .	167
4.69	^{13}C -NMR spectrum of P12 .	167
4.70	^1H -NMR spectrum of P13 .	168
4.71	^{13}C -NMR spectrum of P13 .	168
4.72	^1H -NMR spectrum of P14 .	169
4.73	^{13}C -NMR spectrum of P14 .	169
4.74	^1H -NMR spectrum of P15 .	170
4.75	^{13}C -NMR spectrum of P15 .	170
4.76	^1H -NMR spectrum of P16 .	171
4.77	^{13}C -NMR spectrum of P16 .	171
4.78	^1H -NMR spectrum of P23 .	172
4.79	^{13}C -NMR spectrum of P23 .	172
4.80	^1H -NMR spectrum of P24 .	173
4.81	^{13}C -NMR spectrum of P24 .	173
4.82	^1H -NMR spectrum of P25 .	174
4.83	^{13}C -NMR spectrum of P25 .	174
4.84	^1H -NMR spectrum of P26 .	175
4.85	^{13}C -NMR spectrum of P26 .	175
4.86	^1H -NMR spectrum of P36 .	176
4.87	^{13}C -NMR spectrum of P36 .	176